FINAL REPORT

RESEARCH STUDY ON STABILIZATION AND CONTROL

MODERN SAMPLED-DATA CONTROL THEORY

SYSTEMS RESEARCH LABORATORY

P.O. BOX 2277, STATION A
3206 VALLEY BROOK DRIVE
CHAMPAIGN, ILLINOIS 61820

PREPARED FOR GEORGE C. MARSHALL SPACE FLIGHT CENTER

HUNTSVILLE, ALABAMA

FINAL REPORT

DIGITAL CONTROLLER DESIGN

subtitle:

ANALYSIS OF THE ANNULAR SUSPENSION

POINTING SYSTEM

March 1, 1979

B. C. Kuo

Contract No. NAS8-32358 1-7-ED-07418(1F)

PREPARED FOR GEORGE C. MARSHALL SPACE FLIGHT CENTER

HUNTSVILLE, ALABAMA

SYSTEMS RESEARCH LABORATORY

P.O. BOX 2277, STATION A

CHAMPAIGN, ILLINOIS 61820

TABLE OF CONTENT

1. SIMPLIFIED MODELS OF THE ANNULAR SUSPENSION AND POINTING SYSTEM (ASPS)

1.1 Introduction [1]

The Annular Suspension and Pointing System (ASPS) is a payload auxiliary pointing device of the Space Shuttle. The ASPS is comprised of two major subassemblies, a vernier and a coarse pointing subsystem.

The experiment is attached to a mounting plate/rim combination which is suspended on magnetic bearing/actuators (MBA's) strategically located about the rim. Fine pointing is achieved by "gimballing" the plate/rim within the MBA gaps. Control about the experiment line-of-sight is obtained through the use of a non-contacting rim drive and positioning torquer. All sensors used to close the servo loops on the vernier system are noncontacting elements. Therefore, the experiment is a free-flyer constrained only by the magnetic forces generated by the control loops.

The configuration of the ASPS is shown in Fig. 1-1. The payload/plate/rim combination is mounted on a set of coarse gimbals; an elevation and a lateral coarse gimbal, which provide the slewing and coarse pointing capability of the system. The pointing system concept is unique in that the vernier and coarse pointing subsystem are separate entities. This approach allows for sub-arcsecond pointing of the payload at any coarse gimbal position.

The three functions provided by the ASPS are: (1) pointing the payload, (2) centering the payload in the magnetic actuator assembly, and (3) tracking the payload mounting plate and shuttle motions by the coarse gimbals. Rate and position errors sensed by gyros and celestial sensors located on the payload are processed by a controller which subsequently commands appropriate actuator force to point the payload. Proximeter sensors associated with the actuator clusters detect the payload translation errors which are subsequently processed by the

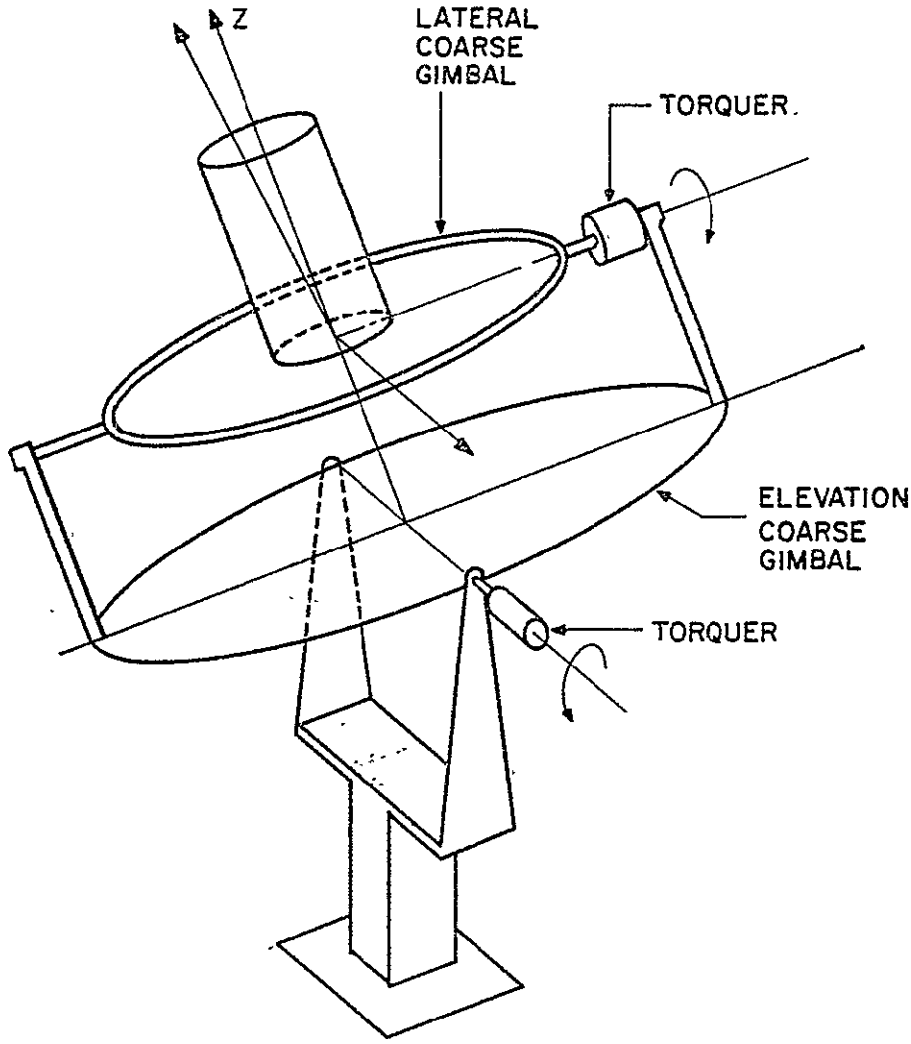

Figure I-1. ASPS configuration.

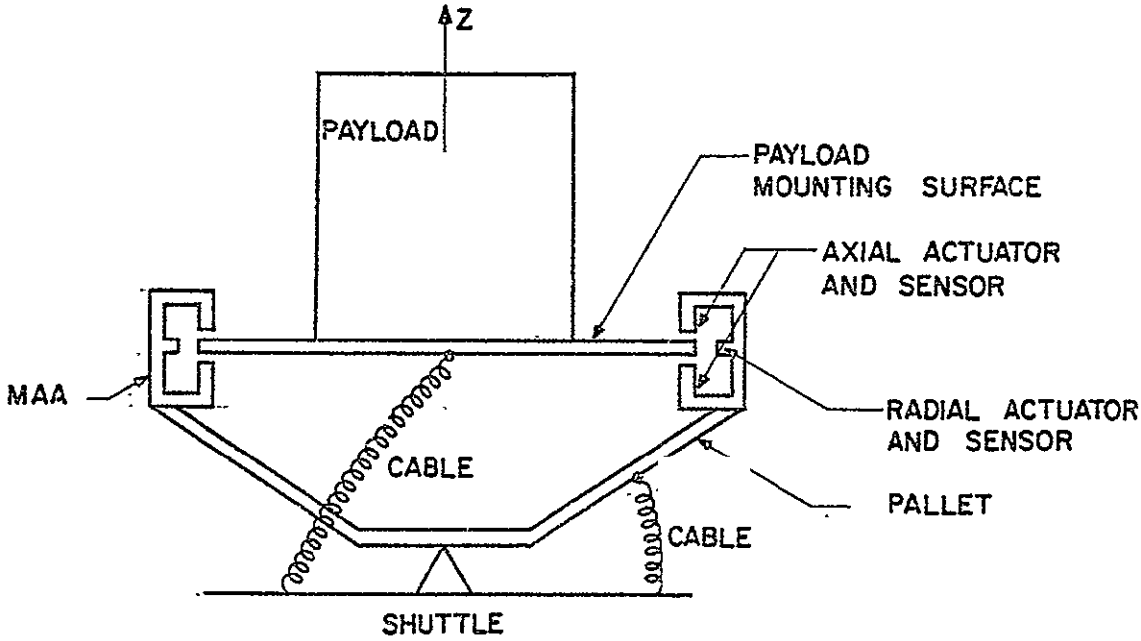

Figure I-2. Payload and magnetic actuator assembly.

controller and used to ascertain the appropriate centering forces.

Figure 1-2 shows the payload and its mounting surface which is controlled by the magnetic actuator assembly (MAA). The cables shown are for the purpose of connecting electric power from the shuttle to the payload and the MAA on the pallet.

1.2 The Planar Model of the ASPS [2]

In this section the equations of motion of a simplified planar model of the ASPS are derived.

The small-angle, small-displacement model shown in Fig. 1-3 is planar with four degrees of freedom and is composed of a mount, a gimbal assembly (elevation), a pallet with magnetic actuators, and a payload. The pallet has one rotational degree of freedom relative to the mount, and the payload has two translational and one rotational degrees of freedom relative to the pallet.

Let the four degrees of freedom be

ϕ_1 = attitude degree of freedom of the pallet relative to the mount

ϕ_2 = attitude degree of freedom of the payload relative to the pallet

x_1 = translation degree of freedom of the payload relative to the pallet

z_1 = translation degree of freedom of the payload relative to the pallet

The following coordinates are defined:

(x_0,z_0) = inertial axes

(x_G,z_G) = inertial axes rotated through an angle of ϕ_M relative to the (x_0,z_0) axes, (ϕ_M is defined as the gimbal angle).

(x_m,z_m) = axes fixed at the pallet center of gravity (CG)

(x_1,z_1) = static axes of the payload

(x_i,z_i) = axes fixed at the payload center of gravity (CG)

(x_j,z_j) = axes fixed at the center of the base of the payload.

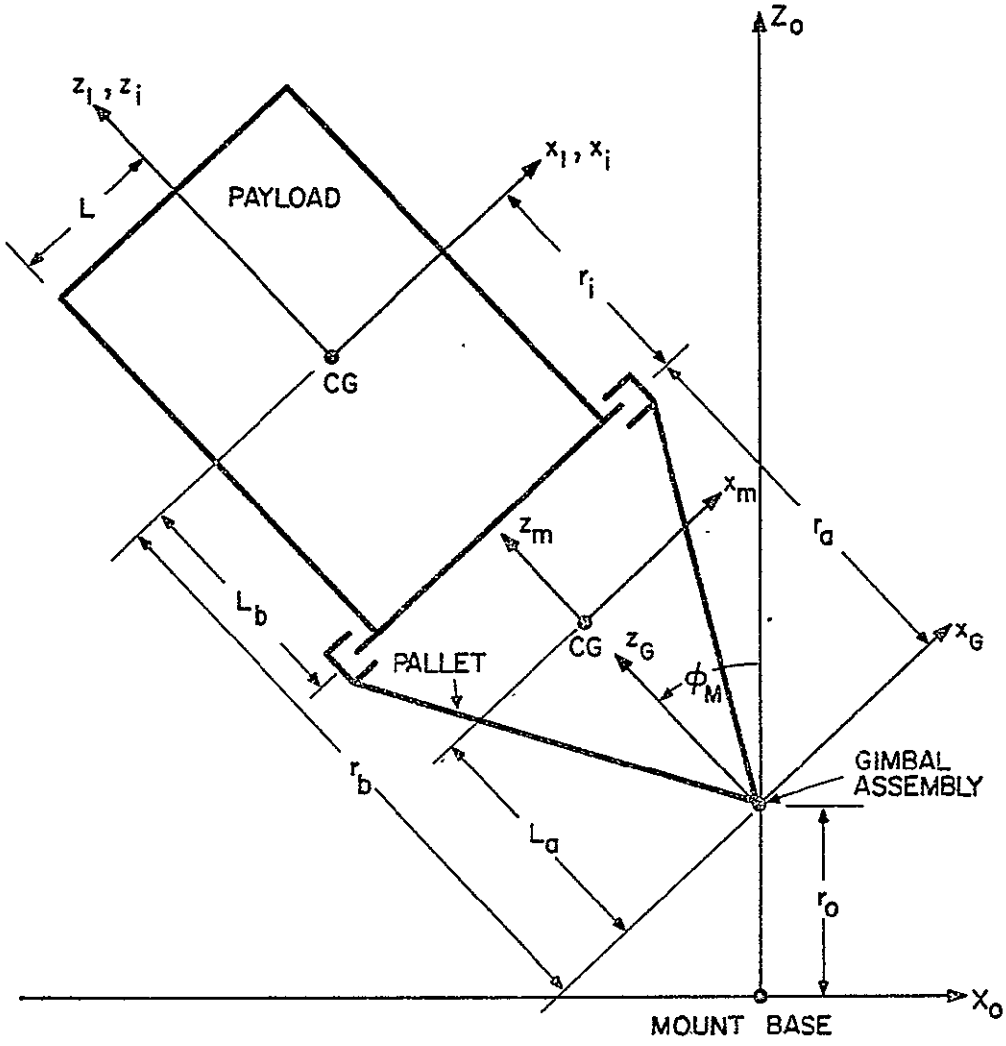

Figure 1-3. Planar ASPS model.

The following system parameters are defined:

M_i = mass of the payload = 600 Kg

M_m = mass of the pallet = 82 Kg

J_m = inertia of the pallet about its mass center = 3.1 Kg-m^2

J_i = inertia of the payload about its mass center = 503 Kg-m^2

L = radius of the payload = 0.406 m

L_a = distance from the gimbal to the pallet CG = 0.2064 m

L_b = distance from the pallet center to the payload CG = 1.486 m

r_a = distance from the gimbal assembly to the pallet center = 0.47 m

r_b = distance from the gimbal assembly to the payload CG = 1.956 m

r_0 = distance from the mount base to the gimbal assembly = 0.75 m

Since the payload is suspended with respect to the pallet, there are many ways of fixing its coordinates for the motion of rotation. In other words, the angle ϕ_2 can be defined in a number of ways. Figure 1-4 illustrates the small-angle rotation of the pallet and the payload with ϕ_2 measured as the angle between the coordinate axes of (x_l,z_l) and (x_j,z_j). This configuration is defined as Model 1 of the ASPS. Figure 1-5 illustrates the model of the ASPS with ϕ_2 measured at the CG of the payload; i.e., between the axes of (x_l,z_l) and (x_i,z_i).

The following coordinate transformations are identified:

Transformation from the static pallet axes to the mount axes:

$$T_G = \begin{bmatrix} \cos\phi_M & -\sin\phi_M \\ \sin\phi_M & \cos\phi_M \end{bmatrix} \tag{1-1}$$

Transformation from the dynamic pallet axes to the static pallet axis:

$$T_l = \begin{bmatrix} \cos\phi_l & -\sin\phi_l \\ \sin\phi_l & \cos\phi_l \end{bmatrix} \cong \begin{bmatrix} 1 & -\phi_l \\ \phi_l & 1 \end{bmatrix} \tag{1-2}$$

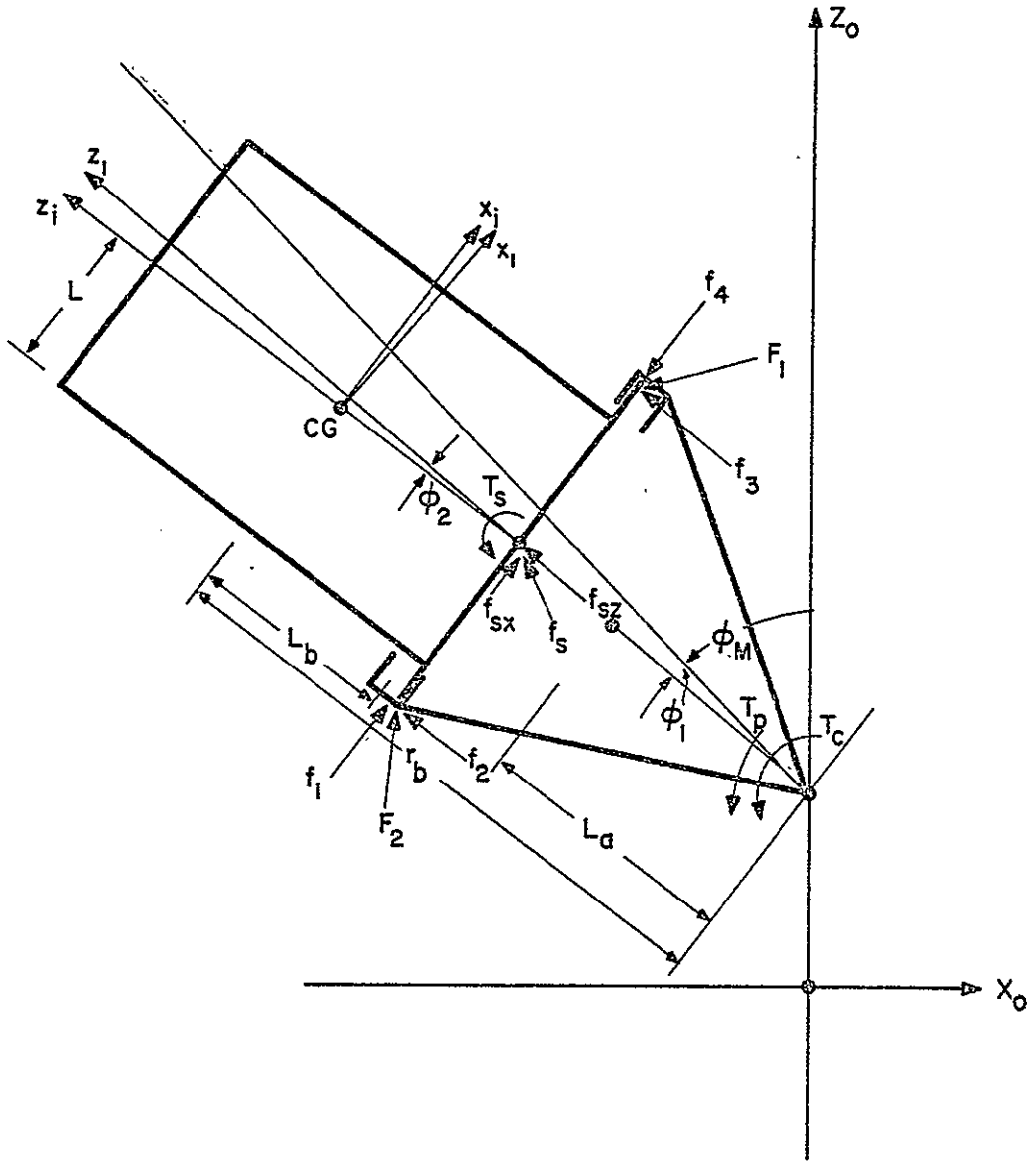

Figure 1-4. Planar ASPS Model 1.

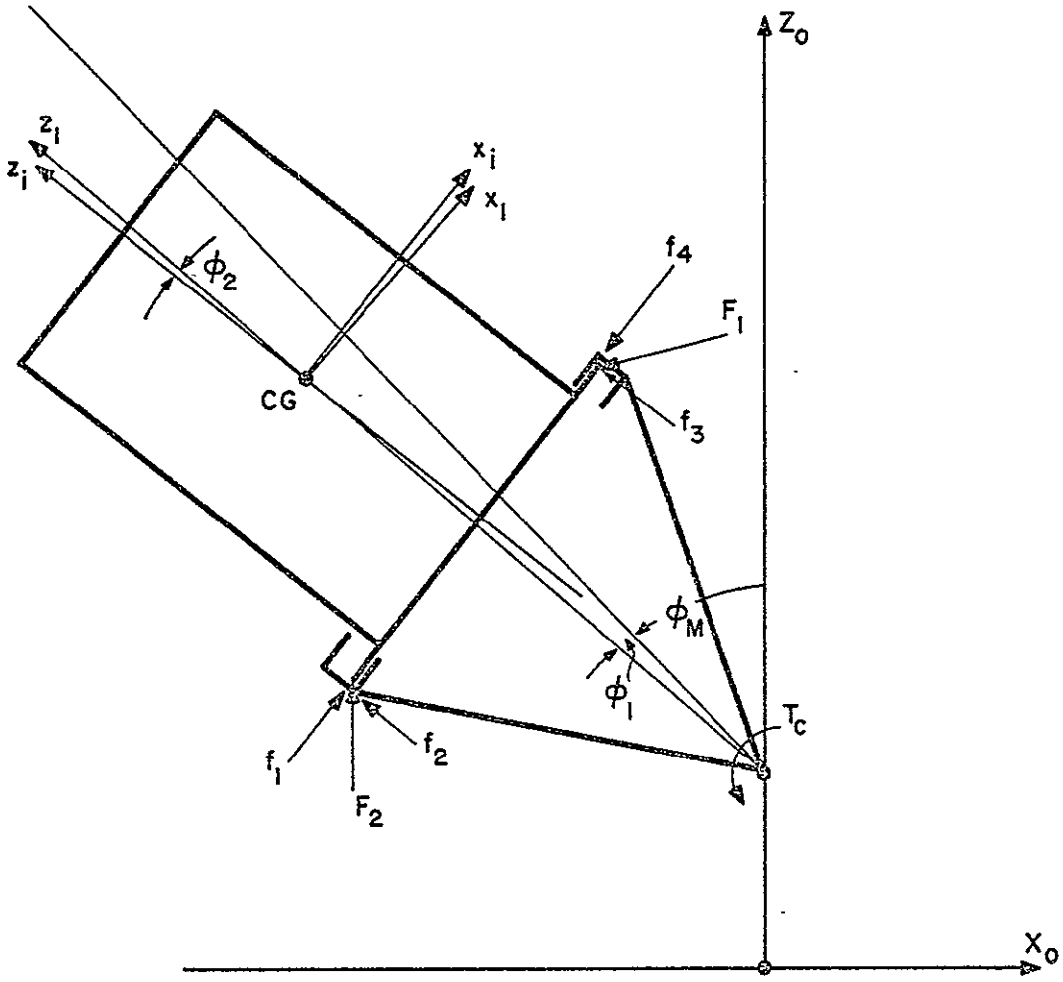

Figure 1-5. Planar ASPS Model 2.

Transformation from the dynamic payload axes to the dynamic pallet axes:

$$T_2 = \begin{bmatrix} \cos\phi_2 & -\sin\phi_2 \\ \sin\phi_2 & \cos\phi_2 \end{bmatrix} = \begin{bmatrix} 1 & -\phi_2 \\ \phi_2 & 1 \end{bmatrix} \qquad (1\text{-}3)$$

The force vectors applied to the payload by the magnetic actuator assembly are defined as:

$$F_1 = \begin{bmatrix} f_4 \\ f_3 \end{bmatrix} = \text{magnetic force applied at the positive } x_m \text{ displacement} \qquad (1\text{-}4)$$

$$F_2 = \begin{bmatrix} f_1 \\ f_2 \end{bmatrix} = \text{magnetic force applied at the negative } x_m \text{ displacement} \qquad (1\text{-}5)$$

The forces F_1 and F_2 are illustrated as shown in Fig. 1-5.

The torque applied by the gimbal assembly is designated as T_c, as shown in Fig. 1-5.

The following vector distances are defined for the pallet and the payload.

R_1 = vector distance from the gimbal assembly to the payload point of application of F_1

R_2 = vector distance from the gimbal assembly to the payload point of application of F_2

R_3 = vector distance from the gimbal assembly to the pallet point of application of F_1

R_4 = vector distance from the gimbal assembly to the pallet point of application of F_2.

Equations of Motion of Model 1

Using the degrees of freedom defined in the preceding sections, the kinetic energy of the system in Fig. 1-4 is

$$T = \text{K.E.} = \frac{1}{2}\dot{R}_m' M_m \dot{R}_m + \frac{1}{2}\dot{R}_i' M_i \dot{R}_i + \frac{1}{2}J_m\dot{\phi}_1^2 + \frac{1}{2}J_i(\dot{\phi}_1 + \dot{\phi}_2)^2 \qquad (1\text{-}6)$$

where the primes denote the transpose of a matrix, and

$$\dot{R}_m = \begin{bmatrix} -L_a \\ 0 \end{bmatrix} \dot{\phi}_1 \tag{1-7}$$

$$\dot{R}_i = \begin{bmatrix} \dot{x}_1 \\ \dot{z}_1 \end{bmatrix} + \begin{bmatrix} -L_b \\ 0 \end{bmatrix} \dot{\phi}_2 + \begin{bmatrix} -r_b \\ 0 \end{bmatrix} \dot{\phi}_1 \tag{1-8}$$

Substitution of Eqs. (1-7) and (1-8) into Eq. (1-6) gives

$$T = \text{K.E.} = \frac{1}{2}M_m L_a^2 \dot{\phi}_1^2 + \frac{1}{2}M_i \dot{z}_1^2 + \frac{1}{2}M_i (\dot{x}_1 - r_b \dot{\phi}_1 - L_b \dot{\phi}_2)^2 + \frac{1}{2}J_m \dot{\phi}_1^2 + \frac{1}{2}J_i (\dot{\phi}_1 + \dot{\phi}_2)^2 \tag{1-9}$$

Let the spring force applied to the system payload due to the cable be designated as

$$f_s = \begin{bmatrix} f_{sx}(x_1) \\ f_{sz}(z_1) \end{bmatrix}, \tag{1-10}$$

and the spring torque applied to the payload due to the cable be $T_s(\phi_2)$. The spring torque applied to the pallet due to the cable is denoted as $T_p(\phi_1)$.

The relation between the force $\overline{F}$ and the potential of the system, U, is

$$\overline{F} = -\nabla U \tag{1-11}$$

Thus,

$$U = U_0 - \int \overline{F} \cdot d\overline{x} \tag{1-12}$$

where U_0 = constant.

The potential energy of Model 1 is

$$U = U_0 - \{(f_1 - f_4)x_1 + (f_2 + F_3)z_1 + \int_0^{\phi_2} T_s(\phi)\,d\phi + \int_0^{z_1} f_{sz}(z)\,dz + \int_0^{x_1} f_{sx}(x)\,dx$$

$$+ (f_3 - f_2)L\phi_2 + \int_0^{\phi_1} T_c(\phi)\,d\phi + \int_0^{\phi_1} T_p(\phi)\,d\phi \tag{1-13}$$

The Lagrangian is defined as

$$\mathcal{L} = \text{K.E.} - U \tag{1-14}$$

Then from Eqs. (1-9) and (1-13), we get

$$\mathcal{L} = \frac{1}{2}M_m L_a^2\dot{\phi}_1^2 + \frac{1}{2}M_i\dot{z}_1^2 + \frac{1}{2}M_i(\dot{x}_1 - r_b\dot{\phi}_1 - L_b\dot{\phi}_2)^2 + \frac{1}{2}J_m\dot{\phi}_1^2 + \frac{1}{2}J_i(\dot{\phi}_1 + \dot{\phi}_2)^2$$

$$+ (f_1 - f_4)x_1 + (f_2 + F_3)z_1 + \int_0^{\phi_2} T_s(\phi)d\phi + \int_0^{z_1} f_{sz}(z)dz + \int_0^{x_1} f_{sx}(x)dx$$

$$+ (f_3 - f_2)L\phi_2 + \int_0^{\phi_1} T_c(\phi)d\phi + \int_0^{\phi_1} T_p(\phi)d\phi - U_0 \qquad (1\text{-}15)$$

The Lagrange equation of motion is

$$\frac{\partial\mathcal{L}}{\partial x_i} - \frac{d}{dt}\left(\frac{\partial}{\partial\dot{x}_i}\right) = 0 \qquad i = 1,2,3,4 \qquad (1\text{-}16)$$

where $x_1 = x_1$, $x_2 = z_1$, $x_3 = \phi_1$ and $x_4 = \phi_2$.

For i = 1, we have

$$\frac{\partial\mathcal{L}}{\partial x_1} = f_1 - f_4 + f_{sx}(x_1) \qquad (1\text{-}17)$$

$$\frac{\partial\mathcal{L}}{\partial\dot{x}_1} = M_i(\dot{x}_1 - r_b\dot{\phi}_1 - L_b\dot{\phi}_2)$$

Thus,

$$\frac{\partial\mathcal{L}}{\partial x_1} - \frac{d}{dt}\left(\frac{\partial}{\partial\dot{x}_i}\right) = -M_i\ddot{x}_1 + M_i r_b\ddot{\phi}_1 + M_i L_b\ddot{\phi}_2 + (f_1 - f_4) + f_{sx}(x_1) = 0 \qquad (1\text{-}18)$$

For i = 2, we have

$$\frac{\partial\mathcal{L}}{\partial z_1} = f_2 + f_3 + f_{sz}(z_1)$$

$$\frac{\partial\mathcal{L}}{\partial\dot{z}_1} = M_i\dot{z}_i$$

Then,

$$\frac{\partial\mathcal{L}}{\partial z_1} - \frac{d}{dt}\left(\frac{\partial}{\partial\dot{z}_1}\right) = -M_i\ddot{z}_i + (f_2 + f_3) + f_{sz}(z_1) = 0 \qquad (1\text{-}19)$$

For i = 3, we have

$$\frac{\partial\mathcal{L}}{\partial\phi_1} = T_c(\phi_1) + T_p(\phi_1)$$

$$\frac{\partial\mathcal{L}}{\partial\dot{\phi}_1} = M_m L_{az}^2\dot{\phi}_1 + M_i(-r_b\dot{x}_i + r_b^2\dot{\phi}_1 + r_b L_b\dot{\phi}_2) + J_m\dot{\phi}_1 + J_i\dot{\phi}_1 + J_i\dot{\phi}_2$$

$$\frac{\partial}{\partial \phi_1} - \frac{d}{dt}\left(\frac{\partial \mathcal{L}}{\partial \dot{\phi}_1}\right) = T_c(\phi_1) + T_p(\phi_1) + M_i r_b \ddot{x}_1$$

$$- (J_m + J_i + M_m L_a^2 + M_i r_b^2)\ddot{\phi}_1 - (J_i + M_i L_b r_b)\ddot{\phi}_2 = 0 \quad (1\text{-}20)$$

For i = 4, we have

$$\frac{\partial \mathcal{L}}{\partial \phi_2} = (f_3 - f_2)L + T_s(\phi_2)$$

$$\frac{\partial \mathcal{L}}{\partial \dot{\phi}_2} = -M_i L_b \dot{x}_1 + r_b L_b M_i \dot{\phi}_1 + M_i L_b^2 \dot{\phi}_2 + J_i \dot{\phi}_1 + J_i \dot{\phi}_2$$

$$\frac{\partial \mathcal{L}}{\partial \phi_2} - \frac{d}{dt}\left(\frac{\partial}{\partial \dot{\phi}_2}\right) = T_s(\phi_2) + (f_3 - f_2)L + M_i L_b \ddot{x}_1$$

$$- (M_i L_b r_b + J_i)\ddot{\phi}_1 - (M_i L_b^2 + J_i)\ddot{\phi}_2 = 0 \quad (1\text{-}21)$$

The Lagrange equations in Eqs. (1-18), (1-19), (1-20) and (1-21) are written in matrix form as follows:

$$\begin{bmatrix} M_i & 0 & -M_i r_b & -M_i L_b \\ 0 & M_i & 0 & 0 \\ -M_i r_b & 0 & J_m+J_i+M_m L_a^2+M_i r_b^2 & J_i+M_i L_b r_b \\ -M_i L_b & 0 & J_i+M_i L_b r_b & J_i+M_i L_b^2 \end{bmatrix} \begin{bmatrix} \ddot{x}_1 \\ \ddot{z}_1 \\ \ddot{\phi}_1 \\ \ddot{\phi}_2 \end{bmatrix} = \begin{bmatrix} f_1-f_4+f_{sx}(x_1) \\ f_2+f_3+f_{sx}(z_1) \\ T_c(\phi_1)+T_p(\phi_1) \\ (f_3-f_2)L+T_s(\phi_2) \end{bmatrix} \quad (1\text{-}22)$$

Equations of Motion of Model 2

For the ASPS system Model 2, the kinetic energy of the system is still given by Eq. (1-6), and $\dot{R}_m$ is as defined in Eq. (1-7), except that

$$\dot{R}_i = \begin{bmatrix} \dot{x}_1 \\ \dot{z}_1 \end{bmatrix} + \begin{bmatrix} -r_b \\ 0 \end{bmatrix} \dot{\phi}_1 \quad (1\text{-}23)$$

Substitution of Eqs. (1-7) and (1-23) into Eq. (1-6) gives

$$K.E. = \frac{1}{2}M_m L_a^2 \dot{\phi}_1^2 + \frac{1}{2}M_i \dot{z}_1^2 + \frac{1}{2}M_i (\dot{x}_1 - r_b \dot{\phi}_1)^2 + \frac{1}{2}J_m \dot{\phi}_1^2 + \frac{1}{2}J_i (\dot{\phi}_1 + \dot{\phi}_2)^2 \quad (1\text{-}24)$$

The potential energy of the Model 2 is

$$U = U_0 - \{(f_1 - f_4)x_1 + \int_0^{x_1} f_{sx}(x)dx + (f_2 + f_3)z_1 + \int_0^{z_1} f_{sz}(z)dz + \int_0^{\phi_2} T_s(\phi)d\phi$$

$$+ \int_0^{\phi_1} T_c(\phi)d\phi + \int_0^{\phi_1} T_p(\phi)d\phi + (f_3 - f_2)L\phi_2 + (f_1 - f_4)L_b\phi_2\} \qquad (1\text{-}25)$$

The Lagrangian $\mathcal{L}$ is given by

$$\mathcal{L} = \text{K.E.} - U = \frac{1}{2}M_m L_a^2\dot{\phi}_1^2 + \frac{1}{2}M_i\dot{z}_1^2 + \frac{1}{2}M_i(\dot{x}_1 - r_b\dot{\phi}_1)^2 + \frac{1}{2}J_m\dot{\phi}_1^2 + \frac{1}{2}J_i(\dot{\phi}_1 + \dot{\phi}_2)^2$$

$$+ (f_1 - f_4)x_1 + \int_0^{x_1} f_{sx}(x)dx + (f_2 + f_3)z_1 + \int_0^{z_1} f_{sz}(z)dz$$

$$+ \int_0^{\phi_2} T_s(\phi)d\phi + \int_0^{\phi_1} T_c(\phi)d\phi + \int_0^{\phi_1} T_p(\phi)d\phi + \{(f_3 - f_2)L$$

$$+ (f_1 - f_4)L_b\}\phi_2 - U_0 \qquad (1\text{-}26)$$

The Lagrange equation of motion is given by Eq. (1-16).

Following the same procedure as for Model 1, the Lagrange equations of Model 2 are derived by use of Eqs. (1-16) and (1-26), and the result is

$$\begin{bmatrix} M_i & 0 & -M_i r_b & 0 \\ 0 & M_i & 0 & 0 \\ -M_i r_b & 0 & J_m+J_i+M_m L_a^2+M_i r_b^2 & J_i \\ 0 & 0 & J_i & J_i \end{bmatrix} \begin{bmatrix} \ddot{x}_1 \\ \ddot{z}_1 \\ \ddot{\phi}_1 \\ \ddot{\phi}_2 \end{bmatrix} = \begin{bmatrix} f_1-f_4+f_{sx}(x_1) \\ f_2+f_3+f_{sz}(z_1) \\ T_c(\phi_1)+T_p(\phi_1) \\ (f_3-f_2)L+(f_1-f_4)L_b+T_s(\phi_2) \end{bmatrix}$$

$$(1\text{-}27)$$

In the analysis conducted in the ensuing sections the equations of motions of Model 2 will be used. One reason for this selection is that the mass matrix of Eq. (1-27) is simpler than that of Model 1 in Eq. (1-22). Another reason for using Model 2 is that the model uses the center of gravity of the payload as the reference point of rotation, which is more logical.

Substitution of the system parameters into Eq. (1-27), we have

$$\begin{bmatrix} 600 & 0 & -1173.6 & 0 \\ 0 & 600 & 0 & 0 \\ -1173.6 & 0 & 2805.15 & 503 \\ 0 & 0 & 503 & 503 \end{bmatrix} \begin{bmatrix} \ddot{x}_1 \\ \ddot{z}_1 \\ \ddot{\phi}_1 \\ \ddot{\phi}_2 \end{bmatrix} \quad \begin{bmatrix} f_1 - f_4 + f_{sx}(x_1) \\ f_2 + f_3 + f_{sz}(z_1) \\ T_c(\phi_1) + T_p(\phi_1) \\ (f_3 - f_2 L + (f_1 - f_4) L_b + T_s(\phi_2) \end{bmatrix} \tag{1-28}$$

1.3 Control of the Z_1 Dynamics of the Payload

Equation (1-28) indicates that the z_1 dynamics of the ASPS are not coupled to the other three degrees of freedom. The z_1 dynamics are described by

$$M_1 \ddot{z}_1 = f_2 + f_3 + f_{sz}(z_1) \tag{1-29}$$

The magnetic actuator forces $f_2 + f_3$ are controlled by feeding back the variables z_1 and $\dot{z}_1$. The control equation is

$$f_2 + f_3 = -K_p z_1 - K_r \dot{z}_1 \tag{1-30}$$

where $K_p = 37.861$ N/m and $K_r = 211.01$ N/m/sec.

Substitution of Eq. (1-30) into Eq. (1-29), we have

$$M_1 \ddot{z}_1 = -K_p z_1 - K_r \dot{z}_1 + f_{sz}(z_1) \tag{1-31}$$

Figure 1-6 shows the state diagram of the z_1 dynamics of the ASPS with the continuous-data position-plus-rate controller. The notation $N_{sz}(z_1)$ in the state diagram represents the functional relation of the wire cable which is attached to the center of the payload mounting surface.

If the wire cable is modelling by a linear spring, $N_{sz}(z_1)$ is simply a constant, $-K_s$ (N/m); that is,

$$f_{sz}(z_1) = -K_s z_1 \tag{1-32}$$

A nonlinear spring characteristic for $N_{sz}(z_1)$ is shown in Fig. 1-7. However, since the mass of the payload is 600 Kg, and the spring constant is

only 0.35 N/m, the effect of the wire cable on the payload dynamics is not going to be substantial.

The characteristic equation of the continuous-data ASPS z_1 dynamic system with the linear wire cable spring characteristic is

$$M_i s^2 + K_r s + K_p + K_s = 0 \tag{1-33}$$

or

$$600s^2 + 211.01s + 38.211 = 0 \tag{1-34}$$

The damping ratio of the system is

$$\zeta = 0.6968 \tag{1-35}$$

and the undamped natural frequency is

$$\omega_n = 0.2524 \text{ rad/sec} \tag{1-36}$$

Analysis of the Digital ASPS z_1 Dynamics

When the z_1 dynamics of the ASPS are controlled by a digital position-plus-rate controller, the dynamic equation is

$$M_i \ddot{z}_1 + K_s z_1 = f_2(t) + f_3(t) \tag{1-37}$$

where

$$f_2(t) + f_3(t) = f_2(kT) + f_3(kT) \qquad kT \leq t < (k+1)T \tag{1-38}$$

Then the control equation is

$$f_2(kT) + f_3(kt) = -K_p z_i(kT) - K_r \dot{z}_i(kT) \tag{1-39}$$

Figure 1-8 shows the block diagram of the linear digital ASPS payload (z_1 dynamics).

Since all the system parameters are given, except the sampling period T, we shall study the maximum value of T for asymptotic stability.

The characteristic equation of the digital system in Fig. 1-8 is

$$\Delta(z) = 1 + \frac{1}{M_i}(1 - z^{-1})\mathfrak{Z}\left\{\frac{K_r/s^2}{1 + \frac{K_r}{M_i}s^{-2}} + \frac{K_p/s^3}{1 + \frac{K_s}{M_i}s^{-2}}\right\} = 0 \tag{1-40}$$

The z-transforms in the last equation are evaluated as follows:

$$\mathcal{Z}\left[\frac{1}{s^2+\frac{K_s}{M_i}}\right]=\frac{\sqrt{\frac{M_i}{K_s}}\,z\sin\sqrt{\frac{K_s}{M_i}}\,T}{z^2-2z\cos\sqrt{\frac{K_s}{M_i}}\,T+1} \tag{1-41}$$

$$\mathcal{Z}\left[\frac{1}{s(s^2+\frac{K_s}{M_i})}\right]=\frac{M_i}{K_s}\left[\frac{z}{z-1}-\frac{z(z-\cos\sqrt{K_s/M_i}\,T)}{z^2-2z\cos\sqrt{K_s/M_i}\,T+1}\right] \tag{1-42}$$

Substitution of the last two equations into Eq. (1-40) and simplifying, we have

$$z^2+\left[\frac{K_r}{\sqrt{M_iK_s}}\sin\sqrt{\frac{K_s}{M_i}}\,T-\frac{K_p}{K_s}\cos\sqrt{\frac{K_s}{M_i}}\,T+\frac{K_p}{K_s}-2\cos\sqrt{\frac{K_s}{M_i}}\,T\right]z+1+\frac{K_p}{K_s}-\frac{K_p}{K_s}\cos\sqrt{\frac{K_s}{M_i}}\,T$$

$$-\frac{K_r}{\sqrt{M_iK_s}}\sin\sqrt{\frac{K_s}{M_i}}\,T=0 \tag{1-43}$$

Substituting the system parameters into the last equation, yielding,

$$z^2+(14.5597\sin 0.02415T-110.1688\cos 0.02415T+108.1688)z+1-14.5597\sin 0.02415T$$
$$-108.1688\cos 0.02415T+108.1688=0 \tag{1-44}$$

The roots of the last equation as a function of T are tabulated below and the root locus diagram with T as a variable parameter is shown in Fig. 1-9. The critical value of T for asymptotic stability is approximately 5.7 sec.

Sampling period T (sec)	Characteristic Equation	Roots
0.1	$z^2-1.96z+0.965=0$	$0.98\pm j0.069$
0.5	$z^2-1.816z+0.832=0$	$0.908\pm j0.0864$
1.0	$z^2-1.6163z+0.680=0$	$0.808\pm j0.164$
2.0	$z^2-1.1686z+0.4232=0$	$0.584\pm j0.286$
3.0	$z^2-0.657z+0.2298=0$	$0.328\pm j0.349$

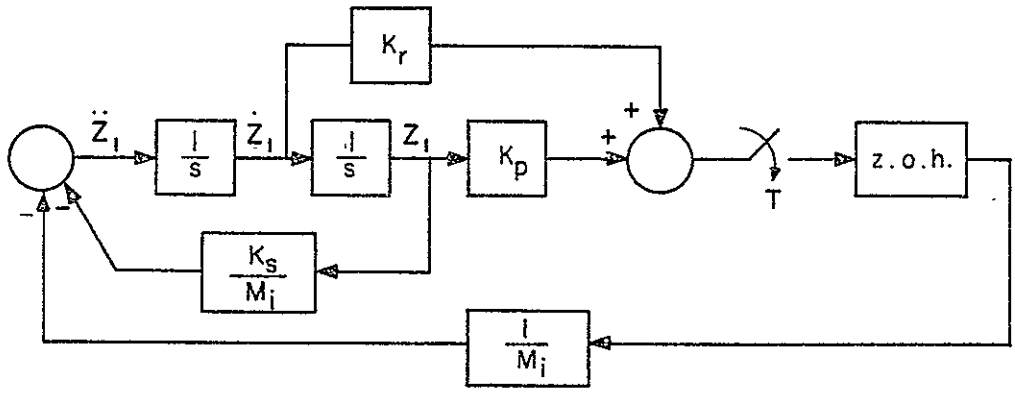

Figure 1-8. Block diagram of the linear digital ASPS payload z_1 dynamics).

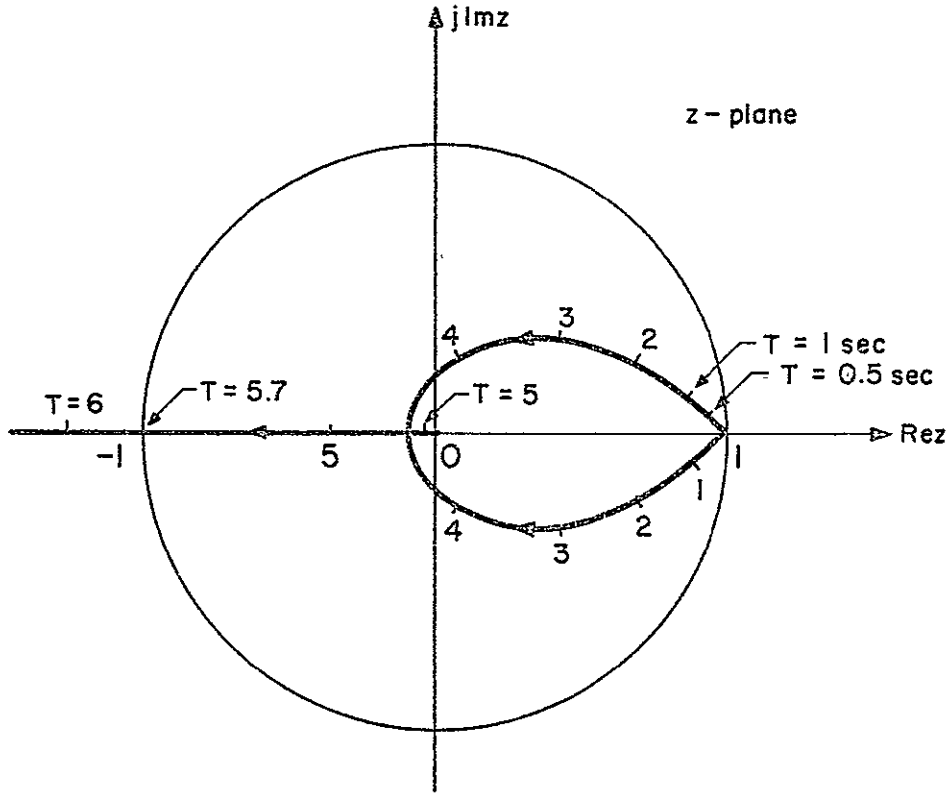

Figure 1-9. Root loci of z_i dynamics of the digital ASPS payload as the sampling period T varies.

4.0	$z^2 - 0.0821z + 0.1 = 0$	$0.041 \pm j\ 0.3135$
5.0	$z^2 + 0.556z + 0.0338 = 0$	-0.4865, -0.0695
5.7	$z^2 + 1.04z + 0.02533 = 0$	-1.01, -0.025
6.0	$z^2 + 1.257z + 0.03124 = 0$	-1.23, -0.0254

The time responses of the digital system in Fig. 1-8 for various sampling periods are shown in Fig. 1-10. The initial value of $z_1(t)$ is chosen to be 0.002 m, since the static bearing gap of z_1 is only 0.0076 m, so that the maximum constraints on the magnitude of z_1 are $\pm$0.0038 m. The time responses in Fig. 1-10 substantiates the root locus findings; when T = 6 sec, the closed-loop system is unstable. The time responses are quite good for T less than or equal to 3 seconds.

Effects of Quantization

The block diagram of the digital ASPS payload z_1 dynamics with the quantization effect is shown in Fig. 1-11. The input-output characteristics of the quantizer are illustrated in Fig. 1-12. The quantization level is denoted by h in meter.

The effects of quantization can be classified into three catagories: (1) stable system with steady-state error, (2) unstable system with sustained oscillation, and (3) unstable system with unbounded responses. The last case is possible since no saturation is assumed in the system model.

The steady-state error due to quatization can be determined by using the least-upper bound method [3] and the condition of sustained oscillations is found by use of the discrete describing function.

The "characteristic equation" of the system shown in Fig. 1-11 is written as

$$\Delta(z) = 1 + Q(z)(1 - z^{-1})\mathcal{Z}\left\{\frac{1}{M_i s^2}\,\frac{K_r + K_p/s}{1 + \frac{K_s}{M_i}\,s^{-2}}\right\} = 0 \qquad (1\text{-}45)$$

where Q(z) denotes the discrete describing function of the quantizer.

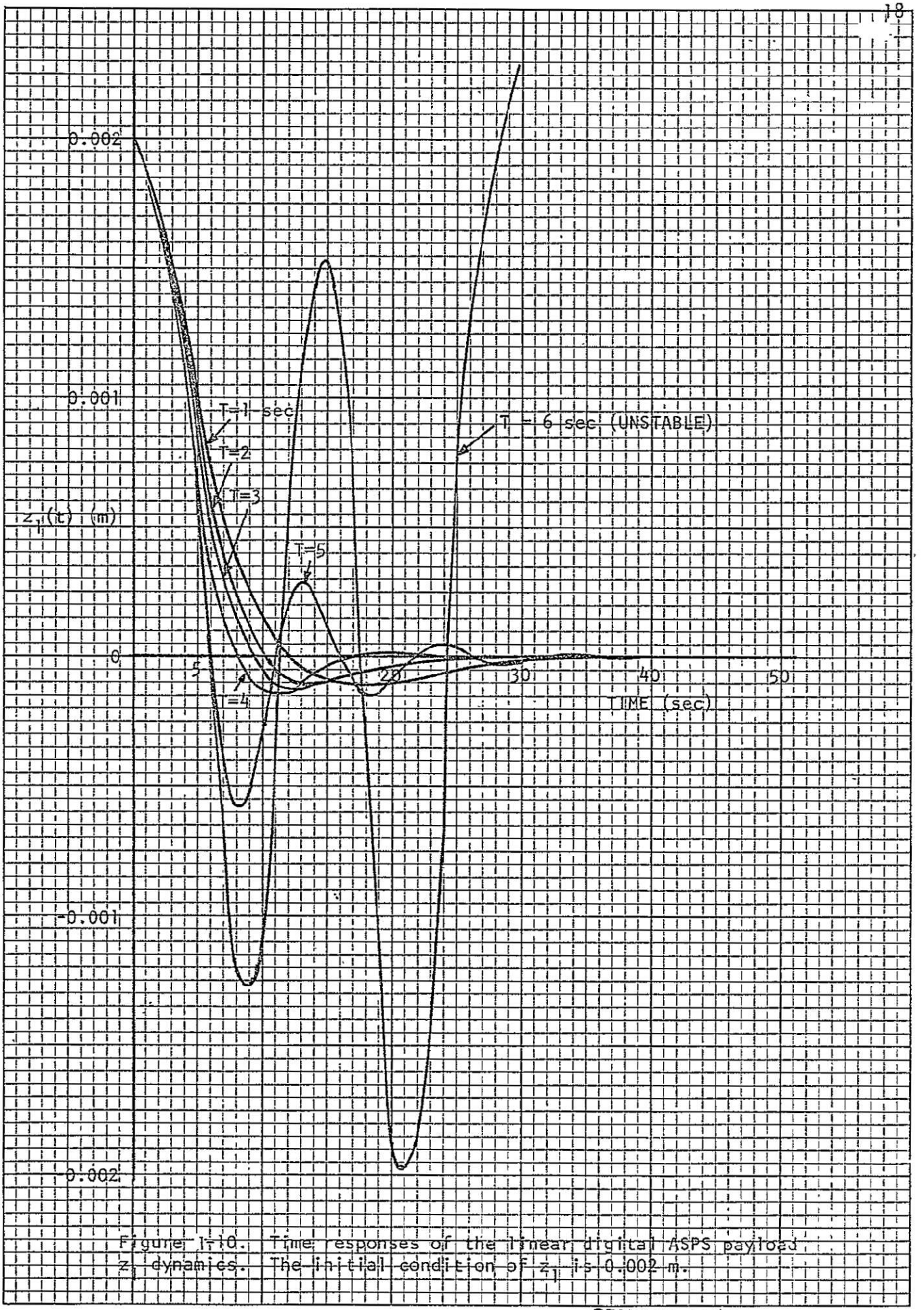

Figure I-10. Time responses of the linear digital ASPS payload z_1 dynamics. The initial condition of z_1 is 0.002 m.

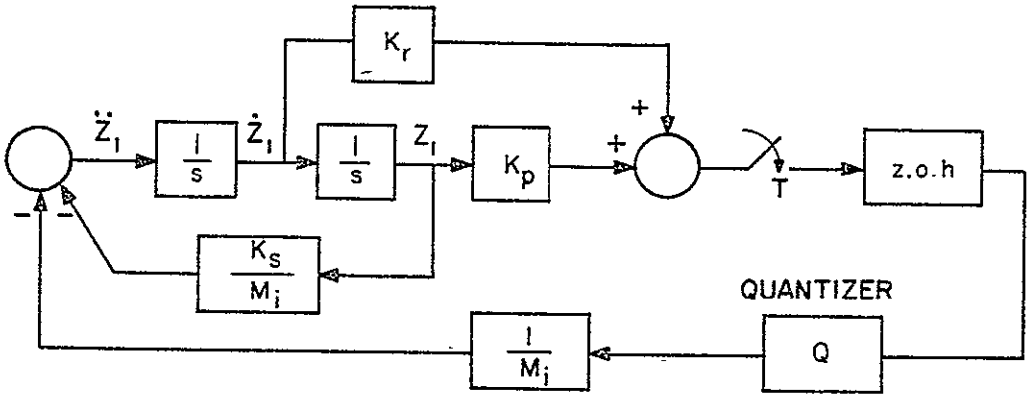

Figure 1-11. Block diagram of the digital ASPS payload z_1 dynamics with quantization.

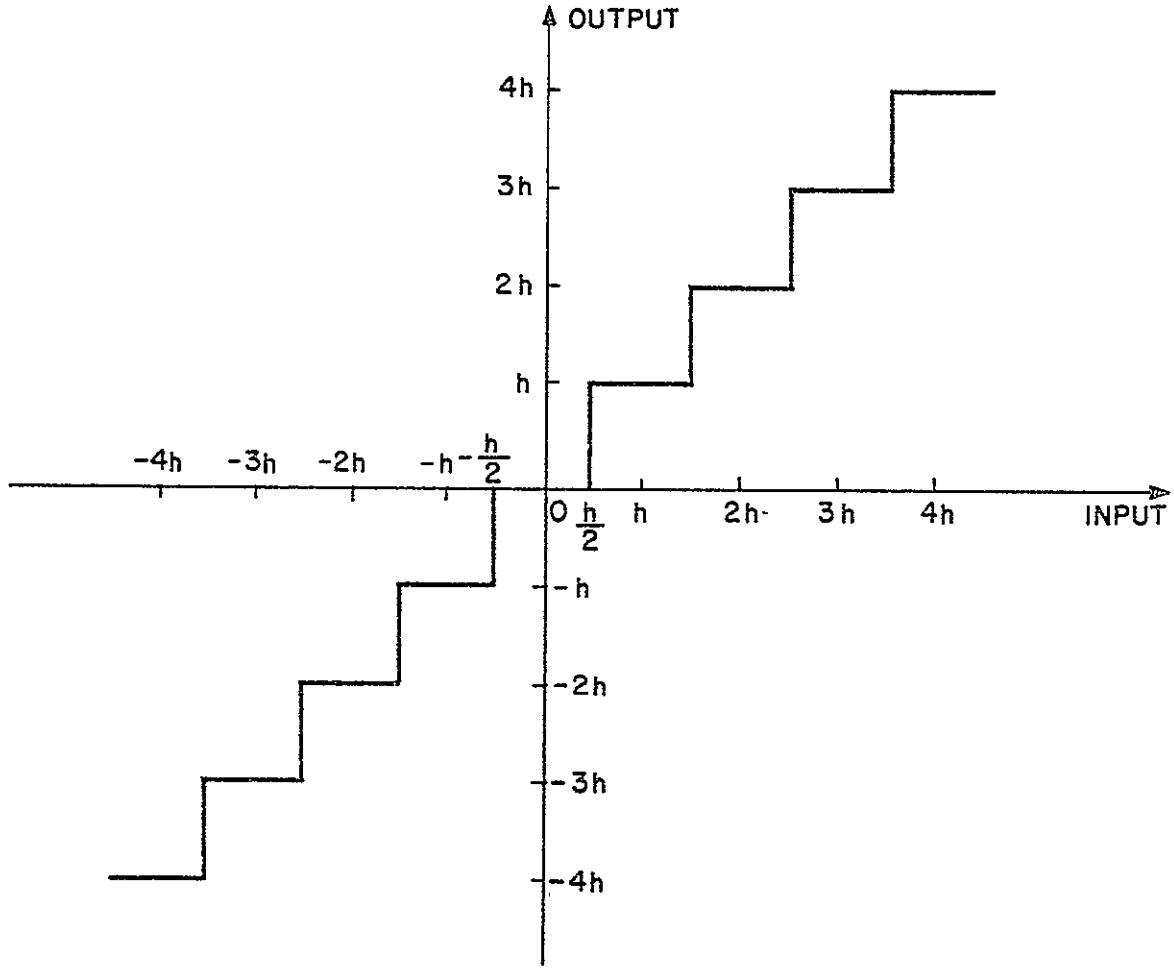

Figure 1-12. Input-output characteristics of a quantizer.

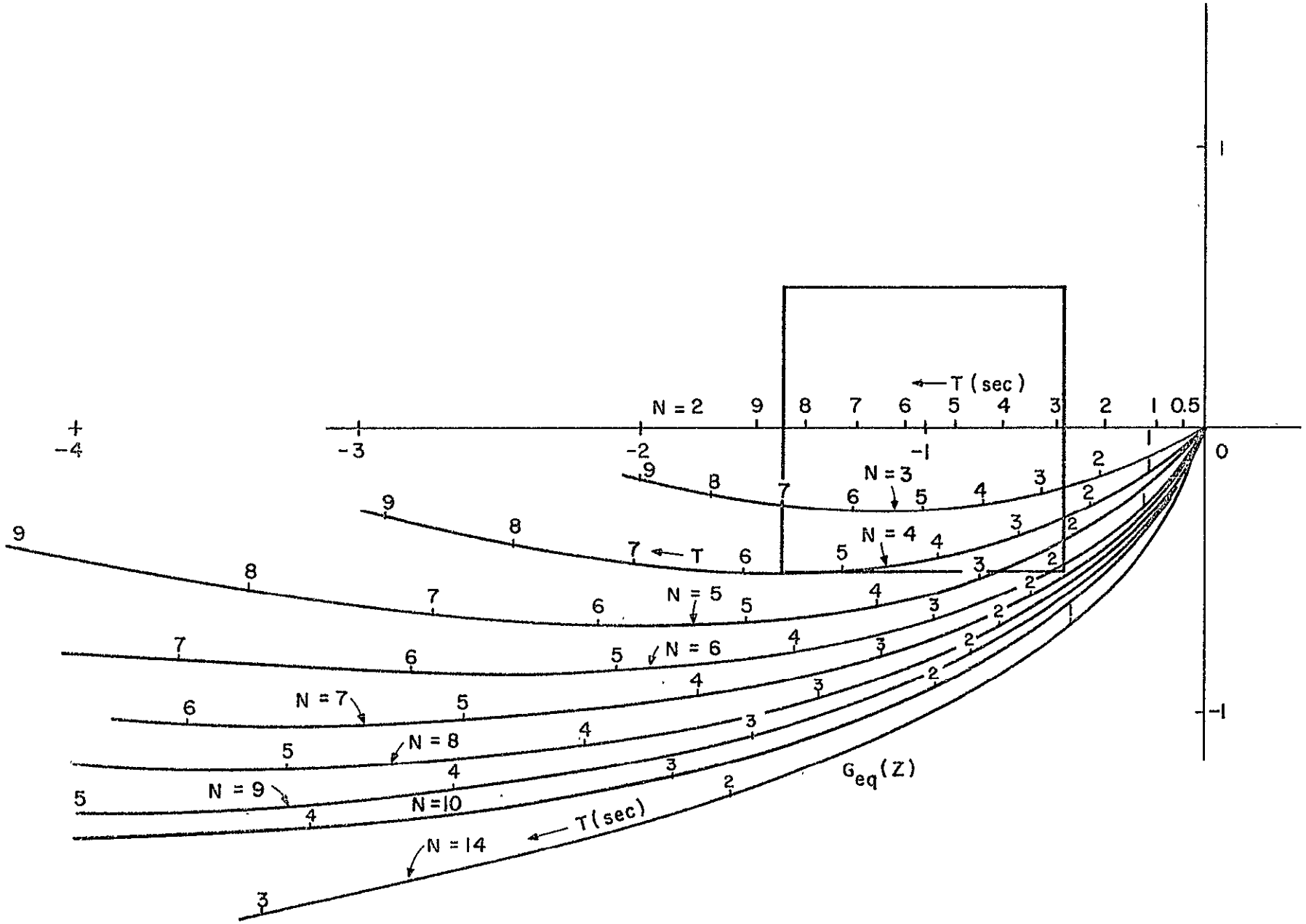

Figure 1-13. $G_{eq}(z)$ plots and critical region bounds of quantizer discrete describing function of ASPS payload z_1 dynamics; K_s = 0.35 N/m.

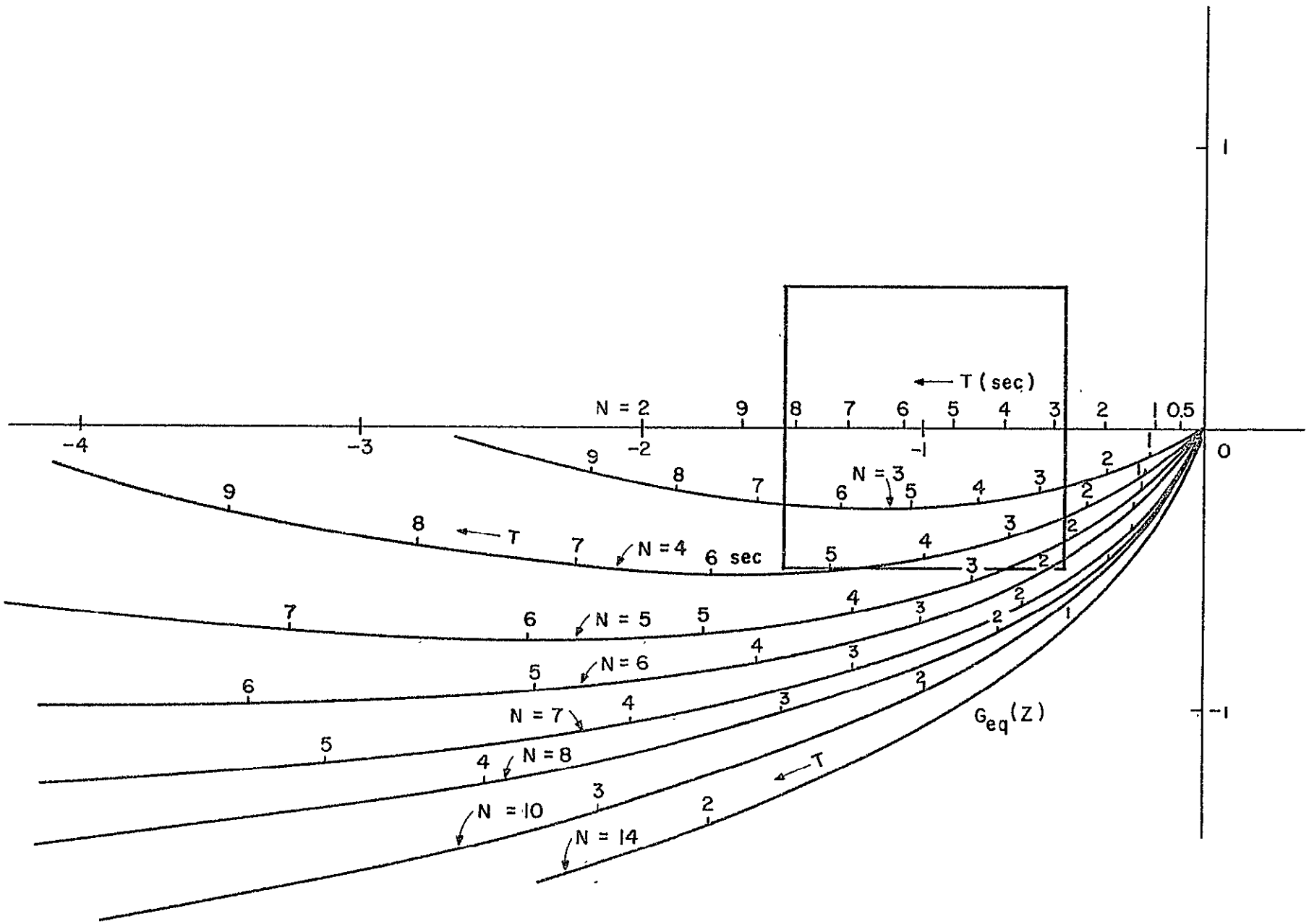

Figure 1-14. $G_{eq}(z)$ plots and critical region bounds of quantizer discrete describing function of ASPS payload z_1 dynamics; K_s = 3.5 N/m.

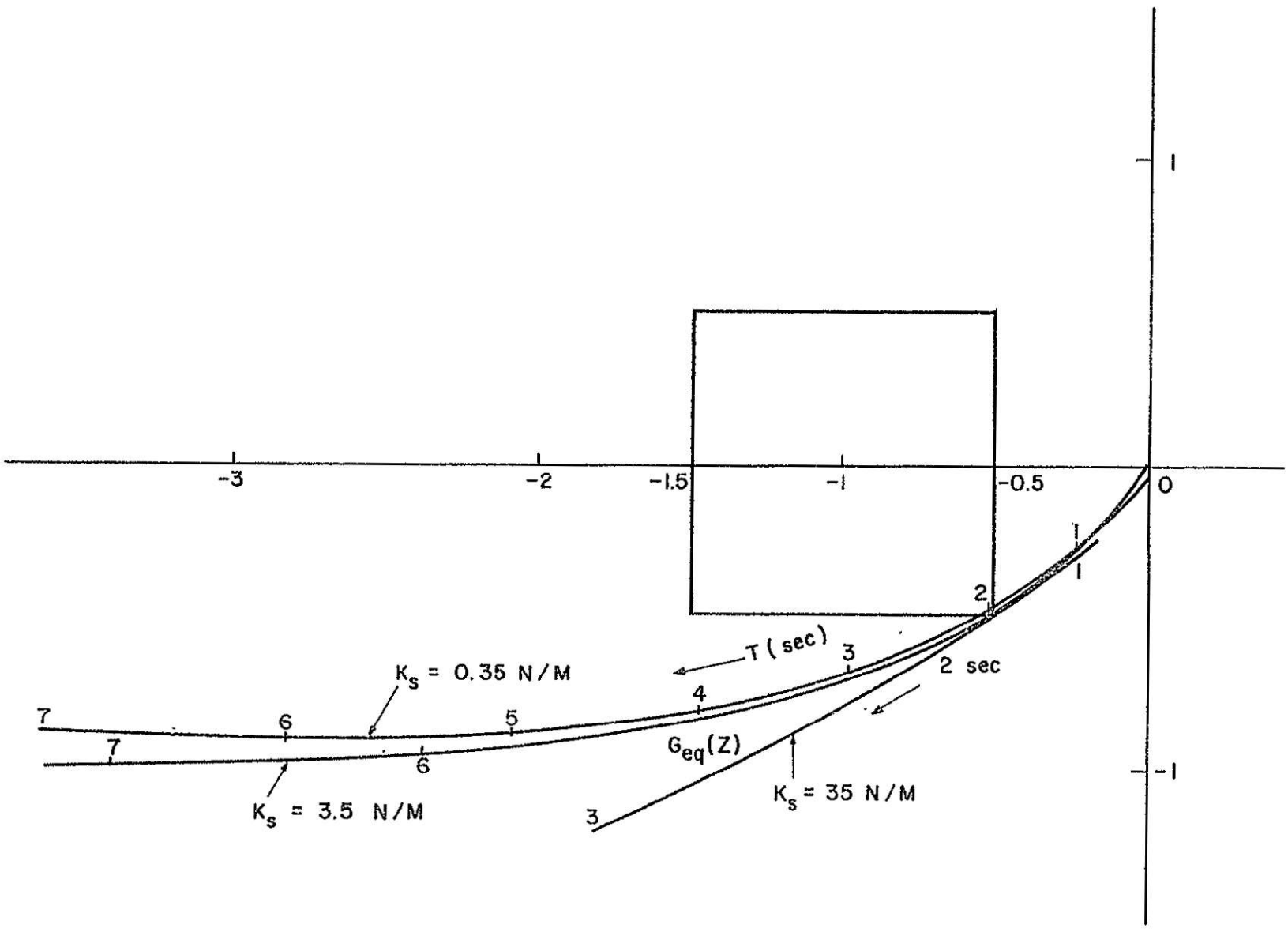

Figure 1-15. $G_{eq}(z)$ plots for N = 6 and K_s = 0.35, 3.5 and 35 N/m and critical region bounds of quantizer discrete describing function of ASPS payload z_1 dynamics.

The z-transform of the last equation is evaluated using the results in Eqs. (1-41) and (1-42). Equation (1-45) becomes

$$\Delta(z) = 1 + Q(z)G_{eq}(z) = 0 \qquad (1\text{-}46)$$

where

$$G_{eq}(z) = \frac{\left(\frac{K_r}{\sqrt{M_i K_s}}\sin\sqrt{\frac{K_s}{M_i}}\,T - \frac{K_p}{K_s}\cos\sqrt{\frac{K_s}{M_i}}\,T + \frac{K_p}{K_s}\right)z - \frac{K_r}{\sqrt{M_i K_s}}\sin\sqrt{\frac{K_s}{M_i}}\,T - \frac{K_p}{K_s}\cos\sqrt{\frac{K_s}{M_i}}\,T + \frac{K_p}{K_s}}{z^2 - 2z\cos\sqrt{\frac{K_s}{M_i}}\,T + 1} \qquad (1\text{-}47)$$

For $K_p = 37.861$, $K_r = 211.01$, $M_i = 600$, and $K_s = 0.35$, the last equation is simplified to

$$G_{eq}(z) = \frac{14.5597\sin 0.02415T - 108.1688\cos 0.02415T + 108.1688)z - 14.5597\sin 0.02415T}{z^2 - 2z\cos 0.02415T + 1} \qquad (1\text{-}48)$$

$$\underline{\qquad -108.1688\cos 0.02415T + 108.1688}$$

Figure 1-13 shows the plots of $G_{eq}(z)$ for various periods of sustained oscillations $T_c = NT$, $N = 2,3,4,\ldots$. The sampling period T varies along the curves. The square block in the figure which is centered at -1 represents the bounds on the critical regions of $-1/Q(z)$ [4] . Theoretically, the intersects between the critical regions of $-1/Q(z)$ and $G_{eq}(z)$ represent conditions of self-sustained oscillations. It is clear from Fig. 1-13 that the system should be free from sustained oscillations for all sampling periods less than 2 seconds.

Figure 1-14 illustrates the $G_{eq}(z)$ plots for $K_s = 3.5$ N/m, 10 times the nominal value. As pointed out earlier, since the mass of the payload is so large, the light spring effect of the wire cable does not materially affect the performance of the system. Figure 1-15 further illustrates that even with $K_s = 35$ N/m, 100 times the nominal value, the characteristics of the system for sampling periods less than 2 seconds are not significantly affected.

The least-upper bound error analysis of the quantization effect is performed by referring to the system block diagram shown in Fig. 1-16. The quantizer is

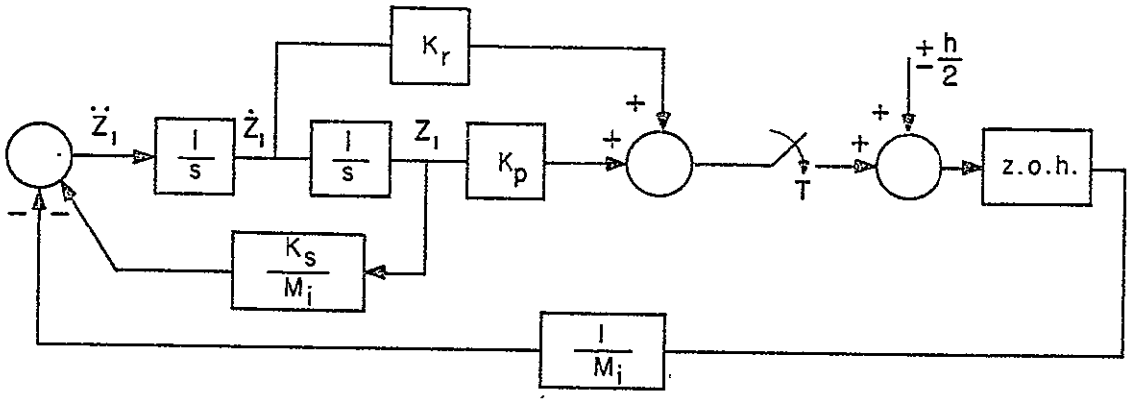

Figure 1-16. Block diagram of the digital ASPS payload z_1 dynamics for the least-upper bound analysis of quantization effects.

```
      DIMENSION PRMT(5),Y(2),DERY(2),AUX(8,2)
      EXTERNAL FCT,OUTP
      COMMON Z,ZDOT,T,AKSMI,AMINV,V1,TPRT,TEND,PRTIME,V1Z,V1H
      COMMON AMI,AKZ,AKP,AKR,TCP,H,AV1H,IV1H,V1H0

      ALL TIME INPUTS SHOULD BE INTEGRAL MULTIPLES OF TINT.

      H=2.**-4
      TCP=1.
      TEND=400.
      TPRT=0.5
      TINT=0.5E-3
      Z0=0.002
      ZDOT0=0.
      ERROR=1.E-5
      AMI=600.
      AKS=0.35
      AKP=37.861
      AKR=211.01
      AKSMI=AKS/AMI
      AMINV=1./AMI
      T=0.
```


Figure 1-17. Computer program of the simulation of the ASPS payload z_1 dynamics with quantization.

```
      PRTIME=-TPRT
      PRMT(1)=T
      PRMT(2)=TEND
      PRMT(3)=TINT
      PRMT(4)=EPROR
      DERY(1)=0.5
      DERY(2)=0.5
      NDIM=2
      Y(1)=Z0
      Y(2)=ZDOT0
      CALL RKGS(PRMT,Y,DERY,NDIM,IHLF,FCT,OUTP,AUX)
      END
      SUBROUTINE FCT(TIME,Y,DERY)
      DIMENSION Y(2),DERY(2)
      COMMON Z,ZDOT,T,AKSMI,AMINV,V1,TPRT,TEND,PRTIME,V1S,V1H,
      COMMON AMI,AKS,AKP,AKR,TSP,H,AV1H,IV1H,V1H0
      Z=Y(1)
      ZDOT=Y(2)
      V1=AKP*Z+AKR*ZDOT
      IF(TIME-T)40,50,50
50    T=T+TSP
      V1S=V1
40    V1H=V1S
      IF(V1H.LT.0)GO TO 20
      AV1H=(V1H/H)+0.5
      GO TO 30
20    AV1H=(V1H/H)-0.5
30    CONTINUE
      IV1H=IFIX(AV1H)
      V1H0=FLOAT(IV1H)*H
      Z2DOT=-AKSMI*Z-AMINV*V1H0
      DERY(1)=ZDOT
      DERY(2)=Z2DOT
      RETURN
      END
      SUBROUTINE OUTP(TIME,Y,DERY,IHLF,NDIM,PRMT)
      DIMENSION Y(2),DERY(2),PRMT(5)
      COMMON Z,ZDOT,T,AKSMI,AMINV,V1,TPRT,TEND,PRTIME,V1S,V1H
      COMMON AMI,AKS,AKP,AKR,TSP,H,AV1H,IV1H,V1H0
      IF((TIME-PRTIME).LT.TPRT)RETURN
      PRTIME=PRTIME+TPRT
      WRITE(5,100) TIME,V1,V1H,V1H0,(Y(I),I=1,2),IHLF
100   FORMAT(1X,F5.2,1X,E12.5,1X,E12.5,1X,E12.5,1X,2(1X,E12.5),1X,I2)
      RETURN
      END
```

Figure I-17. Computer program of the simulation of the ASPS payload z_1 dynamics with quantization.

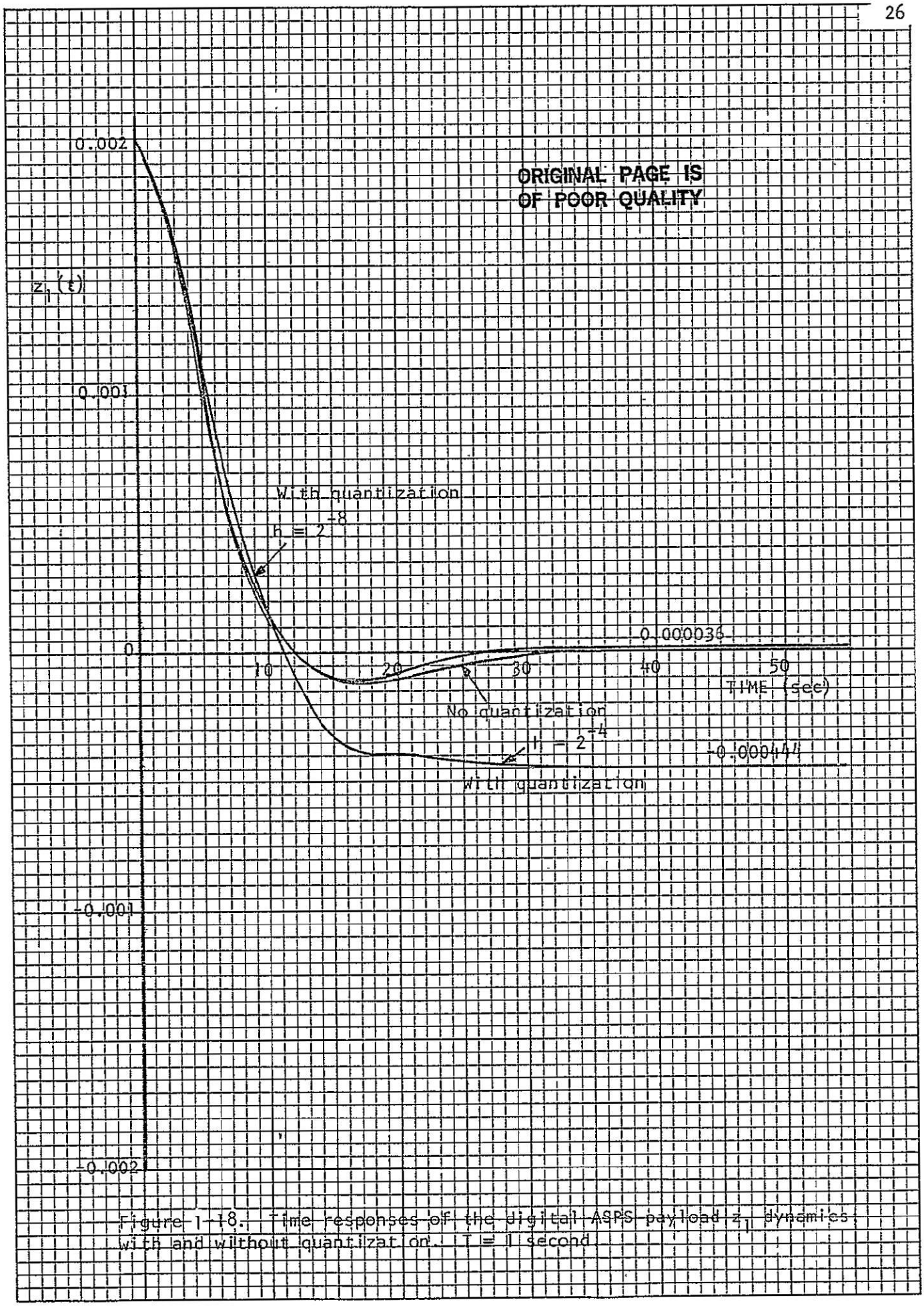

Figure 1-18. Time responses of the digital ASPS payload z_1 dynamics with and without quantization. $T = 1$ second

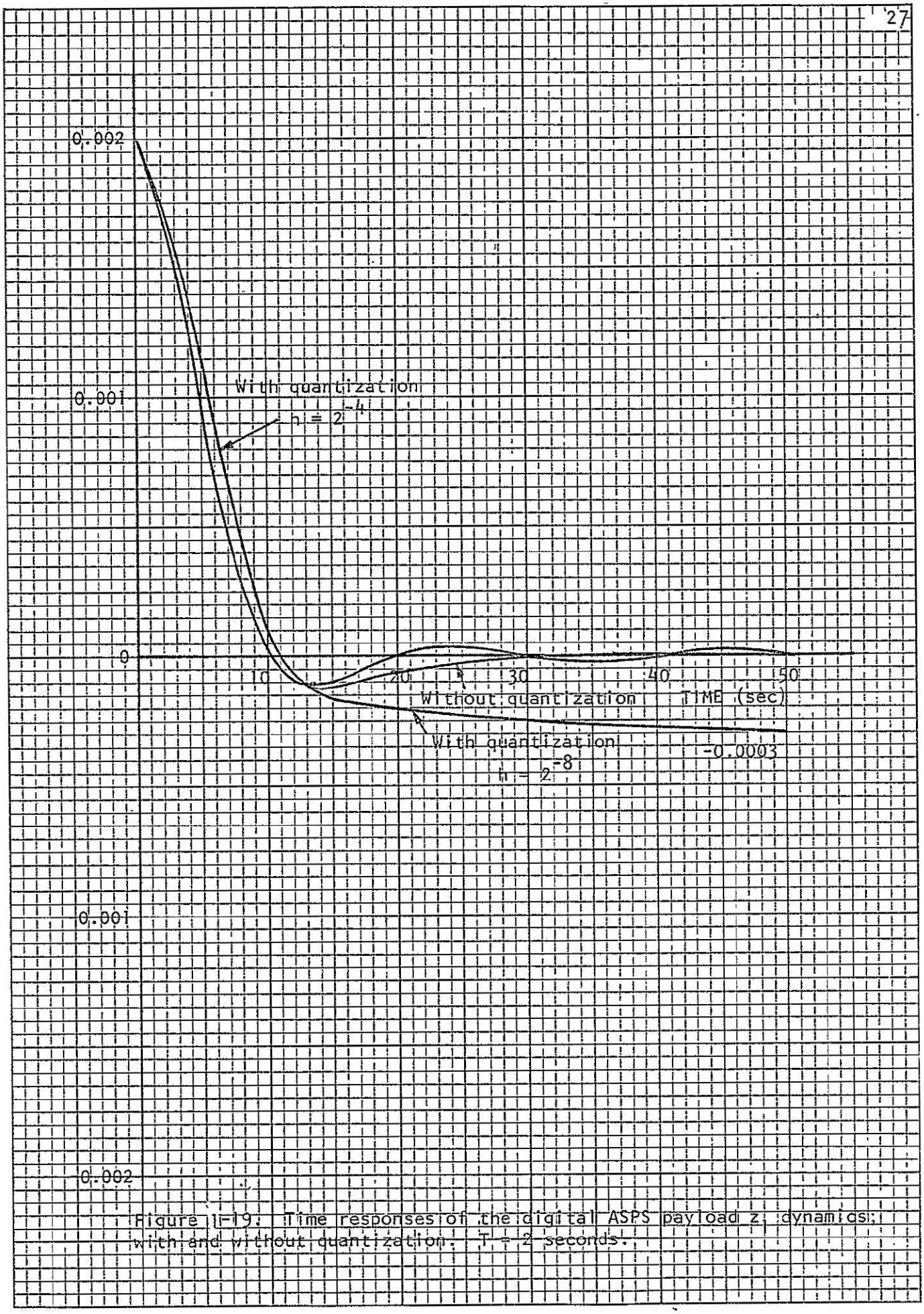

Figure II-19. Time responses of the digital ASPS payload z dynamics with and without quantization. T = 2 seconds.

replaced by the noise input with an amplitude of $\pm h/2$.

The z-transform of the displacement z_1 due to the noise input is

$$Z_1(z) = \frac{(1 - z^{-1})}{\Delta(z)} \mathcal{Z}\left[\frac{1}{M_i s^3(1 + K_s s^{-2}/M_i)}\right] (\pm h/2)\frac{z}{z - 1} \tag{1-49}$$

where $\Delta(z)$ is as given in Eq. (1-40).

In Eq. (1-49),

$$(1 - z^{-1})\mathcal{Z}\left[\frac{1}{M_i s^3(1 + K_s s^{-2}/M_i)}\right] = (1 - z^{-1})\mathcal{Z}\left[\frac{1}{M_i s(s^2 + K_s/M_i)}\right]$$

$$= \frac{1}{K_s} \frac{(z + 1)(1 - \cos\sqrt{K_s/M_i}\, T)}{z^2 - 2z\cos\sqrt{K_s/M_i}\, T + 1} \tag{1-50}$$

Thus,

$$Z_1(z) = \frac{\frac{1}{K_s}(z + 1)(1 - \cos\sqrt{K_s/M_i}\, T)(\frac{\pm h}{2})(\frac{z}{z - 1})}{z^2 + \left(\frac{K_r}{\sqrt{M_i K_s}} \sin\sqrt{\frac{K_s}{M_i}}\, T - \frac{K_p}{K_s}\cos\sqrt{\frac{K_s}{M_i}}\, T + \frac{K_p}{K_s} - 2\cos\sqrt{\frac{K_s}{M_i}}\, T\right) z + 1 + \frac{K_p}{K_s}} \tag{1-51}$$

$$- \frac{K_p}{K_s}\cos\sqrt{\frac{K_s}{M_i}}\, T - \frac{K_r}{\sqrt{M_i K_s}} \sin\sqrt{\frac{K_s}{M_i}}\, T$$

The final steady-state value of $z_1(kT)$ is given by

$$\lim_{k\to\infty} z_1(kT) = \lim_{z=1} (1 - z^{-1})$$

$$= \frac{\frac{2}{K_s}(1 - \cos\frac{K_s}{M_i} T)(\pm \frac{h}{2})}{2(1 + \frac{K_p}{K_s})(1 - \cos\frac{K_s}{M_i} T)} = \frac{\pm \frac{h}{2}}{K_s + K_p} \tag{1-52}$$

This result shows that the least-upper bound on the steady-state value of $z_1(kT)$ due to quantization is inversely proportional to K_s and K_p.

For the given values of K_s and K_p, we have

$$\lim_{k\to\infty} z_1(kT) = \frac{\pm\frac{h}{2}}{38.211} = \pm\, 0.013085237h \qquad (1\text{-}53)$$

Thus, for a quantization level of 2^{-4}, the final error in z_1 is ± 0.000817827 m, whereas it is ± 0.000051114 m for a quantization level of 2^{-8}.

1.4 Computer Simulation of the ASPS Payload $\dot{z}_1$ Dynamics with Quantization

In this section the z_1 dynamics of the ASPS payload are simulated to study the effects of quantization. The computer program is given in Fig. 1-17.

Figure 1-18 illustrates the time responses of $z_1(t)$ of the ASPS payload with and without quantization, for the sampling period of T = 1 second. The initial value of $z_1(t)$ was chosen to be 0.002 m. As predicted by the discrete describing function analysis, the system does not exhibit any sustained oscillations when T = 1 sec. However, the nonzero quantization levels did produce steady-state errors in $z_1(t)$. The computer simulated results and the results obtained by the least-upper bound method are tabulated below for comparison. It is expected that the errors predicted by the least-upper bound method will be greater, since it is a worst-case study.

Sampling Period T = 1 sec

Quantization level h (m)	$z_1(\infty)$ least-upper bound (m)	$z_1(\infty)$ simulation (m)
2^{-4}	$\pm$ 0.0008178	-0.000444
2^{-8}	$\pm$ 0.000051114	0.000036

Figure 1-18 also shows that with the quantization level of 2^{-8} (8 bits), the time response of $z_1(t)$ is very close to that of $z_1(t)$ without quantization, so that a larger word length seems unnecessary unless a smaller steady-state error is required.

Figure 1-19 illustrates the time responses of $z_1(t)$ for T = 2 sec. For $h = 2^{-4}$, the error is -0.0003 at t = 50 sec and still increasing. For $h = 2^{-8}$,

the response actually exhibited a sustained oscillation with a peak-to-peak amplitude of 0.000066 m. As shown in Fig. 1-13, when T = 2 sec, the system is marginal in generating sustained oscillations. It should be noted that the digital computer is not the most suitable for simulating digital systems with quantizers, since the computer itself is a digital system with its own quantization levels. However, the results obtained here are conclusive enough to indicate the quantization effects in the ASPS payload, and are useful in the selection of the sampling period and the quantization level.

For sampling periods greater than 2 seconds, the computer simulation results showed that sustained oscillations always existed.

1.5 Nonlinear Spring Effect of Wire Cable on the ASPS Payload z_1 Dynamics

In the preceding sections the wire cable attached to the ASPS payload was modelled as a linear spring with a spring constant of K_s. In the z_1 direction the spring constant K_s is given as 0.35 N/m. It was shown in the last section that since the mass of the payload is so large (600 Kg), the light spring effect of the wire cable will not have a significant effect on the dynamics of the payload. This would be true whether the wire cable is modelled as a linear spring or a nonlinear spring.

The block diagram of the digital ASPS payload z_1 dynamics with the nonlinear wire cable spring characteristic is shown in Fig. 1-20. As shown in Fig. 1-20, the nonlinear spring characteristic is defined by the parameters K_s and h_{wf}.

The simulation program for the system is given in Fig. 1-21. Figures 1-22 through 1-24 show the time responses of z_1 with the initial consition $z_1(0) = 0.002$ m and under the following three conditions:

(a) linear spring, $K_s = 0.35$ N/m

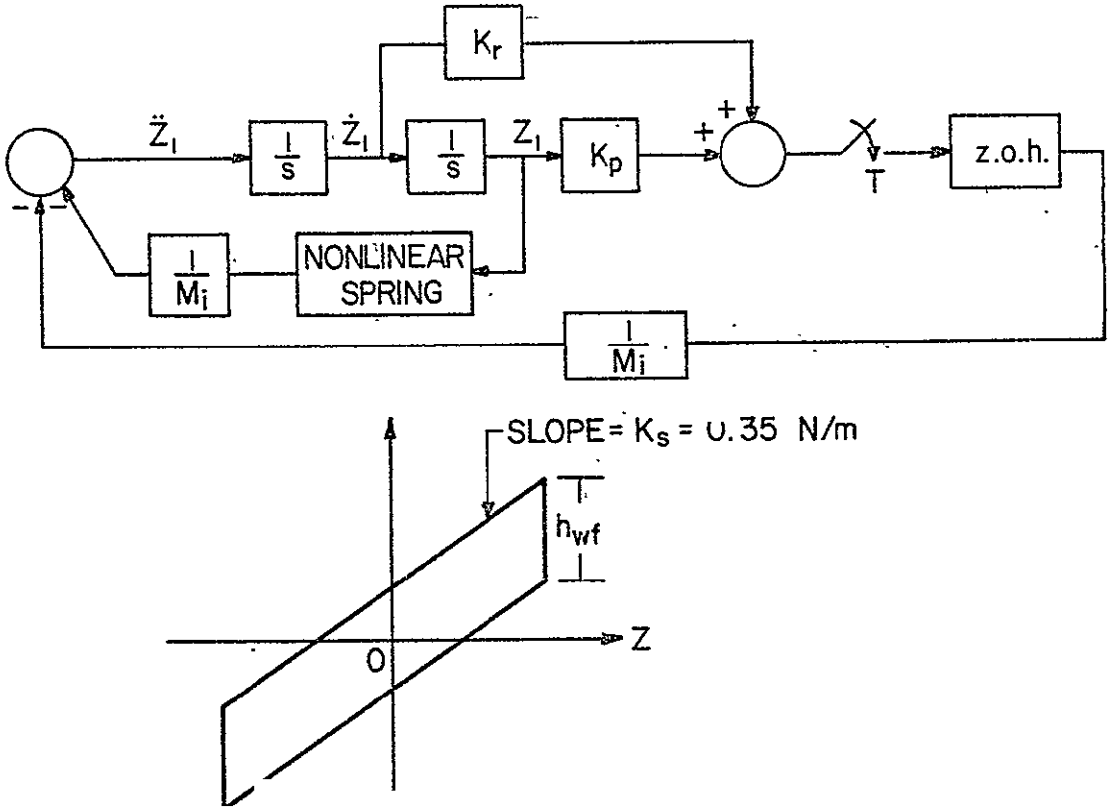

Figure 1-20. Block diagram of the digital ASPS payload z_1 dynamics with nonlinear wire cable characteristic.

(b) nonlinear spring, K_s = 0.35 N/m, h_{wf} = 0.00014 N

(c) nonlinear spring, K_s = 0.35 N/m, h_{wf} = 0.00028 N.

Figure 1-22 shows that for the scale chosen for z_1 in that figure, the time responses of all the three cases are nearly identical. Figure -23 shows the three responses between t = 10 sec and t = 100 sec with the z_1 scale expanded. Figure j-24 shows the three responses between t = 25 sec and t = 100 sec with an even more expanded scale for z_1. Note that the use of the nonlinear spring model for the wire cable creates a nonzero steady-state

```
 TYPE RSIM.F4
       DIMENSION PRMT(5),Y(2),DERY(2),AUX(8,2)
       EXTERNAL FCT,OUTP
       COMMON Z,ZDOT,T,AKSMI,AMINV,V1,TPRT,TEND,AKS,AMI,NPRT,IV1
C
C      ALL TIME INPUTS SHOULD BE INTEGRAL MULTIPLES OF TINT.
C
       OPEN(UNIT=6,DEVICE='DSK',FILE='FOR06.DAT',ACCESS='SEQOUT')
       TSP=2.
       H=2.**-10
       TEND=100.
       TPRT=0.5
       TINT=1.E-2
       ZO=0.002
       ZDOTO=0.
       AMI=600.
       AKS=0.35
       AKP=37.861
       AKR=211.01
       AKSMI=AKS/AMI
       AMINV=1./AMI
       Z=ZO
       ZDOT=ZDOTO
       T=0.
       NPRT=0
       PRMT(3)=TINT
       PRMT(4)=0.001*ZO
       DERY(1)=0.5
       DERY(2)=0.5
       NDIM=2
10     IF(T.GE.TEND) CALL EXIT
       V1=AKP*Z+AKR*ZDOT
       PRMT(1)=T
       PRMT(2)=T+TSP
       Y(1)=Z
       Y(2)=ZDOT
       CALL RKGS(PRMT,Y,DERY,NDIM,IHLF,FCT,OUTP,AUX)
       GO TO 10
       END
       SUBROUTINE FCT(X,Y,DERY)
       DIMENSION Y(2),DERY(2)
       COMMON Z,ZDOT,T,AKSMI,AMINV,V1,TPRT,TEND,AKS,AMI,NPRT,IV1
       DERY(1)=Y(2)
       DERY(2)=-FORCE(Y(1),Y(2))-AMINV*V1
       RETURN
       END
       SUBROUTINE OUTP(X,Y,DERY,IHLF,NDIM,PRMT)
       DIMENSION Y(2),DERY(2),PRMT(5)
       COMMON Z,ZDOT,T,AKSMI,AMINV,V1,TPRT,TEND,AKS,AMI,NPRT,IV1
       IF(X.GT.TEND) PRMT(5)=1.
       T=X
       IF(X.LT.TPRT*FLOAT(NPRT)) RETURN
       WRITE(6,100) IHLF,X,V1,(Y(I),I=1,2)
100    FORMAT(1X,I2,3X,1PE10.4,1P3E11.3)
       Z=Y(1)
       ZDOT=Y(2)
       NPRT=NPRT+1
       RETURN
       END
       FUNCTION FORCE(X,XDOT)
       COMMON Z,ZDOT,T,AKSMI,AMINV,V1,TPRT,TEND,AKS,AMI,NPRT,IV1
       HWF=0.00028
       IF(XDOT)1,2,3
1      FORCE = (AKS*X-HWF/2.)/AMI
       GO TO 4
2      FORCE = AKSMI*X
       GO TO 4
3      FORCE = (AKS*X+HWF/2.)/AMI
4      RETURN
       END
```

ORIGINAL PAGE IS
OF POOR QUALITY

Figure 7-21. Computer simulation program of the ASPS payload z_1 dynamics with nonlinear wire cable characteristic.

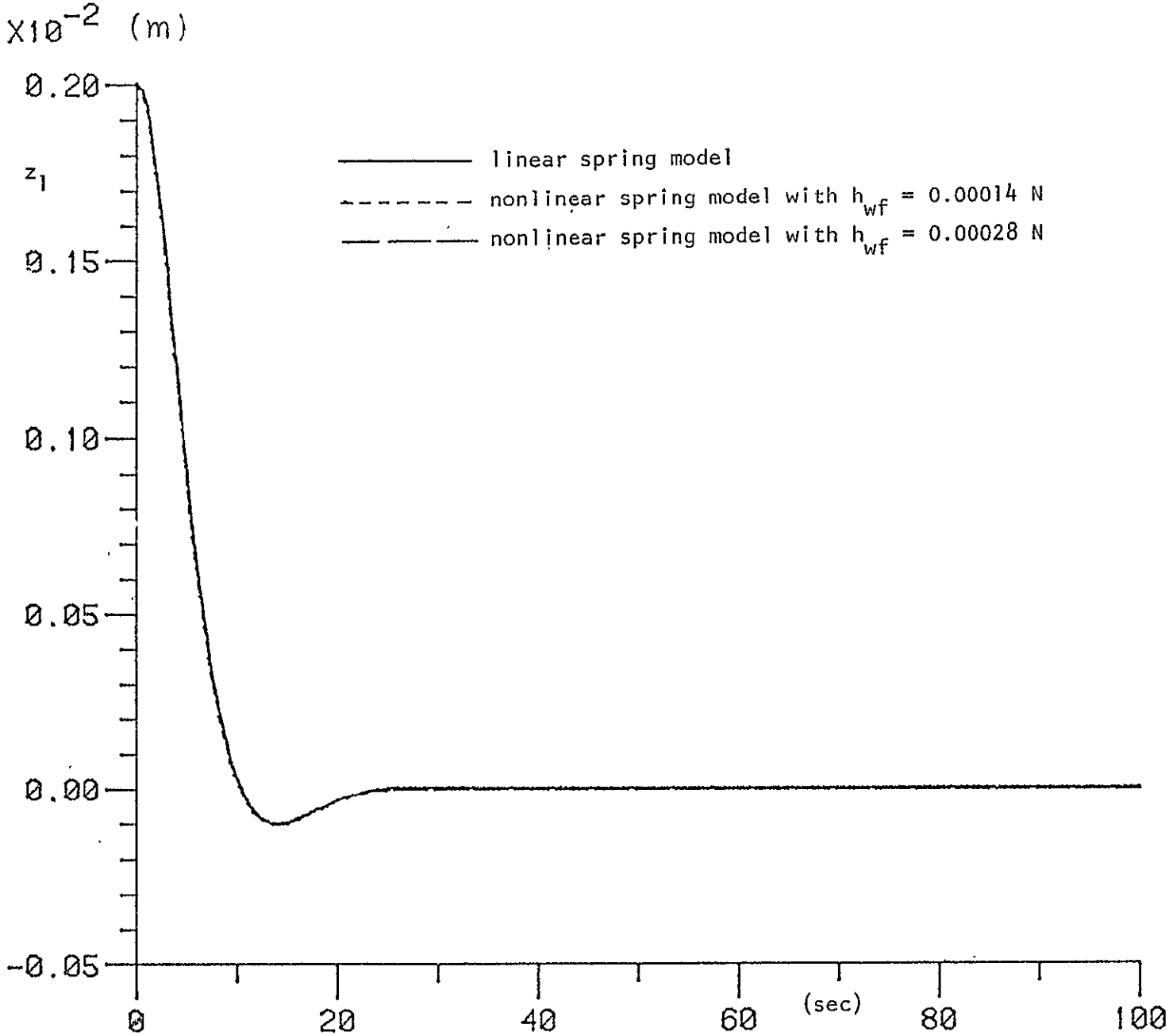

Figure 1-22. Time responses of the digital ASPS payload z_1 dynamics with nonlinear wire cable characteristic.

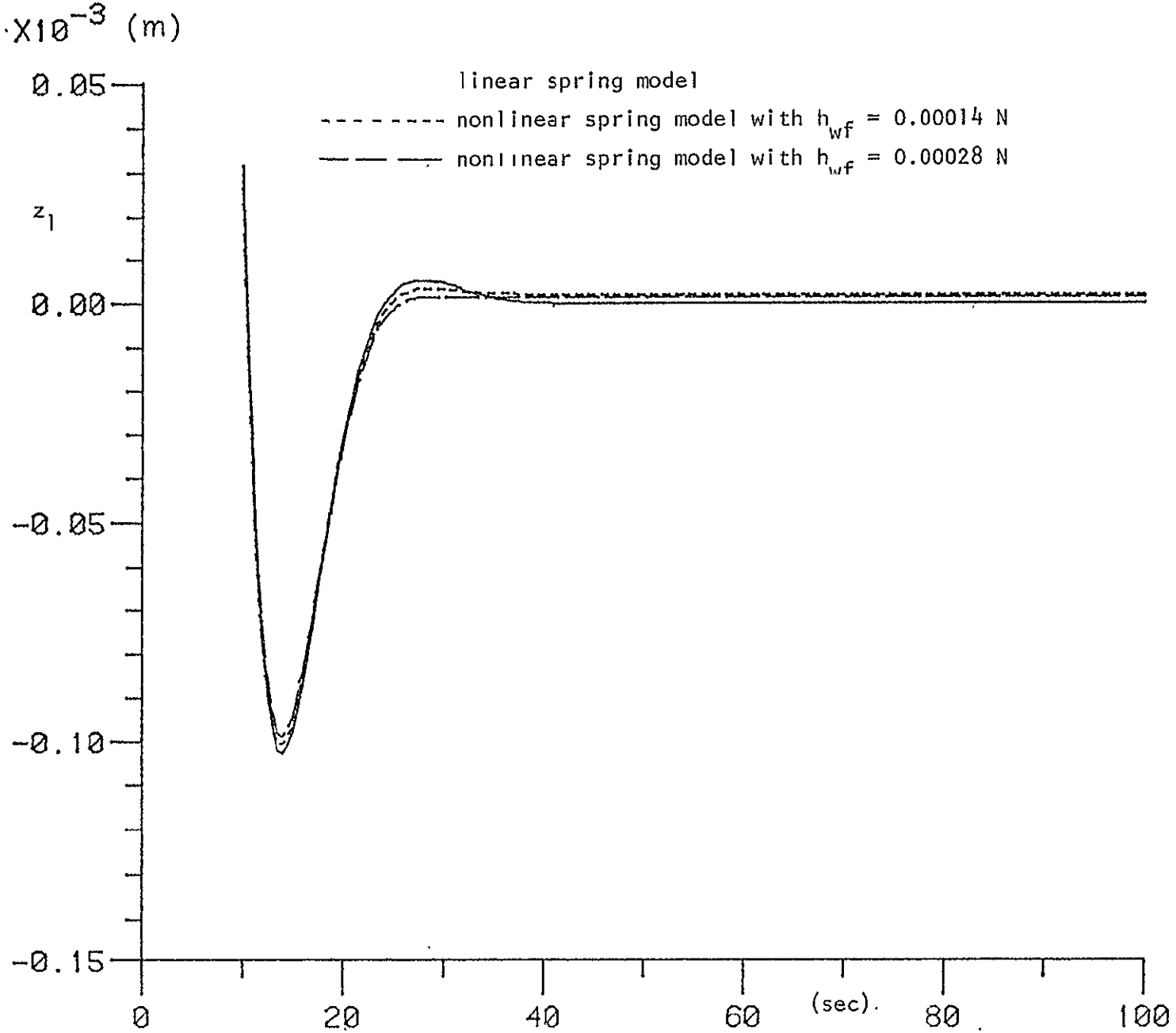

Figure 1-23. Time responses of the digital ASPS payload z_1 dynamics with nonlinear wire cable characteristic.

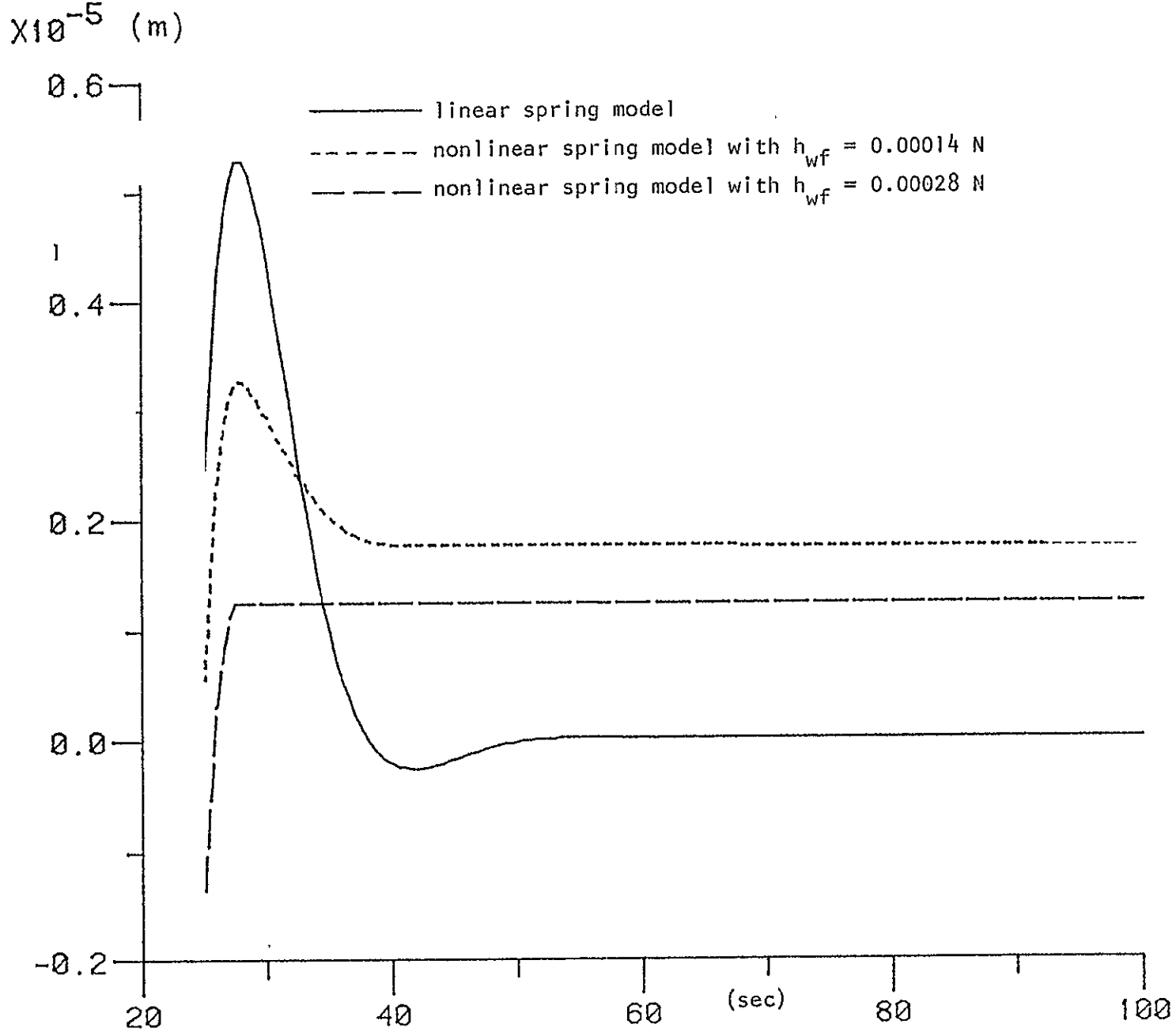

Figure 1-24. Time responses of the digital ASPS payload z_1 dynamics with nonlinear wire cable characteristic.

error for z_1. With h_{wf} =.0.00014 N the steady-state error is 0.18×10^{-5} m, and with h_{wf} = 0.00028 N the steady-state error is 0.12×10^{-5} m. Since these errors are extremely small, it may be concluded again that the wire cable effect on the ASPS payload may be neglected whether a linear or a nonlinear spring model is used.

II. CONTROLLER DESIGN FOR THE ANNULAR SUSPENSION AND POINTING SYSTEM (ASPS)

2.1 Introduction

In the preceding chapter the equations of motion of the ASPS with respect to the planar models of Figs. 1-4 and 1-5 have been derived. The Lagrange equations of the planar ASPS model 2 shown in Fig. 1-5 have been selected for analysis and design of the system. These equations are repeated as follows:

$$\begin{bmatrix} M_i & 0 & -M_i r_b & 0 \\ 0 & M_i & 0 & 0 \\ -M_i r_b & 0 & J_m+J_i+M_m L_a^2+M_i r_b^2 & J_i \\ 0 & 0 & J_i & J_i \end{bmatrix} \begin{bmatrix} \ddot{x}_1 \\ \ddot{z}_1 \\ \ddot{\phi}_1 \\ \ddot{\phi}_2 \end{bmatrix} = \begin{bmatrix} f_1 - f_4 + f_{sx}(x_1) \\ f_2 + f_3 + f_{sz}(z_1) \\ T_c(\phi_1) + T_p(\phi_1) \\ (f_3 - f_2)L + (f_1 - f_4)L_b + T_s(\phi_2) \end{bmatrix} \tag{2-1}$$

The last equation shows that the z_1 dynamics of the payload are decoupled from the other three degrees of freedom. The z_1 dynamics have been thoroughly studied in Chapter 1, and both the analog and the digital controllers have been designed. The main objective of this chapter is to study the dynamics related to the x_1, ϕ_1 and ϕ_2 axes which are coupled.

In the ensueing sections an analog controller for the control of the x_1, ϕ_1 and ϕ_2 dynamics is designed by pole-placement techniques.

2.2 Analytical Model of the x_1, ϕ_1 and ϕ_2 Axes

After eliminating the z_1 dynamics, Eq. (2-1) is reduced to the following form:

$$\begin{aligned} \ddot{x}_1 &= a\ddot{\phi}_1 + b\left((f_1 - f_4) + f_{sx}(x_1)\right) \\ \ddot{\phi}_1 &= c\ddot{x}_1 - d\ddot{\phi}_2 + e\left(T_c(\phi_1) + T_p(\phi_1)\right) \\ \ddot{\phi}_2 &= -\ddot{\phi}_1 + f\left((f_3 - f_2)L + (f_1 - f_4)L_b + T_s(\phi_2)\right) \end{aligned} \tag{2-2}$$

where

$$a = r_b = 1.956$$

$$b = 1/M_i = 0.00167$$

$$c = \frac{M_i r_b}{J_m + J_i + M_m L_a^2 + M_i r_b^2} = 0.4184$$

$$d = \frac{J_i}{J_m + J_i + M_m L_a^2 + M_i r_b^2} = 0.1793$$

$$e = \frac{1}{J_m + J_i + M_m L_a^2 + M_i r_b^2} = 0.000356$$

$$f = 1/J_i = 0.001988$$

In Eq. (2-2) $f_{sx}(x_1)$ denotes the linear spring force due to the wire cable attached to the payload.

For linear analysis, $f_{sx}(x_1)$ is assumed to be directly proportional to x_1; i.e.,

$$f_{sx}(x_1) = -K_s x_1 \tag{2-3}$$

where $K_s = 1.051$ N/m.

Similarly, $T_s(\phi_2)$ denotes the equivalent spring torque due to the wire cable attached to the payload, and $T_p(\phi_1)$ denotes the spring torque due to the wire cable attached to the pallet. Thus,

$$T_s(\phi_2) = -K_{s2}\phi_2 \tag{2-4}$$

$$T_p(\phi_1) = -K_{s1}\phi_1 \tag{2-5}$$

where $K_{s1} = K_{s2} = 0.005$ N/m.

Figure 2-1 shows a block diagram of the ASPS dynamics of the x_1, ϕ_1 and ϕ_2 axes as modelled by Eq. (2-2). Note that the linear system is of the sixth order with three inputs. The input eT_c denotes the torque which is applied to the pallet by the gimbal assembly. The input $f_1 - f_4$ represents the net magnetic forces applied at the base of the payload by the magnetic actuator assembly, and the input $fL(f_3 - f_2)$ denotes similar magnetic forces due to the

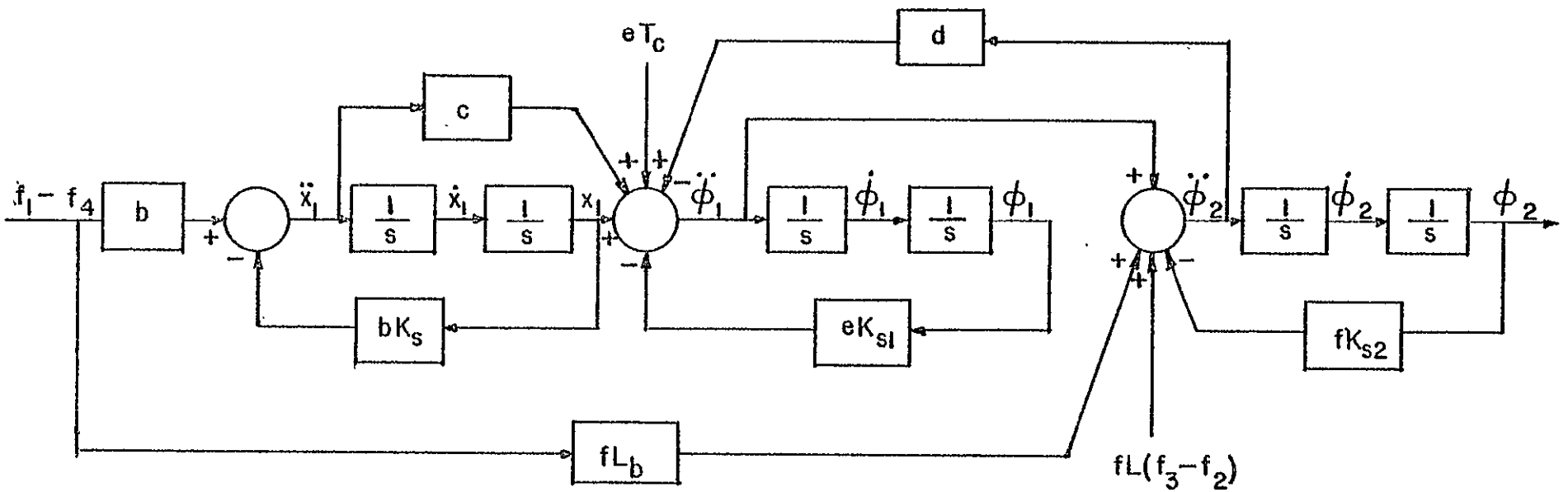

Figure 2-1. Block diagram of the x_1, ϕ_1, ϕ_2 dynamics of the ASPS.

magnetic actuator assembly.

2.3 Design of An Analog Controller For the ASPS By Pole Placement

In this section we shall design an analog controller for the ASPS to control the dynamics of the x_1, ϕ_1, and ϕ_2 axes. As shown in Fig. 2-1 there are three inputs that can be used through the magnetic actuator assembly forces and the gimbal torque to control the attitudes of x_1, ϕ_1 and ϕ_2.

Let us assume that the controls of the x_1, ϕ_1 and ϕ_2 dynamics of the ASPS can be achieved through state feedback. Specifically, we construct the three inputs as follows:

$$f_1 - f_4 = -K_p x_1 - K_r \dot{x}_1 \tag{2-6}$$

$$T_c = -K_1 \int \phi_1 dt - K_2 \phi_2 - K_3 \dot{\phi}_1 \tag{2-7}$$

$$(f_3 - f_2)L + (f_1 - f_4)L_b = -K_4 \int \phi_2 dt - K_5 \phi_2 - K_6 \dot{\phi}_2 \tag{2-8}$$

where K_p, K_r, K_1, K_2, K_3, K_4, K_5 and K_6 are constant gains whose values are to be determined.

The block diagram of the ASPS with state-variable feedbacks as defined in Eqs. (2-6), (2-7) and (2-8) is shown in Fig. 2-2.

In order to evaluate the characteristic equation of the closed-loop ASPS we represent the block diagram of Fig. 2-2 by the simplified signal flow graph in Fig. 2-3.

The branch gains a, c and d in Fig. 2-3 have been defined previously. The loop gains used in Fig. 2-3 are defined as

$$\Delta_1 = -b\left(K_r s^{-1} + (K_p + K_s)s^{-2}\right) \tag{2-9}$$

$$\Delta_2 = -e\left(K_3 s^{-1} + (K_2 + K_{s1})s^{-2} + K_1 s^{-3}\right) \tag{2-10}$$

$$\Delta_3 = -f\left(K_6 s^{-1} + (K_5 + K_{s2})s^{-2} + K_4 s^{-3}\right) \tag{2-11}$$

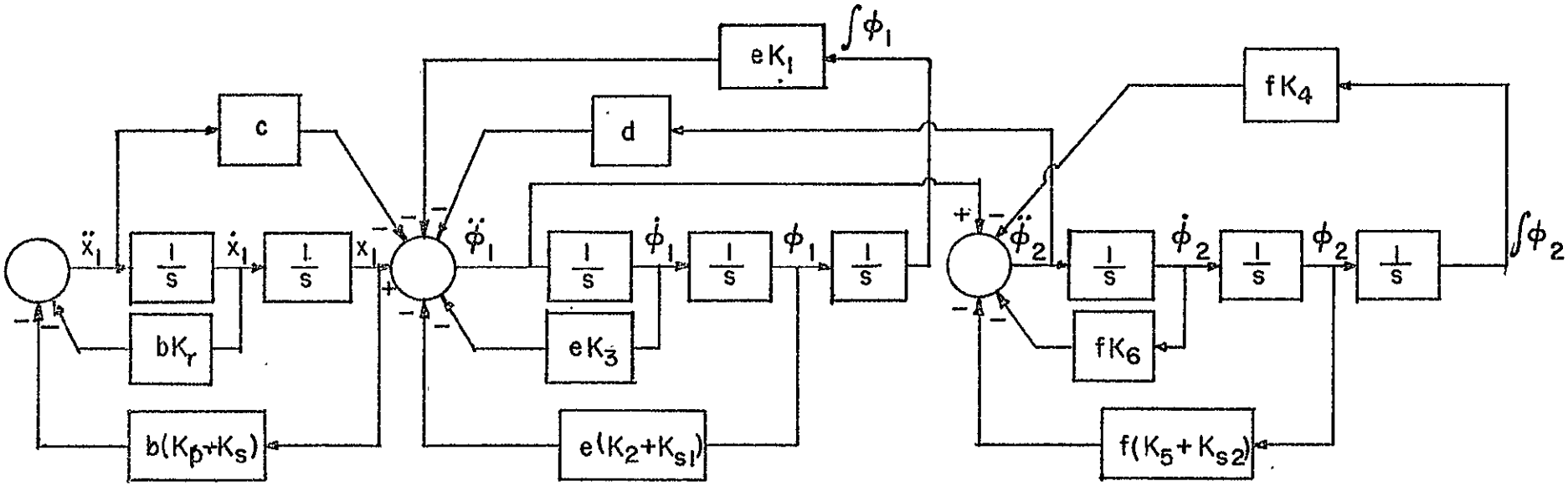

Figure 2-2. Block diagram of the ASPS dynamics with state-variable feedback controls.

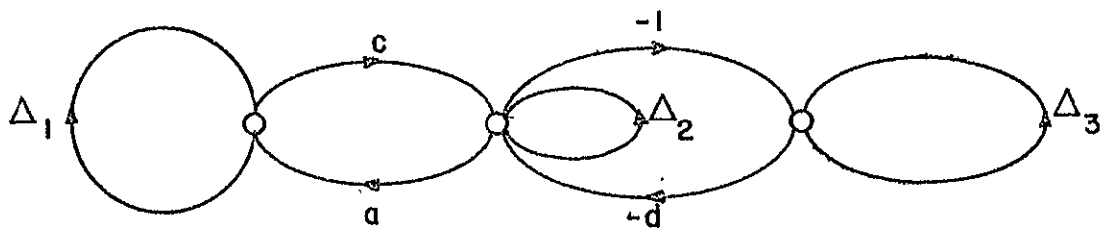

Figure 2-3. A simplified signal flow graph of the system shown in Figure 2-2.

The design objective is to determine the feedback gain constants K_p, K_r, K_1, K_2, K_3, K_4, K_5 and K_6 such that the eigenvalues of the closed-loop ASPS are at certain specified locations.

The first step of the design problem is concerned with the determination of the characteristic equation of the closed-loop system. This is accomplished by applying the Mason's gain formula to the signal flow graph in Fig. 2-3. The result is

$$\Delta = 1 - \Delta_1 - \Delta_2 - \Delta_3 - ca - d + \Delta_1(\Delta_2 + \Delta_3 + d) + ac\Delta_3 + \Delta_2\Delta_3 - \Delta_1\Delta_2\Delta_3 = 0 \tag{2-12}$$

Substitution of the relations for Δ_1, Δ_2 and Δ_3 into the last equation, and rearranging, we get

$$a_8s^8 + a_7s^7 + a_6s^6 + a_5s^5 + a_4s^4 + a_3s^3 + a_2s^2 + a_1s + a_0 = 0 \tag{2-13}$$

where

$$a_8 = 1 - ac - d$$

$$a_7 = b(1 - d)K_r + eK_3 + f(1 - ac)K_6$$

$$a_6 = b(1 - d)K_p + b(1 - d)K_s + e(K_2 + K_{s1}) + f(K_5 + K_{s2}) + beK_rK_3 + efK_3K_6 + bfK_rK_6 - acf(K_5 + K_{s2})$$

$$a_5 = eK_1 + f(1 - ac)K_4 + beK_3(K_p + K_s) + beK_r(K_2 + K_{s1}) + efK_6(K_2 + K_{s1}) + efK_3(K_5 + K_{s2}) + bfK_6(K_p + K_s) + bfK_r(K_5 + K_{s2}) + befK_3K_6K_r$$

$$a_4 = be(K_p + K_s)(K_2 + K_{s1}) + K_1K_rbe + efK_1K_6 + ef(K_2 + K_{s1})(K_5 + K_{s2}) + efK_3K_4 + bf(K_p + K_s)(K_5 + K_{s2}) + bfK_rK_4 + bef((K_p + K_s)K_3K_6 + K_rK_6(K_2 + K_{s1}) + K_rK_3(K_5 + K_{s2}))$$

$$a_3 = beK_1(K_p + K_s) + efK_1(K_5 + K_{s2}) + efK_4(K_2 + K_{s1}) + bfK_4(K_p + K_s)$$
$$+ bef\{K_rK_1K_6 + K_r(K_2 + K_{s1})(K_5 + K_{s2}) + K_rK_3K_4 + (K_p + K_s)K_6(K_2 + K_{s1})$$
$$+ (K_p + K_s)K_3(K_s + K_{s2})\}$$

$$a_2 = efK_1K_4 + bef\{(K_p + K_s)K_1K_6 + (K_p + K_s)(K_2 + K_{s1})(K_5 + K_{s2}) + (K_p + K_s)K_3K_4$$
$$+ K_rK_1(K_5 + K_{s2}) + K_rK_4(K_2 + K_{s1})\}$$

$$a_1 = bef\{K_1K_4K_r + K_4(K_p + K_s)(K_2 + K_{s1}) + K_1(K_p + K_s)(K_5 + K_{s2})\}$$

$$a_0 = befK_1K_4(K_p + K_s)$$

In these nine coefficients, the values of a, b, c, d, e, f, K_{s1}, K_{s2} and K_s are known, and the values of K_p, K_r, K_1, K_2, K_3, K_4, K_5 and K_6 are to be determined for a given set of roots of Eq. (2-13).

Let the desired roots of Eq. (2-13) be λ_1, λ_2, λ_3, λ_4, λ_5, λ_6, λ_7 and λ_8. The condition for these roots to be solutions of Eq. (2-13) is

$$a_8 \prod_{i=1}^{8} (s - \lambda_i) = \sum_{i=0}^{8} a_i s^i \tag{2-14}$$

Expanding the left-hand side of Eq. (2-14), we have the equation,

$$a_8 s^8 + g_7(\underline{\lambda})s^7 + g_6(\underline{\lambda})s^6 + g_5(\underline{\lambda})s^5 + g_4(\underline{\lambda})s^4 + g_3(\underline{\lambda})s^3 + g_2(\underline{\lambda})s^2 + g_1(\underline{\lambda})s^-$$
$$+ g_0(\underline{\lambda}) = \sum_{i=0}^{8} a_i s^i \tag{2-15}$$

where

$$\underline{\lambda} = (\lambda_1, \lambda_2, \lambda_3, \lambda_4, \lambda_5, \lambda_6, \lambda_7, \lambda_8)'$$

denotes the vector of eigenvalues, and $g_i(\underline{\lambda})$ $(i = 0, 1, 2, \ldots, 7)$ are known once $\underline{\lambda}$ is given. In fact, it is simple to see that

$$a_i(K_p, K_r, K_1, K_2, K_3, K_4, K_5, K_6) = g_i(\underline{\lambda}) \tag{2-16}$$

for $i = 0, 1, 2, \ldots, 7$.

Define

$$u_1 = f_1 - f_4 \tag{2-17}$$

$$u_2 = T_c \tag{2-18}$$

$$u_3 = (f_3 - f_2)L + (f_1 - f_4)L_6 \tag{2-19}$$

Equations (2-17), (2-18) and (2-19) specify the three inputs to the ASPS which is an eighth-order system with the state equation

$$\begin{bmatrix} \dot{x}_1 \\ \dot{x}_2 \\ \dot{x}_3 \\ \dot{x}_4 \\ \dot{x}_5 \\ \dot{x}_6 \\ \dot{x}_7 \\ \dot{x}_8 \end{bmatrix} = \begin{bmatrix} 0 & 1 & 0 & 0 & 0 & 0 & 0 & 0 \\ a_{21} & 0 & 0 & a_{24} & 0 & 0 & a_{27} & 0 \\ 0 & 0 & 0 & 1 & 0 & 0 & 0 & 0 \\ 0 & 0 & 0 & 0 & 1 & 0 & 0 & 0 \\ a_{51} & 0 & 0 & a_{54} & 0 & 0 & a_{57} & 0 \\ 0 & 0 & 0 & 0 & 0 & 0 & 1 & 0 \\ 0 & 0 & 0 & 0 & 0 & 0 & 0 & 1 \\ a_{81} & 0 & 0 & a_{84} & 0 & 0 & a_{87} & 0 \end{bmatrix} \begin{bmatrix} x_1 \\ x_2 \\ x_3 \\ x_4 \\ x_5 \\ x_6 \\ x_7 \\ x_8 \end{bmatrix} + \begin{bmatrix} 0 & 0 & 0 \\ b_{21} & b_{22} & b_{23} \\ 0 & 0 & 0 \\ 0 & 0 & 0 \\ b_{51} & b_{52} & b_{53} \\ 0 & 0 & 0 \\ 0 & 0 & 0 \\ b_{81} & b_{82} & b_{83} \end{bmatrix} \begin{bmatrix} u_1 \\ u_2 \\ u_3 \end{bmatrix} \tag{2-20}$$

where

$$x_1 = x$$

$$x_2 = \dot{x}$$

$$x_3 = \int \phi_1 dt$$

$$x_4 = \phi_1$$

$$x_5 = \dot{\phi}_1$$

$$x_6 = \int \phi_2 dt$$

$$x_7 = \phi_2$$

$$x_8 = \dot{\phi}_2$$

and the entries of the matrices of the state equation are determined by the open-loop ASPS. The numerical values of these elements are:

$$a_{21} = -0.6120962971$$

$a_{24} = -0.0014844271$

$a_{27} = 0.0014844271$

$a_{51} = -0.312026593$

$a_{54} = -0.0007589096$

$a_{57} = 0.0007589096$

$a_{81} = 0.312026593$

$a_{84} = 0.0007589096$

$a_{87} = -0.0007688499$

$b_{21} = 0.5823745791$

$b_{22} = 0.2968854358$

$b_{23} = -0.2968854358$

$b_{51} = 0.2968854358$

$b_{52} = 0.1517819201$

$b_{53} = -0.1517819201$

$b_{81} = -0.2968854358$

$b_{82} = -0.1517819201$

$b_{83} = 0.1703268144$

Equation (2-20) describes the system part of the block diagram of Fig. 2-4. In order to use the state feedback to realize a controller, it is necessary that the system is completely controllable. The controllability of the ASPS is determined as follows:

Let Eq. (2-20) be written as

$$\dot{\underline{x}}(t) = A\underline{x}(t) + B\underline{u}(t)$$

The necessary and sufficient conditions for the system to be controllable are that the matrix

$$U = \begin{pmatrix} B & AB & A^2B & \cdots & A^7B \end{pmatrix} \qquad (2\text{-}21)$$

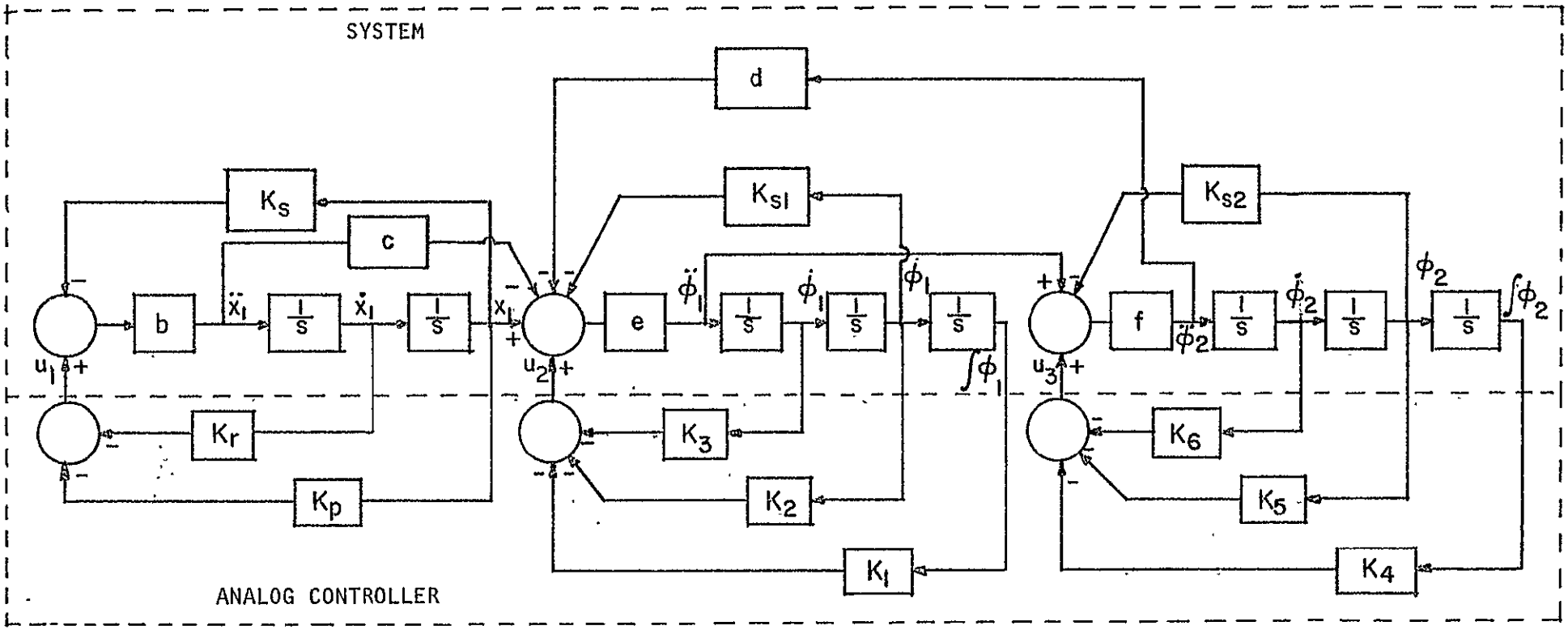

Figure 2-4. Block diagram of the ASPS dynamics and the design of the analog controller.

be of rank eight. In the matrix B, as shown in Eq. (2-20), there are three non-zero rows. The determinant of these three rows is

$$\det \begin{bmatrix} b_{21} & b_{22} & b_{23} \\ b_{51} & b_{52} & b_{53} \\ b_{81} & b_{82} & b_{83} \end{bmatrix} = 0.0000046913 \neq 0 \qquad (2\text{-}22)$$

Thus, we have

$$\text{Rank}(B) = 3 \qquad (2\text{-}23)$$

Also, the matrix

$$AB = \begin{bmatrix} b_{21} & b_{22} & b_{23} \\ 0 & 0 & 0 \\ 0 & 0 & 0 \\ b_{51} & b_{52} & b_{53} \\ 0 & 0 & 0 \\ 0 & 0 & 0 \\ b_{81} & b_{82} & b_{83} \\ 0 & 0 & 0 \end{bmatrix} \qquad (2\text{-}24)$$

has three independent columns. These columns are linearly independent on the columns of B. Therefore,

$$\text{Rank}(AB) = 3$$

and

$$\text{Rank}(B \quad AB) = 6$$

Furthermore, in the matrix A^2B, we have

$$A^2B = \begin{bmatrix} 0 & 0 & 0 \\ a_{21}b_{21}+a_{24}b_{51}+a_{27}b_{81} & a_{21}b_{22}+a_{24}b_{52}+a_{27}b_{82} & a_{21}b_{23}+a_{24}b_{52}+a_{27}b_{83} \\ b_{51} & b_{52} & b_{53} \\ 0 & 0 & 0 \\ a_{51}b_{21}+a_{54}b_{51}+a_{57}b_{81} & a_{51}b_{22}+a_{54}b_{52}+a_{57}b_{82} & a_{51}b_{23}+a_{54}b_{53}+a_{57}b_{83} \\ b_{81} & b_{82} & b_{83} \\ 0 & 0 & 0 \\ a_{81}b_{21}+a_{84}b_{51}+a_{87}b_{81} & a_{81}b_{22}+a_{84}b_{52}+a_{87}b_{82} & a_{81}b_{23}+a_{84}b_{53}+a_{87}b_{83} \end{bmatrix} \quad (2\text{-}25)$$

If the rank of A^2B is greater than or equal to two, the matrix U in Eq. (2-21) will have full rank. Consider the two following rows of AB:

$$\begin{pmatrix} b_{51} & b_{52} & b_{53} \end{pmatrix} \qquad \text{and} \qquad \begin{pmatrix} b_{81} & b_{82} & b_{83} \end{pmatrix}$$

It is obvious that these are linearly independent. Therefore,

$$\text{Rank}(A^2B) \geq 2$$

Also notice that the third and sixth rows of the matrices B and AB have all zero elements. Therefore, there are at least two linearly independent columns in matrix A^2B which is also linearly independent of the columns of the matrix $\begin{pmatrix} B & AB \end{pmatrix}$. Thus, we have the conclusion that

$$\text{Rank}(U) = 8$$

and the full rank of matrix U implies the complete controllability of the ASPS.

With the controllability of the system estabilished, it is now possible to select the eigenvalues of the closed-loop ASPS by using state feedback described in Eqs. (2-6), (2-7) and (2-8); i.e.,

$$u_1 = -K_p x_1 - K_r \dot{x}_1$$

$$u_2 = -K_1 \int \phi_1 dt - K_2 \phi_2 - K_3 \dot{\phi}_1 \qquad (2\text{-}26)$$

$$u_3 = -K_4 \int \phi_2 dt - K_5 \phi_2 - K_6 \dot{\phi}_2$$

The closed-loop control system can be described by

$$\dot{\underline{x}}(t) = (A + BG)\underline{x}(t) = \hat{A}\underline{x}(t) \qquad (2\text{-}27)$$

where the matrices A and B are as in Eq. (2-20), and G is the feedback gain matrix and is given by

$$G = \begin{bmatrix} -K_p & -K_r & 0 & 0 & 0 & 0 & 0 & 0 \\ 0 & 0 & -K_1 & -K_2 & -K_3 & 0 & 0 & 0 \\ 0 & 0 & 0 & 0 & 0 & -K_4 & -K_5 & -K_6 \end{bmatrix} \qquad (2\text{-}28)$$

It is the objective of the design problem to choose a set of feedback gains such that the roots of the characteristic equation are as specified. The roots must satisfy the following equation:

$$\det(sI - \hat{A}) = 0$$

If a closed-loop system is to be designed such that it has a bandwidth of one Hertz, then the eigenvalues are chosen as

$$\lambda_1, \lambda_2 = -7.16 \pm j8.75$$

$$\lambda_3, \lambda_4 = -42.16 \pm j72.67$$

$$\lambda_5 = -11.41$$

$$\lambda_6 = -109.15$$

$$\lambda_7 = -24.21$$

$$\lambda_8 = -6.54$$

In this case, the eigenvalues must satisfy the following equation:

$$\det(sI - \hat{A}) = \prod_{i=1}^{8} (s - \lambda_i) \tag{2-30}$$

where λ_i ($i = 1, 2, \ldots, 8$) are specified in Eq. (2-29).

After expansion of both sides of Eq. (2-30), the coefficients corresponding to the same powers of s must be equal. Thus, eight nonlinear algebraic equations are formed which must be solved to give the eight unknown parameters in the feedback matrix G in Eq. (2-28).

Given the eigenvalues specified in Eq. (2-29), the coefficients of the right-hand side of Eq. (2-20) can be computed. We have

$$\begin{aligned}\prod_{i=1}^{8} (s - \lambda_i) = {} & s^8 + 2.49936\times10^2 s^7 + 2.84334\times10^4 s^6 + 1.9438\times10^6 s^5 \\ & + 6.6624\times10^7 s^4 + 1.2103\times10^9 s^3 + 1.2699\times10^{10} s^2 + 7.3946\times10^{10} s \\ & + 1.78289\times10^{11}\end{aligned} \tag{2-31}$$

After algebraic manipulation, we have

$$\det(sI - \hat{A}) = s^8 + \frac{a_7}{a_8}s^7 + \frac{a_6}{a_8}s^6 + \frac{a_5}{a_8}s^5 + \frac{a_4}{a_8}s^4 + \frac{a_3}{a_8}s^3 + \frac{a_2}{a_8}s^2 + \frac{a_1}{a_8}s + \frac{a_0}{a_8}$$

where $a_0, a_1, \ldots, a_8$ are defined in Eq. (2-13).

Therefore, a system of equations is obtained,

$$a_7 = 2.49936\times10^2 \times 0.2349\times10^{-2} = 0.5871$$

$$a_6 = 2.84334\ 10^4 \times 0.2349\times10^{-2} = 0.6679\times10^2$$

$$a_5 = 1.9438\times10^6 \times 0.2349\times10^{-2} = 0.4566\times10^4$$

$$a_4 = 6.6624\times10^7 \times 0.2349\times10^{-2} = 0.1565\times10^6$$

$$a_3 = 1.2103\times10^9 \times 0.2349\times10^{-2} = 0.2843\times10^7$$

$$a_2 = 1.2699\times10^{10} \times 0.2349\times10^{-2} = 0.2983\times10^8$$

$$a_1 = 7.3946\times10^{10} \times 0.2349\times10^{-2} = 0.1737\times10^9$$

$$a_0 = 1.7829\times10^{11} \times 0.2349\times10^{-2} = 0.4188\times10^9$$

A computer program was written to solve the set of equations involving $a_0, a_1, \ldots, a_7$, using the Brown's method. The feedback gains are solved and are tabulated as follows:

$K_p = 91338$

$K_r = 10081$

$K_1 = 6460200$

$K_2 = 569930$

$K_3 = -48943$

$K_4 = 600900$

$K_5 = 129920$

$K_6 = 11756$

The computer program is tabulated in Table 2-1.

Table 2-1. Computer Program For the Computation of The Feedback Gains of the Closed-Loop ASPS By Means of the Brown's Method

```
      IMPLICIT REAL*8(A-H,O-Z)
      DIMENSION ROOTS(2,50)
      COMMON AKSX,AKSP,AKSS,RB,AMI,A33,AJ,A,B,C,D,E,F,DD(51)
      TYPE 5
5     FORMAT(2X,'THE DEGREE OF P(X) =    '$)
      ACCEPT 6,N
6     FORMAT(I2)
      TYPE 7
7     FORMAT(/'  SPECIFY THE ROOTS OF P(X) IN THE FOLLOWING:'//2X,
     &'*** ALL COMPLEX ROOTS MUST BE IN COMPLEX CONJUGATE PAIRS ',
     &'AND THE'/2X,'    ONE WITH NEGATIVE IMAGINARY PART SHOULD BE ',
     &'SPECIFIED FIRST.***'/)
      DO 1 I=1,N
      TYPE 2,I
2     FORMAT(/2X,'REAL(ROOT',I2,') =    '$)
      ACCEPT 9,ROOTS(1,I)
      TYPE 3,I
3     FORMAT(2X,'IMAG(ROOT',I2,') =    '$)
      ACCEPT 9,ROOTS(2,I)
1     CONTINUE
      TYPE 8
8     FORMAT(/2X,'LEADING COEFFICIENT =    '$)
      ACCEPT 9,COE1
9     FORMAT(F12.5)
      CALL RECON(ROOTS,COE1,DD,N)
      TYPE 10,N
10    FORMAT(/2X,'COEFFICIENTS OF P(X) STARTING FROM THAT OF X**',
     &I2,':'/)
      TYPE 4,(DD(I),I=1,N+1)
4     FORMAT(2X,D12.5)
C
C---SYSTEM CONSTANTS
C
      AKSX=1.051
      AKSP=0.005
      AKSS=0.005
      RB=1.95
      AMI=600.
      A33=2805.15
      AJ=503.
      A=RB
      B=1./AMI
      C=AMI*RB/A33
      D=AJ/A33
      E=1./A33
      F=1./AJ
C
      CALL SOLVER(N)
      STOP
      END
```

Table 2-1. (Continued)

```
      SUBROUTINE RECON (ROOTS,A,    D,N)
      DIMENSION ROOTS(2,30),D(51)
                                          REAL*8 ROOTS,A,D,T,U
      DO 1 I=1,N
      D(I)=0.0
    1 CONTINUE
      D(N+1)=1.0
      NS=N+1
      DO 10 I=1,N
      NL=NS-I
      IF (ROOTS(2,I)) 3,7,10
    3 T=ROOTS(1,I)**2+ROOTS(2,I)**2
      U=2.0*ROOTS(1,I)
      DO 5 J=NL,N
      D(J-1)=T*D(J-1)-U*D(J)+D(J+1)
    5 CONTINUE
      D(N)=T*D(N)-U*D(N+1)
      GO TO 9
    7 T=-ROOTS(1,I)
      DO 8 J=NL,N
      D(J)=T*D(J)+D(J+1)
    8 CONTINUE
    9 D(N+1)=T*D(N+1)
   10 CONTINUE
      DO 11 II=1,NS
      D(II)=D(II)*A
   11 CONTINUE
      RETURN
      END
      SUBROUTINE SOLVER(N)
      REAL*8 X(50),DUM2(50,55)
      INTEGER*4 DUM1(50,51),CNAME(50)
C
C---INITIAL GUESSES OF THE SOLUTION
C
      X(1)=0.105
      X(2)=0.915405
      X(3)=-0.48905
      X(4)=0.5706
      X(5)=0.64607
      X(6)=0.117505
      X(7)=0.1306
      X(8)=0.606
C
C---SPECIFY NAMES FOR EACH COEFFICIENTS FOR PRINTOUT
C
      CNAME(1)='G'
      CNAME(2)='H'
      CNAME(3)='I'
      CNAME(4)='Q'
      CNAME(5)='R'
      CNAME(6)='W'
      CNAME(7)='T'
      CNAME(8)='U'
```

Table 2-1. (Continued)

```
C
C---OTHER PARAMETERS TO BE SPECIFIED
C
      NSIG=12    ! THE NUMBER OF SIGNIFICANT DIGITS DESIRED
      IP=0    ! PRINT STEP NO. AND IMPROVED APPROXIMATION IF IP=1
      NIT=500    ! MAXIMUM NUMBER OF ITERATIONS TO BE USED
C
      CALL BROWN1(N,NIT,NSIG,ING,X,DUM1,DUM2,IP,50)
      IF(ING.EQ.0) WRITE(5,10000)
10000 FORMAT(///'   **A JACOBIAN RELATED MATRIX WAS SINGULAR--'/
     &       'INDICATIVE OF THE PROCESS ''BLOWING-UP''.**')
      WRITE(5,10001) NIT
10001 FORMAT('   **NUMBER OF ITERATIONS = ',I3,'**')
      WRITE(5,10004)
10004 FORMAT('   **FEEDBACK COEFFICIENTS:'/)
      WRITE(5,10002)(CNAME(J),X(J),J=1,N)
10002 FORMAT(10X,A3,' =  ',D12.5)
      RETURN
      END
      SUBROUTINE VRTHF(X,Y,K)
      IMPLICIT REAL*8(A-H,O-Z)
      DIMENSION X(1),ARSR(10,1)
      COMMON AKSX,AKSP,AKSS,RO,ANI,A33,AJ,A,B,C,D,E,F,DD(51)
      G=X(1)
      H=X(2)
      P=X(3)
      Q=X(4)
      R=X(5)
      W=X(6)
      T=X(7)
      U=X(8)
      G1=-B*G
      G2=-B*(H+AKSX)
      G3=-A*C
      G4=-E*P
      G5=-E*(Q+AKSP)
      G6=-E*R
      G7=0
      G8=-F*W
      G9=-F*(T+AKSS)
      G10=-F*U
C---THE VECTOR ARSR(I,1) CONTAINS THE COEFFICIENTS OF THE N-TH
C---DEGREE POLYNOMIAL ORDERED FROM POWER N TO POWER 0 OF X --
C---ARSR(1,1) IS THE COEFFICIENT OF X**N. ARSR(2,1) IS THE COEFFI-
C---CIENT OF X**(N-1), ETC.
      ARSR(1,1)=1.-G3-G7
      GO TO (1,2,3,4,5,6,7,8),K
1     ARSR(2,1)=-G1-G4-G8+G1*G7+G3*G8
      Y=ARSR(2,1)/ARSR(1,1)-DD(2)/DD(1)
      RETURN
2     ARSR(3,1)=-G2-G5-G9+G1*G4+G1*G8+G2*G7+G3*G9+G4*G8
      Y=ARSR(3,1)/ARSR(1,1)-DD(3)/DD(1)
      RETURN
3     ARSR(4,1)=-G6-G10+G1*G5+G1*G9+G2*G4+G2*G8+G3*G10
     &          +G4*G9+G5*G8-G1*G4*G8
      Y=ARSR(4,1)/ARSR(1,1)-DD(4)/DD(1)
      RETURN
4     ARSR(5,1)=G1*G6+G1*G10+G2*G5+G2*G9+G4*G10+G5*G9
     &          +G6*G8-G2*G4*G8-G1*G5*G8-G1*G4*G9
      Y=ARSR(5,1)/ARSR(1,1)-DD(5)/DD(1)
      RETURN
```

Table 2-1. (Continued)

```
5       ARSR(6,1)=G2*G6+G2*G10+G5*G10+G6*G9-G2*G5*G8-G1*G6*G8
                -G2*G4*G9-G1*G5*G9-G1*G4*G10
        Y=ARSR(6,1)/ARSR(1,1)-DD(6)/DD(1)
        RETURN
6       ARSR(7,1)=G6*G10-G2*G6*G8-G2*G5*G9-G1*G6*G9-G2*G4*G10
                -G1*G5*G10
        Y=ARSR(7,1)/ARSR(1,1)-DD(7)/DD(1)
        RETURN
7       ARSR(8,1)=-G2*G6*G9-G2*G5*G10-G1*G6*G10
        Y=ARSR(8,1)/ARSR(1,1)-DD(8)/DD(1)
        RETURN
8       ARSR(9,1)=-G2*G6*G10
        Y=ARSR(9,1)/ARSR(1,1)-DD(9)/DD(1)
        RETURN
        END
      SUBROUTINE BROWNZ(N,NIT,NSIG,ING,X,INTER,COE,IP,L)
      REAL*8 X(1),COE(L,1),RELC,HOLD,H,F,FPLUS,DMAX,TEST,CR
      DIMENSION INTER(L,1)
C**** THE PARAMETERS NIT,NSIG,ING,INTER ARE MAXIT,NUMSIG,SINGULAR,POINT--
C**** ER OF THE ALGORITHM 316 RESPECTIVELY AND INTER(1,N+1),COE(I,N+2),
C**** COE(I,N+3) ARE ISUB(I),PART(I),TEMP(I) RESPECTIVELY.
      NUERO=1
      ING=1
      RELC=10.**(-NSIG)
      C1=0.E0
      C2=1.E20
      DO 91 M=1,NIT
      DO 10 J=1,N
10    INTER(1,J)=J
      DO 50 K=1,N
      IF(K.GT.1) CALL BKSUBT(K,N,X,COE,INTER,L)
      CALL VKTHF(X,F,K)
      FTR=0.001
11    LLY=0
      DO 20 I=K,N
      ITEMP=INTER(K,I)
      HOLD=X(ITEMP)
      H=FTR*HOLD
      IF(H.EQ.0.00) H=0.00100
      X(ITEMP)=HOLD+H
      IF(K.GT.1) CALL BKSUBT(K,N,X,COE,INTER,L)
      CALL VKTHF(X,FPLUS,K)
      COE(ITEMP,N+2)=(FPLUS-F)/H
      X(ITEMP)=HOLD
      C3=DABS(COE(ITEMP,N+2))
      IF(C3.EQ.C1) GO TO 18
      C4=DABS(F/C3)
      IF(C4.LE.C2) GO TO 20
18    LLY=LLY+1
20    CONTINUE
      IF(LLY.LE.(N-K)) GO TO 21
      FTR=FTR*10
      IF(FTR.GT.0.5) GO TO 100
      GO TO 11
21    IF(K.LT.N) GO TO 22
      IF(C3.EQ.C1) GO TO 100
      COE(K,N+1)=0.D0
      KMAX=ITEMP
      GO TO 41
22    KMAX=INTER(K,K)
      DMAX=DABS(COE(KMAX,N+2))
      KPLUS=K+1
```

Table 2-1. (Continued)

```
      DO 30 I=KPLUS,N
      JSUB=INTER(K,I)
      TEST=DABS(COE(JSUB,N+2))
      IF(TEST.LT.BMAX) GO TO 23
      BMAX=TEST
      INTER(KPLUS,I)=KMAX
      KMAX=JSUB
      GO TO 30
23    INTER(KPLUS,I)=JSUB
30    CONTINUE
      IF(DABS(COE(KMAX,N+2)).EQ.C1) GO TO 100
      INTER(K,N+1)=KMAX
      COE(K,N+1)=0.D0
      DO 40 J=KPLUS,N
      JSUB=INTER(KPLUS,J)
      COE(K,JSUB)=-COE(JSUB,N+2)/COE(KMAX,N+2)
40    COE(K,N+1)=COE(K,N+1)+COE(JSUB,N+2)*X(JSUB)
41    COE(K,N+1)=(COE(K,N+1)-F)/COE(KMAX,N+2)+X(KMAX)
50    CONTINUE
      X(KMAX)=COE(N,N+1)
      IF(N.GT.1) CALL BKSUBT(N,N,X,COE,INTER,L)
      IF(M.EQ.1) GO TO 80
      DO 60 I=1,N
      IF (X(I).EQ.C1) GO TO 58
      CR=DABS((COE(I,N+3)-X(1))/X(I))
      GO TO 59
58    CR=DABS(COE(I,N+3))
59    IF(CR.GT.RELC) GO TO 70
60    CONTINUE
      NVERG=NVERG+1
      IF(NVERG.GE.3) GO TO 111
      GO TO 80
70    NVERG=0
80    DO 90 I=1,N
90    COE(I,N+3)=X(I)
      IF(IP.EQ.0) GO TO 91
      WRITE(6,200) M,(X(I),I=1,N)
200   FORMAT(I10,5D20.10/10X,5D20.10)
91    CONTINUE
      RETURN
100   ING=0
      RETURN
111   NIT=M-1
      RETURN
      END
      SUBROUTINE BKSUBT(K,N,X,COE,INTER,L)
      REAL*8 X(1),COE(L,1)
      DIMENSION INTER(L,1)
      KN=K-1
      DO 20 I=1,KN
      KM=K-I+1
      KMAX=INTER(KM-1,N+1)
      X(KMAX)=0.D0
      DO 10 J=KM,N
      JSUB=INTER(KM,J)
10    X(KMAX)=X(KMAX)+COE(KM-1,JSUB)*X(JSUB)
20    X(KMAX)=X(KMAX)+COE(KM-1,N+1)
      RETURN
      END
```

2.4 Time Responses of the Analog ASPS Designed by Pole Placement

The time responses of the closed-loop ASPS with the analog controller designed by the pole-placement design conducted in the last section are studied by computer simulation.

The listings of the computer simulation program are given in Table 2-2.

The initial values of $x_1(t)$, $\phi_1(t)$, and $\phi_2(t)$ are:

$$x_1(0) = 2 \times 10^{-3}$$

$$\phi_1(0) = 0.013$$

$$\phi_2(0) = 0.013$$

It should be noted that no nonlinear characteristics are considered in the system model and the simulations.

Figure 2-5 shows the time response of $x_1(t)$ with the indicated initial condition. As indicated, the time response of $x_1(t)$ decays to zero very rapidly, and the vertical axis of Fig. 2-5 is in a logarithmic scale.

Figure 2-6 shows the time response of $\phi_1(t)$ with the given initial condition. Again, the response decays to zero so rapidly over the 4-second interval that the vertical axis is in logarithmic.

The response of $\phi_2(t)$ is the fastest of the three, and a time response plot could not be made realistically over a 4-second time interval. Thus, the values of the response of $\phi_2(t)$ are tabulated in Table 2-3.

Table 2-2. Computer Program For the Simulation of the Analog ASPS with Controller Designed by Pole Placement

```
      DIMENSION PRMT(5),Y(8),DERY(8),AUX(8,2)
      EXTERNAL FCT,OUTP
      COMMON X,XDOT,PHI1,PHI1DT,PHI1IN,PHI2,PHI2DT,PHI2IN,T,
     &  V1,V2,V3,AJ,AMI,AKSX,AKSP,AKSS,A33,TPRT,RB,DELTA,
     &  A0,B0,C0,D0,E,F,TEND,
     &  NPRT,IV1,IV2,IV3,LINE
     &  OPEN(UNIT=6,DEVICE='DSK',FILE='FOR20.DAT',ACCESS='SEQOUT')

      LINE=0
      H=0.
      TEND=100.
      TPRT=0.25
      TINT=0.5E-3
C-----SET INITIAL CONDITIONS
      X=2.0E-3
      XDOT=0.
      PHI1=0.013
      PHI1DT=0.
      PHI1IN=0.
      PHI2=0.013
      PHI2DT=0.
      PHI2IN=0.
      AMI=600.
      AKSX=1.051
      AKSP=0.005
      AKSS=0.005
      AJ=503.
      A33=2805.1
      RB=1.956
      A0=RB
      B0=1./AMI
      C0=AMI*RB/A33
      D0=AJ/A33
      E=1./A33
      F=1./AJ
      DELTA=1.-A0*C0-D0
      T=0.
      NPRT=0
      PRMT(3)=TINT
      PRMT(4)=0.05*X
      DO 99 I=1,8
99    DERY(I)=0.125
      NDIM=8

      PRMT(1)=T
      PRMT(2)=TEND
      Y(1)=X
      Y(2)=XDOT
      Y(3)=PHI1IN
      Y(4)=PHI1
      Y(5)=PHI1DT
      Y(6)=PHI2IN
      Y(7)=PHI2
      Y(8)=PHI2DT

      CALL RKGS(PRMT,Y,DERY,NDIM,IHLF,FCT,OUTP,AUX)
      STOP
      END
```

Table 2-2 (continued).

```
      SUBROUTINE FCT(XX,Y,DERY)
      DIMENSION  Y(8),DER(8)
      COMMON X,XOUT,PHI1,PH11DT,PHI11N,PHI2,PHI2DT,PHI2IN,T,
     &  V1,V2,V3,AJ,AMI,AKSX,AKSP,AKSS,A33,TPRT,R8,DELTA,
     &  A0,B0,C0,D0,E,F,TEND,
     &  NPRT,IV1,IV2,IV3,LINE
      V1=0.913805*Y(1)+0.100105*Y(2)
      V2=0.646027*Y(3)+0.569930*Y(4)-0.489305*Y(5)
      V3=0.000906*Y(6)+0.129208*Y(7)+0.117505*Y(8)
      DERY(1)=Y(2)
      DERY(2)=((-V1*B0-AKSX*B0*Y(1))*(1.-D0)+A0*((-V2-AKSP*Y(4))*E
     &        +(V3+AKSS*Y(7))*F*D0))/DELTA
      DERY(3)=Y(4)
      DERY(4)=Y(5)
      DERY(5)=((-V2-AKSP*Y(4))*E-(V1+AKSX*Y(1))*B0*C0
     &         +(V3+AKSS*Y(7))*D0*F)/DELTA
      DERY(6)=Y(7)
      DERY(7)=Y(8)
      DERY(8)=(-V3-AKSS*Y(7))*F*(1.-A0*C0)+(V2+AKSP*Y(4))*E
     &         +(V1+AKSX*Y(1))*B0*C0)/DELTA
      RETURN
      END
      SUBROUTINE OUTP(XX,Y,DERY,IHLF,NDIM,PRMT)
      DIMENSION Y(8),DERY(8),PRMT(5)
      COMMON X,XOUT,PHI1,PH11DT,PHI11N,PHI2,PHI2DT,PHI2IN,T,
     &  V1,V2,V3,AJ,AMI,AKSX,AKSP,AKSS,A33,TPRT,R8,DELTA,
     &  A0,B0,C0,D0,E,F,TEND,
     &  NPRT,IV1,IV2,IV3,LINE
      IF(XX.GT.TEND) PRMT(5)=1.
      T=XX
      IF(XX.LT.TPRT*FLOAT(NPRT)) RETURN
      LINE=LINE+1
      WRITE(6,100) IHLF,XX,(Y(I),I=1,8)
100   FORMAT(1X,I2,3X,1PE10.4,1P8E11.3)
      X=Y(1)
      XDOT=Y(2)
      PHI1IN=Y(3)
      PHI1=Y(4)
      PHI1DT=Y(5)
      PHI2IN=Y(6)
      PHI2=Y(7)
      PHI2DT=Y(8)
      NPRT=NPRT+1
      WRITE(5,100) IHLF,XX,(Y(I),I=1,8)
      LINE=0
200   RETURN
      END
```

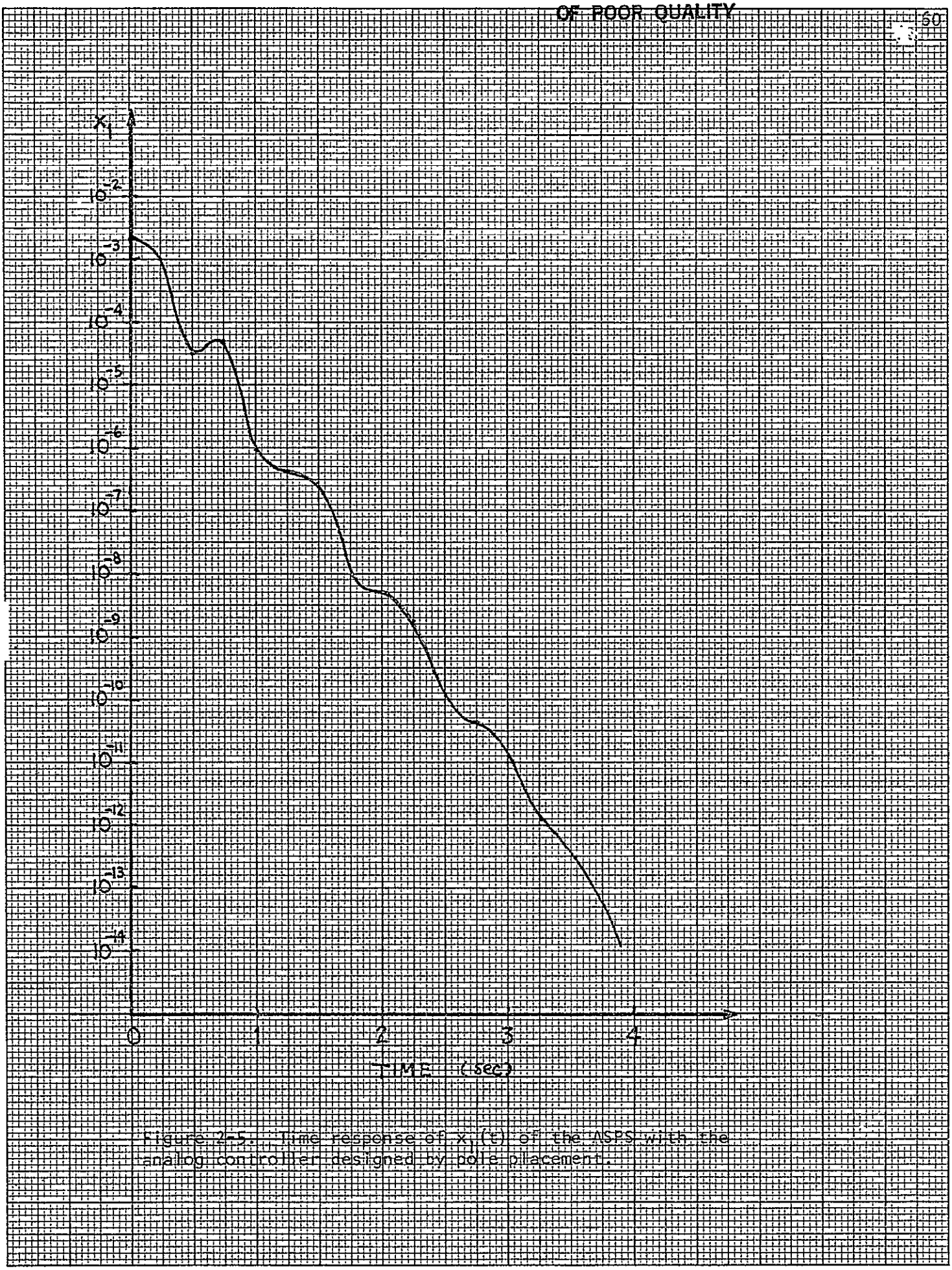

Figure 2-5. Time response of $x_1(t)$ of the ASPS with the analog controller designed by pole placement.

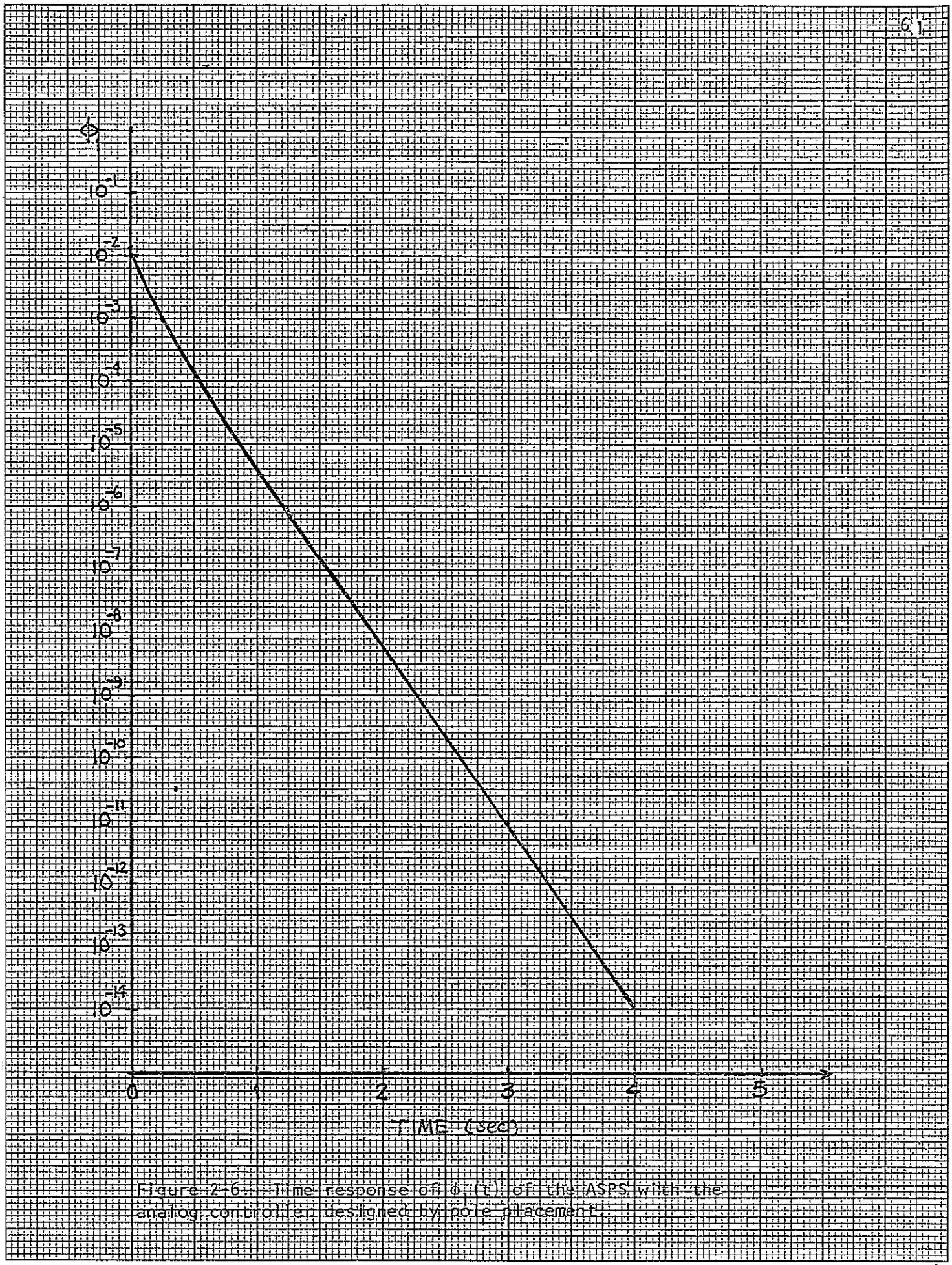

Figure 2-6. Time response of $\phi_1(t)$ of the ASPS with the analog controller designed by pole placement.

Table 2-3. Time Response of ϕ_2 of The ASPS With The Analog Controller Designed by Pole Placement

Time (sec)	$\phi_2(t)$ (rad)
0	1.3×10^{-2}
0.25	-4.342×10^{-3}
0.50	-3.43×10^{-4}
0.75	1.626×10^{-4}
1.00	-1.30×10^{-5}
1.25	5.361×10^{-7}
1.50	7.984×10^{-7}
1.75	-6.162×10^{-8}
2.00	3.742×10^{-9}
2.25	-2.212×10^{-10}
2.5	9.579×10^{-11}
2.75	1.834×10^{-11}
3.00	-2.312×10^{-13}
3.25	7.007×10^{-13}
3.75	9.804×10^{-14}

III. SAMPLED-DATA CONTROL OF THE ANNULAR SUSPENSION AND POINTING SYSTEM (ASPS)

3.1 The Sampled-Data Controller

The sampled-data controller for the ASPS is obtained by incorporating sample-and-hold devices in the control inputs for the dynamics of x_1, $_1$ and $_2$, using the same feedback gains as designed in the analog controller. The design objective is to select an appropriate sampling period T for the sampled-data ASPS.

The sampled-data ASPS is represented by the block diagram of Fig. 3-1. The Q blocks represent the effect of quantization which will not be considered at present.

3.2 Stability Analysis of the Sampled-Data ASPS by the z-Transform

The signal flow graph representation of Fig. 3-1 is shown in Fig. 3-2. The following equations are written directly from the signal flow graph.

$$u_1 = \left[-bG_h\left(\frac{K_p}{s^2} + \frac{K_r}{s}\right)\left(1 - G_3 - G_4 - G_5 + G_3G_5\right)u_1^* - eaG_h\left(\frac{K_p}{s^2} + \frac{K_r}{s}\right)\left(1 - G_5\right)u_2^* + adfG_h\left(\frac{K_p}{s^2} + \frac{K_r}{s}\right)u_3^*\right]/\Delta \qquad (3\text{-}1)$$

$$u_2 = \left[-bcG_h\left(\frac{K_3}{s} + \frac{K_2}{s^2} + \frac{K_1}{s^3}\right)\left(1 - G_5\right)u_1^* - eG_h\left(\frac{K_3}{s} + \frac{K_2}{s^2} + \frac{K_1}{s^3}\right)\left(1 - G_1 - G_5 + G_1G_5\right)u_2^* + dfG_h\left(\frac{K_3}{s} + \frac{K_2}{s^2} + \frac{K_1}{s^3}\right)\left(1 - G_1\right)u_3^*\right]/\Delta \qquad (3\text{-}2)$$

$$u_3 = \left[bcG_h\left(\frac{K_6}{s} + \frac{K_5}{s^2} + \frac{K_4}{s^3}\right)u_1^* + eG_h\left(\frac{K_6}{s} + \frac{K_5}{s^2} + \frac{K_4}{s^3}\right)\left(1 - G_1\right)u_2^* - fG_h\left(\frac{K_6}{s} + \frac{K_5}{s^2} + \frac{K_4}{s^3}\right)\left(1 - G_1 - G_2 + G_1G_3\right)u_3^*\right]/\Delta \qquad (3\text{-}3)$$

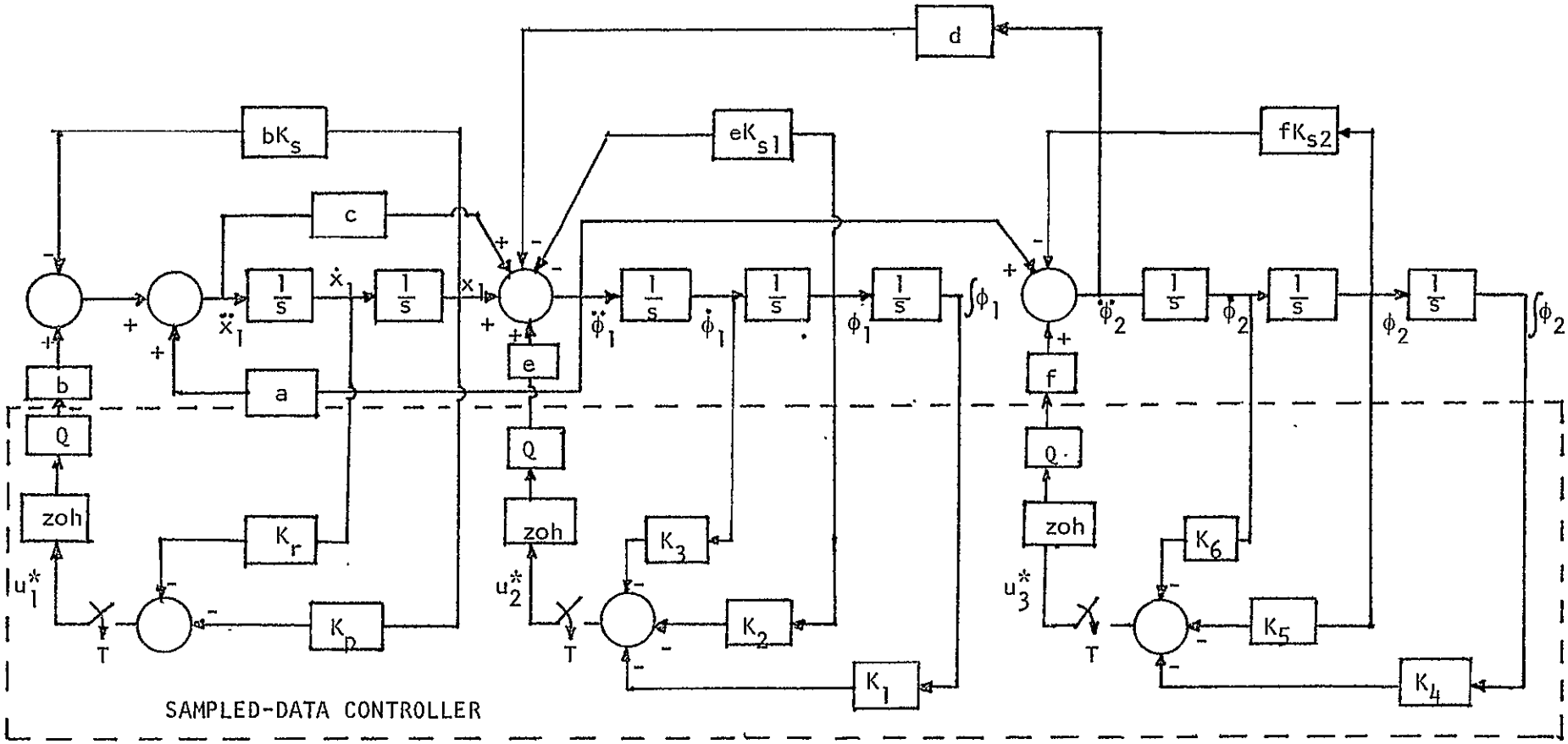

Figure 3-1. Block diagram of the ASPS with the sampled-data controller.

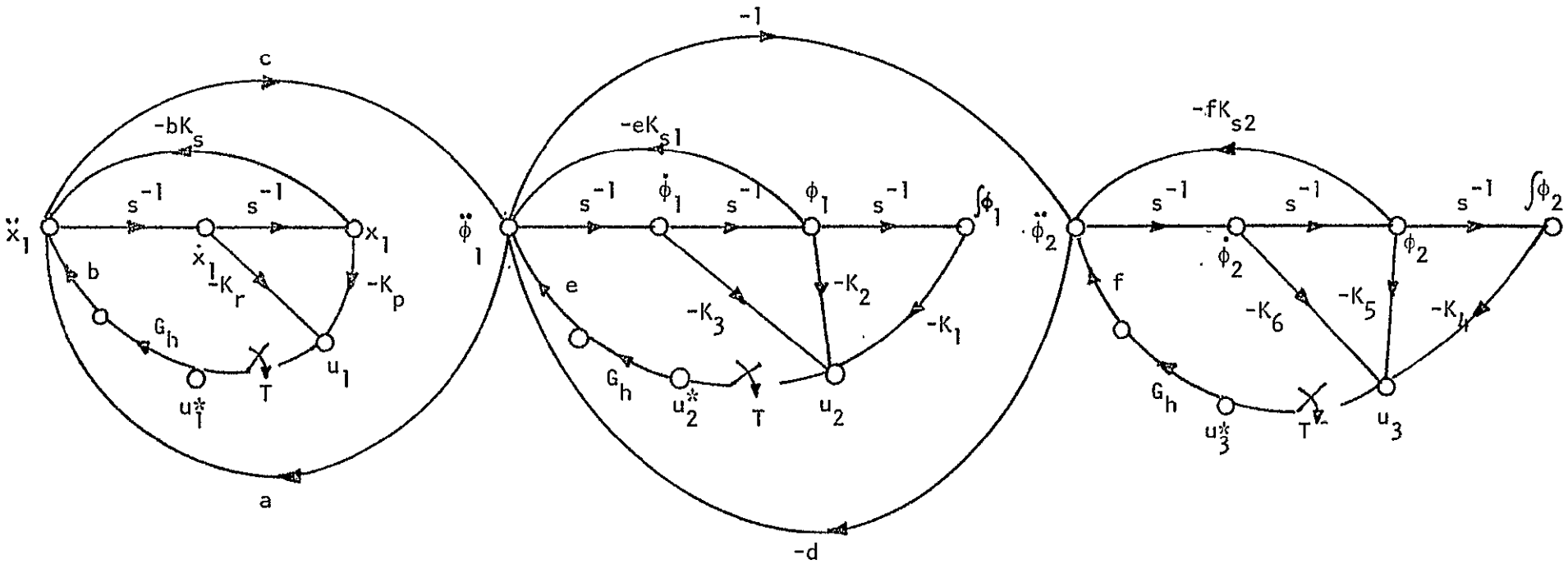

Figure 3-2. Digital signal flow graph of the ASPS.

where

$$G_1 = -bK_s/s^2$$

$$G_2 = ac$$

$$G_3 = -eK_{s1}/s^2$$

$$G_4 = d$$

$$G_5 = -fK_{s2}/s^2$$

$$G_h = (1 - e^{-Ts})/s$$

$$\Delta = 1 - G_1 - G_2 - G_3 = G_4 - G_5 + G_1G_3 + G_1G_4 + G_1G_5 + G_3G_5 + G_2G_5 - G_1G_3G_5$$

Taking the z-transform on both sides of Eqs. (3-1) through (3-3), we have

$$U_1(z) = \mathcal{Z}\left[\frac{G_A}{\Delta}\right] U_1(z) + \mathcal{Z}\left[\frac{G_B}{\Delta}\right] U_2(z) + \mathcal{Z}\left[\frac{G_C}{\Delta}\right] U_3(z) \qquad (3\text{-}4)$$

$$U_2(z) = \mathcal{Z}\left[\frac{G_D}{\Delta}\right] U_1(z) + \mathcal{Z}\left[\frac{G_E}{\Delta}\right] U_2(z) + \mathcal{Z}\left[\frac{G_F}{\Delta}\right] U_3(z) \qquad (3\text{-}5)$$

$$U_3(z) = \mathcal{Z}\left[\frac{G_I}{\Delta}\right] U_1(z) + \mathcal{Z}\left[\frac{G_J}{\Delta}\right] U_2(z) + \mathcal{Z}\left[\frac{G_K}{\Delta}\right] U_3(z) \qquad (3\text{-}6)$$

where

$$G_A = -bG_h\left(\frac{K_p}{s^2} + \frac{K_r}{s}\right)\left(1 - G_3 - G_4 - G_5 + G_3G_5\right)$$

$$G_B = -eaG_h\left(\frac{K_p}{s^2} + \frac{K_r}{s}\right)\left(1 - G_5\right)$$

$$G_C = adfG_h\left(\frac{K_p}{s^2} + \frac{K_r}{s}\right)$$

$$G_D = -bcG_h\left(\frac{K_3}{s} + \frac{K_2}{s^2} + \frac{K_1}{s^3}\right)\left(1 - G_5\right)$$

$$G_E = -eG_h\left(\frac{K_3}{s} + \frac{K_2}{s^2} + \frac{K_1}{s^3}\right)\left(1 - G_1 - G_5 - G_1G_5\right)$$

$$G_F = dfG_h\left(\frac{K_3}{s} + \frac{K_2}{s^2} + \frac{K_1}{s^3}\right)\left(1 - G_1\right)$$

$$G_I = bcG_h\left(\frac{K_6}{s} + \frac{K_5}{s^2} + \frac{K_4}{s^3}\right)$$

$$G_J = eG_h\left(\frac{K_6}{s} + \frac{K_5}{s^2} + \frac{K_4}{s^3}\right)\left(1 - G_1\right)$$

$$G_K = -fG_h\left(\frac{K_6}{s} + \frac{K_5}{s^2} + \frac{K_4}{s^3}\right)\left(1 - G_1 - G_2 - G_3 + G_1G_3\right)$$

Substitution of G_1, G_2, G_3, G_5 and G_h into the last nine equations, we can show by partial fraction expansion that the functions G_A/Δ, G_B/Δ, G_C/Δ, G_D/Δ, G_E/Δ, G_F/Δ, G_I/Δ, G_J/Δ, and G_K/Δ are of the following form:

$$\frac{G_i(s)}{\Delta} = \frac{2(1 - e^{-Ts})}{s}\left(\frac{a_{i1}s + b_{i1}\omega_1}{s^2 + \omega_1^2} + \frac{a_{i2}s + b_{i2}\omega_2}{s^2 + \omega_2^2} + \frac{a_{i3}s + b_{i3}\omega_3}{s^2 + \omega_3^2} + \frac{a_{i4}}{s}\right) \quad (3\text{-}7)$$

where i = A, B, C, D, E, F, I, J and K.

$$\omega_1 = 1.31014\times10^{-3}$$
$$\omega_2 = 3.55991\times10^{-3}$$
$$\omega_3 = 3.77726\times10^{-2}$$

$a_{A1} = 7.6593401\times10^{-6}$ $\quad b_{A1} = 5.2968403\times10^{-2}$

$a_{A2} = -5.2124686\times10^{-4}$ $\quad b_{A2} = -1.3266373$

$a_{A3} = 6.894976$ $\quad b_{A3} = 1.653877\times10^{3}$

$a_{B1} = -3.177573\times10^{-3}$ $\quad b_{B1} = -2.1974837\times10^{1}$

$a_{B2} = -7.8558545\times10^{-3}$ $\quad b_{B2} = -1.999412\times10^{1}$

$a_{B3} = 3.5257182$ $\quad b_{B3} = 8.4570434\times10^{2}$

$a_{C1} = -6.6321553\times10^{-4}$ $\quad b_{C1} = -4.5865363$

$a_{C2} = 3.6432745\times10^{-2}$ $\quad b_{C2} = 9.272583\times10^{1}$

$a_{C3} = -3.5504543$ $\quad b_{C3} = -8.5163773\times10^{2}$

$a_{D1} = 1.1863223\times10^{6}$ $\quad b_{D1} = -1.3711851\times10^{2}$

$a_{D2} = 3.9724468\times10^{5}$ $\quad b_{D2} = -1.2475924\times10^{2}$

$a_{D3} = -1.583584\times10^{6}$ $\quad b_{D3} = 5.2770228\times10^{3}$

$a_{E1} = -6.1833492\times10^{8}$ $\quad b_{E1} = 7.1468909\times10^{4}$

$a_{E2} = -2.7868194\times10^{7}$ $\quad b_{E2} = 8.7523256\times10^{3}$

$a_{E3} = 1.8435832\times10^{5}$ $\quad b_{E3} = -6.1434254\times10^{2}$

$a_{E4} = 1.2920375\times10^{9}$

$a_{F1} = -1.2905753\times10^{8}$ $\quad b_{F1} = 1.4916845\times10^{4}$

$a_{F2} = 1.2924317\times10^{8}$ $\quad b_{F2} = -4.0590328\times10^{4}$

$a_{F3} = -1.8564023\times10^{5}$ $\quad b_{F3} = 6.1865076\times10^{2}$

$a_{I1} = 2.3031281\times10^{4}$ $\quad b_{I1} = -6.5239325$

$a_{I2} = -1.7136123\times10^{5}$ $\quad b_{I2} = 1.318941\times10^{2}$

$a_{I3} = 1.4832586\times10^{5}$ $\quad b_{I3} = -1.2113775\times10^{3}$

$a_{J1} = -1.2004364\times10^{7}$ $\quad b_{J1} = 3.4004041\times10^{3}$

$a_{J2} = 1.202163\times10^{7}$ $\quad b_{J2} = -9.2528628\times10^{3}$

$a_{J3} = -1.7267858\times10^{4}$ $\quad b_{J3} = 1.4102663\times10^{2}$

$a_{K1} = -5.80131\times10^{7}$ $\quad b_{K1} = 4.4651788\times10^{4}$

$a_{K2} = -2.5188685\times10^{6}$ $\quad b_{K2} = 7.1350445\times10^{2}$

$a_{K3} = 4.4225387\times10^{5}$ $\quad b_{K3} = -3.6118882\times10^{3}$

$a_{K4} = 1.2017944\times10^{8}$

$a_{A4} = a_{B4} = a_{C4} = a_{D4} = a_{F4} = a_{I4} = a_{J4} = 0$

Equations (3-4), (3-5) and (3-6) are represented by the digital flow graph of Fig. 3-3. The characteristic equation of the sampled-data ASPS is determined by evaluating the Δ of the signal flow graph of Fig. 3-3. We have

$$\begin{aligned}\Delta(z) = 1 &- \mathcal{Z}\left(\frac{G_A}{\Delta}\right) - \mathcal{Z}\left(\frac{G_E}{\Delta}\right) - \mathcal{Z}\left(\frac{G_K}{\Delta}\right) - \mathcal{Z}\left(\frac{G_D}{\Delta}\right)\mathcal{Z}\left(\frac{G_B}{\Delta}\right) - \mathcal{Z}\left(\frac{G_C}{\Delta}\right)\mathcal{Z}\left(\frac{G_I}{\Delta}\right) - \mathcal{Z}\left(\frac{G_F}{\Delta}\right)\mathcal{Z}\left(\frac{G_J}{\Delta}\right) \\ &- \mathcal{Z}\left(\frac{G_B}{\Delta}\right)\mathcal{Z}\left(\frac{G_I}{\Delta}\right)\mathcal{Z}\left(\frac{G_F}{\Delta}\right) - \mathcal{Z}\left(\frac{G_C}{\Delta}\right)\mathcal{Z}\left(\frac{G_D}{\Delta}\right)\mathcal{Z}\left(\frac{G_J}{\Delta}\right) + \mathcal{Z}\left(\frac{G_A}{\Delta}\right)\mathcal{Z}\left(\frac{G_E}{\Delta}\right) + \mathcal{Z}\left(\frac{G_A}{\Delta}\right)\mathcal{Z}\left(\frac{G_K}{\Delta}\right) \\ &+ \mathcal{Z}\left(\frac{G_A}{\Delta}\right)\mathcal{Z}\left(\frac{G_F}{\Delta}\right)\mathcal{Z}\left(\frac{G_J}{\Delta}\right) + \mathcal{Z}\left(\frac{G_E}{\Delta}\right)\mathcal{Z}\left(\frac{G_K}{\Delta}\right) + \mathcal{Z}\left(\frac{G_E}{\Delta}\right)\mathcal{Z}\left(\frac{G_C}{\Delta}\right)\mathcal{Z}\left(\frac{G_I}{\Delta}\right) \\ &+ \mathcal{Z}\left(\frac{G_K}{\Delta}\right)\mathcal{Z}\left(\frac{G_D}{\Delta}\right)\mathcal{Z}\left(\frac{G_B}{\Delta}\right) - \mathcal{Z}\left(\frac{G_A}{\Delta}\right)\mathcal{Z}\left(\frac{G_E}{\Delta}\right)\mathcal{Z}\left(\frac{G_K}{\Delta}\right) \qquad (3\text{-}8)\end{aligned}$$

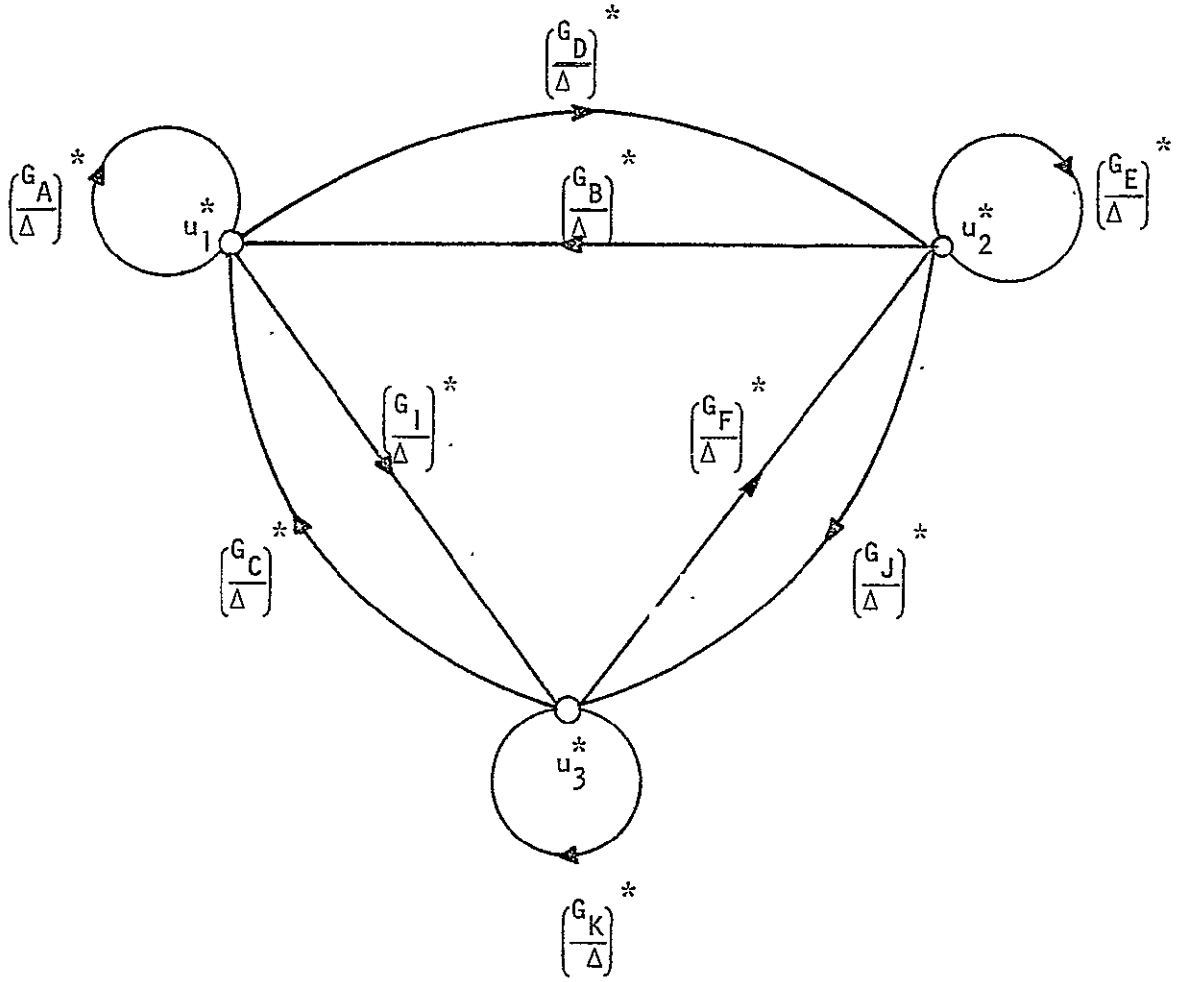

Figure 3-3. Digital signal flow graph of Eqs. (3-3), (3-4) and (3-5).

Since ω_1, ω_2 and ω_3 are small, and $b_{ij}\omega_j \ll a_{ij}$ for i = A, B, C, D, E, F, I, J, K, and j = 1, 2, 3, the z-transform of G_i/Δ can be approximated and simplified. This is justified as follows:

$$\mathcal{Z}\left[\frac{G_A}{\Delta}\right] = 2(1 - z^{-1})\mathcal{Z}\left[\frac{a_{A1}s + b_{A1}\omega_1}{s(s^2 + \omega_1^2)} + \frac{a_{A2}s + b_{A2}\omega_2}{s(s^2 + \omega_2^2)} + \frac{a_{A3}s + b_{A3}\omega_3}{s(s^2 + \omega_3^2)}\right] \tag{3-9}$$

Then

$$\mathcal{Z}\left[\frac{a_{A1}s + b_{A1}\omega_1}{s(s^2 + \omega_1^2)}\right] = \frac{a_{A1}z\sin\omega_1 T}{\omega_1(z^2 - 2z\cos\omega_1 T + 1)} + \frac{b_{A1}}{\omega_1}\left[\frac{z}{z - 1} - \frac{z(z - \cos\omega_1 T)}{z^2 - 2z\cos\omega_1 T + 1}\right] \tag{3-10}$$

For small $\omega_1 T$,

$$\sin\omega_1 T \simeq \omega_1 T$$

$$\cos\omega_1 T \simeq 1$$

Equation (3-10) becomes

$$\mathcal{Z}\left[\frac{a_{A1}s + b_{A1}\omega_1}{s(s^2 + \omega_1^2)}\right] \simeq \frac{a_A zT}{(z - 1)^2} \tag{3-11}$$

Thus, Eq. (3-9) becomes

$$\mathcal{Z}\left[\frac{G_A}{\Delta}\right] \simeq \frac{2T}{z - 1}(a_{A1} + a_{A2} + a_{A3}) = \frac{13.7889T}{z - 1} \tag{3-12}$$

Similarly,

$$\mathcal{Z}\left[\frac{G_B}{\Delta}\right] \simeq \frac{2T}{z - 1}(a_{B1} + a_{B2} + a_{B3}) = \frac{7.029369T}{z - 1} \tag{3-13}$$

$$\mathcal{Z}\left[\frac{G_C}{\Delta}\right] \simeq \frac{2T}{z - 1}(a_{C1} + a_{C2} + a_{C3}) = \frac{-7.029369T}{z - 1} \tag{3-14}$$

$$\mathcal{Z}\left[\frac{G_D}{\Delta}\right] \simeq \frac{2T}{z - 1}(a_{D1} + a_{D2} + a_{D3}) = \frac{-34.04T}{z - 1} \tag{3-15}$$

$$\mathcal{Z}\left[\frac{G_E}{\Delta}\right] \simeq \frac{T}{z - 1}(2a_{E1} + 2a_{E2} + 2a_{E3} + a_{E4}) = \frac{-11T}{z - 1} \tag{3-16}$$

$$\left(\frac{G_F}{\Delta}\right) \simeq \frac{2T}{z-1}(a_{F1} + a_{F2} + a_{F3}) = \frac{-0.46T}{z-1} \tag{3-17}$$

$$\left(\frac{G_I}{\Delta}\right) \simeq \frac{2T}{z-1}(a_{I1} + a_{I2} + a_{I3}) = \frac{-8.18T}{z-1} \tag{3-18}$$

$$\left(\frac{G_J}{\Delta}\right) \simeq \frac{2T}{z-1}(a_{J1} + a_{J2} + a_{J3}) = \frac{-3.716T}{z-1} \tag{3-19}$$

$$\left(\frac{G_K}{\Delta}\right) \simeq \frac{T}{z-1}(2a_{K1} + 2a_{K2} + 2a_{K3} + a_{K4}) = \frac{10.7T}{z-1} \tag{3-20}$$

Substituting these terms into Eq. (3-8) and simplifying, we have the characteristic equation as

$$z^3 - (3 + 13.49T)z^2 + (3 + 26.978T + 361.59T^2)z - (1 + 13.49T + 361.59T^2 + 687T^3) = 0 \tag{3-21}$$

It should be noted that the digital ASPS is originally a twelveth-order system. Because ω_1, ω_2, and ω_3 are very small, the analysis conducted here results in a third-order approximation with the characteristic equation given in Eq. (3-21). When we neglected ω_1, ω_2 and ω_3, in essence we have made a variation on the unit circle in the z-plane. Thus, the stability criterion should be modified to $|z| < 1\pm\varepsilon$ where ε depends on the value of ω_1, ω_2 and ω_3. As a matter of fact, for small sampling periods, the characteristic roots of the system are all very close to the $z = 1$ point in the z-plane.

The roots of Eq. (3-21) for T = 0.001, 0.01 and 0.1 sec are tabulated as follows:

T = 0.001 sec $z = 0.9372,\ 1.038 \pm j0.0604$

T = 0.01 sec $z = 1.0192,\ 1.0578 \pm j0.175$

T = 0.1 sec $z = 1.203,\ 1.573 \pm j1.7478$

Although in a strict sense these roots are all outside the unit circle, and the corresponding system are all unstable, as discussed above, the roots for T = 0.001 sec are so close to the unit circle that if enough accuracy

were carried out in the analysis without approximation, these roots could actually be inside the unit circle. In any case, for T = 0.1 sec or greater the digital system is definitely unstable. As will be verified by computer simulation results in the next chapter, the digital ASPS is stable for T = 0.001 sec and unstable for T = 0.1 sec, with the stability boundary being somewhere around T = 0.0075 sec.

Therefore, the approximation conducted on the z-transform analysis still gave useful results on the stability condition of the digital ASPS with respect to the sampling period T. Because the characteristic roots of the system are all very close to the z = 1 point for stable values of T, an accurate analysis using the exact model is almost impossible even with the aide of a digital computer.

IV. COMPUTER SIMULATION OF THE DIGITAL ASPS

4.1 The Digital ASPS With The Sampled-Data Controller

It was discussed in the preceding chapter that the digital ASPS was obtained by placing sample-and-hold units in the control inputs of the x_1, ϕ_1 and ϕ_2 components, using the same feedback gains as designed for the continuous-data system. The z-transform analysis conducted in the last chapter showed that the digital ASPS is unstable for sampling periods greater than 0.01 seconds approximately.

The computer listing of the simulation program for the digital ASPS without guantization effects is given in Table 4-1.

The simulation results verified that the digital ASPS neglecting quantization is unstable for sampling periods greater than 0.01 second. When the sampling period is less than or equal to 0.075 seconds, the simulated responses remained stable.

Figure 4-1 illustrates the time response of the x_1 dynamics when T = 0.005 seconds. The initial conditions are: $x_1(0) = 2\times10^{-3}$ and $\dot{x}_1(0) = 0$. Figure 4-2 shows the same response of x_1 for t greater than 6 seconds. The vertical scale is changed to show the oscillatory characteristics as the response decays to zero.

Figures 4-3 and 4-4 illustrate the time responses of ϕ_1 and ϕ_2, respectively, when T = 0.005 seconds.

Although the overshoots of the time responses of the digital ASPS are quite large for T = 0.005 sec., it can be shown that these overshoots are substantially reduced by reducing the sampling period T.

4.2 The Digital ASPS With Quantization

In this section the effect of quantization in the sample-and-hold channels of x_1, ϕ_1 and ϕ_2 is investigated by means of computer simulation.

```
      DIMENSION PRMT(5),Y(8),DERY(8),AUX(8,8)
      EXTERNAL FCT,OUTP
      COMMON X,XDOT,PHI1,PHI1DT,PHI1IN,PHI2,PHI2DT,PHI2IN,T,
     &  V1,V2,V3,AJ,AMI,AKSX,AKSP,AKSS,A33,TPRT,RB,DELTA,
     &  A0,B0,C0,D0,E,F,TEND,
     &  NPRT,IV1,IV2,IV3,LINE
      OPEN(UNIT=6,DEVICE='DSK',FILE='FOR20.DAT',ACCESS='SEQOUT')

      LINE=0
      TSP=0.005
      H=0.
      TEND=100.
      TPRT=0.05
      TINT=0.5E-3
C-----SET INITIAL CONDITIONS
      X=2.0E-3
      XDOT=0.
      PHI1=0.013
      PHI1DT=0.
      PHI1IN=0.
      PHI2=0.013
      PHI2DT=0.
      PHI2IN=0.
      AMI=600.
      AKSX=1.051
      AKSP=0.005
      AKSS=0.005
      AJ=503.
      A33=2805.11
      RB=1.956
      A0=RB
      B0=1./AMI
      C0=AMI*RB/A33
      D0=AJ/A33
      E=1./A33
      F=1./AJ
      DELTA=1.-A0*C0-D0
      T=0.
      NPRT=0
      PRMT(3)=TINT
      PRMT(4)=0.01*X
      DO 99 I=1,8
99    DERY(I)=0.125
      NDIM=8
10    IF(T.GE.TEND) CALL EXIT
      V1=0.9133805*X+0.1008105*XDOT
      V2=0.6460207*PHI1IN+0.5693D6*PHI1-0.4894D5*PHI1DT
      V3=0.6009006*PHI2IN+0.1299206*PHI2+0.1175605*PHI2DT

      PRMT(1)=T
      PRMT(2)=T+TSP
      Y(1)=X
      Y(2)=XDOT
      Y(3)=PHI1IN
      Y(4)=PHI1
      Y(5)=PHI1DT
      Y(6)=PHI2IN
      Y(7)=PHI2
      Y(8)=PHI2DT
```

```
      CALL RKGS(PRMT,Y,DERY,NDIM,IHLF,FCT,OUTP,AUX)
      GO TO 10
      END

      SUBROUTINE FCT(XX,Y,DERY)
      DIMENSION  Y(8),DERY(8)
      COMMON X,XDOT,PHI1,PHI1DT,PHI1IN,PHI2,PHI2DT,PHI2IN,T,
     &  V1,V2,V3,AJ,AM1,AKSX,AKSP,AKSS,A33,TPRT,RB,DELTA,
     &  A0,B0,C0,D0,E,F,TEND,
     &  NPRT,IV1,IV2,IV3,LINE
      DERY(1)=Y(2)
      DERY(2)=((-V1*B0-AKSX*B0*Y(1))*(1.-D0)+A0*((-V2-AKSP*Y(4))*E
     &           +(V3+AKSS*Y(7))*F*D0))/DELTA
      DERY(3)=Y(4)
      DERY(4)=Y(5)
      DERY(5)=((-V2-AKSP*Y(4))*E-(V1+AKSX*Y(1))*B0*C0
     &          +(V3+AKSS*Y(7))*D0*F)/DELTA
      DERY(6)=Y(7)
      DERY(7)=Y(8)
      DERY(8)=((-V3-AKSS*Y(7))*F*(1.-A0*C0)+(V2+AKSP*Y(4))*E
     &          +(V1+AKSX*Y(1))*B0*C0)/DELTA
      RETURN
      END
      SUBROUTINE OUTF(XX,Y,DERY,IHLF,NDIM,PRMT)
      DIMENSION Y(8),DERY(8),PRMT(5)
      COMMON X,XDOT,PHI1,PHI1DT,PHI1IN,PHI2,PHI2DT,PHI2IN,T,
     &  V1,V2,V3,AJ,AM1,AKSX,AKSP,AKSS,A33,TPRT,RB,DELTA,
     &  A0,B0,C0,D0,E,F,TEND,
     &  NPRT,IV1,IV2,IV3,LINE
      IF (XX.GT.TEND) PRMT(5)=1.
      T=XX
      IF(XX.LT.TPRT*FLOAT(NPRT)) RETURN
      LINE=LINE+1
      WRITE(6,100) IHLF,XX,(Y(I),I=1,8)
100   FORMAT(1X,I2,3X,1PE10.4,1P8E11.3)
      X=Y(1)
      XDOT=Y(2)
      PHI1IN=Y(3)
      PHI1=Y(4)
      PHI1DT=Y(5)
      PHI2IN=Y(6)
      PHI2=Y(7)
      PHI2DT=Y(8)
      NPRT=NPRT+1
      IF(LINE.LT.10) GO TO 200
      WRITE(5,100) IHLF,XX,(Y(I),I=1,8)
      LINE=0
200   RETURN
      END
```

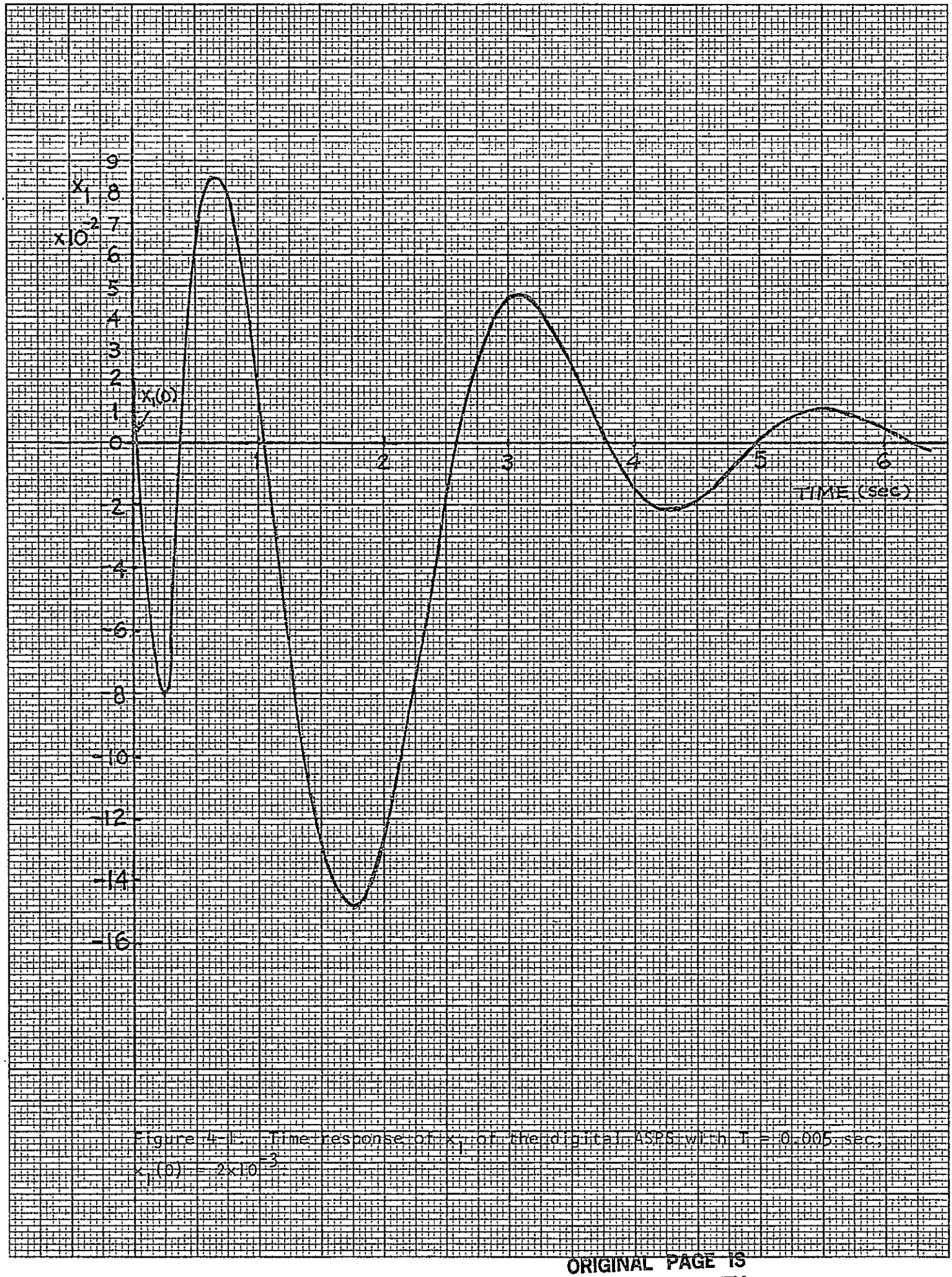

Figure 4-1. Time response of x_1 of the digital ASPS with $T = 0.005$ sec; $x_1(0) = 2 \times 10^{-3}$

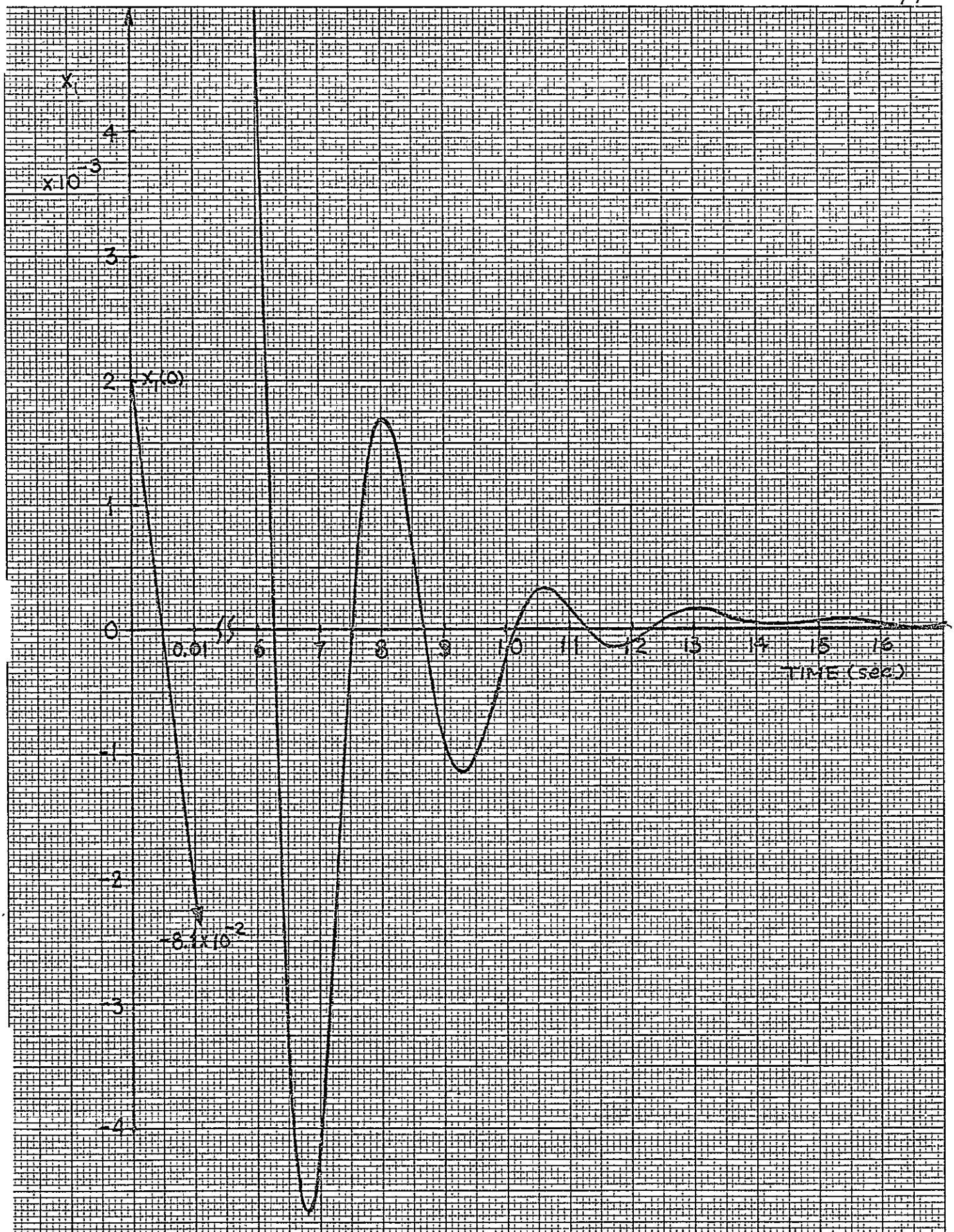

Figure I-2. Time response of x_1 of the digital ASPS with T = 0.005 sec.

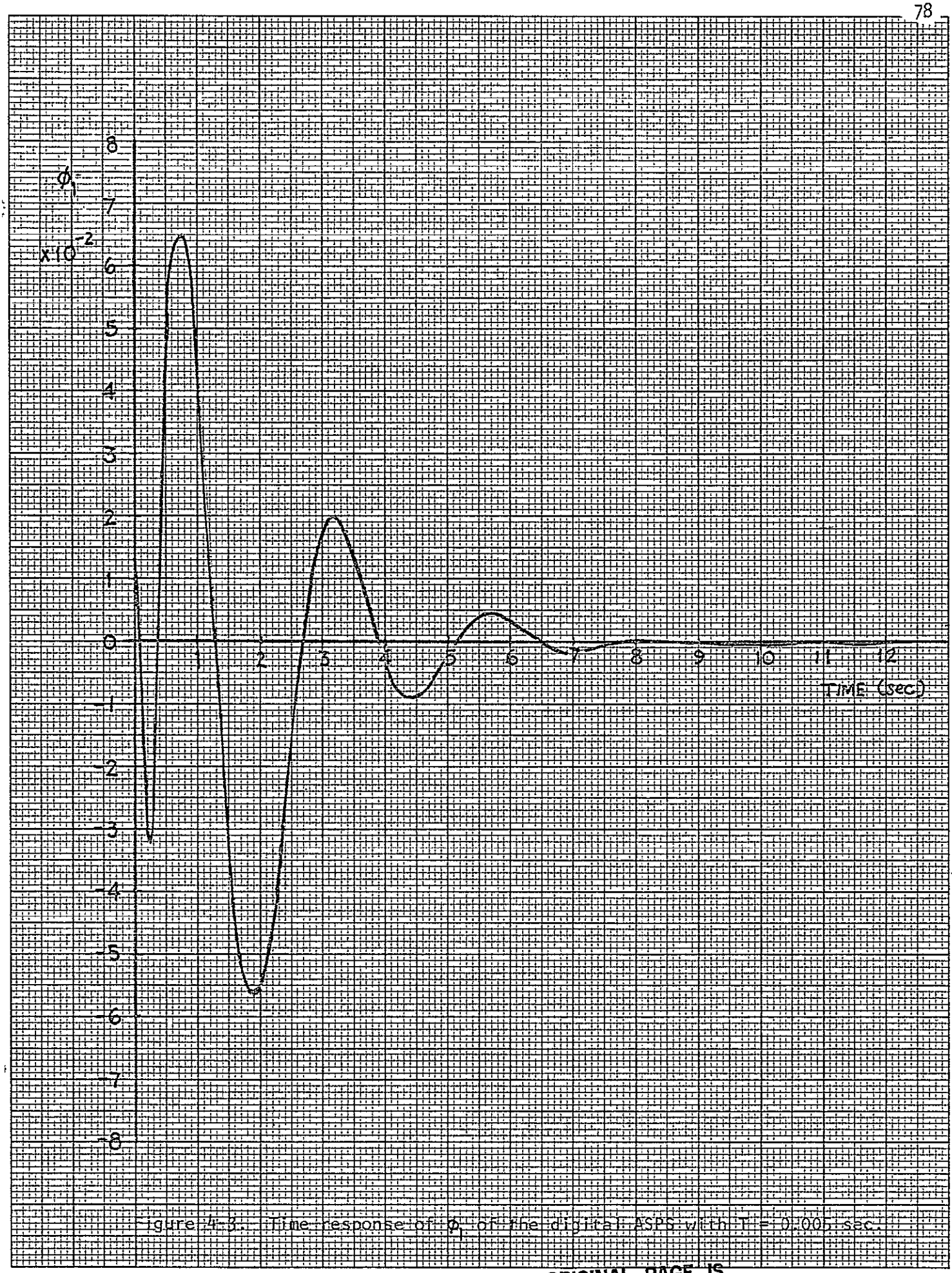

Figure 4.3. Time response of ϕ_1 of the digital ASPS with T = 0.005 sec.

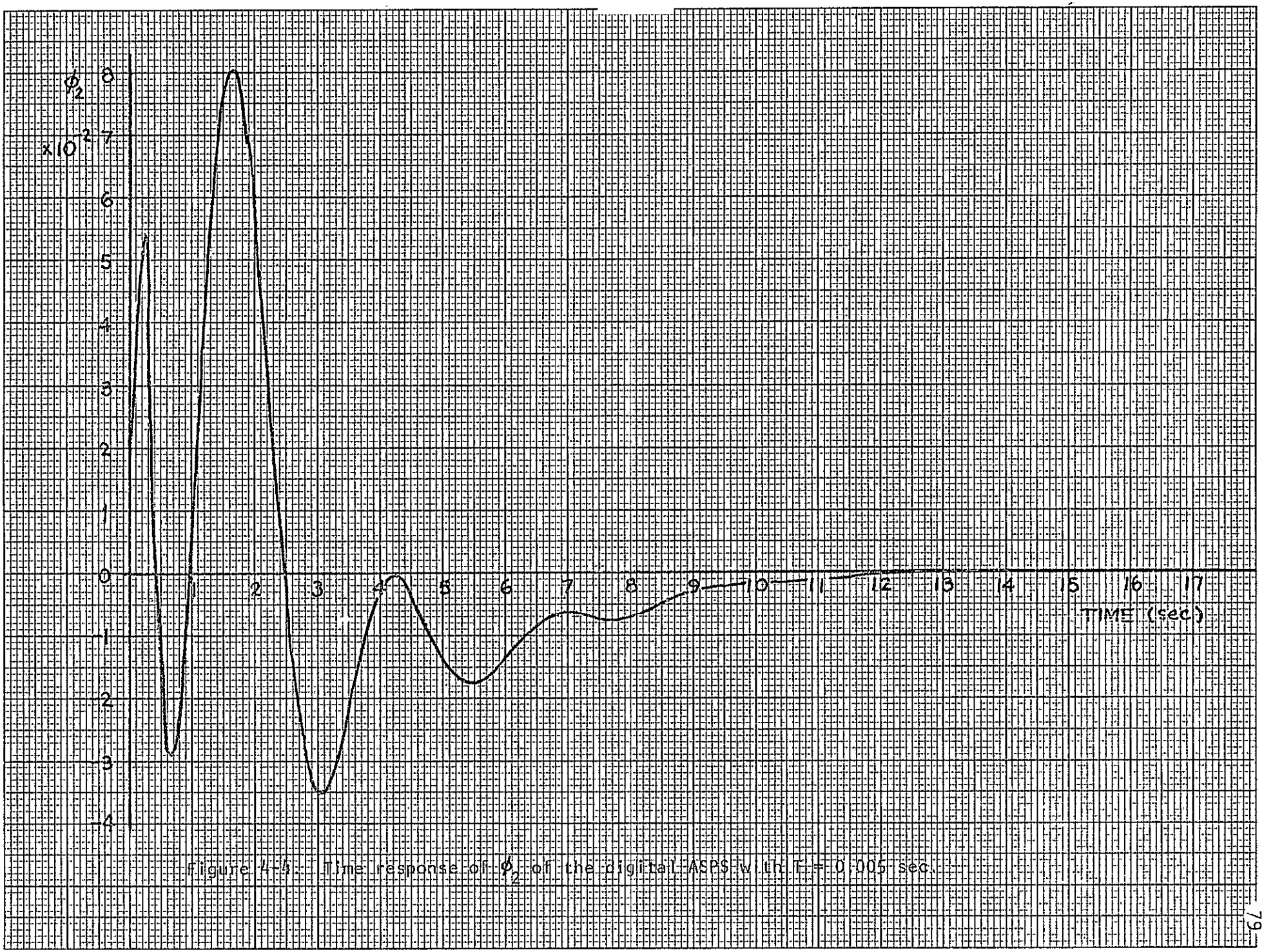

Figure 4-5. Time response of ϕ_2 of the digital ASPS with T = 0.005 sec.

The computer program listing is given in Table 4-2.

When 8-bit quantizers are placed in any or all of the input channels of the digital ASPS the system is still stable, and no sustained oscillations were observed. Figure 4-5 shows the phase plane trajectories of x_1 versus $\dot{x}_1$ of the digital ASPS with and without an 8-bit quantizer. The quantizer is placed only in the x_1 channel.

Figures 4-6 and 4-7 illustrate the time responses of ϕ_1 and ϕ_2, respectively, with the 8-bit quantizer for x_1, and T = 0.005 seconds.

Figure 4-8 gives the phase plane trajectory of x_1 versus $\dot{x}_1$ when a 16-bit quantizer is placed in the x_1 channel only. The trajectory of x_1 with the 8-bit quantizer is also shown in the same figure for comparison. Note that for the same time instants the response of x_1 with the 8-bit quantizer is greater than that of the response with the 16-bit quantizer. The phase plane representation of x_1 is chosen because of the high oscillations in the responses which make the time response difficult to plot.

Figures 4-9 and 4-10 illustrate the time responses of ϕ_1 and ϕ_2, respectively, for T = 0.005 sec and a 16-bit quantizer in the x_1 channel. The overshoots in these responses are smaller than the corresponding ones in Figs. 4-6 and 4-7 which are for the 8-bit quantizer.

Figures 4-11, 4-12 and 4-13 show that results on the responses of x_1, ϕ_1 and ϕ_2, respectively, when an 8-bit quantizer is placed in the ϕ_1 channel only. The sampling period is 0.005 seconds.

Figures 4-14, 4-15 and 4-16 show the time responses of x_1, ϕ_1 and ϕ_2, respectively, when an 8-bit quantizer is placed in the ϕ_2 channel only. The sampling period is 0.005 seconds.

Figures 4-17, 4-18 and 4-19 give the time responses of x_1, ϕ_1 and ϕ_2,

respectively, when an 8-bit quantizer is placed in each of the three control input channels, and the sampling period is 0.002 seconds. As mentioned earlier the oscillations and overshoots are substantially reduced when the sampling period is smaller.

Table 4-2. Computer Simulation Program of the Digital ASPS with Quantization.

```
      DIMENSION PRMT(5),Y(8),DERY(8),AUX(9,9)
      EXTERNAL FCT,OUTP
      COMMON X,XDOT,PHI1,PHI1DT,PHI1IN,PHI2,PHI2DT,PHI2IN,T,
     &  V1,V2,V3,AJ,AMI,AKSX,AKSP,AKSS,A33,TPRI,R0,DELTA,
     &  A0,B0,C0,D0,E,F,TEND,H,
     &  NPRT,IV1,IV2,IV3,LINE
      OPEN(UNIT=6,DEVICE='DSK',FILE='FOR20.DAT',ACCESS='SEQOUT')

      LINE=0
      TSP=0.002
      H=2.**-8
      TEND=100.
      IPRT=0.05
      TINT=0.5E-4
C-----SET INITIAL CONDITIONS
      X=1.0E-3
      XDOT=0.
      PHI1=0.002
      PHI1DT=0.
      PHI1IN=0.
      PHI2=0.002
      PHI2DT=0.
      PHI2IN=0.
      AMI=600.
      AKSX=1.051
      AKSP=0.005
      AKSS=0.005
      AJ=503.
      A33=2805.15
      R0=1.956
      A0=R0
      B0=1./AMI
      C0=AMI*R0/A33
      D0=AJ/A33
      E=1./A33
      F=1./AJ
      DELTA=1.-A0*C0-B0
      T=0.
      NPRT=0
      PRMT(3)=TINT
      PRMT(4)=0.05*X
      DO 99 I=1,8
99    DERY(I)=0.125
      NDIM=8
10    IF(T.GE.TEND) CALL EXIT
      V1=0.913380*X+0.100810*XDOT
      V2=0.846207*PHI1IN+0.569936*PHI1-0.089430*PHI1DT
      V3=0.800906*PHI2IN+0.129206*PHI2+0.117560*PHI2DT

      CALL QUANTZ(V1)
      CALL QUANTZ(V2)
      CALL QUANTZ(V3)

      PRMT(1)=T
      PRMT(2)=T+TSP
```

```
      Y(1)=X
      Y(2)=XDOT
      Y(3)=PHI1IN
      Y(4)=PHI1
      Y(5)=PHI10
      Y(6)=PHI21N
      Y(7)=PHI2
      Y(8)=PHI2DT

      CALL RKGS(PRMT,Y,DERY,NDIM,IHLF,FCT,OUTP,AUX)
      GO TO 10
      END

      SUBROUTINE QUANTZ(XX)
      COMMON X,XDOT,PHI1,PHI1DT,PHI1IN,PHI2,PHI2DT,PHI2IN,T,
     1  V1,V2,V3,AJ,AMI,AK,AX,AKSP,AKS,AM3,TPKT,KB,DELTA,
     2  A0,B0,C0,D0,E,F,TEND,H,
     3  NPRT,IV1,IV2,IV3,LINE
      IF(XX.LT.0.) GO TO 20
      IV=(XX/H)+0.5
      GO TO 30
      IV=(XX/H)-0.5
      XX=FLOAT(IV)*H
      RETURN
      END
```

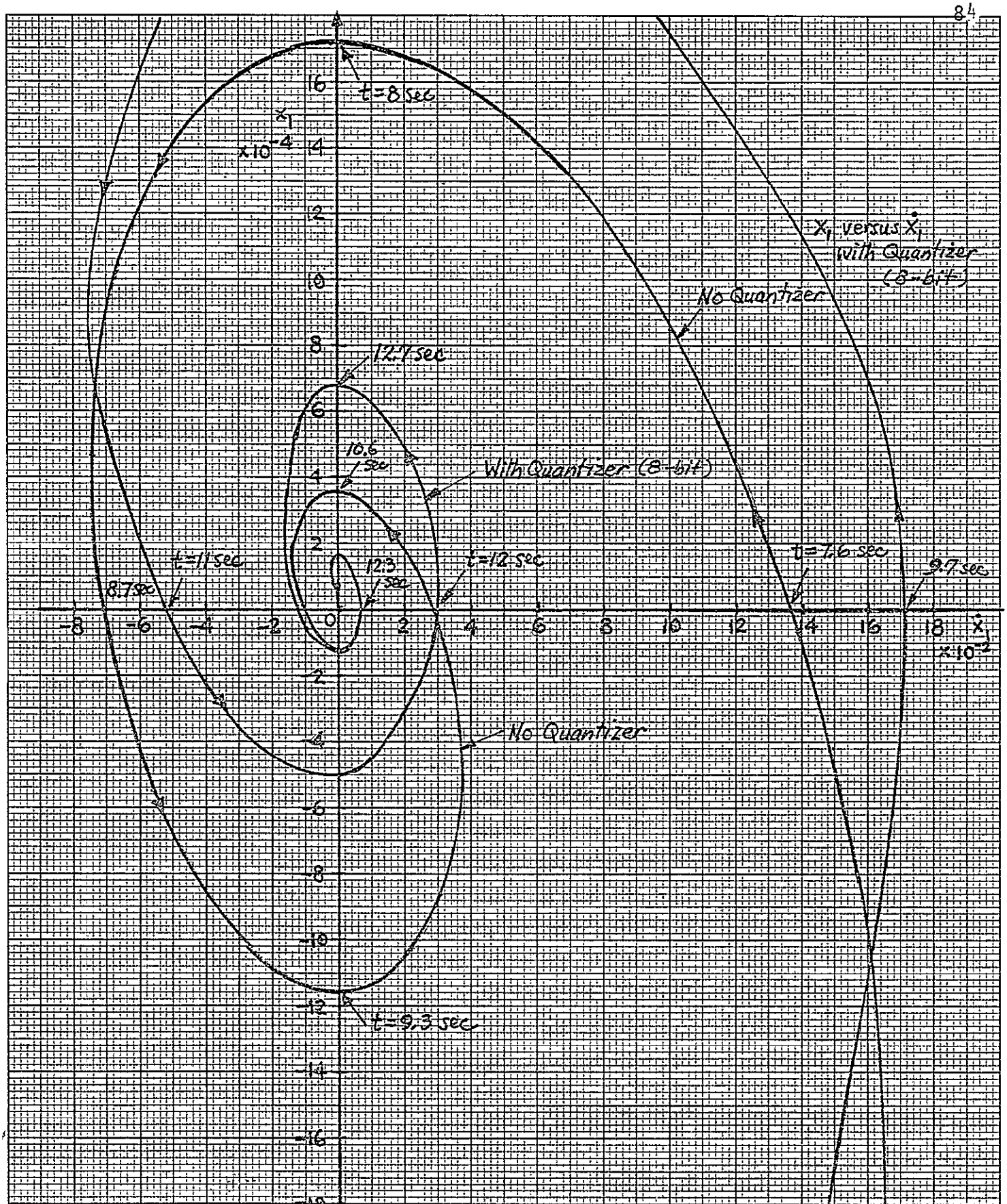

Figure 4-5. Phase plane trajectories of x_1 versus $\dot{x}_1$ of the digital ASPS with and without 8-bit quantizer. T = 0.005 sec. Quantizer is only in the x_1 channel.

Figure 4-6. Time response of ϕ_1 of the digital ASPS with 8-bit quantizer. For T = 0.005 sec. The quantizer is only in the x_1 channel.

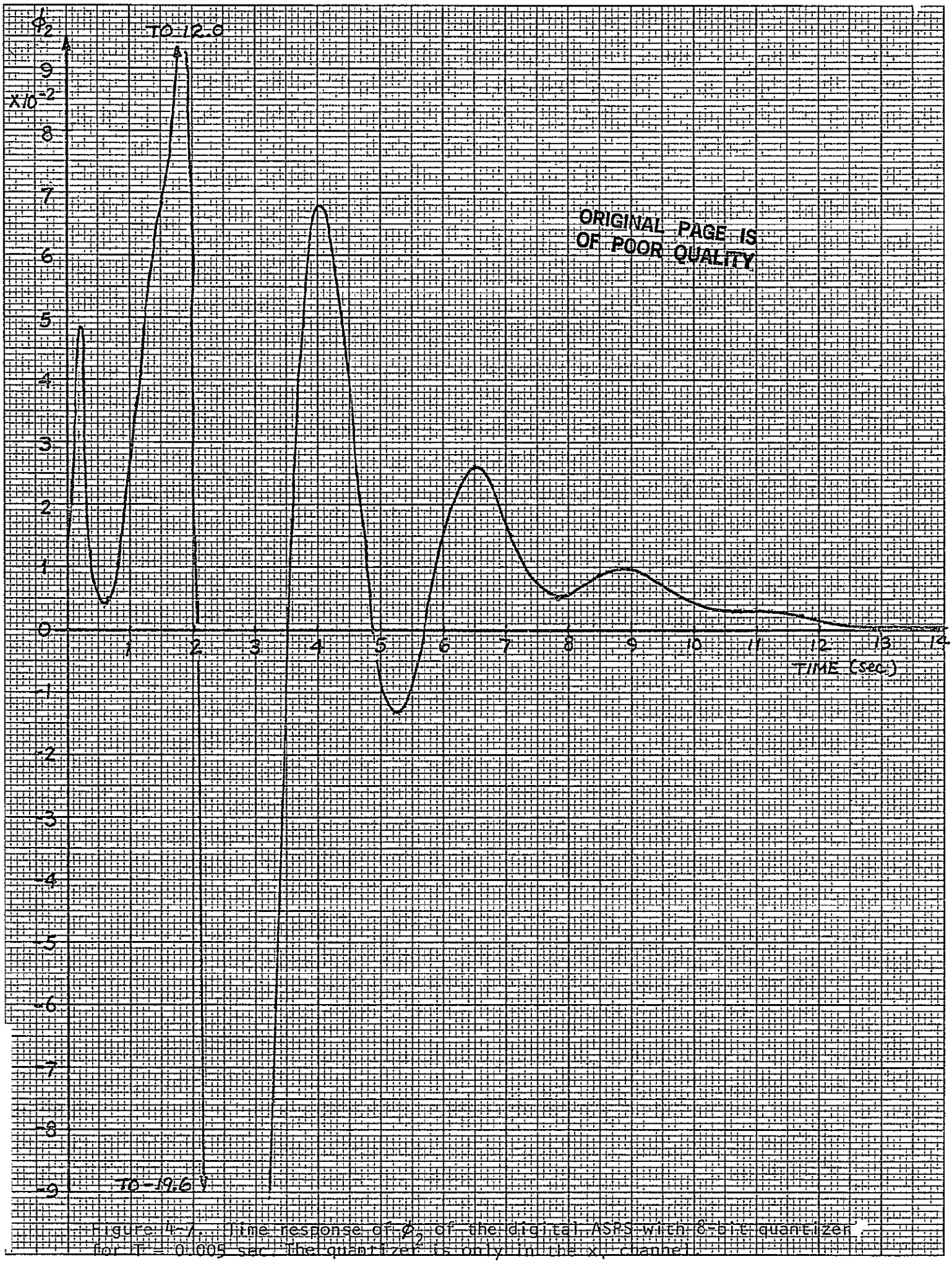

Figure 4-1. Time response of ϕ_2 of the digital ASPS with 8-bit quantizer for T = 0.005 sec. The quantizer is only in the x_1 channel.

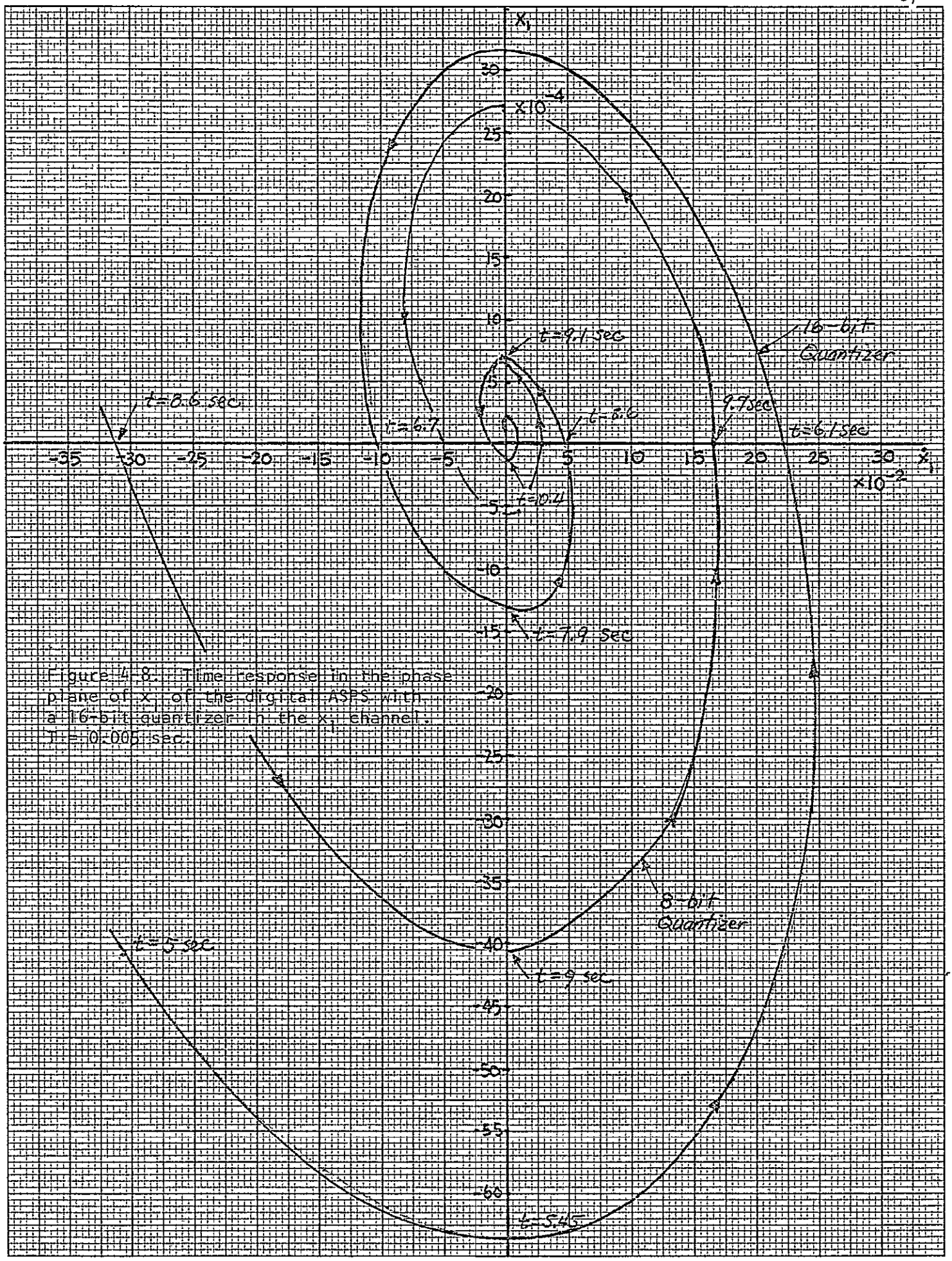

Figure 4.8. Time response in the phase plane of x_1 of the digital ASPS with a 16-bit quantizer in the x_1 channel. T = 0.005 sec.

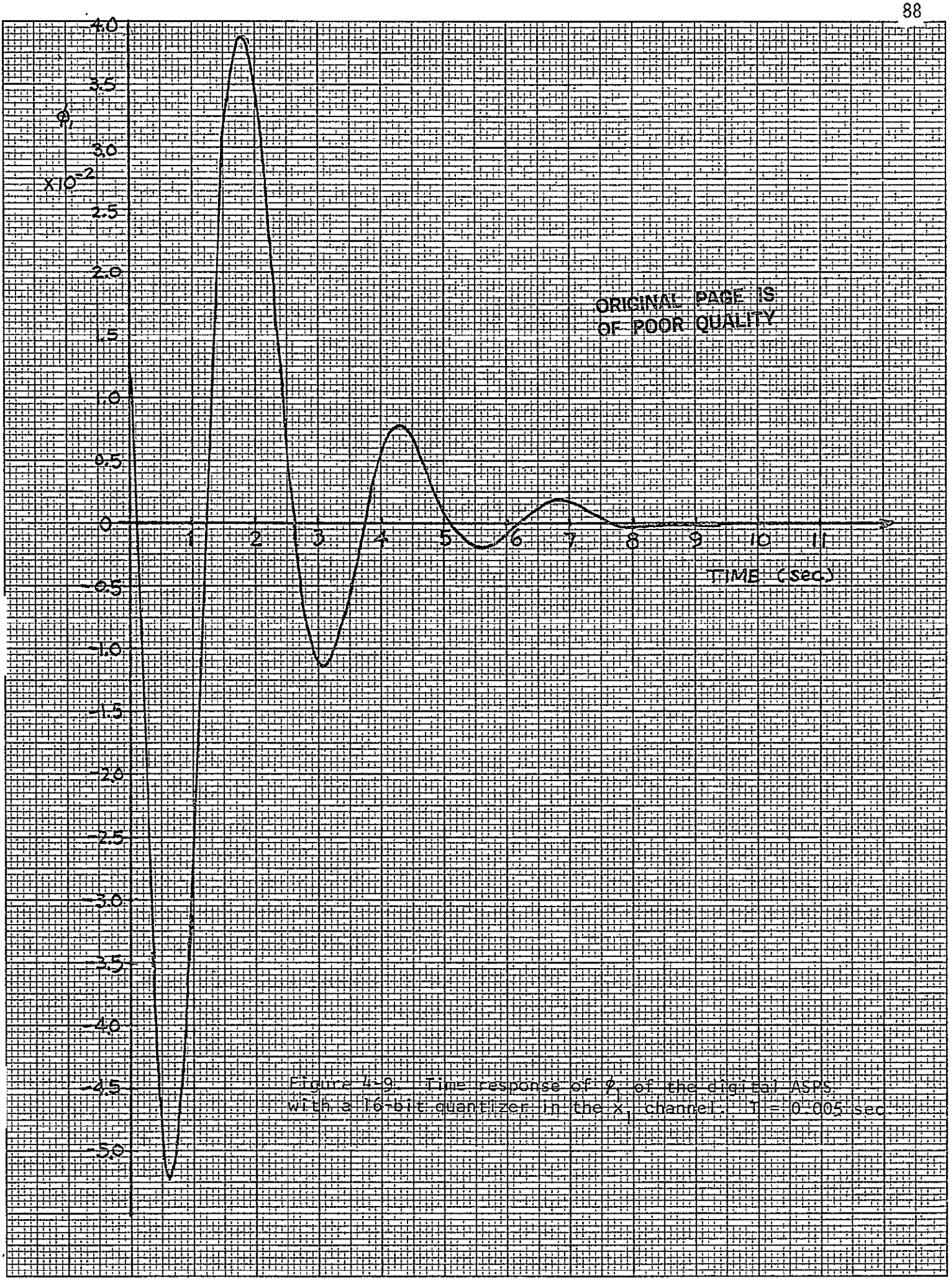

Figure 4-9. Time response of ℓ_1 of the digital ASPS with a 16-bit quantizer in the x_1 channel. T = 0.005 sec.

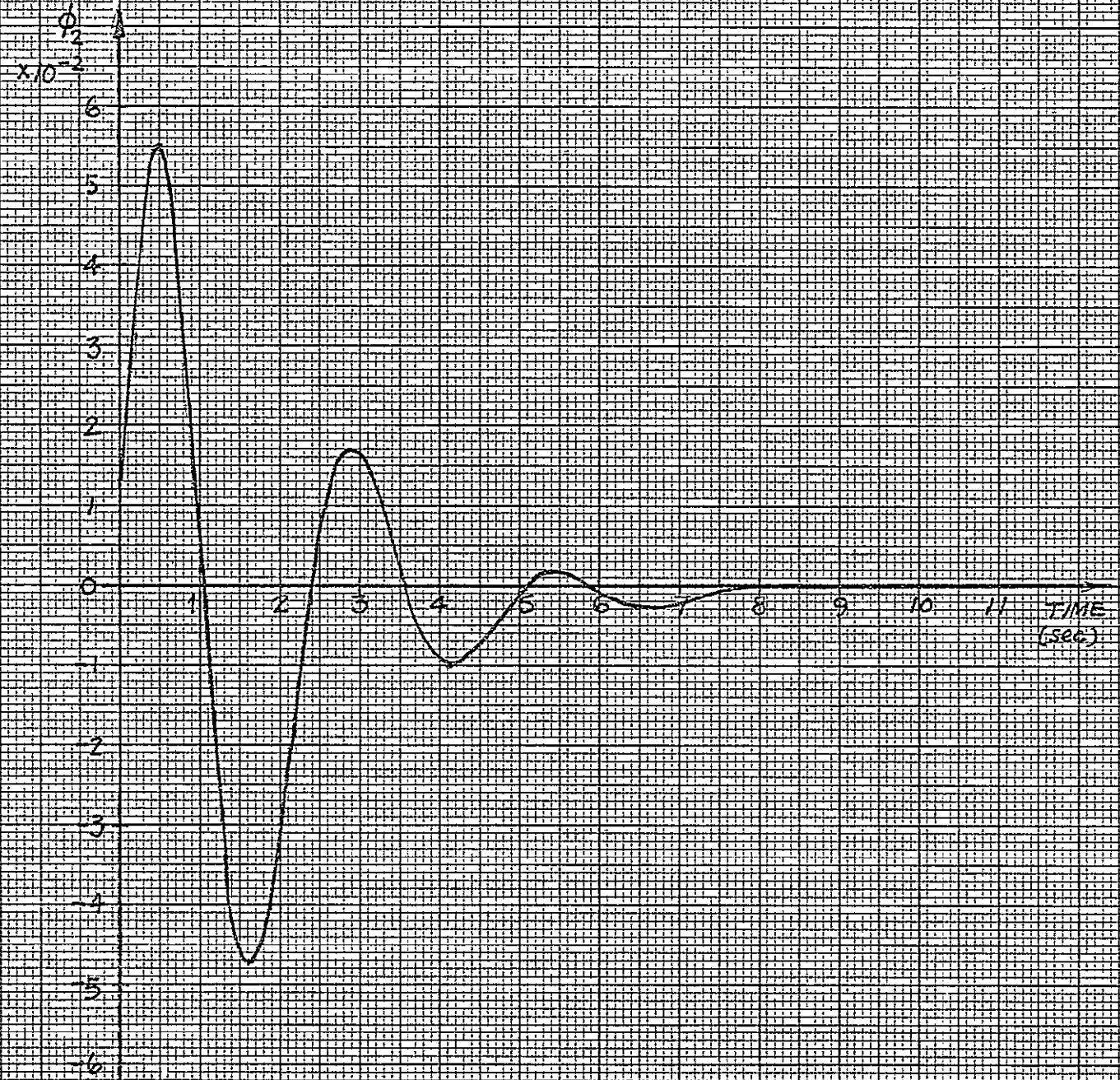

Figure 4-10. Time response of ϕ_2 of the digital ASRS with a 16-bit quantizer in the x_1 channel. $T = 0.005$ sec.

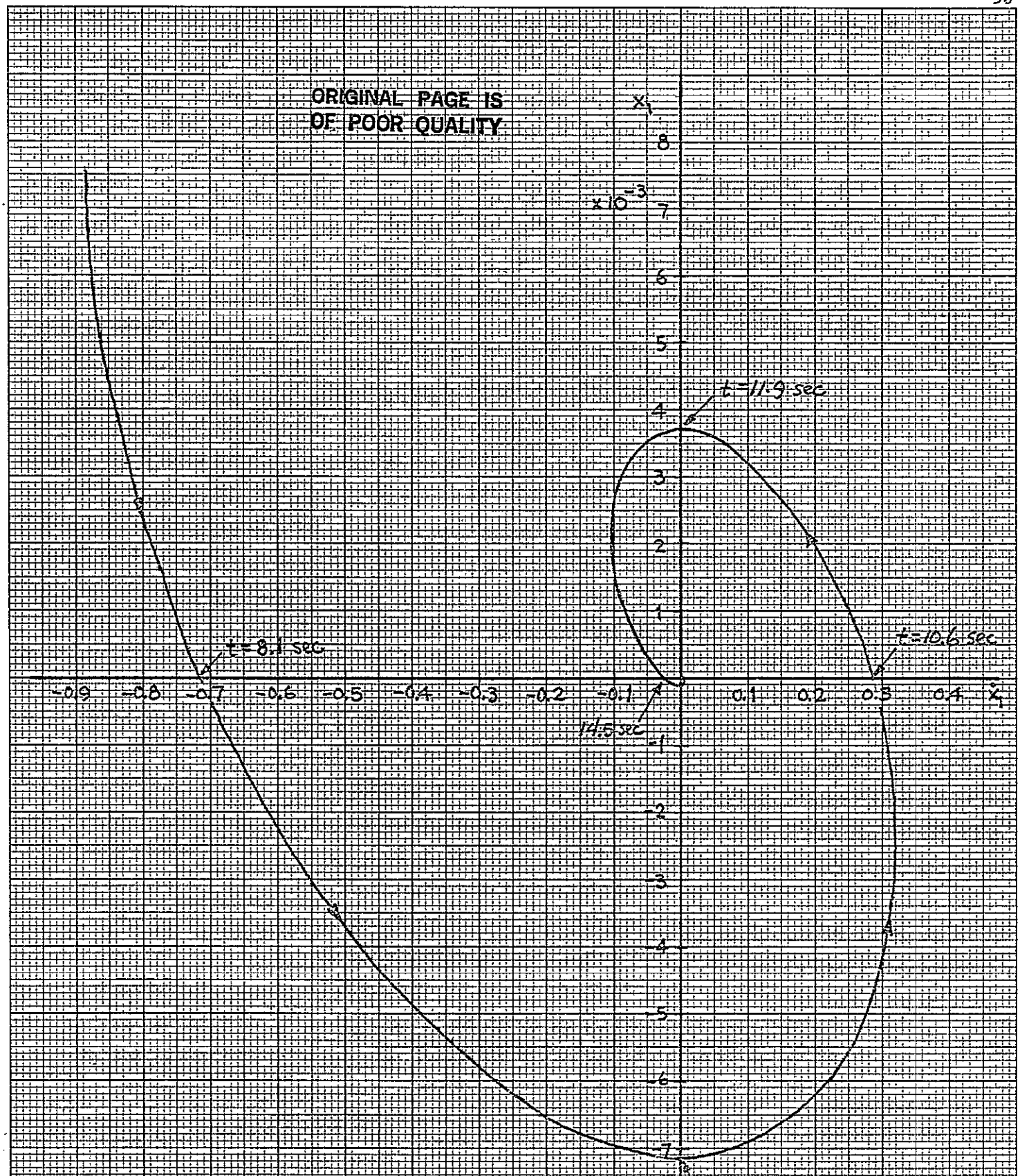

Figure 4-11. Phase plane trajectory of x_1 versus $\dot{x}_1$ of the digital ASPS with an 8-bit quantizer in the ϕ_1 channel. $T = 0.005$ sec.

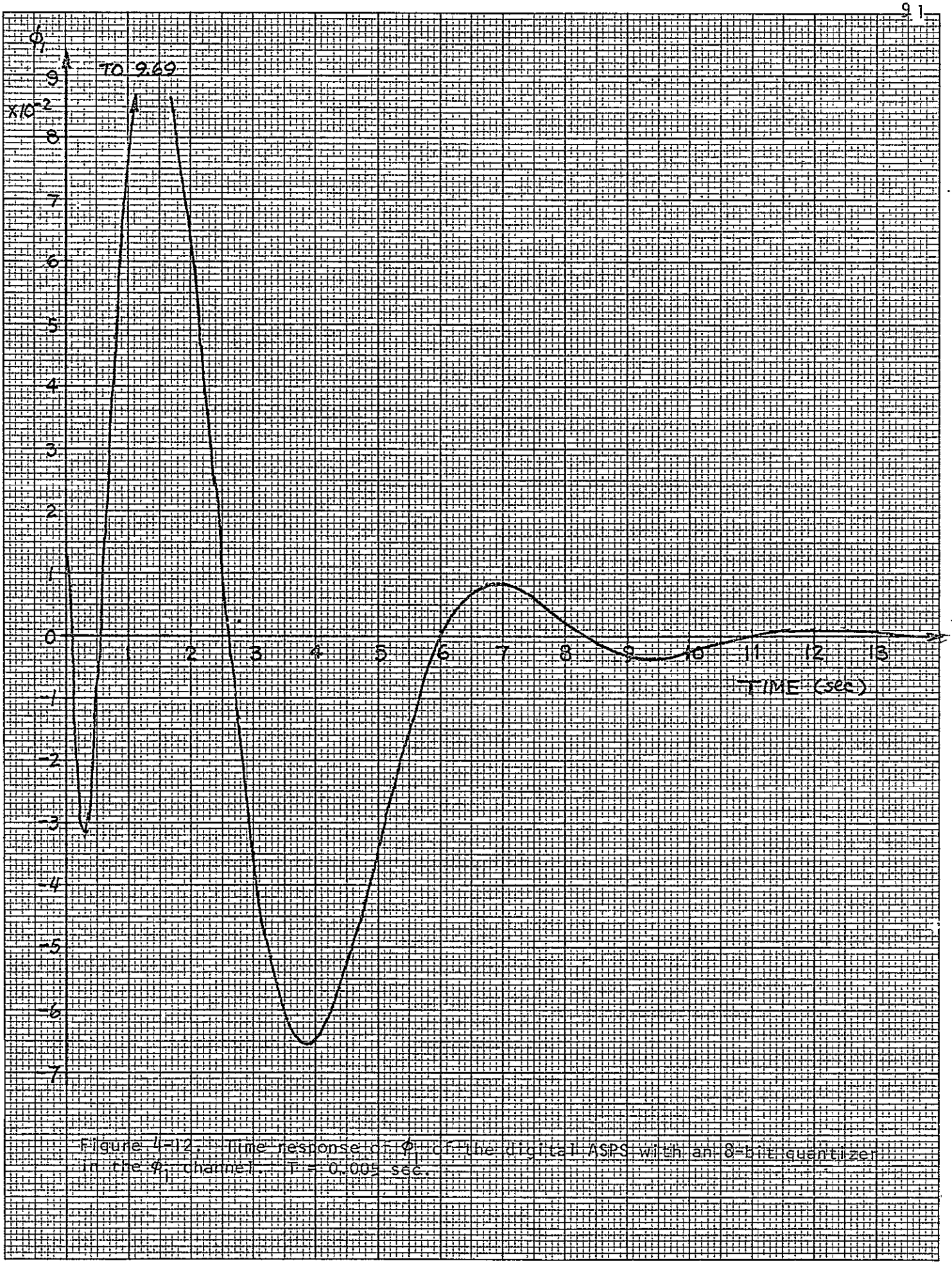

Figure 4-12. Time response of ϕ_1 of the digital ASPS with an 8-bit quantizer in the ϕ_1 channel. T = 0.005 sec.

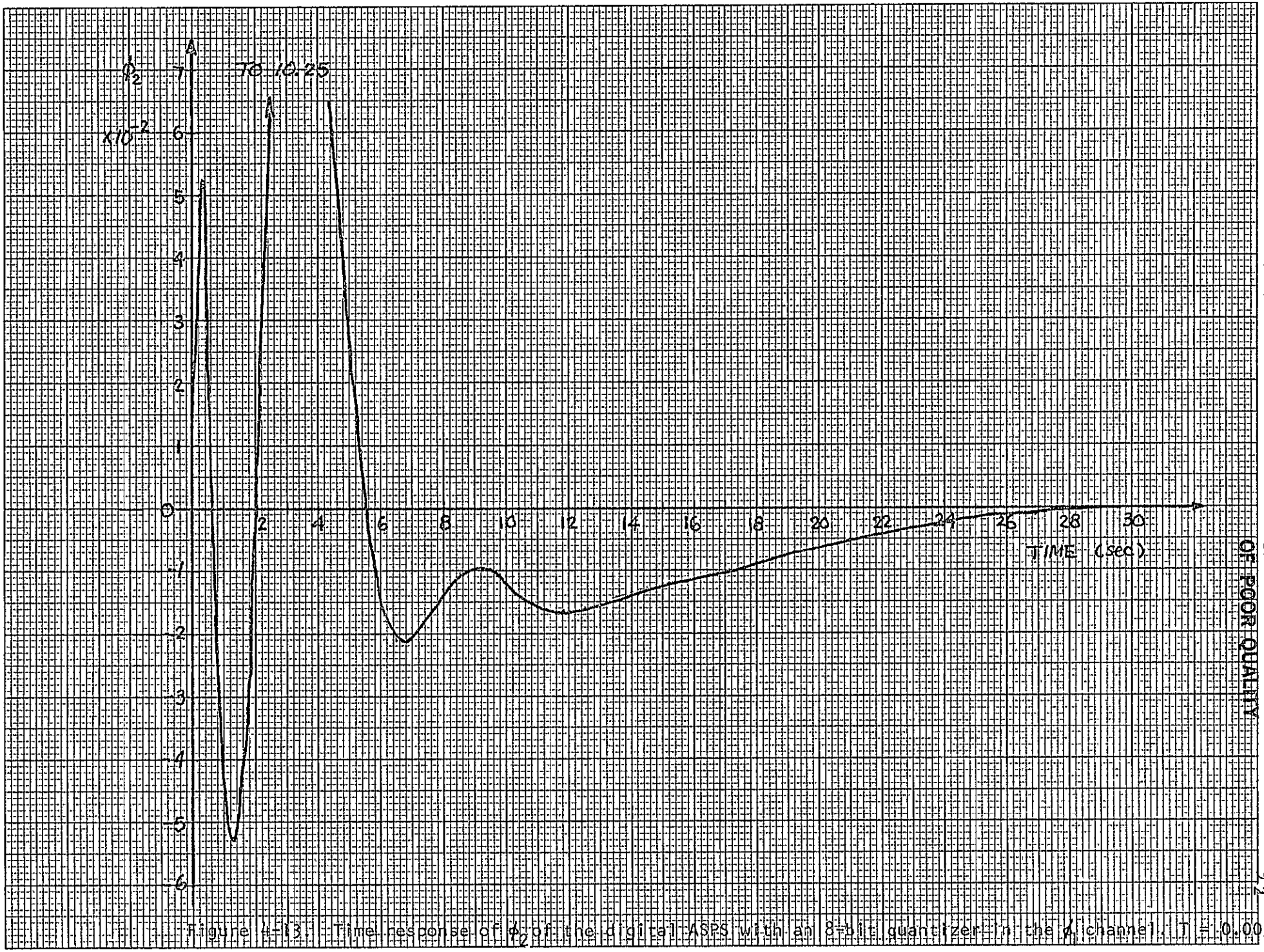

Figure 4-13. Time response of ϕ_{12} of the digital ASPS with an 8-bit quantizer in the ϕ_1 channel. T = 0.005.

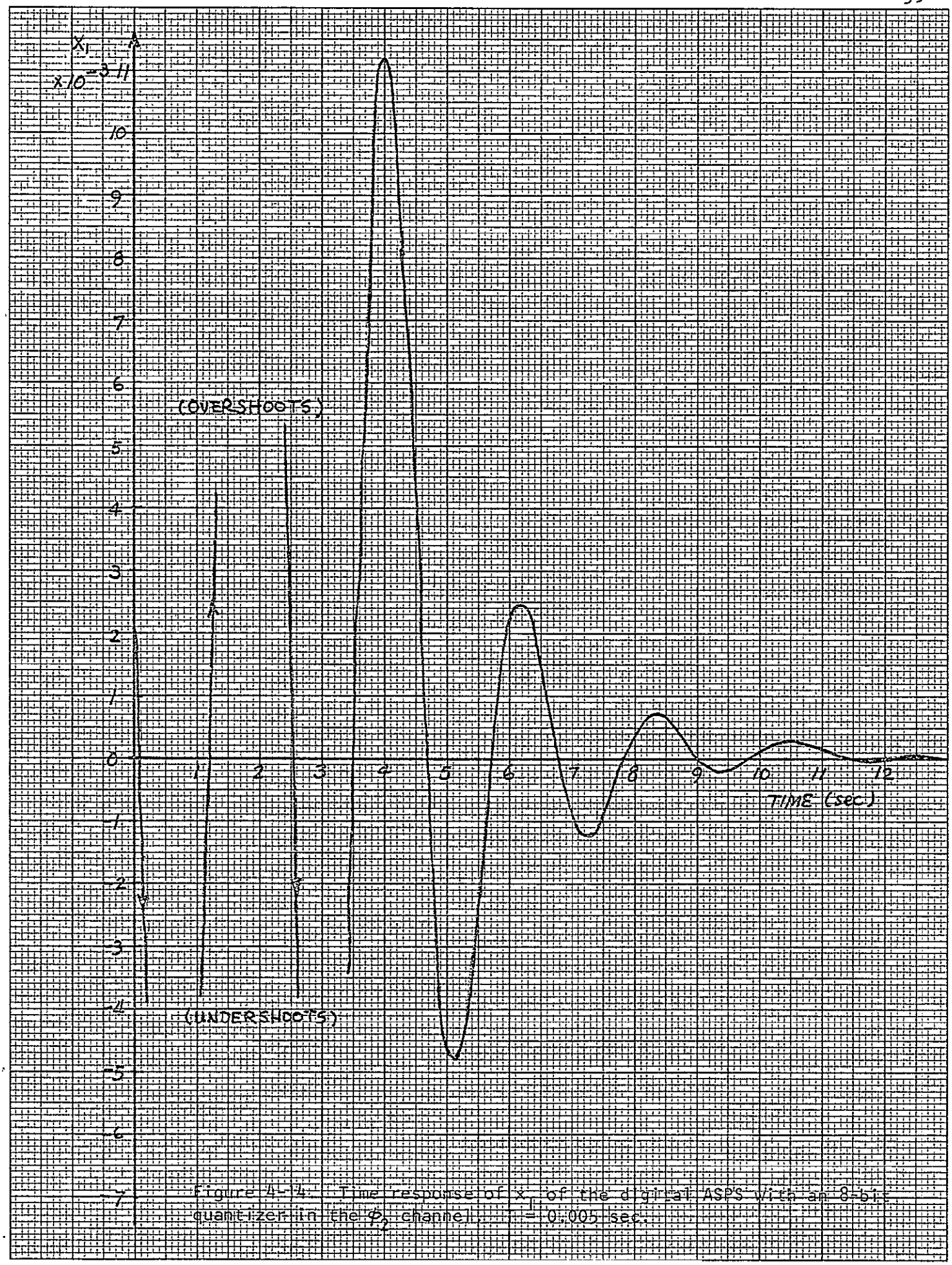

Figure 4-14 Time response of x_1 of the digital ASPS with an 8-bit quantizer in the ϕ_2 channel. $T = 0.005$ sec.

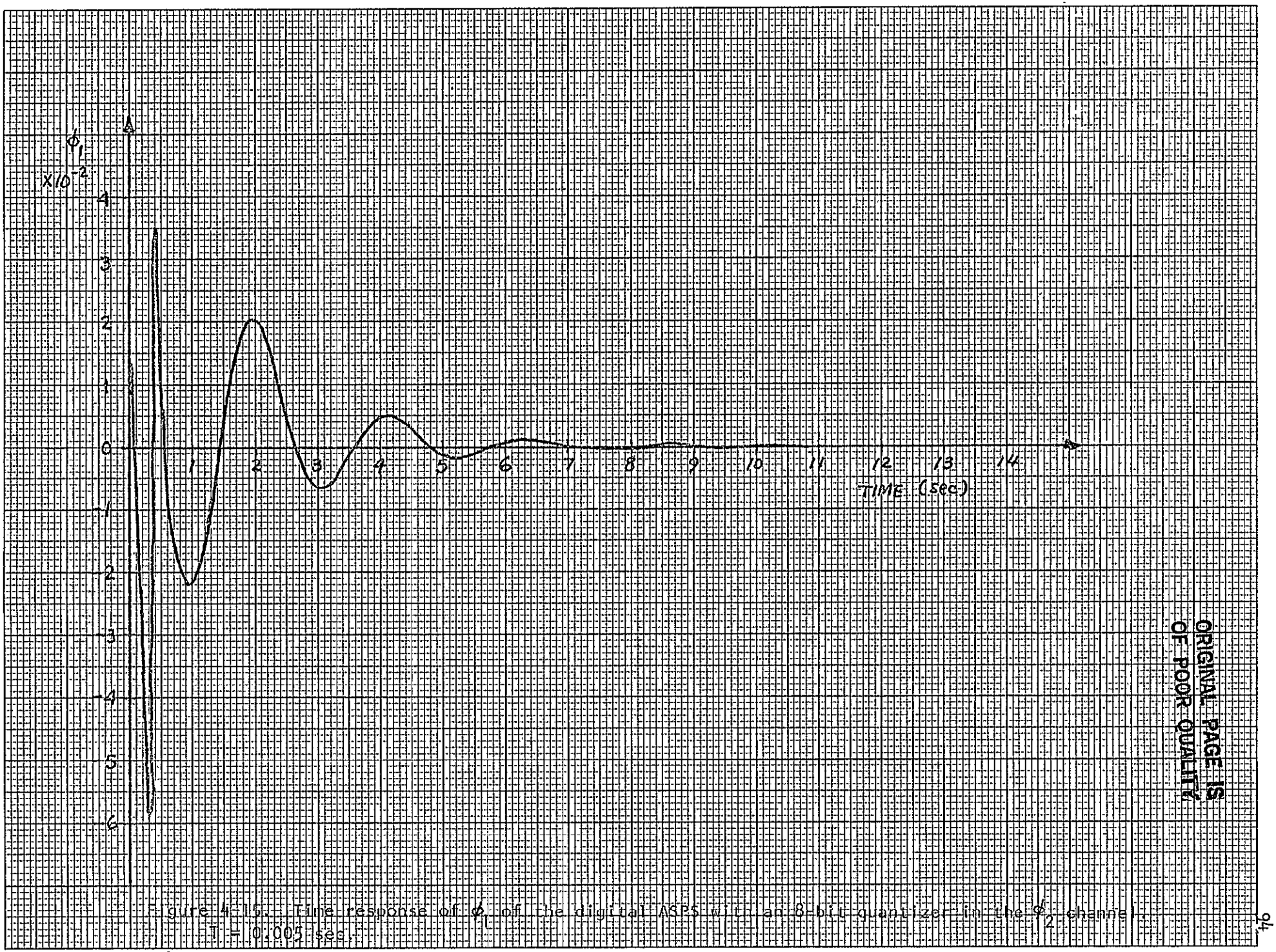

Figure 4-15. Time response of ϕ_1 of the digital ASPS with an 8-bit quantizer in the ϕ_2 channel. T = 0.005 sec.

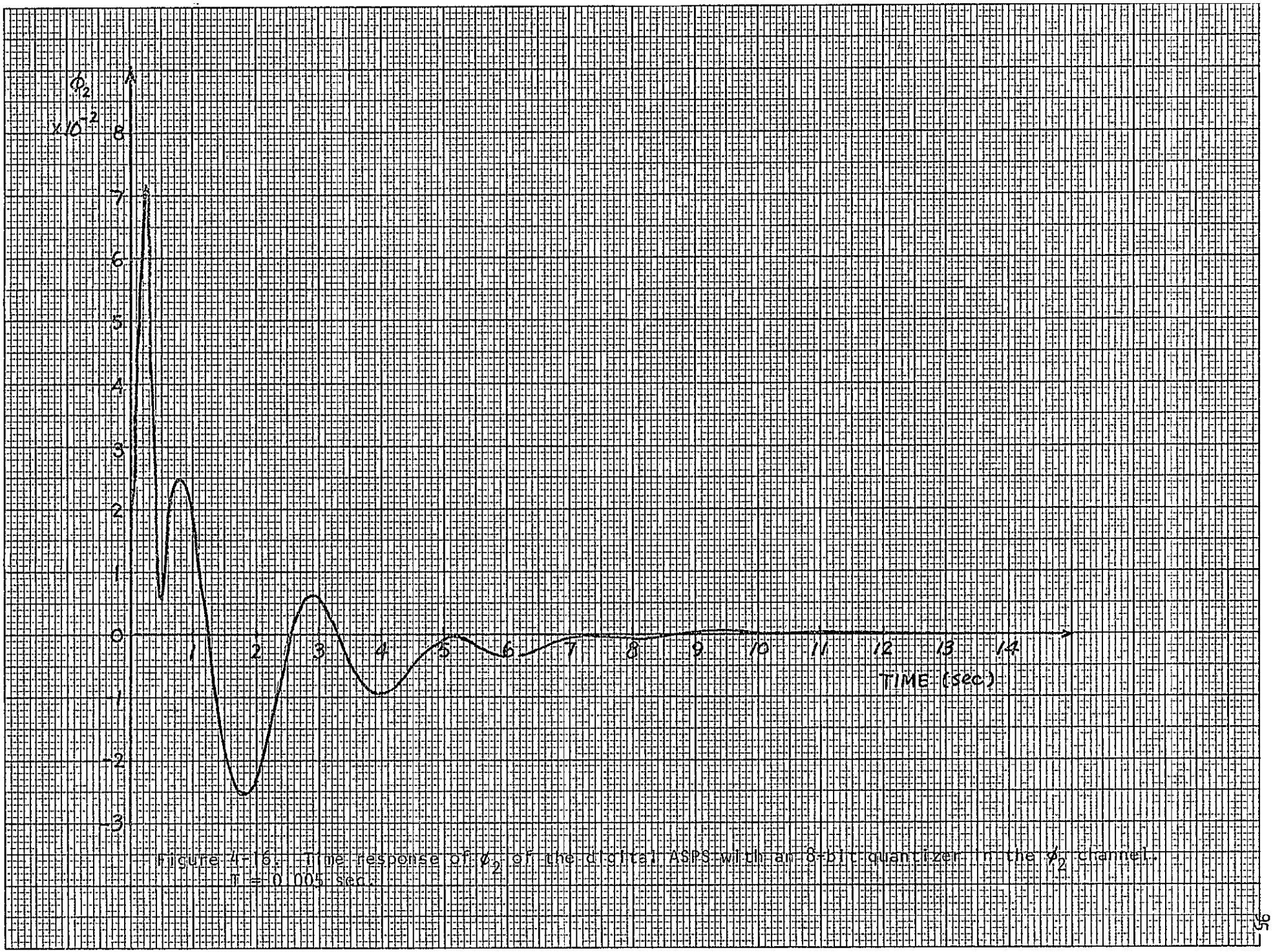

Figure 4-16. Time response of ϕ_2 of the digital ASPS with an 8-bit quantizer in the ϕ_2 channel. $T = 0.005$ sec.

C-2

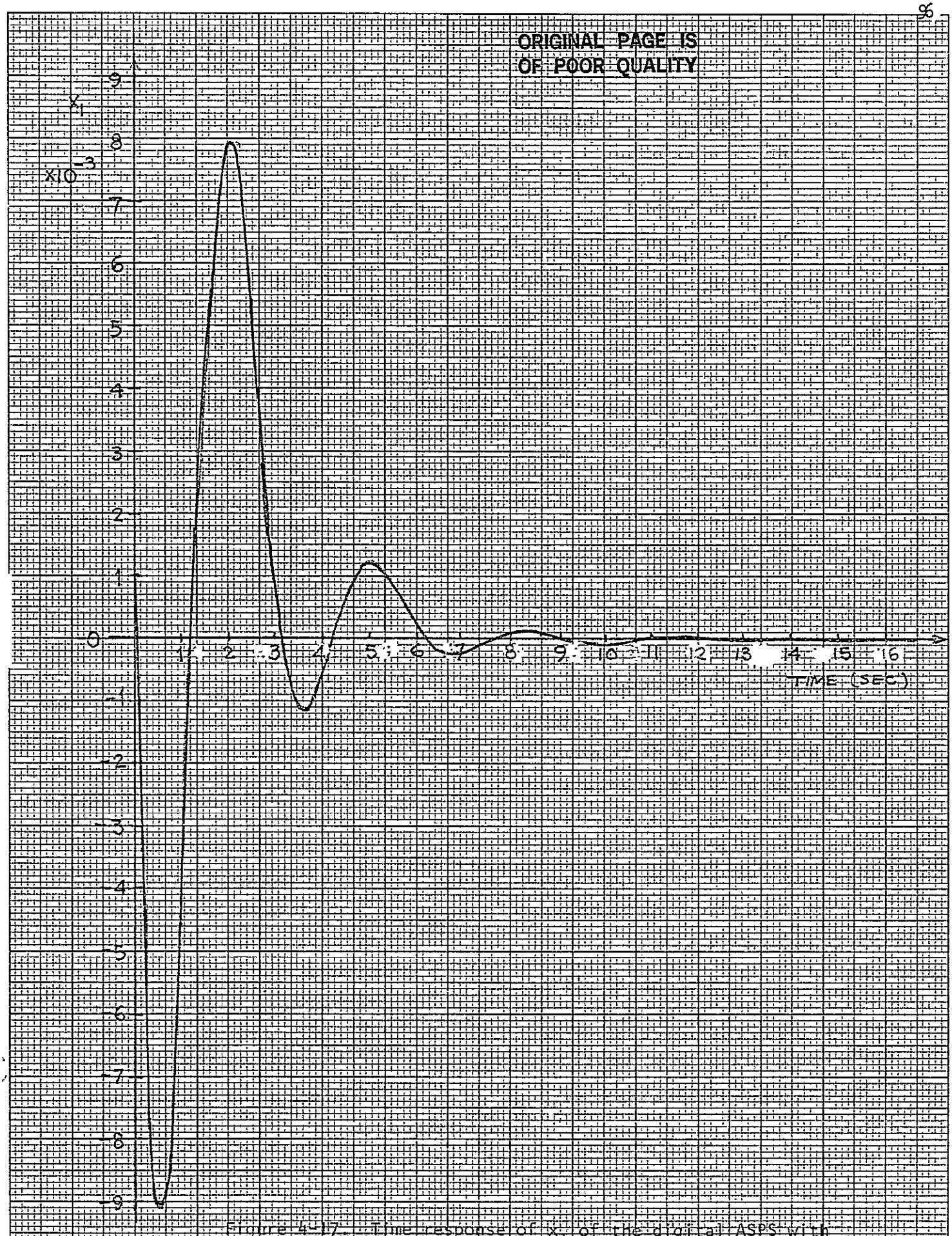

Figure 4-17. Time response of x_1 of the digital ASPS with a quantizer in each of the three channels; 8-bit, T = 0.002 sec.

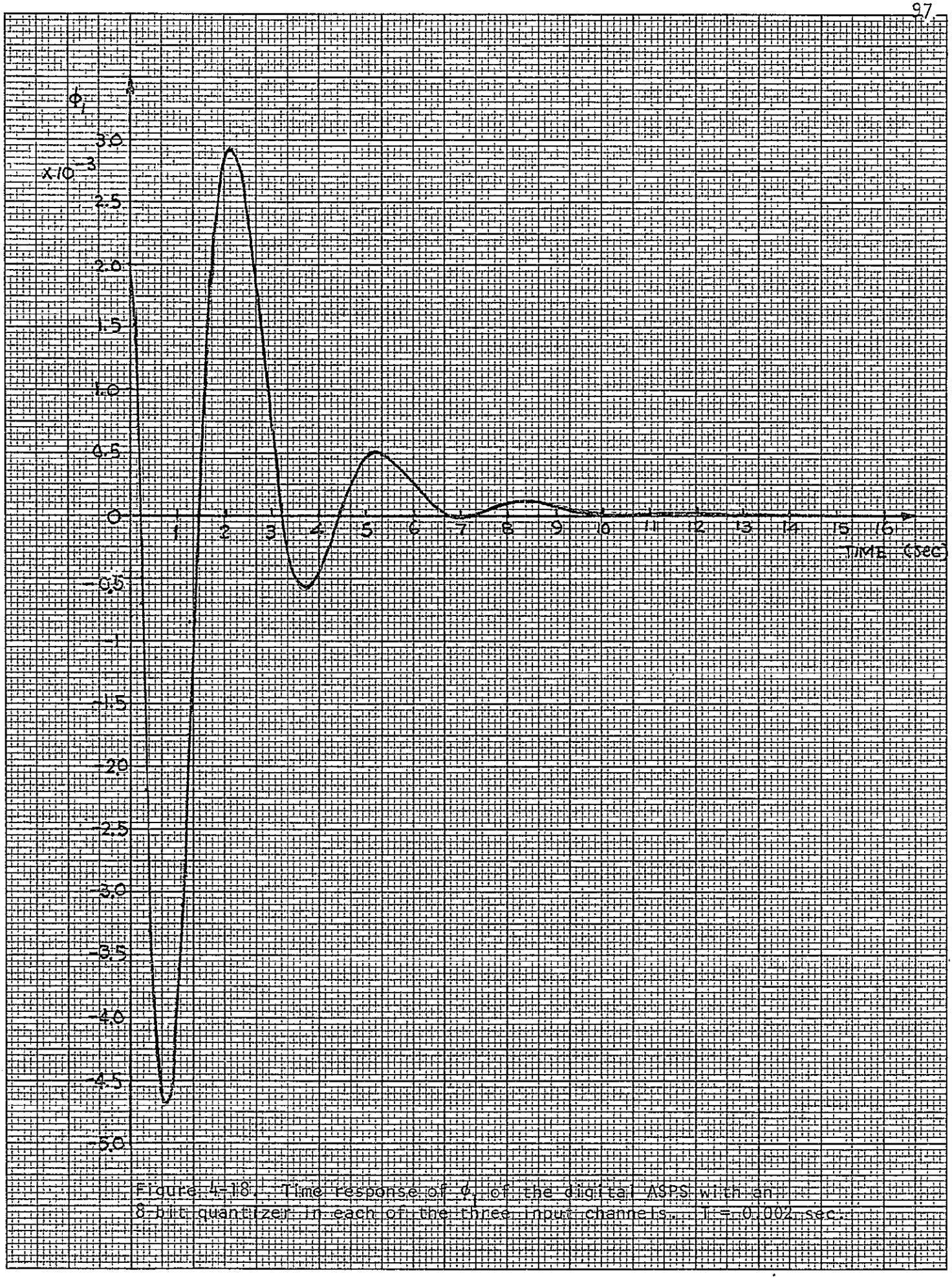

Figure 4-18. Time response of ϕ_1 of the digital ASPS with an 8-bit quantizer in each of the three input channels. T = 0.002 sec.

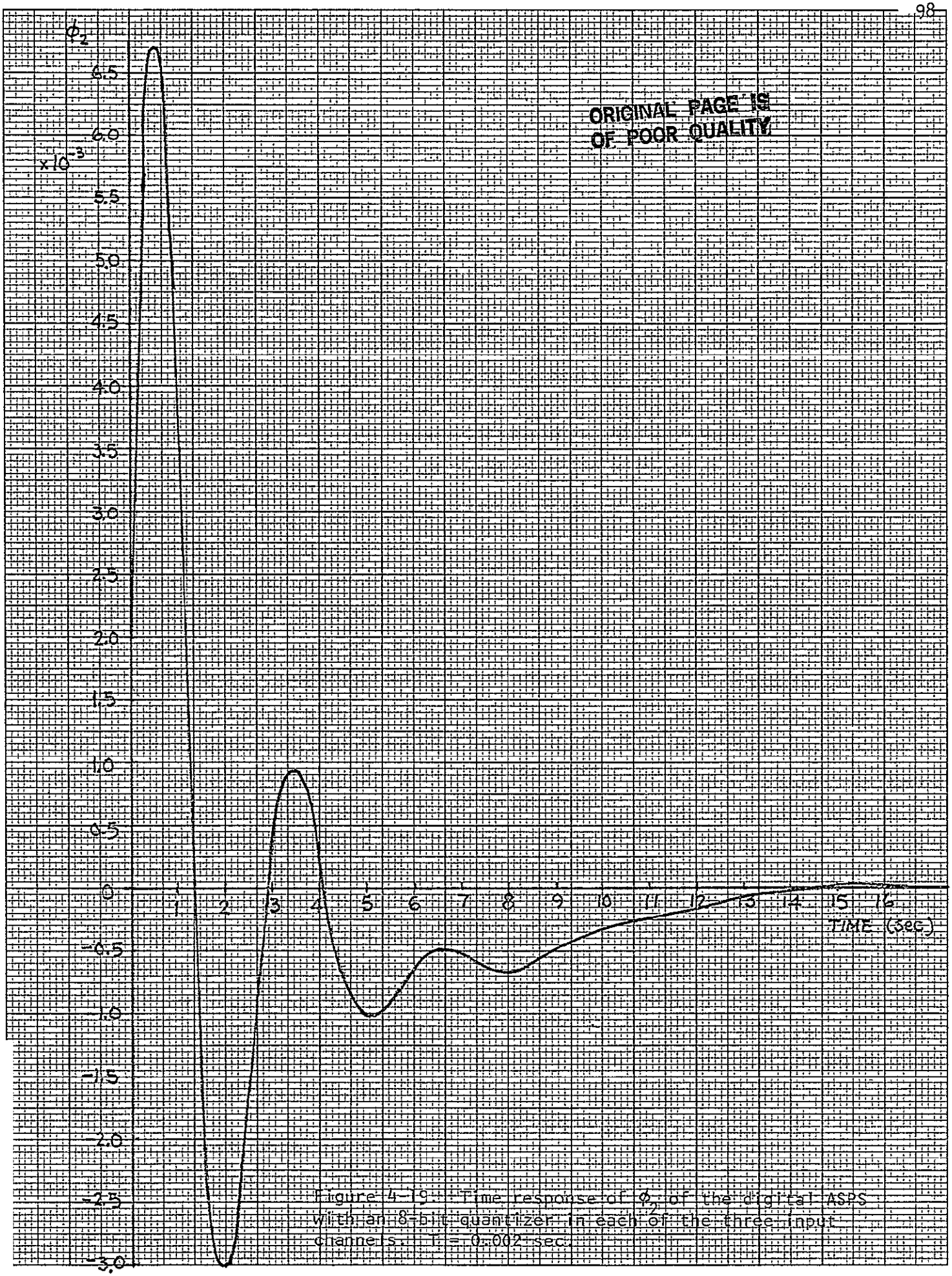

Figure 4-19. Time response of ϕ_2 of the digital ASPS with an 8-bit quantizer in each of the three input channels. T = 0.002 sec.

V. DESIGN OF THE ANALOG ASPS THROUGH DECOUPLING AND POLE PLACEMENT

5.1 Introduction

In Chapter II the analog controllers of the ASPS are designed for the control of the x, ϕ_1 and ϕ_2 dynamics. The eight eigenvalues of the system are assigned so that the overall system has an equivalent bandwidth of 2 Hz. We shall see later that this is not an accurate description of the bandwidth requirements of the system.

The analog controllers consist of eight state-feedback gains with no coupling between x, ϕ_1 and ϕ_2. In other words, the input u_1 of the x component is affected only by feedbacks from x and $\dot{x}$, the input u_2 of the ϕ_1 component is affected only by feedbacks from $\int\phi_1$, ϕ_1 and $\dot{\phi}_1$. Similarly, the input u_3 of the ϕ_2 component is realized by feedback from the states $\int\phi_2$, ϕ_2 and $\dot{\phi}_2$. Therefore, the three independent controllers are essentially PID controllers.

The values of the eight feedback gains are determined by using the Brown's method for pole-placement. The sampled-data version of the x, ϕ_1 and ϕ_2 dynamics of the ASPS was obtained by inserting sample-and-hold devices in the three input channels. It was shown in Chapter III that using the feedback gains designed for the analog system, the sampled-data system is stable for sampling periods less than or equal to 0.0075 seconds. However, this sampling period is still considered to be too small to be economical and practical for the ASPS.

5.2 Design of the Analog ASPS Through Decoupling And Pole Placement

As it turns out the desired bandwidths requirement of the ASPS is as follows:

x_1 dynamics	0.04 Hz
ϕ_1 dynamics	10 Hz

ϕ_2 dynamics 1 Hz

Since the ϕ_1 dynamics is 250 times faster than the x dynamics, it is virtually impossible to find an equivalent bandwidth of the overall system and establish a general eigenvalue requirement for the system. Therefore, it is necessary to decouple the x, ϕ_1 and ϕ_2 dynamics through state feedback and simultaneously place the poles to realize the desired bandwidths for all three system components. The problem is stated as:

Given the system

$$\dot{\underline{x}}(t) = A\underline{x}(t) + B\underline{u}(t) \tag{5-1}$$

where

$$\underline{x}(t) = \begin{bmatrix} x \\ \dot{x} \\ \int\phi_1 \\ \phi_1 \\ \dot{\phi}_1 \\ \int\phi_2 \\ \phi_2 \\ \dot{\phi}_2 \end{bmatrix} = \begin{bmatrix} x_1 \\ x_2 \\ x_3 \\ x_4 \\ x_5 \\ x_6 \\ x_7 \\ x_8 \end{bmatrix} \tag{5-2}$$

$$\underline{u}(t) = \begin{bmatrix} u_1(t) \\ u_2(t) \\ u_3(t) \end{bmatrix} \tag{5-3}$$

A is the 8x8 coefficient matrix and B is the 8x3 input matrix. The state feedback is defined by

$$\underline{u}(t) = -G\underline{x}(t) \tag{5-4}$$

where G is the 3x8 feedback matrix. The elements of G are to be selected so that the coefficient matrix of the closed-loop system, A - BG, has the following form:

$$A - BG = \begin{bmatrix} \Lambda_1 & 0 & 0 \\ 0 & \Lambda_2 & 0 \\ 0 & 0 & \Lambda_3 \end{bmatrix} \tag{5-5}$$

where

Λ_1 is a 2x2 matrix for $\dot{x}$

Λ_2 is a 3x3 matrix for ϕ_1

Λ_3 is a 3x3 matrix for ϕ_2.

The eigenvalues of Λ_1, Λ_2 and Λ_3 are so selected that the bandwidths requirements are satisfied.

Referring to Fig. 2-1 the A matrix of the ASPS has the following form:

$$A = \begin{bmatrix} 0 & 1 & 0 & 0 & 0 & 0 & 0 & 0 \\ a_{21} & 0 & 0 & a_{24} & 0 & 0 & a_{27} & 0 \\ 0 & 0 & 0 & 1 & 0 & 0 & 0 & 0 \\ 0 & 0 & 0 & 0 & 1 & 0 & 0 & 0 \\ a_{51} & 0 & 0 & a_{54} & 0 & 0 & a_{57} & 0 \\ 0 & 0 & 0 & 0 & 0 & 0 & 1 & 0 \\ 0 & 0 & 0 & 0 & 0 & 0 & 0 & 1 \\ a_{81} & 0 & 0 & a_{84} & 0 & 0 & a_{87} & 0 \end{bmatrix} \tag{5-6}$$

The B matrix is written as

$$B = \begin{bmatrix} 0 & 0 & 0 \\ b_{21} & b_{22} & b_{23} \\ 0 & 0 & 0 \\ 0 & 0 & 0 \\ b_{51} & b_{52} & b_{53} \\ 0 & 0 & 0 \\ 0 & 0 & 0 \\ b_{81} & b_{82} & b_{83} \end{bmatrix} \tag{5-7}$$

where the a_{ij}'s and b_{ij}'s in the A and B matrices are given as

$$a_{21} = -0.61207568$$

$$a_{24} = -1.4844272 \times 10^{-3}$$

$$a_{27} = 1.4844272 \times 10^{-3} = -a_{24}$$

$$a_{51} = -0.31202659$$

$$a_{54} = -7.589096 \times 10^{-4}$$

$$a_{57} = 7.589096 \times 10^{-4} = -a_{54}$$

$$a_{81} = 0.31202659$$

$$a_{84} = 7.589096 \times 10^{-4}$$

$$a_{87} = -7.6884996 \times 10^{-4}$$

$$b_{21} = 0.58237458$$

$$b_{22} = 0.29688544$$

$$b_{23} = -0.29688544$$

$$b_{51} = 0.29688544$$

$$b_{52} = 0.15178192$$

$$b_{53} = -0.15178192 = -b_{52}$$

$$b_{81} = -0.29688544$$

$$b_{82} = -0.15178192$$

$$b_{82} = 0.15376999$$

It is simple to show that B has full rank (rank = 3).

Let the feedback matrix be represented by

$$G = \begin{bmatrix} g_{11} & g_{12} & g_{13} & g_{14} & g_{15} & g_{16} & g_{17} & g_{18} \\ g_{21} & g_{22} & g_{23} & g_{24} & g_{25} & g_{26} & g_{27} & g_{28} \\ g_{31} & g_{32} & g_{33} & g_{34} & g_{35} & g_{36} & g_{37} & g_{38} \end{bmatrix} \qquad (5\text{-}8)$$

Then BG becomes

$$BG = \begin{bmatrix} 0 & 0 & 0 & 0 & 0 & 0 & 0 & 0 \\ (BG)_{21} & (BG)_{22} & (BG)_{23} & (BG)_{24} & (BG)_{25} & (BG)_{26} & (BG)_{27} & (BG)_{28} \\ 0 & 0 & 0 & 0 & 0 & 0 & 0 & 0 \\ 0 & 0 & 0 & 0 & 0 & 0 & 0 & 0 \\ (BG)_{51} & (BG)_{52} & (BG)_{53} & (BG)_{54} & (BG)_{55} & (BG)_{56} & (BG)_{57} & (BG)_{58} \\ 0 & 0 & 0 & 0 & 0 & 0 & 0 & 0 \\ 0 & 0 & 0 & 0 & 0 & 0 & 0 & 0 \\ (BG)_{81} & (BG)_{82} & (BG)_{83} & (BG)_{84} & (BG)_{85} & (BG)_{86} & (BG)_{87} & (BG)_{88} \end{bmatrix} \quad (5\text{-}9)$$

where

$$(BG)_{ij} = \sum_{k=1}^{3} b_{ik} g_{kj} \qquad i=1,2,\ldots,8,\ j=1,2,\ldots,8$$

In order for A - BG to be a diagonal matrix, the following relations must hold:

$$(BG)_{23} = a_{23} = 0$$
$$(BG)_{24} = a_{24}$$
$$(BG)_{25} = a_{25} = 0$$
$$(BG)_{26} = a_{26} = 0$$
$$(BG)_{27} = a_{27}$$
$$(BG)_{28} = a_{28} = 0$$
$$(BG)_{51} = a_{51}$$
$$(BG)_{52} = a_{52} = 0$$
$$(BG)_{56} = a_{56} = 0$$
$$(BG)_{57} = a_{57}$$
$$(BG)_{58} = a_{58} = 0$$
$$(BG)_{81} = a_{81}$$
$$(BG)_{82} = a_{82} = 0$$
$$(BG)_{83} = a_{83} = 0$$
$$(BG)_{84} = a_{84}$$

$$(BG)_{85} = a_{85} = 0$$

These equations represent 16 equations with 24 variables in the feedback gains g_{ij} (i=1,2,3; j=1,2,...,8).

For the present design, the x dynamics is specified to have a bandwidth of 0.04 Hz. Since the x dynamics are represented by a second-order system, the bandwidth of the system is given by

$$BW = \omega_n \left(1 - 2\zeta^2 + \sqrt{4\zeta^4 - 4\zeta^2 + 2} \right)^{\frac{1}{2}} \tag{5-11}$$

If we choose the damping ratio ζ to be 0.707, then

$$BW = \omega_n \tag{5-12}$$

where ω_n is the natural undamped frequency.

Therefore, for the x dynamics, the eigenvalues are selected to be at

$$p_1, p_2 = a_1 \pm j a_1 \tag{5-13}$$

where

$$a_1 = - \frac{0.04 \times 2\pi}{\sqrt{2}} = -0.178 \tag{5-14}$$

The ϕ_1 and ϕ_2 dynamics are of the third order. However, we can use second-order approximations by placing the real root far to the left on the real axis in the s-plane. For this case we let the real root of the ϕ_1 dynamics be placed at

$$p_3 = b_2 = -200 \tag{5-15}$$

Then, the complex roots are:

$$p_4, p_5 = a_2 \pm j a_2 \tag{5-16}$$

where

$$a_2 = - \frac{2\pi \times 10}{\sqrt{2}} = -44.436 \tag{5-17}$$

Similarly, for the ϕ_2 dynamics, we let

$$p_6 = b_3 = -20 \tag{5-18}$$

Then,

$$p_7, p_8 = a_3 \pm ja_3 \tag{5-19}$$

where

$$a_3 = -\frac{2\pi \times 1}{\sqrt{2}} = -4.4436 \tag{5-20}$$

The characteristic equations of the three decoupled subsystems are as follows:

$$\text{x component:} \quad (s - a_1 - ja_1)(s + a_1 + ja_1)$$
$$= s^2 - 2a_1 s + 2a_1^2 = 0 \tag{5-21}$$

$$\phi_1 \text{ component:} \quad (s - b_2)(s - a_2 - ja_2)(s - a_2 + ja_2)$$
$$= (s - b_2)(s^2 - 2a_2 s + 2a_2^2)$$
$$= s^3 - (2a_2 + b_2)s^2 + (2a_2^2 + 2a_2 b_2)s - 2a_2^2 b_2 = 0 \tag{5-22}$$

$$\phi_2 \text{ componwnt:} \quad (s - b_3)(s - a_3 - ja_3)(s - a_3 + ja_3)$$
$$= (s - b_3)(s^2 - 2a_3 s + 2a_3^2)$$
$$= s^3 - (2a_3 + b_3)s^2 + (2a_3^2 + 2a_3 b_3)s - 2a_3^2 b_3 = 0 \tag{5-23}$$

If there exists a set of feedback gains such that the decoupling of the subsystems x, ϕ_1 and ϕ_2 can be accomplished, then the decoupled closed-loop system will have the independent characteristic equations of Eqs. (5-21), (5-22) and (5-23).

Let the matrix A of Eq. (5-6) be written as

$$A = \left[\begin{array}{c|c|c} A_{11} & X & X \\ \hline X & A_{22} & X \\ \hline X & X & A_{33} \end{array}\right] \tag{5-24}$$

where A_{11} denotes a 2x2 matrix, A_{22} and A_{33} are 3x3 matrices. The submatrices denoted by X contain elements which are unimportant for the immediate development.

In view of Eqs. (5-5) and (5-9), the decoupled x dynamics with state feedback can be expressed as

$$\begin{bmatrix} \dot{x}_1 \\ \dot{x}_2 \end{bmatrix} = \Lambda_1 \begin{bmatrix} x_1 \\ x_2 \end{bmatrix} \tag{5-25}$$

where

$$\Lambda_1 = A_{11} - \begin{bmatrix} 0 & 0 \\ (BG)_{21} & (BG)_{22} \end{bmatrix} = \begin{bmatrix} 0 & 1 \\ a_{21} - (BG)_{21} & -(BG)_{22} \end{bmatrix} \tag{5-26}$$

The characteristic equation of Λ_1 is

$$|sI - \Lambda_1| = \begin{vmatrix} s & -1 \\ a_{21} - (BG)_{21} & s + (BG)_{22} \end{vmatrix}$$

$$= s^2 + (BG)_{22}s - a_{21} + (BG)_{21} = 0 \tag{5-27}$$

Similarly, the decoupled ϕ_1 dynamics with state feedback is described by

$$\begin{bmatrix} \dot{x}_3 \\ \dot{x}_4 \\ \dot{x}_5 \end{bmatrix} = \Lambda_2 \begin{bmatrix} x_3 \\ x_4 \\ x_5 \end{bmatrix} \tag{5-28}$$

where

$$\Lambda_2 = A_{22} - \begin{bmatrix} 0 & 0 & 0 \\ 0 & 0 & 0 \\ (BG)_{53} & (BG)_{54} & (BG)_{55} \end{bmatrix}$$

$$= \begin{bmatrix} 0 & 1 & 0 \\ 0 & 0 & 1 \\ -(BG)_{53} & a_{54} - (BG)_{54} & -(BG)_{55} \end{bmatrix} \tag{5-29}$$

The characteristic equation of Λ_2 is

$$|sI - \Lambda_2| = \begin{vmatrix} s & -1 & 0 \\ 0 & s & -1 \\ (BG)_{53} & -a_{54} + (BG)_{54} & s + (BG)_{55} \end{vmatrix}$$

$$= s^3 + (BG)_{55}s^2 + \left((BG)_{54} - a_{54}\right)s + (BG)_{53} = 0 \qquad (5\text{-}30)$$

For the ϕ_2 component, the decoupled closed-loop state equations are

$$\begin{bmatrix} \dot{x}_6 \\ \dot{x}_7 \\ \dot{x}_8 \end{bmatrix} = \Lambda_3 \begin{bmatrix} x_6 \\ x_7 \\ x_8 \end{bmatrix} \qquad (5\text{-}31)$$

where

$$\Lambda_3 = A_{33} - \begin{bmatrix} 0 & 0 & 0 \\ 0 & 0 & 0 \\ (BG)_{86} & (BG)_{87} & (BG)_{88} \end{bmatrix}$$

$$= \begin{bmatrix} 0 & 1 & 0 \\ 0 & 0 & 1 \\ -(BG)_{86} & a_{87} - (BG)_{87} & -(BG)_{88} \end{bmatrix} \qquad (5\text{-}32)$$

The characteristic equation of Λ_3 is

$$|sI - \Lambda_3| = \begin{vmatrix} s & -1 & 0 \\ 0 & s & -1 \\ (BG)_{86} & -a_{87} + (BG)_{87} & s + (BG)_{88} \end{vmatrix}$$

$$= s^3 + (BG)_{88}s^2 + \left((BG)_{87} - a_{87}\right)s + (BG)_{86} = 0 \qquad (5\text{-}33)$$

For pole placement, in order tc meet the bandwidth requirements, the corresponding coefficients of the characteristic equations in Eqs. (5-27), (5-30) and (5-33) must match those of Eqs. (5-21), (5-22) and (5-23), respectively.

Thus, for pole-placement,

$$s^2 - 2a_1 s + 2a_1^2 = s^2 + (BG)_{22}s + (BG)_{21} - a_{21} \qquad (5\text{-}34)$$

$$s^3 - (2a_2 + b_2)s^2 + (2a_2^2 + 2a_2 b_2)s - 2a_2^2 b_2$$

$$= s^3 + (BG)_{55}s^2 + \left((BG)_{54} - a_{54}\right)s + (BG)_{53} \qquad (5\text{-}35)$$

$$s^3 - (2a_3 + b_3)s^2 + (2a_3^2 + 2a_3b_3)s - 2a_3^2b_3$$
$$= s^3 + (BG)_{88}s^2 + \left((BG)_{87} - a_{87}\right)s + (BG)_{86} \qquad (5\text{-}36)$$

Equating the like coefficients in the above three equations, we have

$$\begin{aligned}
(BG)_{22} &= b_{21}g_{12} + b_{22}g_{22} + b_{23}g_{32} = -2a_1 \\
(BG)_{21} &= b_{21}g_{11} + b_{22}g_{21} + b_{23}g_{31} = 2a_1^2 + a_{21} \\
(BG)_{55} &= b_{51}g_{15} + b_{52}g_{25} + g_{53}g_{35} = -(2a_2 + b_2) \\
(BG)_{54} &= b_{51}g_{14} + b_{52}g_{24} + b_{53}g_{34} = 2a_2^2 + 2a_2b_2 + a_{54} \\
(BG)_{53} &= b_{51}g_{13} + b_{52}g_{23} + b_{53}g_{33} = -2a_2^2b_2 \\
(BG)_{88} &= b_{81}g_{18} + b_{82}g_{28} + b_{83}g_{38} = -(2a_3 + b_3) \\
(BG)_{87} &= b_{81}g_{17} + b_{82}g_{27} + b_{83}g_{37} = 2a_3^2 + 2a_3b_3 + a_{87} \\
(BG)_{86} &= b_{81}g_{16} + b_{82}g_{26} + b_{83}g_{36} = -2a_3^2b_3
\end{aligned} \qquad (5\text{-}37)$$

Notice that the 16 constraint equations on the feedback gains in Eq. (5-10) are conditions on decoupling of the three subsystems, whereas the 8 constraint equations in Eq. (5-37) are the conditions for pole placement. The 24 constraint equations contain 24 unknowns in the elements of the feedback matrix G, g_{ij}, i=1, 2,3, j=1,2,...,8.

The 24 constraint equations in Eqs. (5-10) and (5-37) can be written as

$$WG = C \qquad (5\text{-}38)$$

where

$$W = \begin{bmatrix} b_{21} & b_{22} & b_{23} \\ b_{51} & b_{52} & b_{53} \\ b_{81} & b_{82} & b_{83} \end{bmatrix}$$

G is the feedback matrix given in Eq. (5-8), and C is a 3x8 matrix whose elements are composed of a_1, a_2, a_3, b_1, b_2, b_3, and a_{ij}, i=1,2,...,8, j=1,2,...,8.

The feedback gain matrix G can be solved form Eq. (5-38) if W is nonsingular.

$$G = W^{-1}C \qquad (5\text{-}39)$$

to be nonsingular, it is necessary and sufficient for B to have full rank.

atrix

or the system parameters given for the ASPS, the feedback matrix is solved

q. (5-39), and the results are given as follows:

$$g_{11} = 36.449$$

$$g_{12} = 212.4$$

$$g_{13} = -9.256981248 \times 10^{8}$$

$$g_{14} = -2.5471626624 \times 10^{7}$$

$$g_{15} = -3.3892568 \times 10^{5}$$

$$g_{16} = 0$$

$$g_{17} = 0$$

$$g_{18} = 0$$

$$g_{21} = -73.35$$

$$g_{22} = -415.4544$$

$$g_{23} = 2.2126125552 \times 10^{9}$$

$$g_{24} = 6.0882526771 \times 10^{7}$$

$$g_{25} = 8.1012732 \times 10^{5}$$

$$g_{26} = 3.96750304 \times 10^{5}$$

$$g_{27} = 1.091703152 \times 10^{5}$$

$$g_{28} = 1.452664 \times 10^{4}$$

$$g_{31} = 0$$

$$g_{32} = 0$$

$$g_{33} = 3.96750304 \times 10^{8}$$

$$g_{34} = 1.091703152 \times 10^{7}$$

$$g_{35} = 1.452664 \times 10^{5}$$

$$g_{36} = 3.96750304 \times 10^{5}$$

$$\phi(0.02)=\begin{bmatrix} 9.998\times10^{-1} & 1.999\times10^{-2} & 0 & -2.968\times10^{-7} & -1.979\times10^{-9} & 0 & 2.968\times10^{-7} & 1.979\times10^{-9} \\ -1.224\times10^{-2} & 9.998\times10^{-1} & 0 & -2.968\times10^{-5} & -2.968\times10^{-7} & 0 & 2.968\times10^{-5} & 2.968\times10^{-7} \\ -4.160\times10^{-7} & -2.080\times10^{-9} & 1 & 1.999\times10^{-2} & 1.999\times10^{-4} & 0 & 1.011\times10^{-9} & 5.059\times10^{-12} \\ -6.240\times10^{-5} & -4.160\times10^{-7} & 0 & 9.999\times10^{-1} & 1.999\times10^{-2} & 0 & 1.517\times10^{-7} & 1.011\times10^{-9} \\ -6.240\times10^{-3} & -6.240\times10^{-5} & 0 & -1.517\times10^{-5} & 9.999\times10^{-1} & 0 & 1.517\times10^{-5} & 1.517\times10^{-7} \\ 4.160\times10^{-7} & 2.080\times10^{-9} & 0 & 1.011\times10^{-9} & 5.059\times10^{-12} & 1 & 1.999\times10^{-2} & 1.999\times10^{-4} \\ 6.240\times10^{-5} & 4.160\times10^{-7} & 0 & 1.517\times10^{-7} & 1.011\times10^{-9} & 0 & 9.999\times10^{-1} & 1.999\times10^{-2} \\ 6.240\times10^{-3} & 6.240\times10^{-5} & 0 & 1.517\times10^{-5} & 1.517\times10^{-7} & 0 & -1.537\times10^{-5} & 9.999\times10^{-1} \end{bmatrix} \tag{6-12}$$

$$\theta(0.02) = \begin{bmatrix} 1.164\times10^{-4} & 5.937\times10^{-5} & -5.937\times10^{-5} \\ 1.164\times10^{-2} & 5.937\times10^{-3} & -5.937\times10^{-3} \\ 3.958\times10^{-7} & 2.023\times10^{-7} & -2.023\times10^{-7} \\ 5.937\times10^{-5} & 3.035\times10^{-5} & -3.035\times10^{-5} \\ 5.937\times10^{-3} & 3.035\times10^{-3} & -3.035\times10^{-3} \\ -3.958\times10^{-7} & -2.023\times10^{-7} & 2.050\times10^{-7} \\ -5.937\times10^{-5} & -3.035\times10^{-5} & 3.075\times10^{-5} \\ -5.937\times10^{-3} & -3.035\times10^{-3} & 3.075\times10^{-3} \end{bmatrix} \tag{6-13}$$

For the same bandwidth requirements described in Chapter 5, the following eigenvalues are selected in the s-plane:

x component: (0.04 Hz bandwidth)

$p_1, p_2 = -0.178 \pm j0.178$

ϕ_1 component: (10 Hz bandwidth)

$p_3 = -200$

$$p_4,\ p_5 = -44.436 \pm j44.436$$

ϕ_2 component: (1 Hz bandwidth)

$$p_6 = -20$$

$$p_7,\ p_8 = -4.4436 \pm j4.4436$$

Using the transformation $z = e^{Ts}$, these eigenvalues are transformed into the z-plane. The corresponding z-plane eigenvalues are:

x: $z_1,\ z_2 = 0.9964457 \pm j0.0035417$

ϕ_1: $z_3 = 0.01831564$

$z_4,\ z_5 = 0.2592945 \pm j0.3191948$

ϕ_2: $z_6 = 0.67032$

$z_7,\ z_8 = 0.911366 \pm j0.096987$

The condition of decoupling of the closed-loop digital system given in Eq. (6-8) results in 42 constraint equations. This is due to the fact that Eq. (6-8) represents 64 scalar equations, but there are 42 zero elements in the matrix. The pole placements of the eighth-order system would produce 8 more constraint equations, so there are only 24 unknowns in the feedback matrix G. Therefore, in general, there would not be a set of solutions with more equations than unknowns. However, a closer look at the elements of $\phi(T)$ and $\theta(T)$ reveals that some of the elements are extremely small so that a good approximation can be obtained by assuming that these small elements are zeros. In other words, the state transition matrix $\phi(0.02)$ given in Eq. (6-12) can be approximated by the following matrix.

$$\phi(0.02) \simeq \left[\begin{array}{cc|ccc|ccc} 9.998\times10^{-1} & 1.999\times10^{-2} & 0 & 0 & 0 & 0 & 0 & 0 \\ -1.224\times10^{-2} & 9.998\times10^{-1} & 0 & -2.968\times10^{-5} & -2.968\times10^{-7} & 0 & 2.968\times10^{-5} & 2.968\times10^{-7} \\ \hline 0 & 0 & 1 & 1.999\times10^{-2} & 1.999\times10^{-4} & 0 & 0 & 0 \\ 0 & 0 & 0 & 9.999\times10^{-1} & 1.999\times10^{-2} & 0 & 0 & 0 \\ -6.240\times10^{-5} & -4.160\times10^{-7} & 0 & -1.517\times10^{-5} & 9.999\times10^{-1} & 0 & 1.517\times10^{-5} & 1.517\times10^{-7} \\ \hline 0 & 0 & 0 & 0 & 0 & 1 & 1.999\times10^{-2} & 1.999\times10^{-4} \\ 0 & 0 & 0 & 0 & 0 & 0 & 9.999\times10^{-1} & 1.999\times10^{-2} \\ 6.240\times10^{-3} & 6.240\times10^{-5} & 0 & 1.517\times10^{-5} & 1.517\times10^{-7} & 0 & -1.537\times10^{-5} & 9.999\times10^{-1} \end{array}\right] \qquad (6\text{-}14)$$

Similarly, we can approximate $\theta(0.02)$ by the following matrix:

$$\theta(0.02) \simeq \left[\begin{array}{ccc} 0 & 0 & 0 \\ 1.164\times10^{-2} & 5.937\times10^{-3} & -5.937\times10^{-3} \\ \hline 0 & 0 & 0 \\ 0 & 0 & 0 \\ 5.937\times10^{-3} & 3.035\times10^{-3} & -3.035\times10^{-3} \\ \hline 0 & 0 & 0 \\ 0 & 0 & 0 \\ -5.937\times10^{-3} & -3.035\times10^{-3} & 3.075\times10^{-3} \end{array}\right] \qquad (6\text{-}15)$$

Then, the matrix $\theta(0.02)G$ becomes

$$\theta(0.02)G \simeq \left[\begin{array}{cc|ccc|ccc} 0 & 0 & 0 & 0 & 0 & 0 & 0 & 0 \\ (\theta G)_{21} & (\theta G)_{22} & (\theta G)_{23} & (\theta G)_{24} & (\theta G)_{25} & (\theta G)_{26} & (\theta G)_{27} & (\theta G)_{28} \\ \hline 0 & 0 & 0 & 0 & 0 & 0 & 0 & 0 \\ 0 & 0 & 0 & 0 & 0 & 0 & 0 & 0 \\ (\theta G)_{51} & (\theta G)_{52} & (\theta G)_{53} & (\theta G)_{54} & (\theta G)_{55} & (\theta G)_{56} & (\theta G)_{57} & (\theta G)_{58} \\ \hline 0 & 0 & 0 & 0 & 0 & 0 & 0 & 0 \\ 0 & 0 & 0 & 0 & 0 & 0 & 0 & 0 \\ (\theta G)_{81} & (\theta G)_{82} & (\theta G)_{83} & (\theta G)_{84} & (\theta G)_{85} & (\theta G)_{86} & (\theta G)_{87} & (\theta G)_{88} \end{array}\right] \quad (6\text{-}16)$$

Based on Eqs. (6-14), (6-15) and (6-16), the following 16 equations are obtained for decoupling the ϕ - θG matrix:

$$(\theta G)_{23} = \theta_{21}g_{13} + \theta_{22}g_{23} + \theta_{23}g_{33} = \phi_{23} = 0$$

$$(\theta G)_{24} = \theta_{21}g_{14} + \theta_{22}g_{24} + \theta_{23}g_{34} = \phi_{24} = -2.968\times10^{-5}$$

$$(\theta G)_{25} = \theta_{21}g_{15} + \theta_{22}g_{25} + \theta_{23}g_{35} = \phi_{25} = -2.968\times10^{-7}$$

$$(\theta G)_{26} = \theta_{21}g_{16} + \theta_{22}g_{26} + \theta_{23}g_{36} = \phi_{26} = 0$$

$$(\theta G)_{27} = \theta_{21}g_{17} + \theta_{22}g_{27} + \theta_{23}g_{37} = \phi_{27} = 2.968\times10^{-5}$$

$$(\theta G)_{28} = \theta_{21}g_{18} + \theta_{22}g_{28} + \theta_{23}g_{38} = \phi_{28} = 2.968\times10^{-7}$$

$$(\theta G)_{51} = \theta_{51}g_{11} + \theta_{52}g_{21} + \theta_{53}g_{31} = \phi_{51} = -6.240\times10^{-5}$$

$$(\theta G)_{52} = \theta_{51}g_{12} + \theta_{52}g_{22} + \theta_{53}g_{32} = \phi_{52} = -4.160\times10^{-7}$$

$$(\theta G)_{56} = \theta_{51}g_{16} + \theta_{52}g_{26} + \theta_{53}g_{36} = \phi_{56} = 0$$

$$(\theta G)_{57} = \theta_{51}g_{17} + \theta_{52}g_{27} + \theta_{53}g_{37} = \phi_{57} = 1.517\times10^{-5}$$

$$(\theta G)_{58} = \theta_{51}g_{18} + \theta_{52}g_{28} + \theta_{53}g_{38} = \phi_{58} = 1.517\times10^{-7}$$

$$(\theta G)_{81} = \theta_{81}g_{11} + \theta_{82}g_{21} + \theta_{83}g_{32} = \phi_{81} = 6.240\times10^{-3}$$

$$(\theta G)_{82} = \theta_{81}g_{11} + \theta_{82}g_{22} + \theta_{83}g_{32} = \phi_{82} = 6.240\times10^{-5}$$

$$(\theta G)_{83} = \theta_{81}g_{13} + \theta_{82}g_{23} + \theta_{83}g_{33} = \phi_{83} = 0$$

$$(\theta G)_{84} = \theta_{81}g_{14} + \theta_{82}g_{24} + \theta_{83}g_{34} = \phi_{84} = 1.517\times10^{-5}$$

$$(\theta G)_{85} = \theta_{81}g_{15} + \theta_{82}g_{25} + \theta_{83}g_{35} = \phi_{85} = 1.517\times10^{-7}$$

The eight additional constraint equations for the solution of the 24 elements of the feedback gain matrix G come from the pole placement requirements on the submatrices, Λ_1, Λ_2 and Λ_3.

After the matrix ϕ - θG has been decoupled, it can be written as

$$\phi(0.02) - \theta(0.02)G = \left[\begin{array}{c|c|c} \Lambda_1 & 0 & 0 \\ \hline 0 & \Lambda_2 & 0 \\ \hline 0 & 0 & \Lambda_3 \end{array}\right] \qquad (6\text{-}18)$$

where

$$\Lambda_1 = \begin{bmatrix} \phi_{11} & \phi_{12} \\ \phi_{21} & \phi_{22} \end{bmatrix} - \begin{bmatrix} 0 & 0 \\ (\theta G)_{21} & (\theta G)_{22} \end{bmatrix}$$

$$= \begin{bmatrix} \phi_{11} & \phi_{12} \\ \phi_{21} - (\theta G)_{21} & \phi_{22} - (\theta G)_{22} \end{bmatrix} \qquad (6\text{-}19)$$

$$\Lambda_2 = \begin{bmatrix} \phi_{33} & \phi_{34} & \phi_{35} \\ \phi_{43} & \phi_{44} & \phi_{45} \\ \phi_{53} & \phi_{54} & \phi_{55} \end{bmatrix} - \begin{bmatrix} 0 & 0 & 0 \\ 0 & 0 & 0 \\ (\theta G)_{53} & (\theta G)_{54} & (\theta G)_{55} \end{bmatrix}$$

$$= \begin{bmatrix} \phi_{33} & \phi_{34} & \phi_{35} \\ \phi_{43} & \phi_{44} & \phi_{45} \\ \phi_{53} - (\theta G)_{53} & \phi_{54} - (\theta G)_{54} & \phi_{55} - (\theta G)_{55} \end{bmatrix} \qquad (6\text{-}20)$$

$$\Lambda_3 = \begin{bmatrix} \phi_{66} & \phi_{67} & \phi_{68} \\ \phi_{76} & \phi_{77} & \phi_{78} \\ \phi_{86} & \phi_{87} & \phi_{88} \end{bmatrix} - \begin{bmatrix} 0 & 0 & 0 \\ 0 & 0 & 0 \\ (\theta G)_{86} & (\theta G)_{87} & (\theta G)_{88} \end{bmatrix}$$

$$= \begin{bmatrix} \phi_{66} & \phi_{67} & \phi_{68} \\ \phi_{76} & \phi_{77} & \phi_{78} \\ \phi_{86} - (\theta G)_{86} & \phi_{87} - (\theta G)_{87} & \phi_{88} - (\theta G)_{88} \end{bmatrix} \qquad (6\text{-}21)$$

The characteristic equation of the decoupled x dynamics is

$$|zI - \Lambda_1| = \begin{vmatrix} z - \phi_{11} & -\phi_{12} \\ -\phi_{21} + (\theta G)_{21} & z - \phi_{22} + (\theta G)_{22} \end{vmatrix}$$

$$= z^2 + \left((\theta G)_{22} - \phi_{11} - \phi_{22}\right)z + \phi_{11}\phi_{22} - \phi_{11}(\theta G)_{22} + \phi_{12}\left((\theta G)_{21} - \phi_{21}\right)$$

$$= (z + a_1 + jb_1)(z + a_1 - jb_1) \qquad (6\text{-}22)$$

where $a_1 = -0.9964457$ and $b_1 = -0.0035417$.

Now solving for the unknowns in Eq. (6-22), we have

$$(\theta G)_{21} = \theta_{21}g_{11} + \theta_{22}g_{21} + \theta_{23}g_{31}$$

$$= \frac{1}{\phi_{12}}\left(a_1^2 + b_1^2 + \phi_{11}^2 + 2a_1\phi_{11} + \phi_{12}\phi_{21}\right) \qquad (6\text{-}23)$$

$$(\theta G)_{22} = \theta_{21}g_{12} + \theta_{22}g_{22} + \theta_{23}g_{32} = \phi_{11} + \phi_{12} + 2a_1 \qquad (6\text{-}24)$$

For the ϕ_1 dynamics, the characteristic equation of Λ_2 is

$$|zI - \Lambda_2| = \begin{vmatrix} z - \phi_{33} & -\phi_{34} & -\phi_{35} \\ -\phi_{43} & z - \phi_{44} & -\phi_{45} \\ -\phi_{53} + (\theta G)_{53} & -\phi_{54} + (\theta G)_{54} & z - \phi_{55} + (\theta G)_{55} \end{vmatrix}$$

$$= z^3 + \left((\theta G)_{55} - \phi_{55} - \phi_{44} - \phi_{33}\right)z^2 + \left(-(\phi_{44} + \phi_{33})(\theta G)_{55} + \phi_{45}(\theta G)_{54}\right.$$

$$+ \phi_{35}(\theta G)_{53} - \phi_{54}\phi_{45} + \phi_{33}\phi_{55} + \phi_{33}\phi_{44} - \phi_{43}\phi_{34} - \phi_{35}\phi_{53} + \phi_{44}\phi_{45})z$$

$$+ [(\phi_{33}\phi_{44} - \phi_{43}\phi_{34})(\theta G)_{55} + (\phi_{35}\phi_{43} - \phi_{33}\phi_{45})(\theta G)_{54}$$

$$+ (\phi_{34}\phi_{45} - \phi_{35}\phi_{44})(\theta G)_{53} - \phi_{33}\phi_{44}\phi_{55} + \phi_{33}\phi_{54}\phi_{45} + \phi_{43}\phi_{34}\phi_{55}$$

$$- \phi_{43}\phi_{35}\phi_{54} - \phi_{34}\phi_{45}\phi_{53} + \phi_{35}\phi_{44}\phi_{53}) \qquad (6\text{-}25)$$

The desired characteristic equation is written as

$$(z + a_2 + jb_2)(z + a_2 - jb_2)(z + c_2) = 0 \qquad (6\text{-}26)$$

where

$$c_2 = -0.01831564$$

$$a_2 = -0.2592945$$

$$b_2 = -0.3191948$$

Equating Eqs. (6-25) and (6-26), we get

$$(\theta G)_{55} = \theta_{51}g_{15} + \theta_{52}g_{25} + \theta_{53}g_{35} = \phi_{55} + \phi_{44} + 1 + 2a_2 + c_2 \qquad (6\text{-}27)$$

$$(\theta G)_{54} = \theta_{51}g_{14} + \theta_{52}g_{24} + \theta_{53}g_{34}$$

$$= \frac{-\phi_{35}(1 + 2a_2 + a_2^2 + b_2^2)(1 + c_2)}{\phi_{45}(\phi_{35} + \phi_{34}\phi_{45} - \phi_{35}\phi_{44})} + \frac{1}{\phi_{45}}[(\phi_{44} + 1)(\phi_{55} + \phi_{44}$$

$$+ 1 + 2a_2 + c_2) - \phi_{44}\phi_{45} + \phi_{45}\phi_{54} - \phi_{55} - \phi_{44} + 2a_2c_2 + a_2^2 + b_2^2] \qquad (6\text{-}28)$$

$$(\theta G)_{53} = \theta_{51}g_{13} + \theta_{52}g_{23} + \theta_{53}g_{33}$$

$$= \frac{(1 + 2a_2 + a_2^2 + b_2^2)(1 + c_2)}{\phi_{35} + \phi_{34}\phi_{45} - \phi_{35}\phi_{44}} \qquad (6\text{-}29)$$

For the ϕ_2 dynamics, the characteristic equation of Λ_3 is

$$|zI - \Lambda_3| = \begin{vmatrix} z - \phi_{66} & -\phi_{67} & -\phi_{68} \\ -\phi_{76} & -\phi_{77} & -\phi_{78} \\ -\phi_{86} + (\theta G)_{86} & -\phi_{87} + (\theta G)_{87} & z - \phi_{88} + (\theta G)_{88} \end{vmatrix}$$

$$= z^3 + \left((\theta G)_{88} - \phi_{88} - \phi_{77} - \phi_{66}\right)z^2 + \left[-(\phi_{77} + \phi_{66})(\theta G)_{88} + \phi_{78}(\theta G)_{87}\right.$$

$$+ \phi_{68}(\theta G)_{86} - \phi_{87}\phi_{78} + \phi_{66}\phi_{88} + \phi_{66}\phi_{77} - \phi_{76}\phi_{67} - \phi_{68}\phi_{86} + \left.\phi_{77}\phi_{78}\right]z$$

$$+ \left[(\phi_{66}\phi_{77} - \phi_{76}\phi_{67})(\theta G)_{88} + (\phi_{68}\phi_{76} - \phi_{66}\phi_{78})(\theta G)_{87}\right.$$

$$+ (\phi_{67}\phi_{78} - \phi_{68}\phi_{77})(\theta G)_{86} - \phi_{66}\phi_{77}\phi_{88} + \phi_{66}\phi_{87}\phi_{78} + \phi_{76}\phi_{67}\phi_{88}$$

$$\left. - \phi_{76}\phi_{68}\phi_{87} - \phi_{67}\phi_{78}\phi_{86} + \phi_{68}\phi_{77}\phi_{86}\right) \qquad (6\text{-}30)$$

The desired characteristic equation is written as

$$(z + a_3 + jb_3)(z + a_3 - jb_3)(z + c_3) = 0 \qquad (6\text{-}31)$$

where

$$c_3 = -0.67032$$

$$a_3 = -0.911366$$

$$b_3 = -0.096987$$

Equating Eqs. (6-30) and (6-31), we get

$$(\theta G)_{86} = \theta_{81}g_{16} + \theta_{82}g_{26} + \theta_{83}g_{36}$$

$$= \frac{(1 + 2a_3 + a_3^2 + b_3^2)(1 + c_3)}{\phi_{68} + \phi_{67}\phi_{78} - \phi_{68}\phi_{77}} \qquad (6\text{-}32)$$

$$(\theta G)_{87} = \theta_{81}g_{17} + \theta_{82}g_{27} + \theta_{83}g_{37}$$

$$= \frac{-\phi_{68}(1 + 2a_3 + a_3^2 + b_3^2)(1 + c_3)}{\phi_{78}(\phi_{68} + \phi_{67}\phi_{78} - \phi_{68}\phi_{77})} + \frac{1}{\phi_{78}}\left((\phi_{77} + 1)(\phi_{88} + \phi_{77} + 1 + 2a_3 + c_3)\right.$$

$$\left. - \phi_{77}\phi_{78} + \phi_{78}\phi_{87} - \phi_{88} - \phi_{77} + 2a_3c_3 + a_3^2 + b_3^2\right) \qquad (6\text{-}33)$$

$$(\theta G)_{88} = \theta_{81}g_{18} + \theta_{82}g_{28} + \theta_{83}g_{38}$$

$$= \phi_{88} + \phi_{77} + 1 + 2a_3 + c_3 \qquad (6\text{-}34)$$

Equations (6-23), (6-24), (6-27), (6-28), (6-29), (6-32), (6-33) and (6-34) form the additional eight constraint equations, together with the 16 equations in Eq. (6-17) are adequate for the solution of the 24 unknown feedback gains ir

The solution of the 24 constraint equations gives the following results:

$$
\begin{aligned}
g_{11} &= 35.432513595904985 \\
g_{12} &= 209.57461847387285 \\
g_{13} &= -9.368484250209332\times10^{7} \\
g_{14} &= -8.11397701621271032\times10^{6} \\
g_{15} &= -1.4453443216549823\times10^{5} \\
g_{16} &= g_{17} = g_{18} = 0 \\
g_{21} &= -71.361744259885901 \\
g_{22} &= -409.94846384061196 \\
g_{23} &= 2.2392641102247482\times10^{8} \\
g_{24} &= 1.9394105849068884\times10^{7} \\
g_{25} &= 3.454675889387745\times10^{5} \\
g_{26} &= 3.578272520216161\times10^{5} \\
g_{27} &= 1.3239693135355619\times10^{6} \\
g_{28} &= 1.2749737170875715\times10^{4} \\
g_{31} &= g_{32} = 0 \\
g_{33} &= 4.015292755500438\times10^{7} \\
g_{34} &= 3.4776162570406019\times10^{6} \\
g_{35} &= 6.194684677849835\times10^{4} \\
g_{36} &= 3.578272527392904\times10^{5} \\
g_{37} &= 1.3239693094129 44\times10^{6} \\
g_{38} &= 1.2749737129324844\times10^{4}
\end{aligned}
\qquad (6\text{-}35)
$$

VII. COMPUTER SIMULATION AND DESIGN OF THE DIGITAL ASPS

7.1 Introduction

In the preceding chapter the digital ASPS was designed through decoupling and pole placement. In general, the decoupling problem does not have a unique solution. However, in the ASPS it turns out that some of the elements of the matrices $\phi(T)$ and $\theta(T)$ are very small so that the matrix θG can be approximated by a matrix which has only one nonzero row. We recall that the design objective is to realize simultaneously the following bandwidth requirements for the x, ϕ_1 and ϕ_2 components of the system:

x: bandwidth = 0.04 Hz

ϕ_1: bandwidth = 10 Hz

ϕ_2: bandwidth = 1 Hz

However, the "partial" decoupling of these components means that the desired bandwidths cannot be realized directly by the design method outlined in Chapter VI. A trial-and-error method is used to determine the feedback gains to meet the design requirements. The method involves first assuming a desired bandwidth for x, BW = 0.04 Hz, then we compute the required feedback gains, simulate the digital system, and observe the time responses to see if the individual bandwidth requirement is satisfied. If any one of the bandwidth is not satisfied, we adjust the bandwidth of x again, and repeat the process until we come close to the desired bandwidths. Only the bandwidth of x is varied in this case, since the bandwidths of ϕ_1 and ϕ_2 are not so sensitive to parameter variations.

In Chapter VI the digital ASPS was designed using the sampling period of 0.02 seconds. In this chapter larger sampling periods are considered. It is shown that the digital ASPS with state feedback can be stabilized for

a sampling period as large as 0.1 second.

7.2 Computer Simulation Results, T = 0.02 sec

In Chapter VI, we set the sampling period at T = 0.02 sec, and required that the bandwidths are 0.04 Hz, 10 Hz and 1 Hz, respectively for the x, ϕ_1 and ϕ_2 components. These bandwidth requirements correspond to a set of z-plane eigenvalues which the closed-loop system must realize. The corresponding feedback gains are obtained as in Eq. (6-35). The computer program listing for the design and simulation of the digital ASPS is given in Table 7-1. Figure 7-1 shows the time response of x(t) when the feedback gains are as given in Eq. (7-35). Notice that the response is very slow which corresponds to a system with a very narrow bandwidth, certainly much smaller than the desired value of 0.04 Hz. By reassigning the bandwidth of x, it is possible to fine tune the dynamics of x, ϕ_1 and ϕ_2. However, due to the coupling of the three components, it is extremely difficult to obtain the exact responses desired, depending on how the bandwidth is defined. In any case, the closed-loop eigenvalues of the system are placed at the desired location by the state feedback design. The desired eigenvalues are now specified as follows:

x: $z_1, z_2 = 0.964471639922 \pm j0.00342947$

ϕ_1: $z_3 = 0.01831564$

ϕ_2: $z_4, z_5 = 0.2592945 \pm j0.3191948$

$z_6 = 0.67032$

$z_7, z_8 = 0.911366 \pm j0.096987$

Note that only z_1 and z_2 are changed, but the other six roots are still the same as those specified in Chapter VI. The pole-placement design now yields the following feedback gains:

$$g_{11} = 3643.66148126889$$

$$
\begin{aligned}
g_{12} &= 2128.0189640019839 \\
g_{13} &= -9.3684842502093316 \times 10^{7} \\
g_{14} &= -8.11397701621271032 \times 10^{6} \\
g_{15} &= -1.4453443216549823 \times 10^{5} \\
g_{16} &= g_{17} = g_{18} = 0 \\
g_{21} &= -42330.651505108181 \\
g_{22} &= -10394.903057183335 \\
g_{23} &= 2.2392641102247482 \times 10^{8} \\
g_{24} &= 1.9394105849068884 \times 10^{7} \\
g_{25} &= 3.454675889387745 \times 10^{5} \\
g_{26} &= 3.5782725250216161 \times 10^{5} \\
g_{27} &= 1.3239693135355619 \times 10^{6} \\
g_{28} &= 1.2749737170875715 \times 10^{4} \\
g_{31} &= g_{32} = 0 \\
g_{33} &= 4.0152927555004380 \times 10^{7} \\
g_{34} &= 3.4776162570406019 \times 10^{6} \\
g_{35} &= 6.194684677849835 \times 10^{4} \\
g_{36} &= 3.5782725273929039 \times 10^{5} \\
g_{37} &= 1.323969309412944 \times 10^{6} \\
g_{38} &= 1.2749737129324844 \times 10^{4}
\end{aligned}
\qquad (7\text{-}1)
$$

Note that except for g_{11}, g_{12}, g_{21} and g_{22} all the other feedback gains are identical to those given in Eq. (6-35). The time responses of x, ϕ_1 and ϕ_2 for these feedback gains are shown in Figs. 7-2, 7-3 and 7-4, respectively. These responses are very close to having the desired bandwidths.

Table 7-1. Computer Program For the Design and Simulation of the Digital ASPS

```
      IMPLICIT REAL*8 (A-H,O-Z)
C     CALCULATION OF GW AND EN FOR THE POINT AT POINT METHOD
C     CALCULATION BY SERIES SUMMATION
      DIMENSION A(8,8),B(8,3),GO(3,8),GW(3,8),EO(1,1),CW(1,1)
      DIMENSION STMTS(8,8),H(3,8),THETAC(8,3),THETAS(8,3),AC(8,8)
      DIMENSION STMTC(8,8),LW(3),MN(3),WORK1(3,3),WORK2(3,8),WORK3(8,8)
      DIMENSION WORK4(8,8),WORK5(8,8),WORK6(8,8),WORK7(8,8),WORK8(3,8)
        DIMENSION WI(3,3),WO(3,8)
      DET=0.
      KMAX=2000
      N=8
      M=3
      DO 18 I=1,N
      DO 19 J=1,M
      B(I,J)=0.
      H(J,I)=0.
19    GO(J,I)=0.
      DO 18 J=1,N
18    A(I,J)=0.
C
C       SYSTEM CONSTANTS
C
        AMI=600.
        AKSX=1.051
        AKSP=0.005
        AKSS=0.005
        AJ=503.
        A33=2805.15
        RB=1.956
        AO=RB
        BO=1./AMI
        CO=AMI*RB/A33
        DO=AJ/A33
        E=1./A33
        F=1./AJ
        DELTA=1.-AO*CO-DO
C
C       NON-ZERO ENTRIES OF THE MATRICES
C
        A(1,2)=1.
        A(2,1)=-BO*AKSX*(1.-DO)/DELTA
        A(2,4)=-E*AKSP*AO/DELTA
        A(2,7)=AKSS*F*DO*AO/DELTA
        A(3,4)=1.
        A(4,5)=1.
        A(5,1)=-AKSX*BO*CO/DELTA
        A(5,4)=-AKSP*E/DELTA
        A(5,7)=AKSS*DO*F/DELTA
        A(6,7)=1.
```

```
      A(7,8)=1.
      A(8,1)=AKSX*BO*CO/DELTA
      A(8,4)=AKSP*E/DELTA
      A(8,7)=-AKSS*F*(1.-AO*CO)/DELTA
      B(2,1)=BO*(1.-CO)/DELTA
      B(2,2)=E*AO/DELTA
      B(2,3)=-FY00*AO/DELTA
      B(5,1)=BO*CO/DELTA
      B(5,2)=E/DELTA
      B(5,3)=-AO*F/DELTA
      B(8,1)=-BO*CO/DELTA
      B(8,2)=-E/DELTA
      B(8,3)=F*(1.-AO*CO)/DELTA
      GO(1,1)=3.6449E1
      GO(1,2)=2.124E1
      GO(1,3)=-7.2569?1248E8
      GO(1,4)=-?.5471626624E7
      GO(1,5)=-3.389.5568E5
      GO(1,6)=0.E0
      GO(2,1)=-7.355E1
      GO(2,2)=-4.154544E1
      GO(2,3)=2.212612555?E9
      GO(2,4)=6.0882?26624E7
      GO(2,5)=8.1013732E5
      GO(2,6)=3.?6750304?5
      GO(2,7)=1.091703152E5
      GO(2,8)=1.4526640E4
      GO(3,3)=3.96?5030?E8
      GO(3,4)=1.091707152E7
      GO(3,5)=1.45?664?E5
      GO(3,6)=3.96?50304E5
      GO(3,7)=1.091?051E5
      GO(3,8)=1.452664?E4
      H(1,1)=0.99
      H(1,2)=0.01
      H(2,3)=0.01
      H(2,4)=0.98
      H(2,5)=0.01
      H(3,6)=0.01
      H(3,7)=0.98
      H(3,8)=0.01

C
      TYPE 107
        DO 201 J=1,N
201     TYPE 110,(A(J,I),I=1,N)
      TYPE 108
        DO 202 J=1,N
202     TYPE 210,(B(J,I),I=1,M)
      TYPE 109
        DO 203 J=1,M
```

ORIGINAL PAGE IS
OF POOR QUALITY

```
C203      TYPE 110,(GO(J,1),I=1,N)

C-      SAMPLING PERIOD
        T=0.1
        TYPE 101,T
          TYPE 301
301       FORMAT(4X,'FIRST PASS OF STRMAT')
        CALL STRMAT(A,N,T,STMTS,WORK3,K1,WORK4,WORK5)
        IF(K1-KMAX) 30,20,20
30      CALL GMPRD(WORK3,B,THETAS,N,N,M)
          TYPE 401
401       FORMAT(4X,'THE EXP(A*T) MATRIX')
          DO 402 I=1,N
402       TYPE 110,(STMTS(I,J),J=1,N)
          TYPE 403
403       FORMAT(4X,'THE THETA MATRIX')
          DO 404 I=1,N
404       TYPE 210,(THETAS(I,J),J=1,M)
          PI=3.141592653
          DSQ2=1./SQRT(2.)
          FAC1=1.*T*DSQ2*2.*PI
          FAC2=0.8*T*DSQ2*2.*PI
          FAC3=0.13*T*DSQ2*2.*PI
          A1=-DEXP(-FAC1)*DCOS(FAC1)
          B1=-DEXP(-FAC1)*DSIN(FAC1)
          C1=-DEXP(-200.*T)
          A2=-DEXP(-FAC2)*DCOS(FAC2)
          B2=-DEXP(FAC3)*DSIN(FAC2)
          C2=-DEXP(-20.*T)
          A3=-DEXP(-FAC3)*DCOS(FAC3)
          B3=-DEXP(-FAC3)*DSIN(FAC3)
          TYPE 501
501       FORMAT(/4X,'**THE POLES OF THE DISCRETE SYSTEM**:')
          TYPE 502,A1,B1,C1
          TYPE 502,A2,B2,C2
          TYPE 502,A3,B3
502       FORMAT(/4X,1P3E21.12)
          WI(1,1)=THETAS(2,1)
          WI(1,2)=THETAS(2,2)
          WI(1,3)=THETAS(2,3)
          WI(2,1)=THETAS(5,1)
          WI(2,2)=THETAS(5,2)
          WI(2,3)=THETAS(5,3)
          WI(3,1)=THETAS(8,1)
          WI(3,2)=THETAS(8,2)
          WI(3,3)=THETAS(8,3)
          WO(1,1)=(1./STMTS(1,2))*(A3*A3+B3*B3+STMTS(1,1)*STMTS(1,1)
     &      +2.*A3*STMTS(1,1)+STMTS(1,2)*STMTS(2,1))
          WO(2,1)=STMTS(5,1)
          WO(3,1)=STMTS(8,1)
          WO(1,2)=STMTS(1,1)+STMTS(2,2)+2.*A3
```

```
      WO(2,1)=STMTS(4,2)
      WO(3,2)=STMTS(8,2)
      WO(1,3)=STMTS(2,3)
      WO(2,3)=(1.+C1*(A1*A1+B1*B1)*(1.+C1)/(STMTS(4,5)
     &  +STMTS(3,4)*STMTS(4,5)-STMTS(3,5)*STMTS(4,4))
      WO(3,3)=STMTS(8,3)
      WO(1,4)=STMTS(2,4)
      WO(2,4)=(1./STMTS(4,5))*((STMTS(4,4)+1.)*STMTS(5,5)
     &  +STMTS(4,4)+1.+2.*A1+C1)-STMTS(4,4)*STMTS(4,5)
     &  +STMTS(4,5)*STMTS(5,4)-STMTS(5,5)-STMTS(4,4)+2.*A1*C1
     &  +A1*A1+B1*B1)-(STMTS(3,5)/STMTS(4,5))*(1.+2.*A1+
     &  A1*A1+B1*B1)*(1.+C1)/(STMTS(3,5)+STMTS(3,4)*STMTS(4,5)
     &  -STMTS(3,5)*STMTS(4,4))
      WO(3,4)=STMTS(8,4)
      WO(1,5)=STMTS(2,5)
      WO(2,5)=STMTS(5,5)+STMTS(4,4)+1.+2.*A1+C1
      WO(3,5)=STMTS(8,5)
      WO(1,6)=STMTS(2,6)
      WO(2,6)=STMTS(5,6)
      WO(3,6)=(1.+2.*A2+A2*A2+B2*B2)*(1.+C2)/(STMTS(6,8)
     &  +STMTS(6,7)*STMTS(7,8)-STMTS(6,8)*STMTS(7,7))
      WO(1,7)=STMTS(2,7)
      WO(2,7)=STMTS(5,7)
      WO(3,7)=(1./STMTS(7,8))*((STMTS(7,7)+1.)*(STMTS(8,8)
     &  +STMTS(7,7)+1.+2.*A2+C2)-STMTS(7,8)*STMTS(7,8)
     &  +STMTS(7,8)*STMTS(8,7)-STMTS(8,8)*STMTS(7,7)+2.*A2*C2
     &  +A2*A2+B2*B2)-(STMTS(6,8)/STMTS(7,8))*(1.+2.*A2+A2*A2+
     &  +B2*B2)*(1.+C2)/(STMTS(6,8)*STMTS(8,7)*STMTS(7,8)
     &  -STMTS(6,8)*STMTS(7,7))
      WO(1,8)=STMTS(2,8)
      WO(2,8)=STMTS(5,8)
      WO(3,8)=STMTS(8,8)+STMTS(7,7)+1 +2.*A2+C2
      CALL MINV(WI,N,DET,LW,MW)
      CALL GMPRD(WI,WO,GW,M,M,N)
      CALL GMPRD(THETAS,GW,WORK7,N,M,N)
      CALL GMSUB(STMTS,WORK7,WORK6,N,N)
      TYPE 503
503   FORMAT(/4X,'THE FEEDBACK COEFFICIENTS')
      DO 504 I=1,M
      TYPE 505,(GW(I,J),J=1,N)
504   TYPE 506
505   FORMAT(/4X,1P4D25.16)
506   FORMAT(/4X,'*')
      TYPE 507
507   FORMAT(/4X,'THE PHI-THETA*G MATRIX')
      DO 508 I=1,N
508   TYPE 110,(WORK6(I,J),J=1,N)
```

```
      CALL EXIT
100   FORMAT(/4X,4HDET=,1PE12.4)
101   FORMAT(/4X,18HWEIGHTING MATRIX H)
102   FORMAT(/4X,45HCONT. TRANSITION MATRIX FOR CONTINUOUS SYSTEM,10X,
     12HK=,I2)
103   FORMAT(/4X,46HDATE TRANSITION MATRIX FOR SAMPLE DATA SYSTEM,10X,
     12HK=,I2)
104   FORMAT(/4X,2HGW)
105   FORMAT(/4X,'**********',I5,'**********',/,4X,2HT=,E9.2)
106   FORMAT(/4X,2HEW)
110   FORMAT(2X,1P8E14.7)
107   FORMAT(/4X,'THE A MATRIX')
108   FORMAT(/4X,'THE B MATRIX')
109   FORMAT(/4X,'THE QQ MATRIX')
111   FORMAT(/4X,'THE EQ MATRIX')
210     FORMAT(2X,1PE12.4,I2)
      END
        SUBROUTINE GMPRD(A,B,R,N,M,L)
        IMPLICIT REAL*8(A-H,O-Z)
        DIMENSION A(N,M),B(M,L),R(N,L)
        DO 1 I=1,N
        DO 1 J=1,L
        R(I,J)=0.
        DO 1 K=1,M
1       R(I,J)=R(I,J)+A(I,K)*B(K,J)
        RETURN
        END
        SUBROUTINE GMMUL(A,B,R,N,M,L)
        IMPLICIT REAL*8(A-H,O-Z)
        DIMENSION A(1),B(1),R(1)
        IR=0
        IK=-M
        DO 10 K=1,L
        IK=IK+M
        DO 10 J=1,N
        IR=IR+1
        JI=J-N
        IB=IK
        R(IR)=0
        DO 10 I=1,M
        JI=JI+N
        IB=IB+1
10      R(IR)=R(IR)+A(JI)*B(IB)
        RETURN
        END
        SUBROUTINE GMSUB(A,B,R,N,M)
        IMPLICIT REAL*8(A-H,O-Z)
        DIMENSION A(N,M),B(N,M),R(N,M)
        DO 1 I=1,N
        DO 1 J=1,M
1       R(I,J)=A(I,J)-B(I,J)
        RETURN
        END
        SUBROUTINE GMPSC(A,B,C,N,M)
        IMPLICIT REAL*8(A-H,O-Z)
        DIMENSION A(N,M),B(N,M)
        DO 1 I=1,N
```

```
      DO 1 J=1,M
      B(I,J)=A(I,J)*C
      RETURN
      ENTRY
      SUBROUTINE MMAUX(A,B,R,N,M)
      IMPLICIT REAL*8(A-H,O-Z)
      DIMENSION A(N,M),B(N,M),R(N,M)
      DO 1 I=1,N
      DO 1 J=1,M
1     R(I,J)=A(I,J)+B(I,J)
      RETURN
      END
      SUBROUTINE SIRMAT(A,N,T,PHI,THETA,N,W1,W2)
      IMPLICIT REAL*8 (A-H,O-Z)
      DIMENSION A(N,N),PHI(N,N),DELTA(N,N),W1(N,N),W2(N,N)
      N2=N*N
      ALPHA=1.E-5
      BETA=1.E-40
      KMAX=2000
      LIN=0
C
C     INITIALIZATION
C
C
      DO 3 I=1,N
      DO 3 J=1,N
      IF(I-J) 1,2,1
1     PHI(I,J)=0.
      W1(I,J)=0.
      THETA(I,J)=0.
      GO TO 3
2     PHI(I,J)=1.
      W1(I,J)=T
      THETA(I,J)=T
3     CONTINUE
C
C     NORM OF A
C
      TYPE 601
601   FORMAT(/4X,'THE PASSED A MATRIX')
      DO 600 I=1,N
600   TYPE 203,(A(I,J),J=1,N)
      TYPE 602
602   FORMAT(4X,'*')
      ANORM=0.
      DO 4 I=1,N
      DO 4 J=1,N
4     ANORM=ANORM+DABS(A(I,J))
      K=2
C
C     START OF LOOP
```

ORIGINAL PAGE IS
OF POOR QUALITY

```
C
13      AK=K
        CALL GMPRD(A,W2,W2,N,N,N)
        CALL GMADD(W2,PHI,PHI,N,N)
        C=T/AK
101     FORMAT(I6)
        CALL GMPSC(W2,W1,C,N,N)
        CALL GMADD(W1,THETA,THETA,N,N)
203       FORMAT(2X,IPBE14.7)
          IF(AK-ANORM*T) 51,51,7
51        LIN=1
          GO TO 5
7       BNORM=0.
          DO 8 I=1,N
          DO 8 J=1,N
8           BNORM=BNORM+DABS(W2(I,J))
        EPSLON=ANORM*T/(AK+2.)
        TEST=BNORM*ANORM*T/((AK+1.)*(1.-EPSLON))
        DO 9 I=1,N
          DO 9 J=1,N
        IF(DABS(PHI(I,J))-BETA) 9,9,10
10      IF(TEST-ALPHA*DABS(PHI(I,J))) 9,9,52
52        LIN=2
          GO TO 5
9       CONTINUE
        RETURN
5       IF(K-KMAX) 11,12,12
11      K=K+1
          LIN=0
        GO TO 13
12      TYPE 100,K
          TYPE207,LIN
207       FORMAT(4X,'STATUS IS ',I2)
          TYPE 500,ANORM,K
500       FORMAT(/4X,'ANORM=',1PE14.7,'    K=',I5)
        RETURN
100     FORMAT(//20H K GREATER THAN KMAX,I5//)
        END
          SUBROUTINE MINV(A,N,D,L,M)
          IMPLICIT REAL*8(A-H,O-Z)
        DIMENSION A(1),L(1),M(1)
C
C         SEARCH FOR LARGEST ELEMENT
C
        D=1.0
        NK=-N
        DO 80 K=1,N
        NK=NK+N
        L(K)=K
        M(K)=K
        KK=NK+K
```

```
      BIGA=A(KK)
      DO 20 J=K,N
      IZ=IK(J-1)
      DO 20 I=K,N
      IJ=IZ+I
10    IF(ABS(BIGA)-ABS(A(IJ)))15,20,20
15    BIGA=A(IJ)
      L(K)=I
      M(K)=J
20    CONTINUE
C
C        INTERCHANGE ROWS
C
      J=L(K)
      IF(J-K) 35,35,25
25    KI=K-N
      DO 30 I=1,N
      KI=KI+N
      HOLD=-A(KI)
      JI=KI-K+J
      A(KI)=A(JI)
30    A(JI) =HOLD
C
C        INTERCHANGE COLUMNS
C
35    I=M(K)
      IF(I-K) 45,45,38
38    JP=NP(I-1)
      DO 40 J=1,N
      JK=NK+J
      JI=JP+I
      HOLD=-A(JK)
      A(JK)=A(JI)
40    A(JI) =HOLD
C
C        DIVIDE COLUMN BY MINUS PIVOT (VALUE OF PIVOT ELEMENT IS
C        CONTAINED IN BIGA)
C
45    IF(BIGA) 48,46,48
46    D=0.0
      RETURN
48    DO 55 I=1,N
      IF(I-K) 50,55,50
50    IK=NK+I
      A(IK)=A(IK)/(-BIGA)
55    CONTINUE
C
C        REDUCE MATRIX
C
      DO 65 I=1,N
      IK=NK+I
```

ORIGINAL PAGE IS
OF POOR QUALITY

```
      HOLD=A(IK)
      IJ=I-N
      DO 65 J=1,N
      IJ=IJ+N
      IF(I-K) 60,65,60
   60 IF(J-K) 62,65,62
   62 KJ=IJ-I+K
      A(IJ)=HOLD*A(KJ)+A(IJ)
   65 CONTINUE
C
C        DIVIDE ROW BY PIVOT
C
      KJ=K-N
      DO 75 J=1,N
      KJ=KJ+N
      IF(J-K) 70,75,70
   70 A(KJ)=A(KJ)/BIGA
   75 CONTINUE
C
C        PRODUCT OF PIVOTS
C
      D=D*BIGA
C
C        REPLACE PIVOT BY RECIPROCAL
C
      A(KK)=1.0/BIGA
   80 CONTINUE
C
C        FINAL ROW AND COLUMN INTERCHANGE
C
      K=N
  100 K=(K-1)
      IF(K) 150,150,105
  105 I=L(K)
      IF(I-K) 120,120,108
  108 JQ=N*(K-1)
      JR=N*(I-1)
      DO 110 J=1,N
      JK=JQ+J
      HOLD=A(JK)
      JI=JR+J
      A(JK)=-A(JI)
  110 A(JI) =HOLD
  120 J=M(K)
      IF(J-K) 100,100,125
  125 KI=K-N
      DO 130 I=1,N
      KI=KI+N
      HOLD=A(KI)
      JI=KI-K+J
      A(KI)=-A(JI)
  130 A(JI) =HOLD
      GO TO 100
  150 RETURN
      END
```

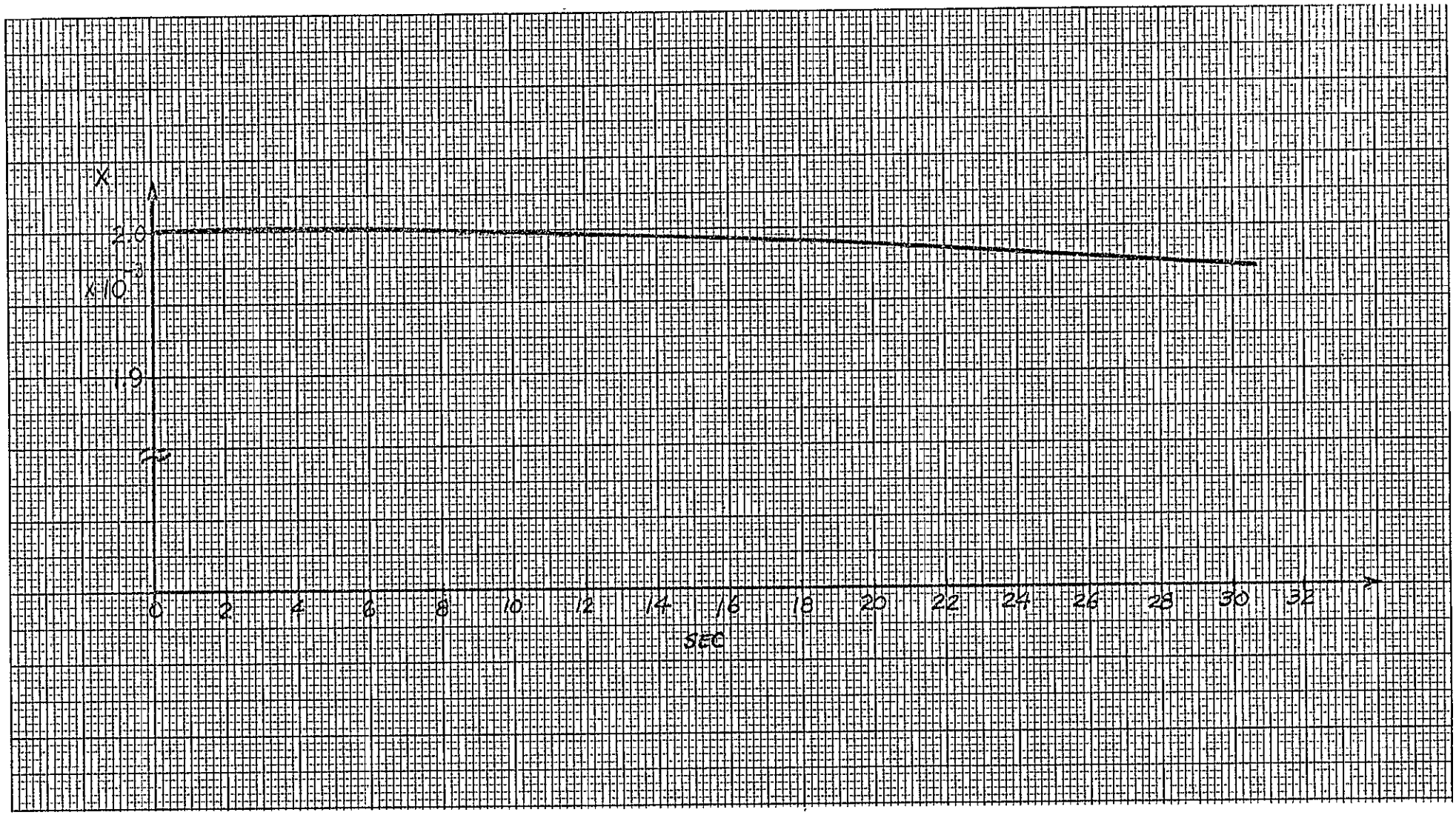

Figure 7-1. Time response of x, T = 0.02 sec, with feedback gains given in Eq. (6-35).

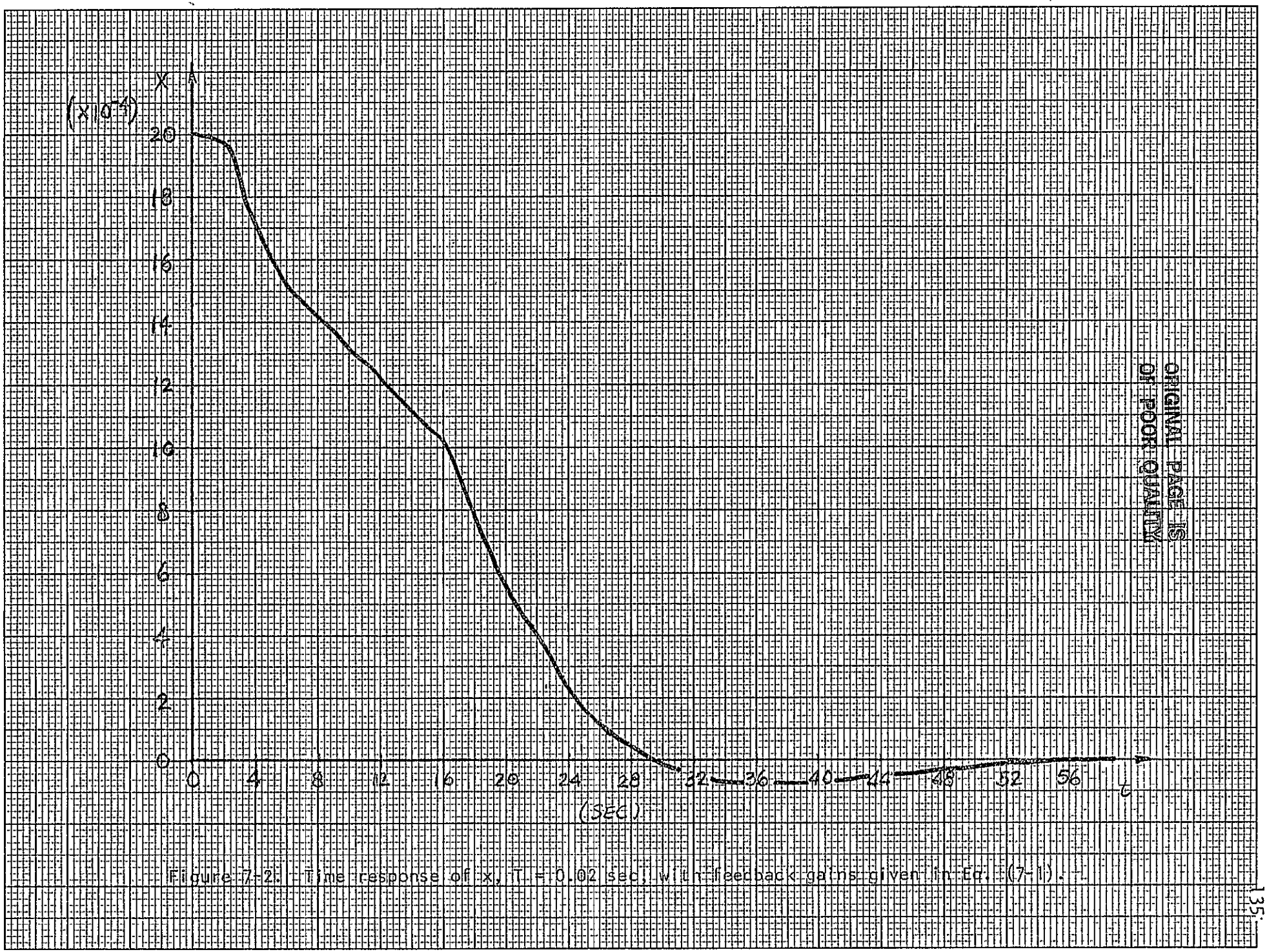

Figure 7-2. Time response of x, T = 0.02 sec, with feedback gains given in Eq. (7-11).

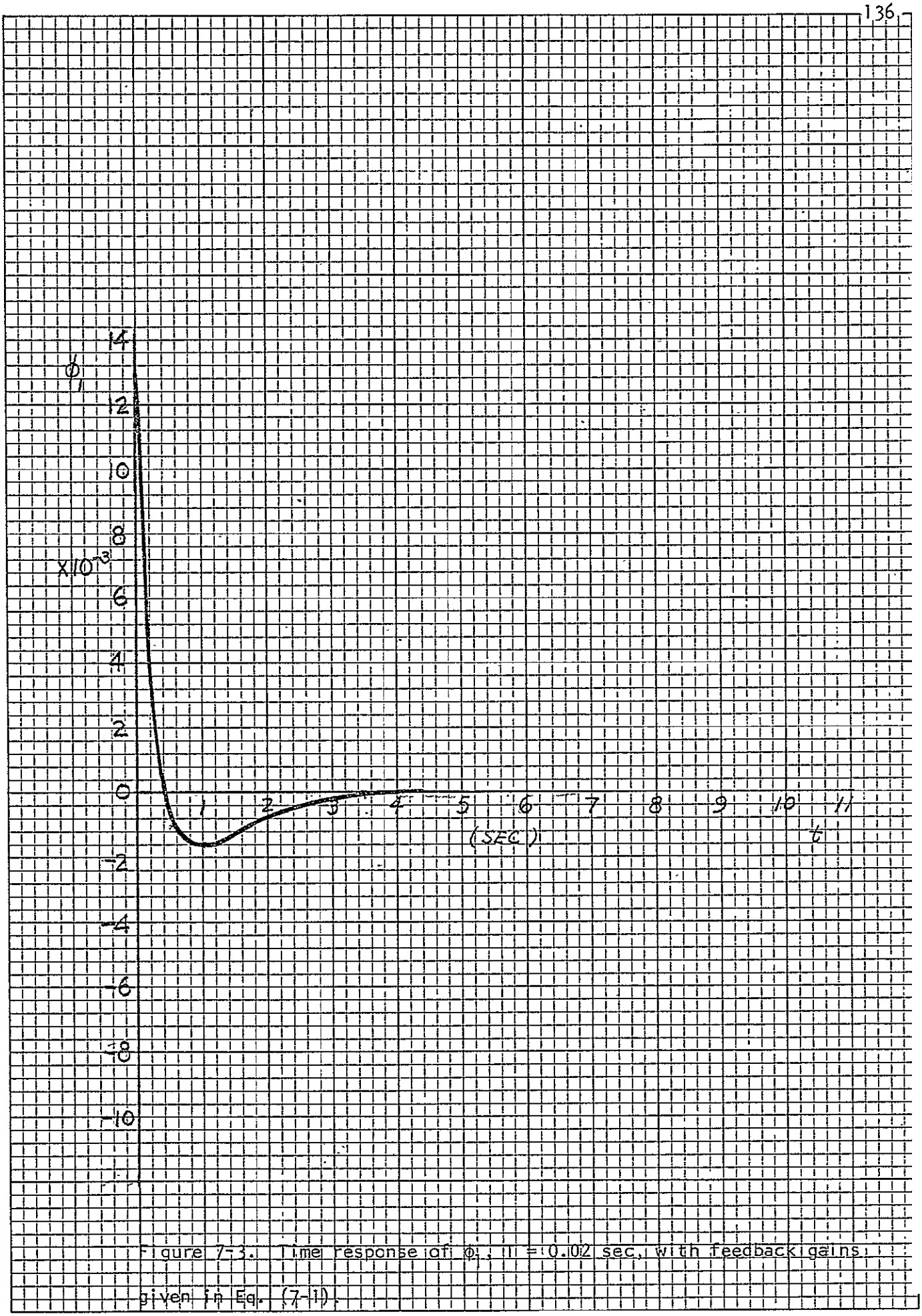

Figure 7-3. Time response of ϕ_1; $\Pi = 0.02$ sec, with feedback gains given in Eq. (7-11).

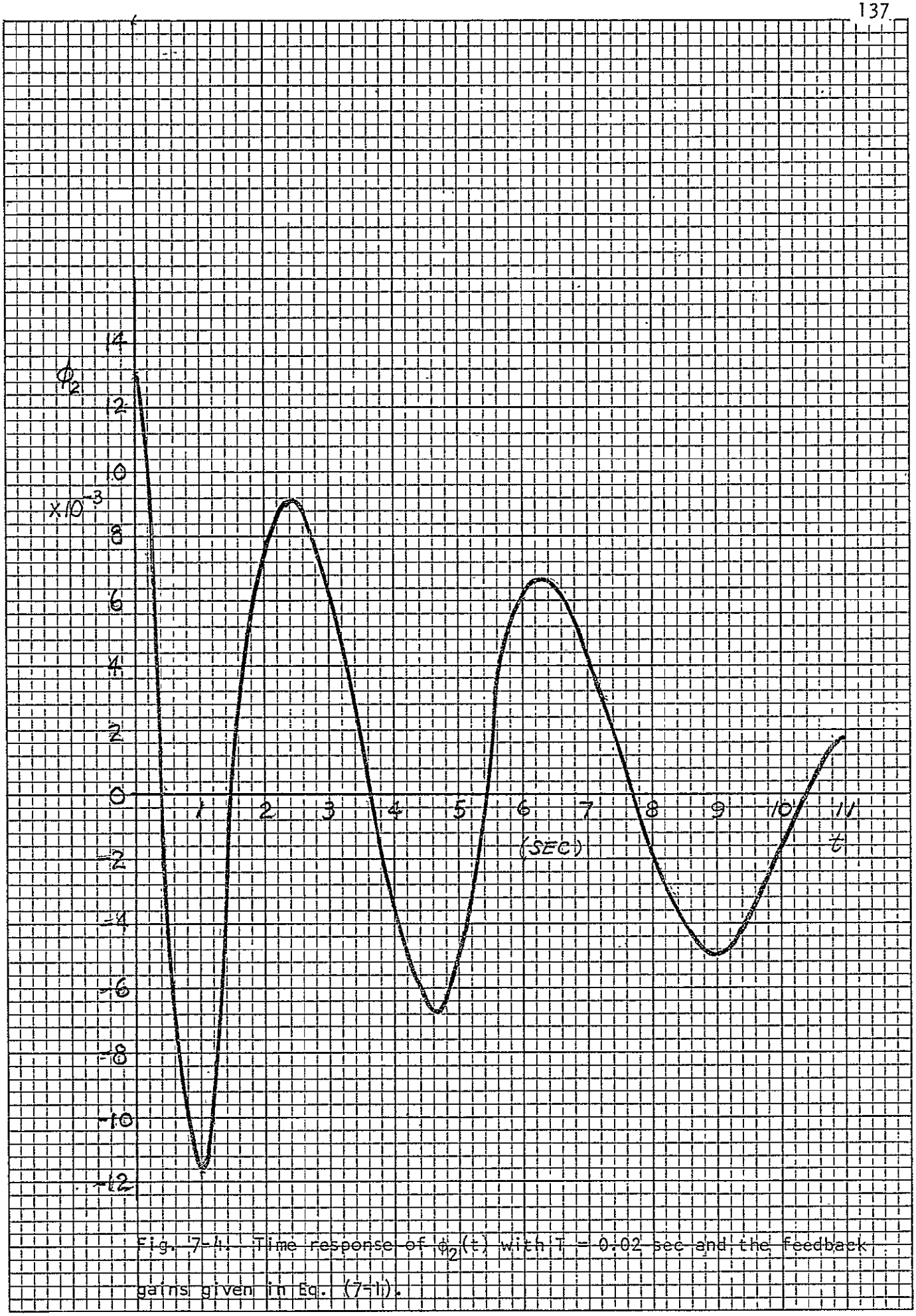

Fig. 7-4. Time response of $\phi_{12}(t)$ with $T = 0.02$ sec and the feedback gains given in Eq. (7-11).

7.3 Computer Simulation Results, T = 0.04 sec

It is of interest to investigate if the sampling period can be increased and still be able to realize state feedback control to achieve the desired bandwidths for the three system components. The sampling period is now increased to 0.04 sec. The matrices $\phi(T)$ and $\theta(T)$ for T = 0.04 sec are given as follows:

$$\phi(0.04) = \begin{bmatrix}
9.995\times10^{-1} & 3.999\times10^{-2} & 0 & -1.187\times10^{-6} & -1.583\times10^{-8} & 0 & 1.187\times10^{-6} & 1.583\times10^{-8} \\
-2.447\times10^{-2} & 9.995\times10^{-1} & 0 & -5.936\times10^{-5} & -1.187\times10^{-6} & 0 & 5.936\times10^{-5} & 1.187\times10^{-6} \\
-3.328\times10^{-6} & -3.33\times10^{-8} & 1 & 3.999\times10^{-2} & 7.999\times10^{-4} & 0 & 8.094\times10^{-9} & 8.094\times10^{-11} \\
-2.496\times10^{-4} & -3.33\times10^{-6} & 0 & 9.999\times10^{-1} & 3.999\times10^{-2} & 0 & 6.070\times10^{-7} & 8.094\times10^{-9} \\
-1.247\times10^{-2} & -2.49\times10^{-4} & 0 & -3.035\times10^{-5} & 9.999\times10^{-1} & 0 & 3.035\times10^{-5} & 6.070\times10^{-7} \\
3.328\times10^{-6} & 3.328\times10^{-8} & 0 & 8.094\times10^{-9} & 8.094\times10^{-11} & 1 & 3.999\times10^{-2} & 7.999\times10^{-4} \\
2.496\times10^{-4} & 3.328\times10^{-6} & 0 & 6.070\times10^{-7} & 8.094\times10^{-9} & 0 & 9.999\times10^{-1} & 3.999\times10^{-2} \\
1.247\times10^{-2} & 2.496\times10^{-4} & 0 & 3.035\times10^{-5} & 8.094\times10^{-7} & 0 & -3.074\times10^{-5} & 9.999\times10^{-1}
\end{bmatrix} \quad (7\text{-}2)$$

$$\theta(0.04) = \begin{bmatrix}
4.658\times10^{-4} & 2.374\times10^{-4} & -2.374\times10^{-4} \\
2.329\times10^{-2} & 1.187\times10^{-2} & -1.187\times10^{-2} \\
3.166\times10^{-6} & 1.618\times10^{-6} & -1.618\times10^{-6} \\
2.374\times10^{-4} & 1.214\times10^{-4} & -1.214\times10^{-4} \\
1.187\times10^{-2} & 6.070\times10^{-3} & -6.070\times10^{-3} \\
-3.166\times10^{-6} & -1.618\times10^{-6} & 1.640\times10^{-6} \\
-2.374\times10^{-4} & -1.214\times10^{-4} & 1.230\times10^{-4} \\
-1.187\times10^{-2} & -6.070\times10^{-3} & 6.149\times10^{-3}
\end{bmatrix} \quad (7\text{-}3)$$

The desired eigenvalues of the closed-loop ASPS are set at:

x: $z_1, z_2 = 0.976901072005 \pm j0.00225733531031$

ϕ_1: $z_3 = 0.0003354626270$

ϕ_2: $z_4, z_5 = 0.0028068097799 \pm j0.003939345$

$z_6 = 0.4493289641172$

$z_7, z_8 = 0.8587194942988 \pm j0.16334107966$

The feedback gains are determined and are tabulated as follows:

$$g_{11} = 3.8178805894610170\times10^{2}$$
$$g_{12} = 6.8560283114373904\times10^{2}$$
$$g_{13} = -1.8228873974050188\times10^{7}$$
$$g_{14} = -2.5313721087607277\times10^{6}$$
$$g_{15} = -8.7845436116937588\times10^{4}$$
$$g_{16} = g_{17} = g_{18} = 0$$
$$g_{21} = -7.4488328494704121 3\times10^{2}$$
$$g_{22} = -1.3410796296921878\times10^{3}$$
$$g_{23} = 4.3570829799433742\times10^{7} \qquad (7\text{-}4)$$
$$g_{24} = 6.0505099423975705\times10^{6}$$
$$g_{25} = 2.0996900572869749\times10^{5}$$
$$g_{26} = 2.0185680288217810\times10^{5}$$
$$g_{27} = 3.6134117793464126\times10^{5}$$
$$g_{28} = 1.0477885260603344\times10^{4}$$
$$g_{31} = g_{32} = 0$$
$$g_{33} = 7.8128183443659252\times10^{6}$$
$$g_{34} = 1.0849353874460890\times10^{6}$$
$$g_{35} = 3.7650182657481631\times10^{4}$$
$$g_{36} = 2.0185680341725262\times10^{5}$$
$$g_{37} = 3.6134117389247105\times10^{5}$$

$$g_{38} = 1.0477885188377713 \times 10^{4}$$

The time responses of $x(t)$, $\phi_1(t)$ and $\phi_2(t)$ for T = 0.04 and the feedback gains as listed above are shown in Figs. 7-5, 7-6 and 7-7, respectively.

7.4 Computer Simulation Results, T = 0.1 sec

Since the on-board computer has a limited capacity and processing speed, it is important that the sampling period of the ASPS should be kept as large as possible. It is well known that in general large sampling periods are detrimental to the stability of digital control systems. In the preceeding sections we have shown the design of the feedback gains for the ASPS to realize the bandwidth requirements with sampling periods of 0.02 and 0.04 seconds. In this section we shall show that the ASPS can be operated with a sampling period as large as 0.1 second.

For T = 0.1 second, the $\phi(T)$ and $\theta(T)$ matrices are,

$$\phi(0.1) =$$

$$\begin{bmatrix}
9.969\times10^{-1} & 9.999\times10^{-2} & 0 & -7.418\times10^{-6} & -2.473\times10^{-7} & 0 & 7.418\times10^{-6} & 2.473\times10^{-7} \\
-6.114\times10^{-2} & 9.969\times10^{-1} & 0 & -1.483\times10^{-4} & -7.418\times10^{-6} & 0 & 1.483\times10^{-4} & 7.418\times10^{-6} \\
-5.199\times10^{-5} & -1.299\times10^{-6} & 1 & 9.999\times10^{-2} & 4.999\times10^{-3} & 0 & 1.264\times10^{-7} & 3.161\times10^{-9} \\
-1.559\times10^{-3} & -5.198\times10^{-5} & 0 & 9.999\times10^{-1} & 9.999\times10^{-2} & 0 & 3.792\times10^{-6} & 1.264\times10^{-7} \\
-3.117\times10^{-2} & -1.559\times10^{-3} & 0 & -7.581\times10^{-5} & 9.999\times10^{-1} & 0 & 7.581\times10^{-5} & 3.792\times10^{-6} \\
5.199\times10^{-5} & 1.299\times10^{-6} & 0 & 1.264\times10^{-7} & 3.161\times10^{-9} & 1 & 9.999\times10^{-2} & 4.999\times10^{-3} \\
1.559\times10^{-3} & 5.198\times10^{-5} & 0 & 3.792\times10^{-6} & 1.264\times10^{-7} & 0 & 9.999\times10^{-1} & 9.999\times10^{-2} \\
3.117\times10^{-2} & 1.559\times10^{-3} & 0 & 7.581\times10^{-5} & 3.793\times10^{-6} & 0 & -7.681\times10^{-5} & 9.999\times10^{-1}
\end{bmatrix} \quad (7\text{-}5)$$

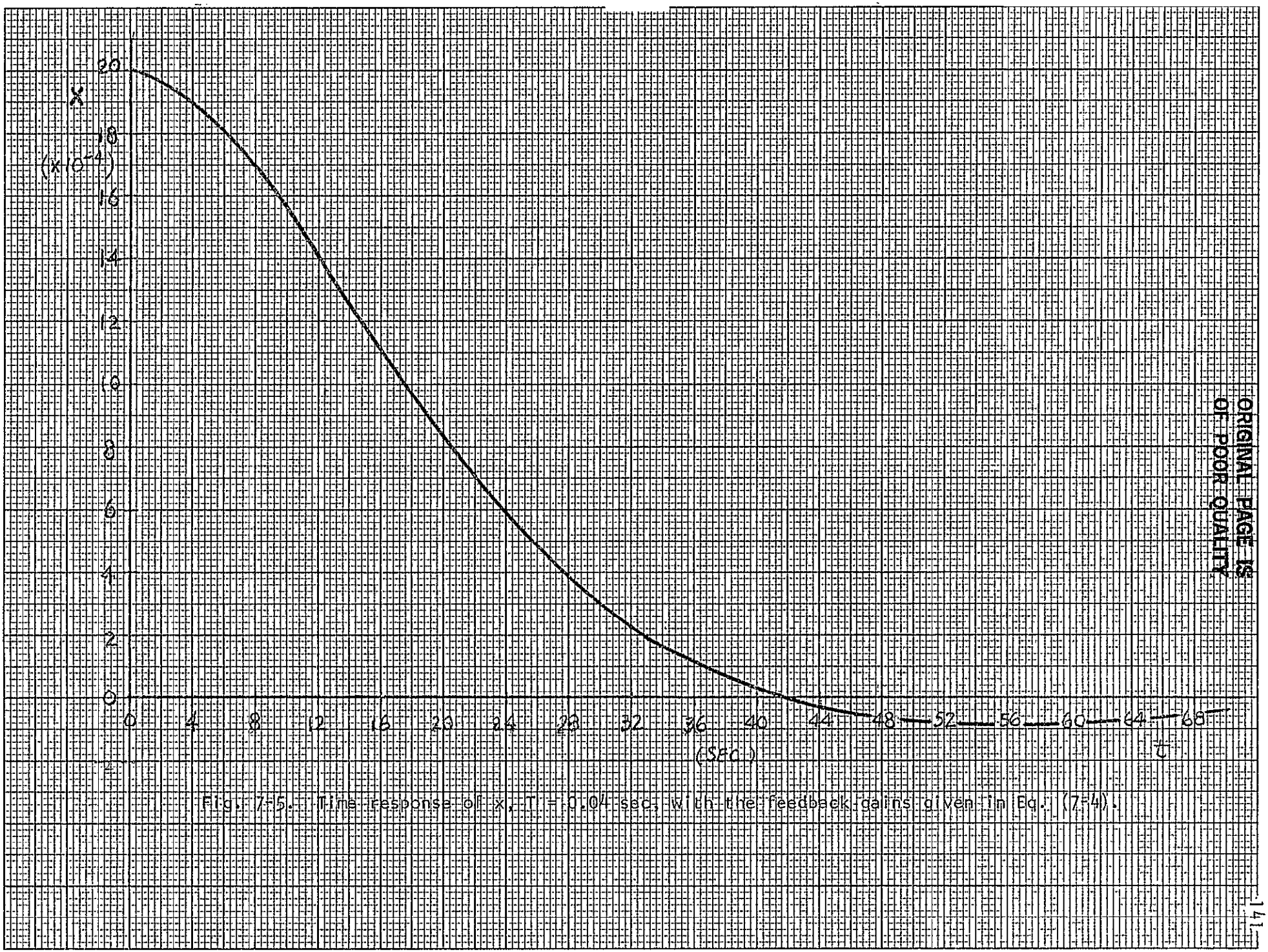

Fig. 7-5. Time response of x, T = 0.04 sec, with the feedback gains given in Eq. (7-4).

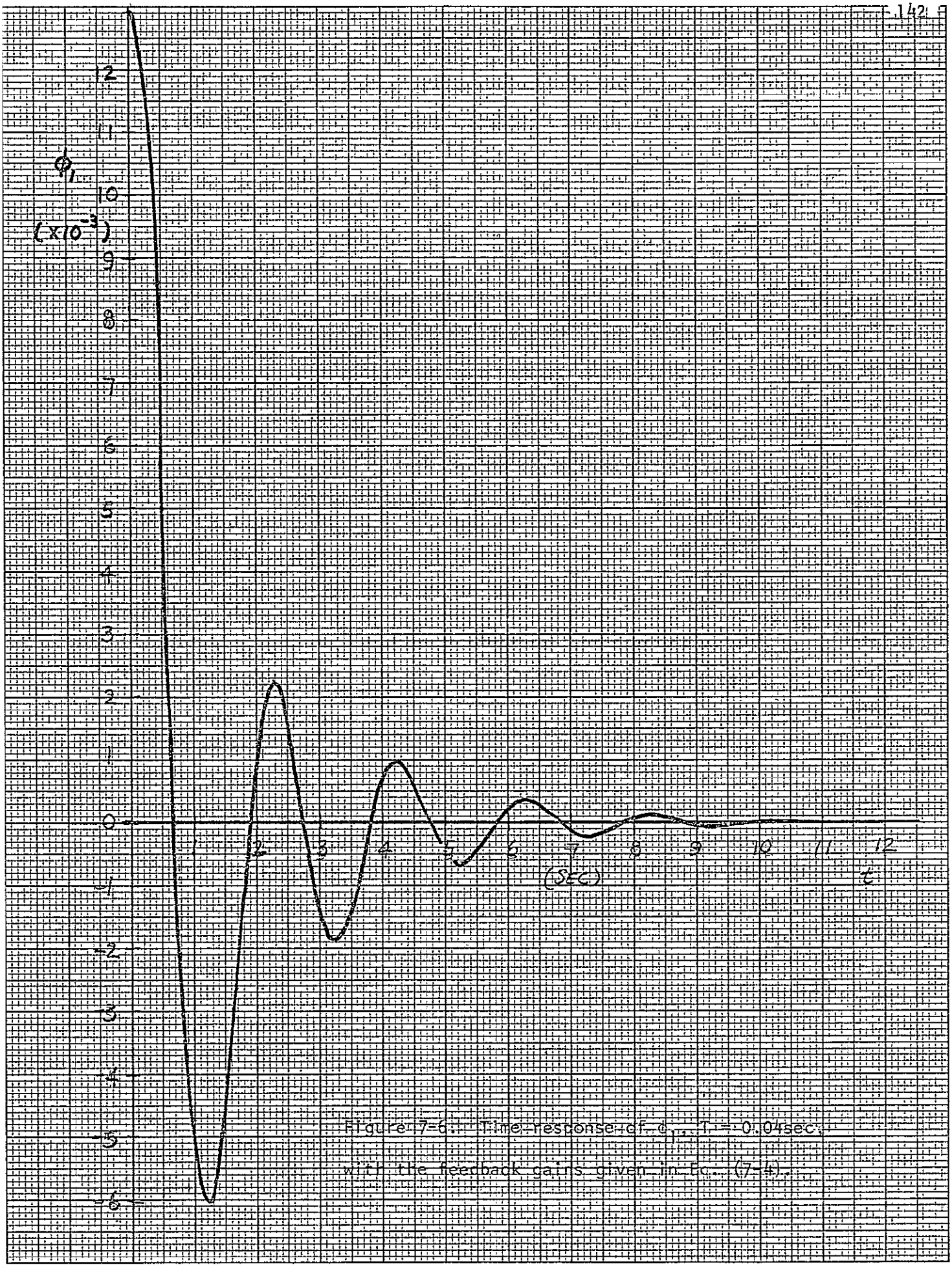

Figure 7-6. Time response of ϕ_1, $T_1 = 0.04$sec, with the feedback gains given in Eq. (7-4).

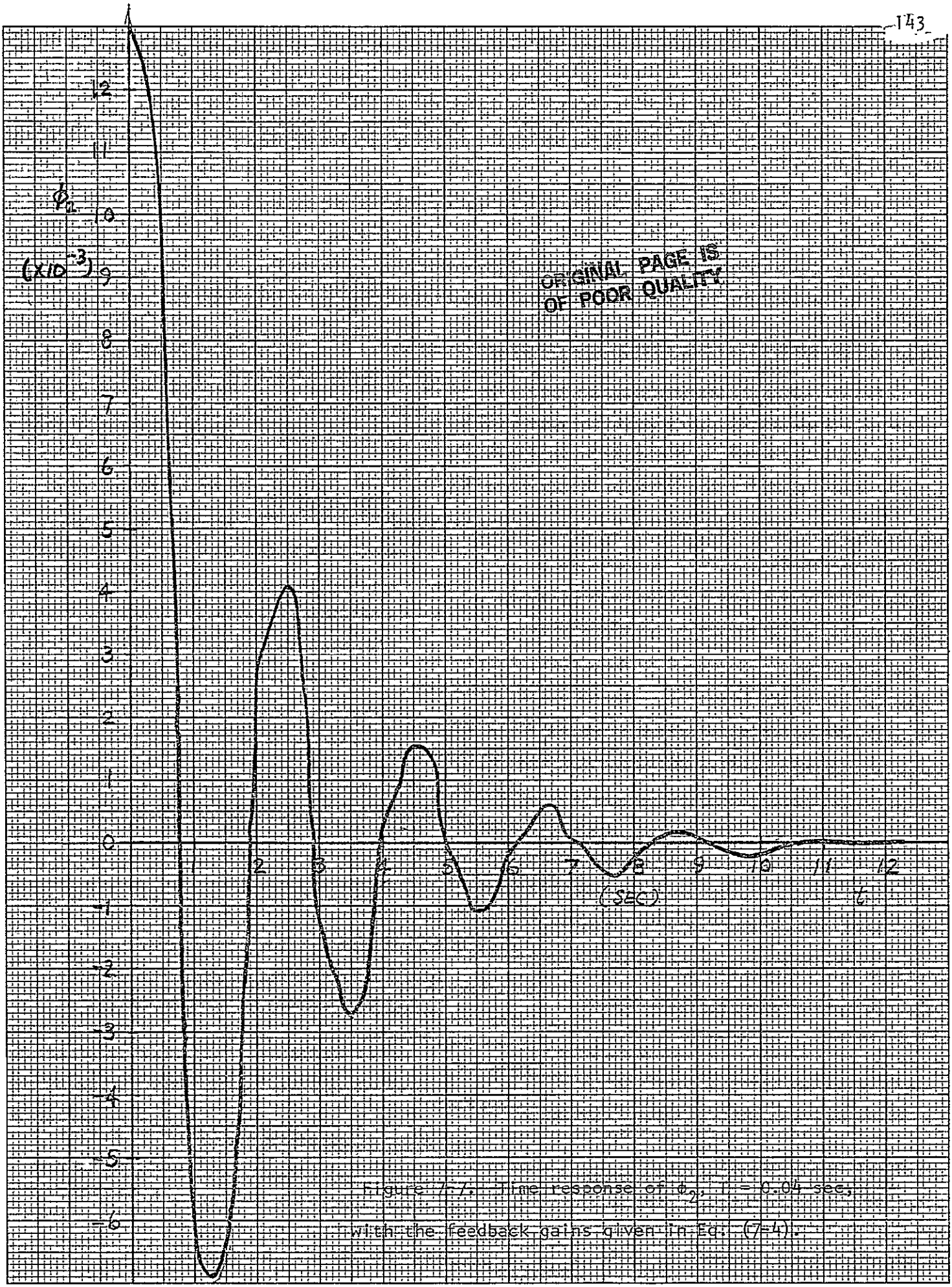

Figure 7.7. Time response of ϕ_2, $\tau = 0.04$ sec, with the feedback gains given in Eq. (7-4).

$$\theta(0.1) = \begin{bmatrix} 2.910\times10^{-3} & 1.484\times10^{-3} & -1.484\times10^{-3} \\ 5.818\times10^{-2} & 2.966\times10^{-2} & -2.966\times10^{-2} \\ 4.947\times10^{-5} & 2.529\times10^{-5} & -2.529\times10^{-5} \\ 1.484\times10^{-3} & 7.585\times10^{-4} & -7.585\times10^{-4} \\ 2.966\times10^{-2} & 1.516\times10^{-2} & -1.516\times10^{-2} \\ -4.947\times10^{-5} & -2.529\times10^{-5} & 2.562\times10^{-5} \\ -1.484\times10^{-3} & -7.585\times10^{-4} & 7.685\times10^{-4} \\ -2.966\times10^{-2} & -1.516\times10^{-2} & 1.536\times10^{-2} \end{bmatrix} \tag{7-6}$$

Corresponding to the desired bandwidths of the three system components, the eigenvalues of the closed-loop digital ASPS are set at:

x: $z_1, z_2 = 0.9423049137666 \pm j\ 0.05448575545211$

ϕ_1: $z_3 = 2.06\times10^{-9}$

ϕ_2: $z_4, z_5 = 0.5790229524118 \pm j0.275632267541$

$z_6 = 0.1353352832366$

$z_7, z_8 = 0.6570647872999 \pm j0.4965162436514$

The feedback gains are determined and are tabulated as follows:

$$\begin{aligned} g_{11} &= 356.54391190867254 \\ g_{12} &= 673.937543782499 \\ g_{13} &= -2.971496035004556\times10^{5} \\ g_{14} &= -2.192918298193871\times10^{5} \\ g_{15} &= -2.1617128726694806\times10^{4} \\ g_{16} &= g_{17} = g_{18} = 0 \\ g_{21} &= -699.45360421649164 \\ g_{22} &= -1318.3208244459652 \\ g_{23} &= 7.102498404377198\times10^{5} \\ g_{24} &= 5.2415343590564353\times10 \end{aligned} \tag{7-7}$$

$$g_{25} = 5.1669468758013832 \times 10^{4}$$

$$g_{26} = 1.5837111307008396 \times 10^{5}$$

$$g_{27} = 8.5497097649640713 \times 10^{4}$$

$$g_{28} = 7799.1724382365824$$

$$g_{31} = g_{32} = 0$$

$$g_{33} = 1.2735706421362781 \times 10^{5}$$

$$g_{34} = 9.3987551465092623 \times 10^{4}$$

$$g_{35} = 9265.0100115225987$$

$$g_{36} = 1.5837111569386454 \times 10^{5}$$

$$g_{37} = 8.5497094066096154 \times 10^{4}$$

$$g_{38} = 7799.1723174474365$$

The time responses of x, ϕ_1 and ϕ_2 of the digital ASPS with T = 0.1 and the feedback gains in Eq. (7-7) are shown in Figs. 7-8, 7-9, and 7-10, respectively. These time responses show that with the proper design, the digital ASPS can operate with a relatively large sampling time without any difficulties.

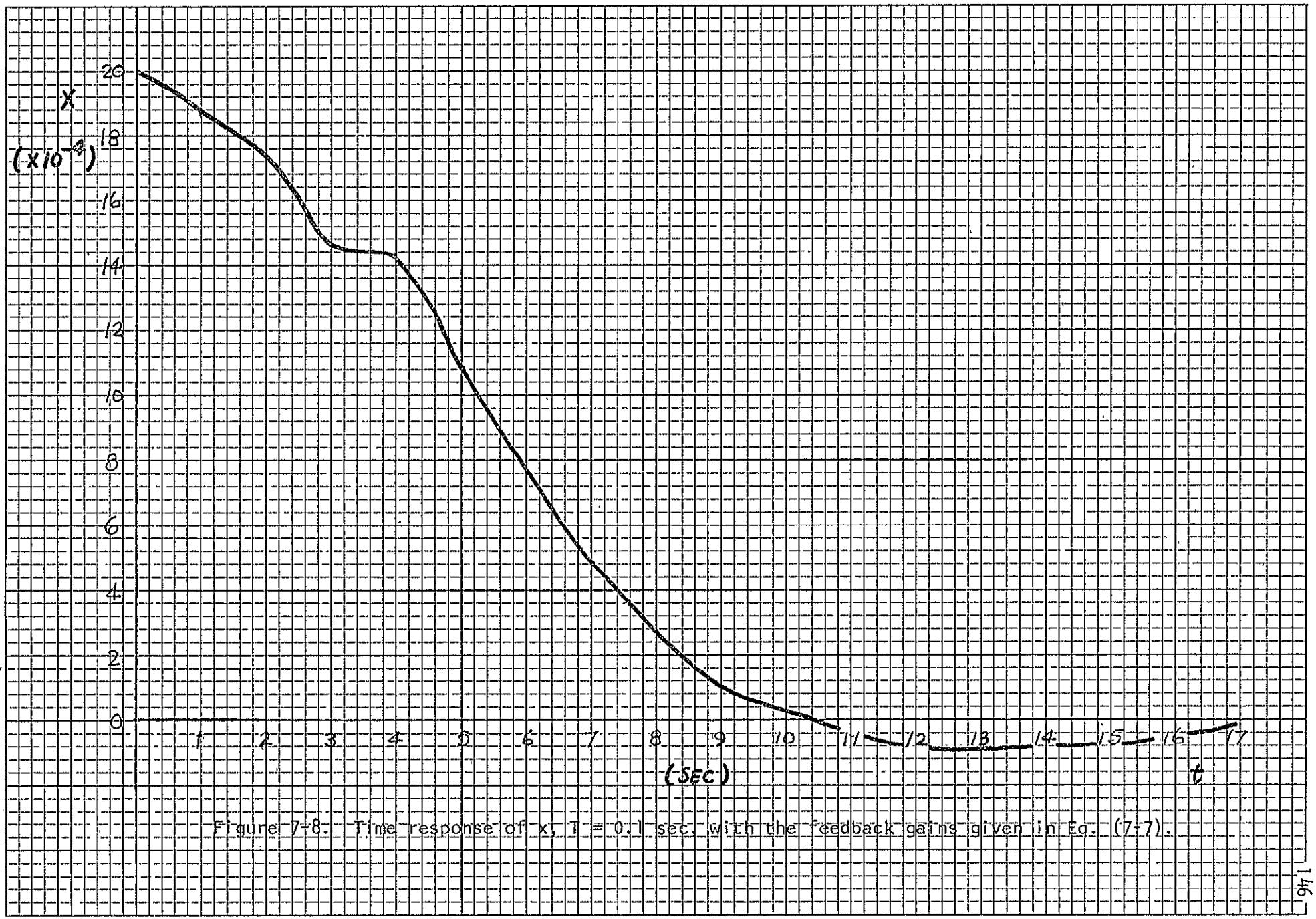

Figure 7-8. Time response of x, T = 0.1 sec, with the feedback gains given in Eq. (7-7).

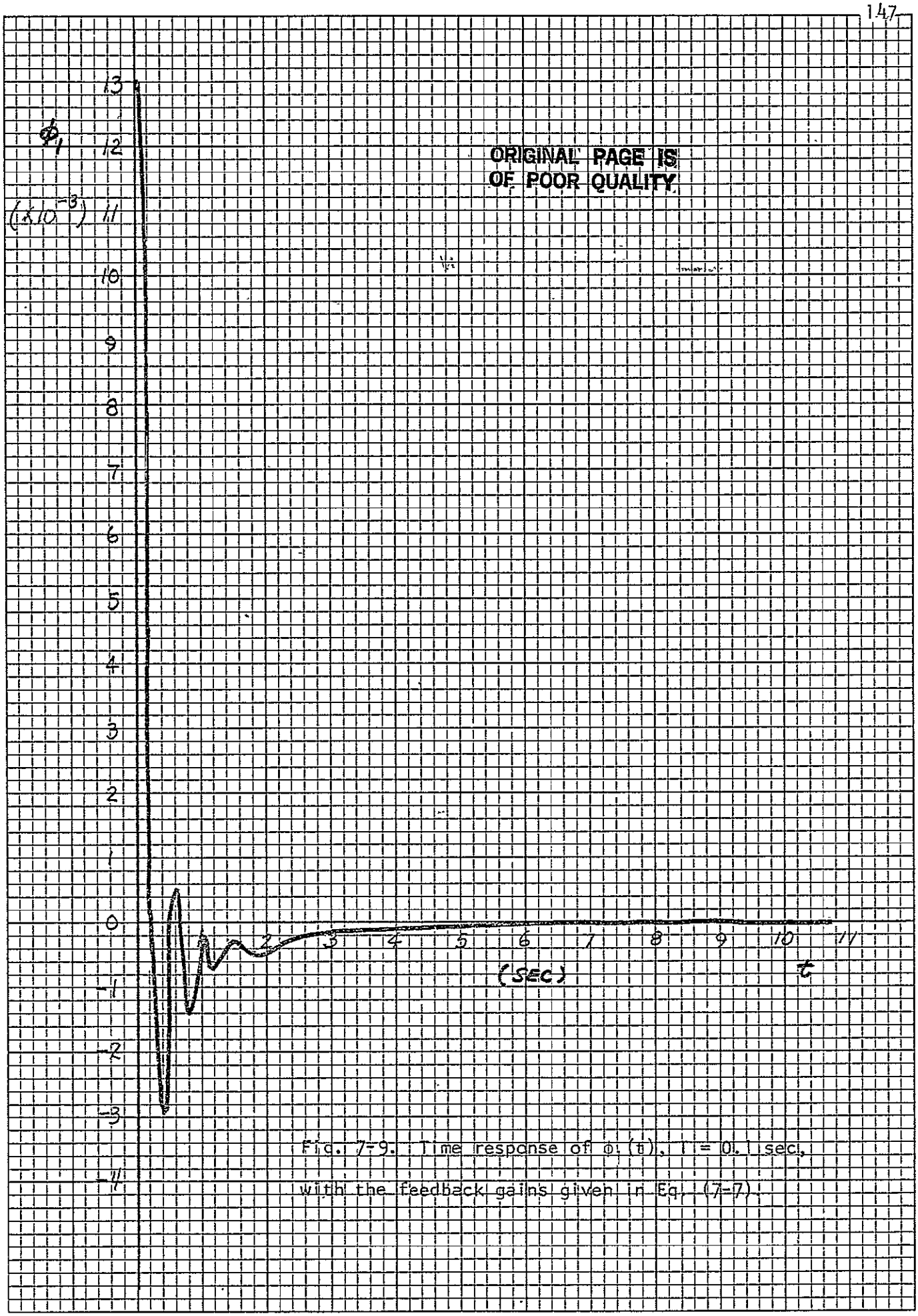

Fig. 7-9. Time response of $\phi_1(t)$, $\tau = 0.1$ sec, with the feedback gains given in Eq. (7-7).

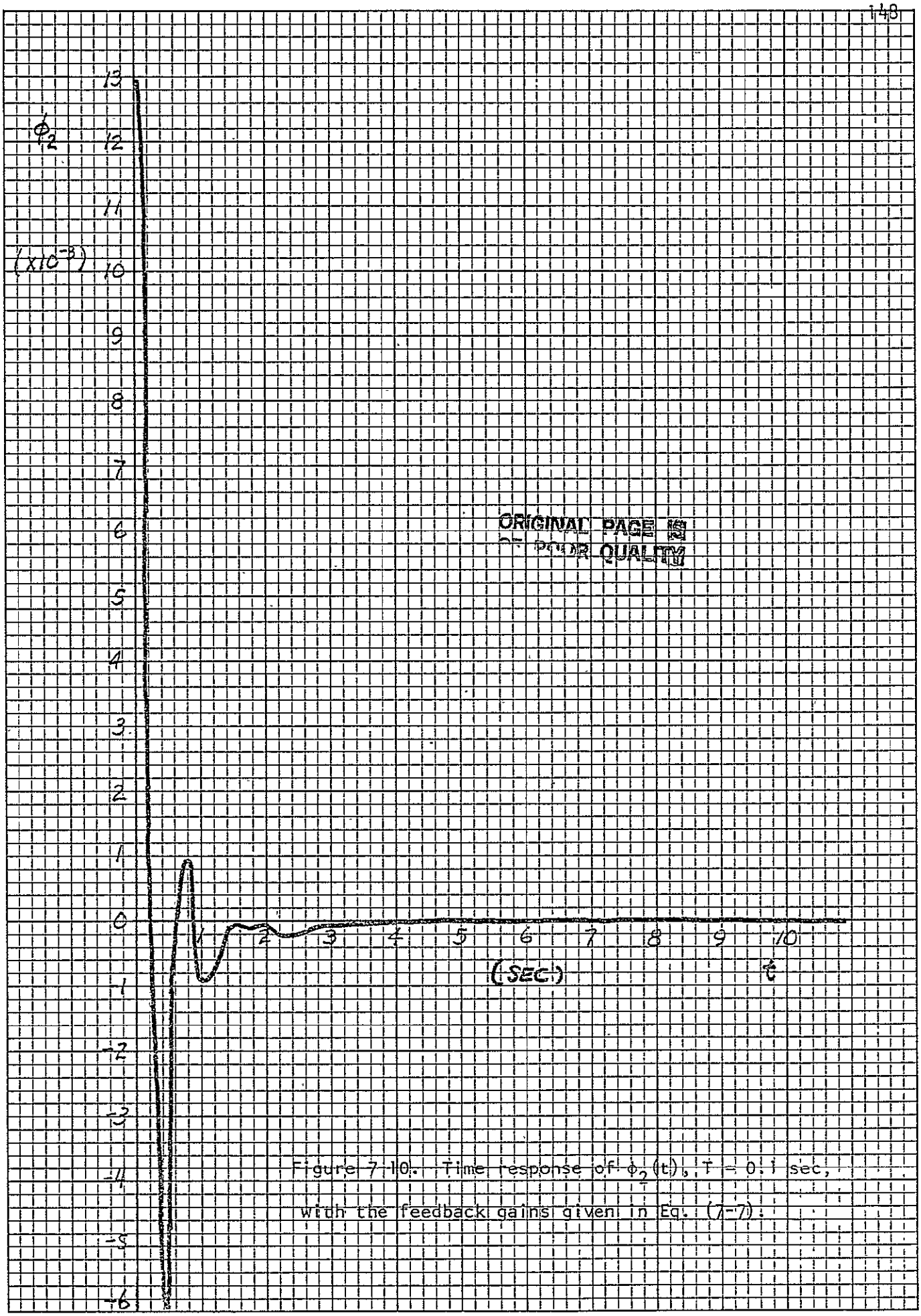

Figure 7-10. Time response of $\phi_2(t)$, $\tau = 0.1$ sec, with the feedback gains given in Eq. (7-7).

VIII. QUANTIZATION EFFECTS IN THE DIGITAL ASPS

8.1 Introduction

In the preceding chapters the digital ASPS was designed through decoupling and pole-placement techniques, and the designed system was simulated on the digital computer. It was shown that the bandwidth requirements were approximately satisfied by digital feedback, and the computer simulation results showed that the responses of the x, ϕ_1 and ϕ_2 dynamics were guite good. With proper design, the digital ASPS can operate with a relatively large sampling period of T = 0.1 sec without any difficulty.

In reality, because of the finite bit length used in a digital computer, the state-feedback gains designed for the decoupled digital ASPS must be quantized. It should also be noted that the quantization effect due to operations in the digital computer is not the same as that introduced by the A/D converter.

In this chapter we shall investigate the effects of amplitude quantization in the digital ASPS with state feedback. In general, it is well-known that quantization can lead to two possible difficulties in system performance. One form of difficulty is sustained oscillations or instability due to amplitude quantization. The second type of performance degradation due to quantization is in the form of steady-state errors.

Although closed-form analytical methods are available for the studies of sustained oscillations and steady-state error due to quantization in digital control systems, the complexity and high-order nature of the closed-loop digital ASPS precludes the effective use of these methods. The discrete describing function method can be applied to the study of sustained oscillations in digital control systems due to one quantizer. However, the closed-loop

digital ASPS has many A/D converters and many quantizers representing the digital computer operation of the feedback gains. The complexity of the system also does not allow an analytical solution to the steady-state error by the maximum-upper-bound method, treating all quantizers as noise sources.

The method adopted in this chapter is computer simulation. It seems that considering all difficulties, computer simulation still resulted in useful conclusions to the problem of quantization.

8.2 Quantization Considerations in the ASPS

In a digital computer a real number is usually represented by two parts: the mantessa and the exponent. Figure 8-1 illustrates the floating-point representation of the number X by an N-bit mantessa M and an exponent part. Thus, X can be expressed as

$$X = M \times B^{e} \tag{8-1}$$

where M is the mantessa, B is the base number, 2 in general, and e is an integer which represents the order of the exponent. The N-bit floating-point number M is generally scaled to be

$$B^{-1} \leq M < 1 \tag{8-2}$$

and two's complement arithmatic is used for denoting negative numbers.

In numerical computation, amplitude quantization is introduced by the finite length of the mantessa. However, the truncation error introduced by the quantization effect is not a fixed value; it depends on the exponential scaling; i.e., it is proportional to B^{e}. Therefore, if the bit length of the mantessa is N, the quantization level is $2^{-N} \times B^{e}$. The quantization of a given number should begin with the calculation of the mantessa M and the exponent e. The flow chart given in Fig. 8-2 shows how the quantization

operation is implemented.

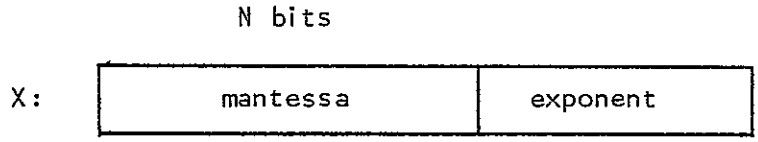

Figure 8-1. Representation of a real number

Table 8-1 shows the subroutine FUNCTION QT(X) which is used for the simulation of the 16-bit quantization of the feedback gains for the digital ASPS.

Table 8-1

```
      FUNCTION QT(X)
      H=2.**-16
      IF(X.NE.0.) GO TO 1
      QT=0.
      RETURN
1     AX=ABS(X)
      SIGN=AX/X
      IF(AX-1.) 2,3,4
3     QT=X
      RETURN
2     K=0
22    IF(AX.GT.10.**(K-1)) GO TO 21
      K=K-1
      GO TO 22
4     K=1
42    IF(AX.LT.10.**K) GO TO 21
      K=K+1
      GO TO 42
21    BX=AX/10.**K
      IV=(BX/H)+0.5
      QT=SIGN*FLOAT(IV)*H*10.**K
      RETURN
      END
```

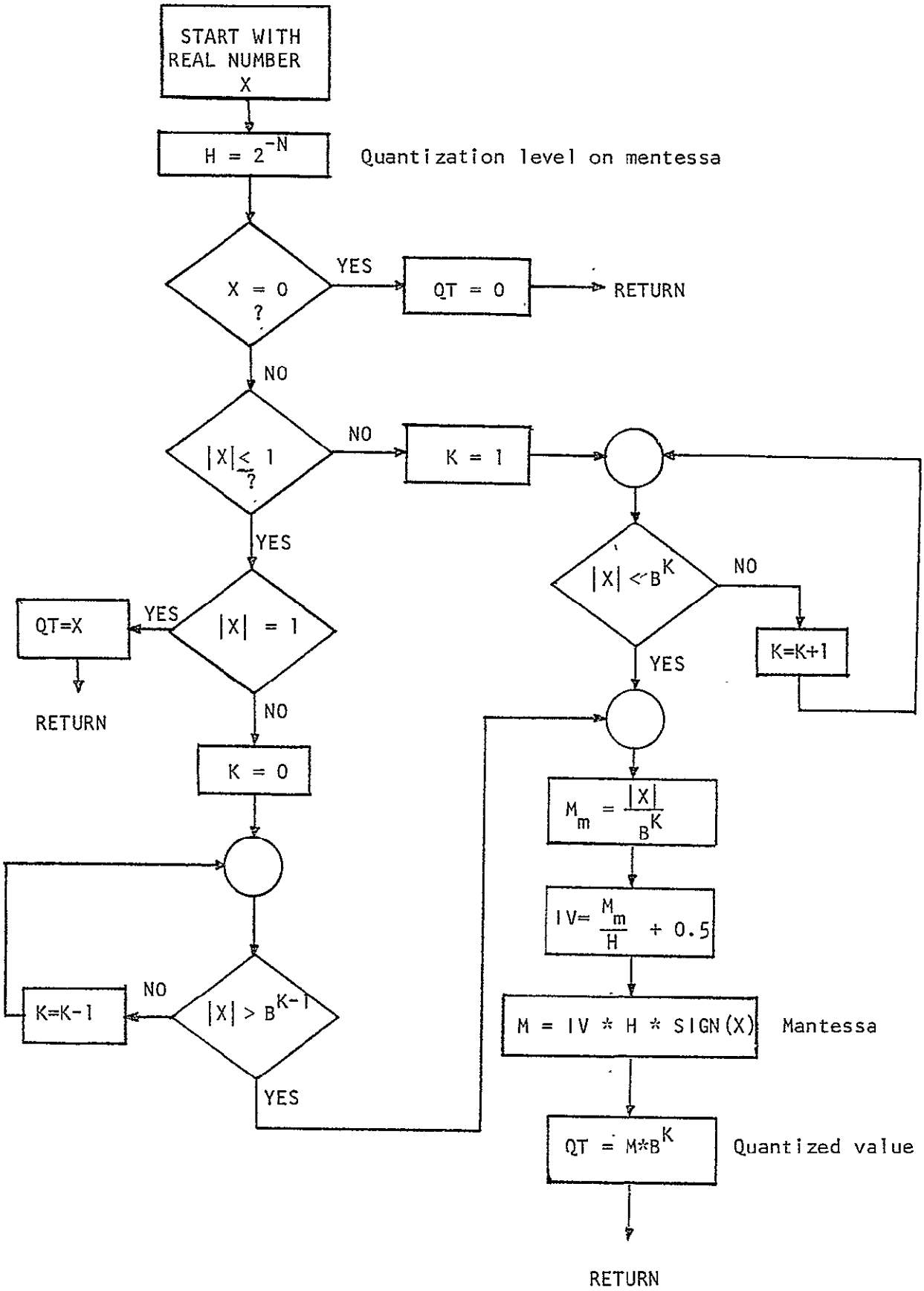

Figure 8-2. Quantization operation.

8.3 Scaling Effects on the A/D Converters

The block diagram of the closed-loop digital ASPS with state feedback is shown in Fig. 8-3. The digital computer which implements the digital controller is interfaced with the ASPS through the A/D and D/A converters.

The A/D converters serve as sample-and-hold devices and quantizers because of their finite bit lengths. If the A/D converter has N bits in the output and is biased with voltage V, then the full-scale input V volts will result in a digital number $1 - 2^{-N}$, which when taken by the digital controller will be interpreted as $V(1 - 2^{-N})$ which is the quantized value of V. Therefore, the A/D converter, together with the necessary I/O port in the computer, can be considered as an A/D converter with normalized 1 volt bias, i.e., simply a quantizer. The functional block diagram is shown in Fig. 8-4.

Since the steady-state error due to quantization is directly related to the quantization level, the accuracy in the responses of the ASPS will depend on the quantization of the A/D converters. The most straightforward method of increasing the accuracy of the system is to increase the bit length of the A/D converter. However, this is an expensive proposition, and the cost can be saved by making use of the scaling technique in the A/D converter.

In the ASPS controller designed in the preceding chapters, the sensor gains were assumed to be unity. For example, if the error in the x component is X meter, we assume that the sensor sensed X volts, and the controller received $Q_N(X)$ as a number for data processing. Because of the quantization effect in the controller, the steady-state error will be confined to be within 2^{-N} meter, where N is the number of bits in the A/D output. In general, N can be 8 or 12 (N = 12 is used here), and the error is apparently not satisfactory.

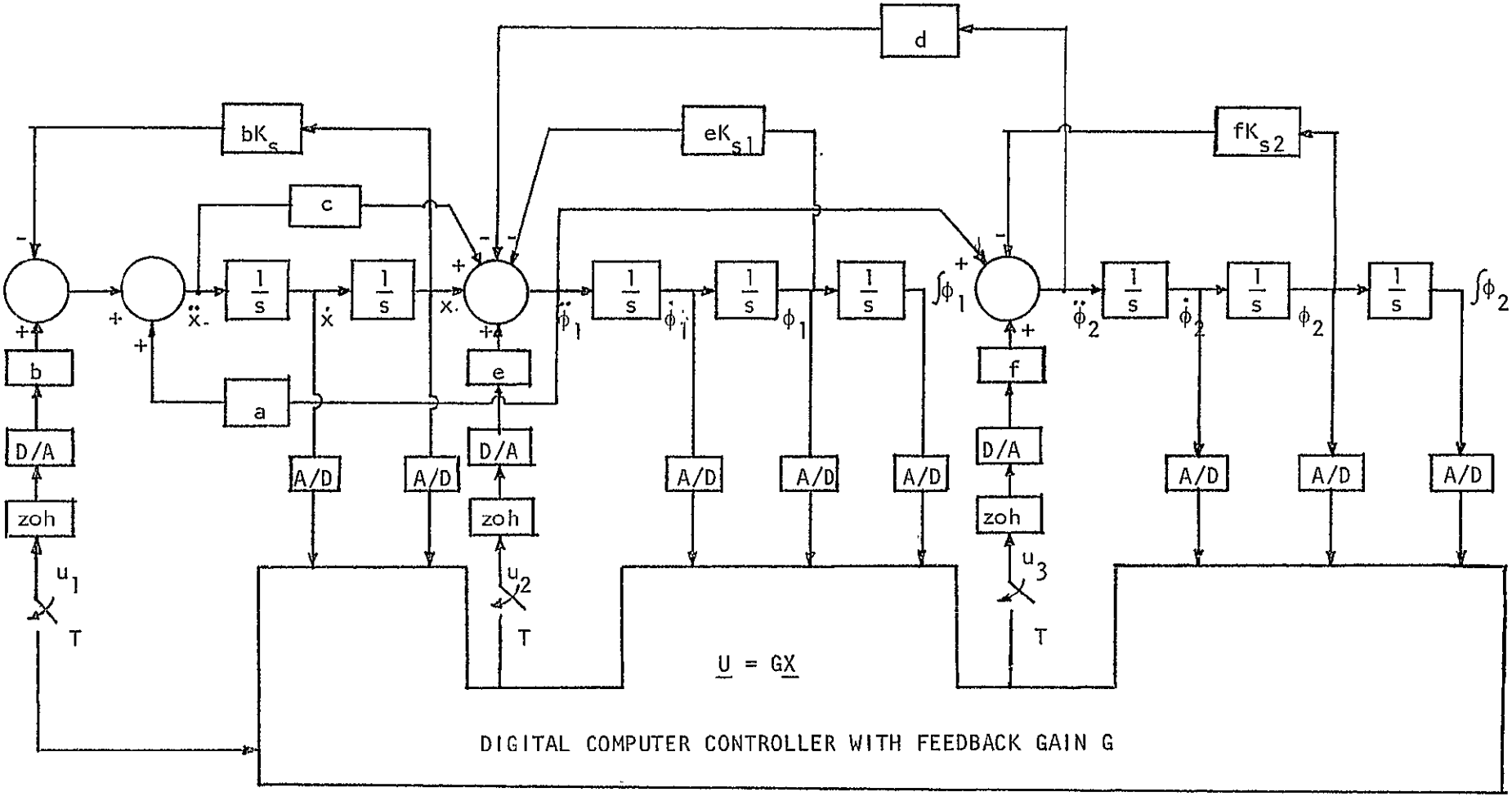

Figure 8-3. Block diagram of the ASPS with the state-feedback digital controller and quantizers.

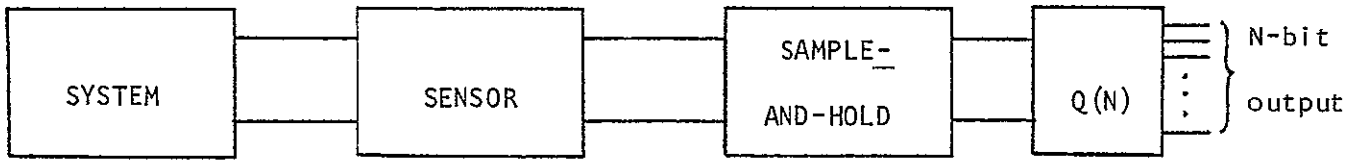

Figure 8-4. Block diagram of A/D conversion.

If a sensor gain of 1000 is introduced before the sample-and-hold, as shown in Fig. 8-4, then the X meter error in the system will be sensed as 1000X mm. After the quantization, the error will be confined to be within 2^{-N} mm. The digital computer takes $Q_n(1000X)$ as an input number, and performs a division-by-1000 to convert it back to the number $Q_N(1000X)/1000 = X$ which is of the appropriate dimension. Since there are reciprocal gain factors at both sides of the quantizer, as shown in Fig. 8-5, the transfer function between points A and B as seen from the quantizer Q is the same as that between points C and D. Therefore, the control scheme thus far designed will not be affected by the application of a sensor gain.

For the eight state variables in the ASPS, it can be seen that the scaling factors for each of these variables will not be the same for best system performance. As a matter of fact, the sensor gain should not be too low so as to have larger quantization error. On the other hand, the sensor gain should not be too high so as to cause saturation in the system.

In actual implementation it is suggested that the possible maximum error be sensed (with a certain sensor gain) as the bias voltage of the A/D converte and the quantized value be divided by that certain sensor gain before it is stored in the certain memory location in the computer. All the feedback gains are retained to be the same as they are designed without the scaling factor.

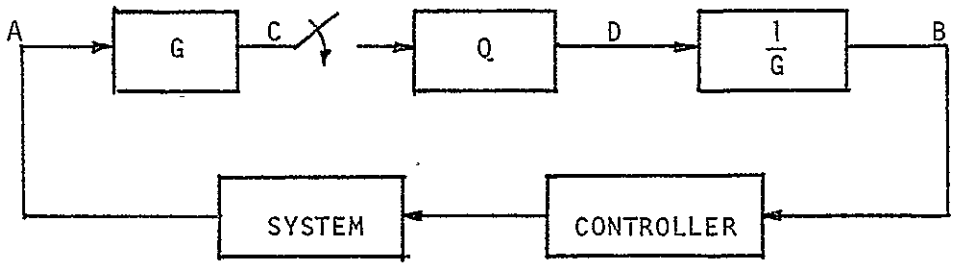

Figure 8-5. Block diagram showing the effect of scaling.

8.4 Computer Simulation of the ASPS With Quantization

In this section the reponses of the digital closed-loop ASPS with quantization are obtained through computer simulation. The block diagram of the system is shown in Fig. 8-3. The sampling period of the system was chosen to be 0.1 sec. The feedback gains of the system are tabulated in Eq. (7-7) and are not repeated here. Eight-bit and 12-bit A/D and D/A converters were used. Since the 16-bit wordlength used in the digital computer is longer than the bit length of the A/D and D/A converters, quantization should be considered when computing the control signals of the ASPS. This process is represented by the subroutine program listed in Table 8-2.

Table 8-2

```
C-------DATA SAMPLING AND A/D CONVERSION

      V1=3.565368652343375E2*Q(X)+6.739349365234375E2*Q(XDOT)
     &   -2.971496601562SE5*Q(PHI1IN)-2.192993164062SE5*Q(PHI1)
     &   -2.161712646484375E4*Q(PHI1DT)
      V2=-6.994476318359375E2*Q(X)-1.318359375E3*Q(XDOT)
     &   +7.102508515625E5*Q(PHI1IN)+5.241546640625E5*Q(PHI1)
     &   +5.166931152343751E4*Q(PHI1DT)+1.583709726562SE5*Q(PHI2IN)
     &   +8.549652148437SE4*Q(PHI2)+7.799224853515625E3*Q(PHI2DT)
      V3=1.273498533515625E5*Q(PHI1IN)+9.398803710937SE4*Q(PHI1)
     &   +9.264984130859375E3*Q(PHI1DT)+1.583709726562SE5*Q(PHI2IN)
     &   +8.549652148437SE4*Q(PHI2)+7.799224853515625E3*Q(PHI2DT)

      V1=Q(V1)
      V2=Q(V2)
      V3=Q(V3)
```

```
      FUNCTION Q(XX)
      COMMON X,XDOT,PHI1,PHI1DT,PHI1IN,PHI2,PHI2DT,PHI2IN,T,
     &  V1,V2,V3,AJ,AMI,AKSX,AKSF,AKSS,A33,TPRT,RB,DELTA,
     &  A0,B0,C0,D0,E,F,TEND,H,
     &  NPRT,IV1,IV2,IV3,LINE
      IF(XX.LT.0.) GO TO 20
      IV=(XX/H)+0.5
      GO TO 30
20    IV=(XX/H)-0.5
30    Q=FLOAT(IV)*H
      RETURN
      END
```


Figure 8-6 shows the responses of the x-dynamics of the ASPS with an initial condition of 2×10^{-3} for the first 60 seconds, with and without quantization. The A/D and D/A converters have 12 bits. Notice that the quantization effect on the transient response is to cause an overshoot in x at the beginning. Figure 8-7 illustrates the response of the x-dynamics beyond 100 seconds (near steady state). Notice that the response cannot be classified as "sustained oscillation", since it is not periodic. However, it does appear that the amplitude of the response has reached a maximum saturated level. In this case, the maximum error due to quantization is less than 1.5 times 2^{-12}.

Figure 8-8 illustrates the response of the ϕ_1-dynamics with the same quantization level as described above. In this case it is seen that the quantization effect was to cause high overshoots in the transient response, but the response quickly reached a bounded steady-state. Figure 8-9 shows the same ϕ_1 response beyond 140 seconds. We see that the maximum steady-state error due to the 12-bit quantization is less than 1.5×10^{-4}. Again, the steady-state response cannot be described as a sustained oscillation.

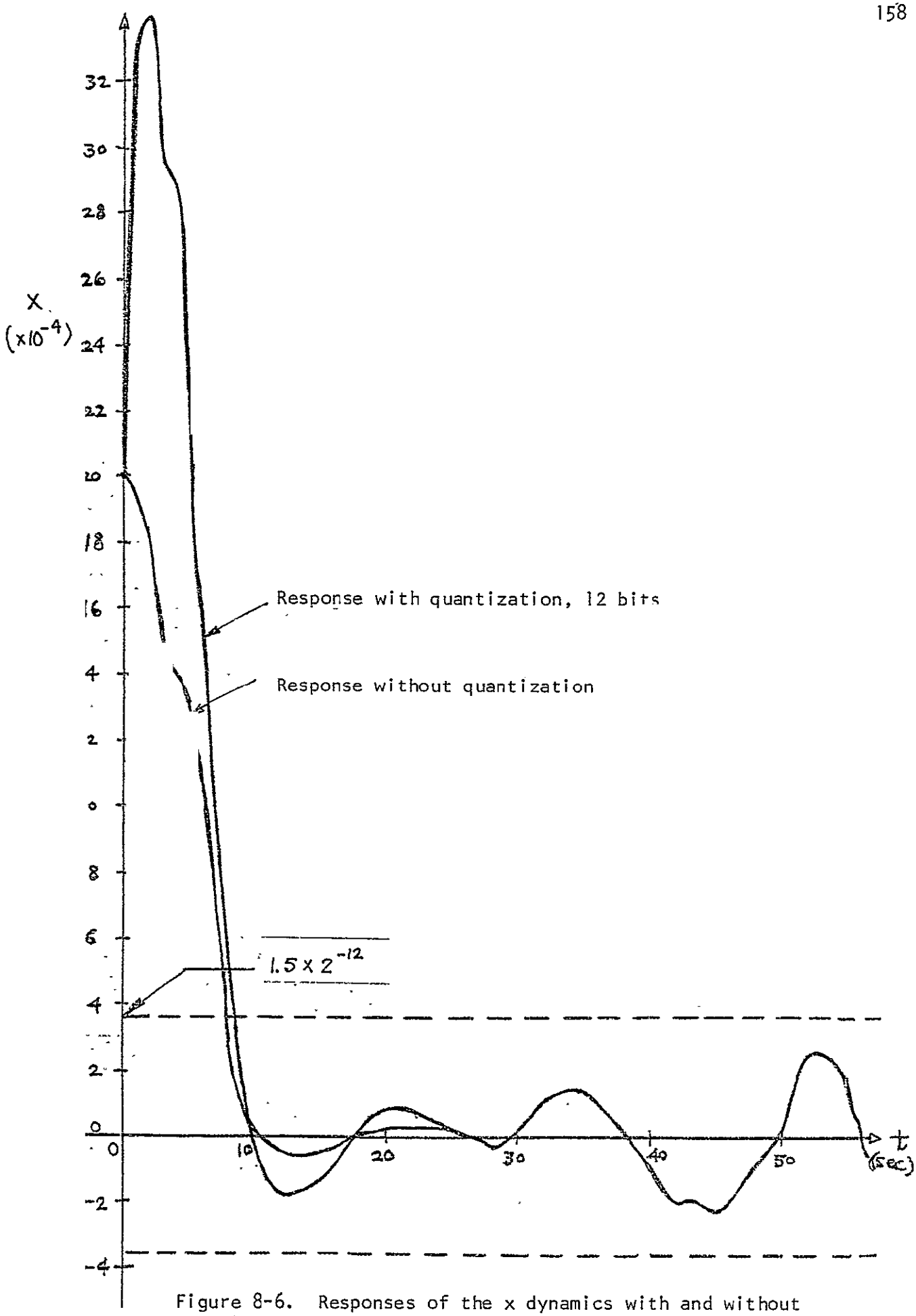

Figure 8-6. Responses of the x dynamics with and without quantization; 12-bit A/D and D/A converters

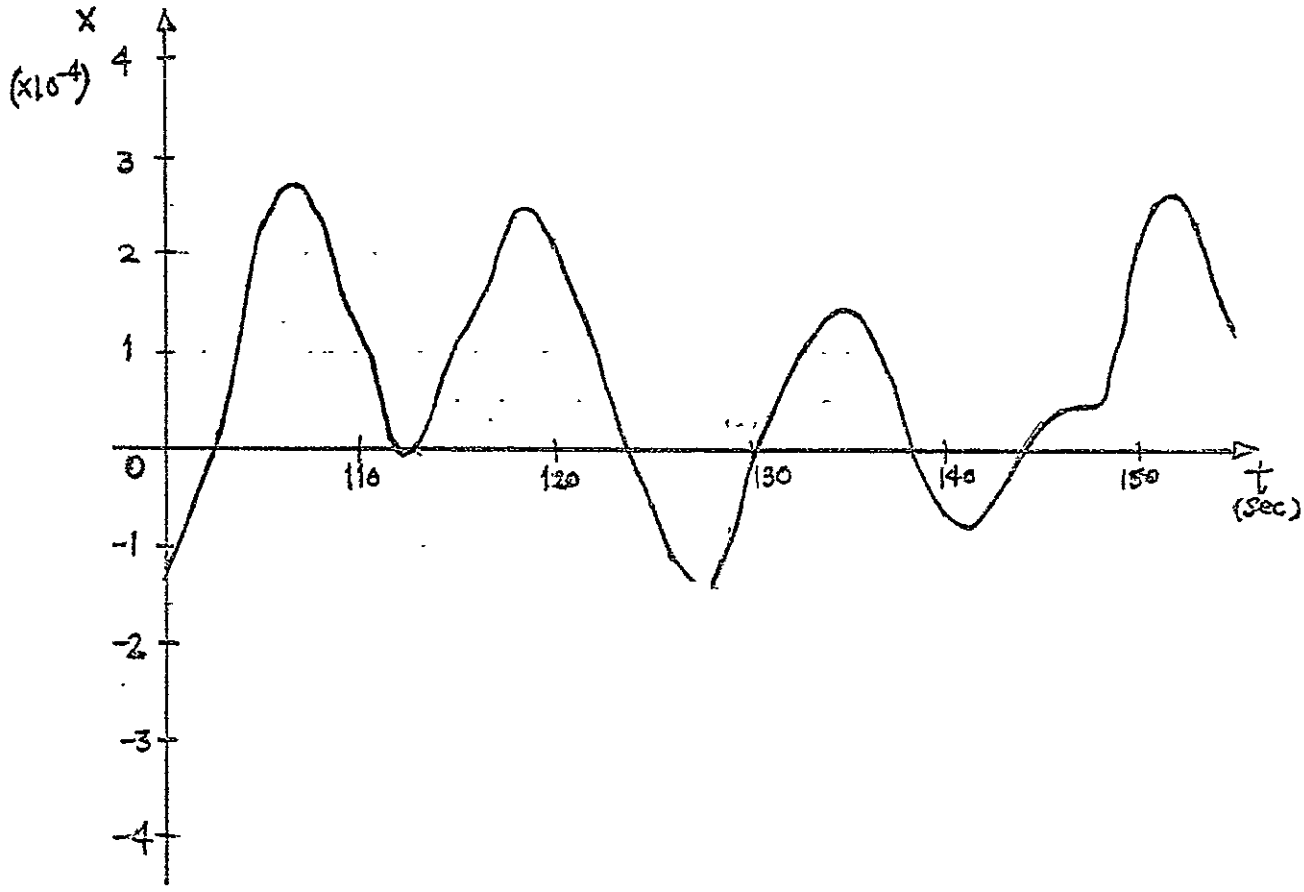

Figure 8-7. Response of the x dynamics near the steady-state with 12-bit A/D and D/A converters.

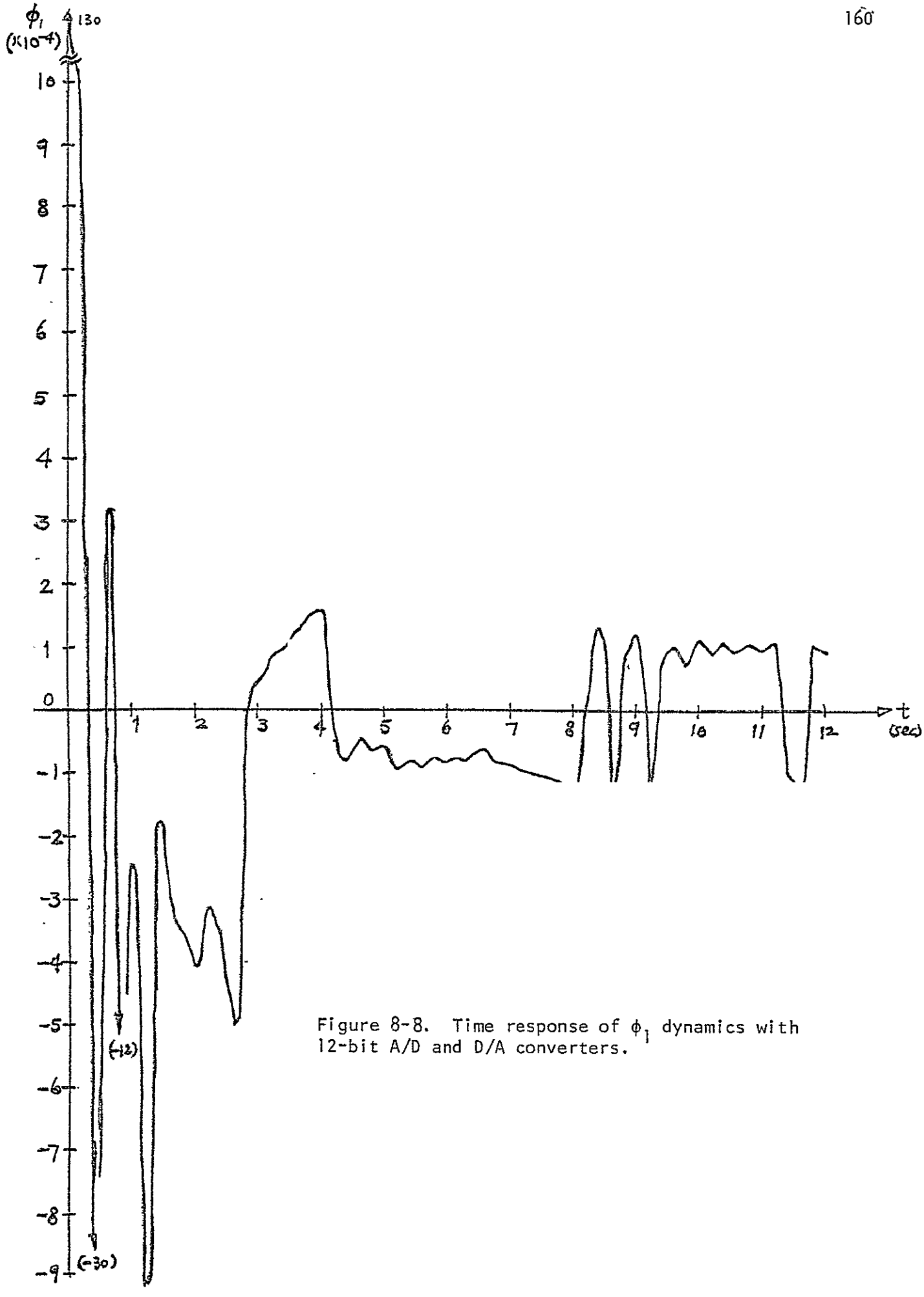

Figure 8-8. Time response of ϕ_1 dynamics with 12-bit A/D and D/A converters.

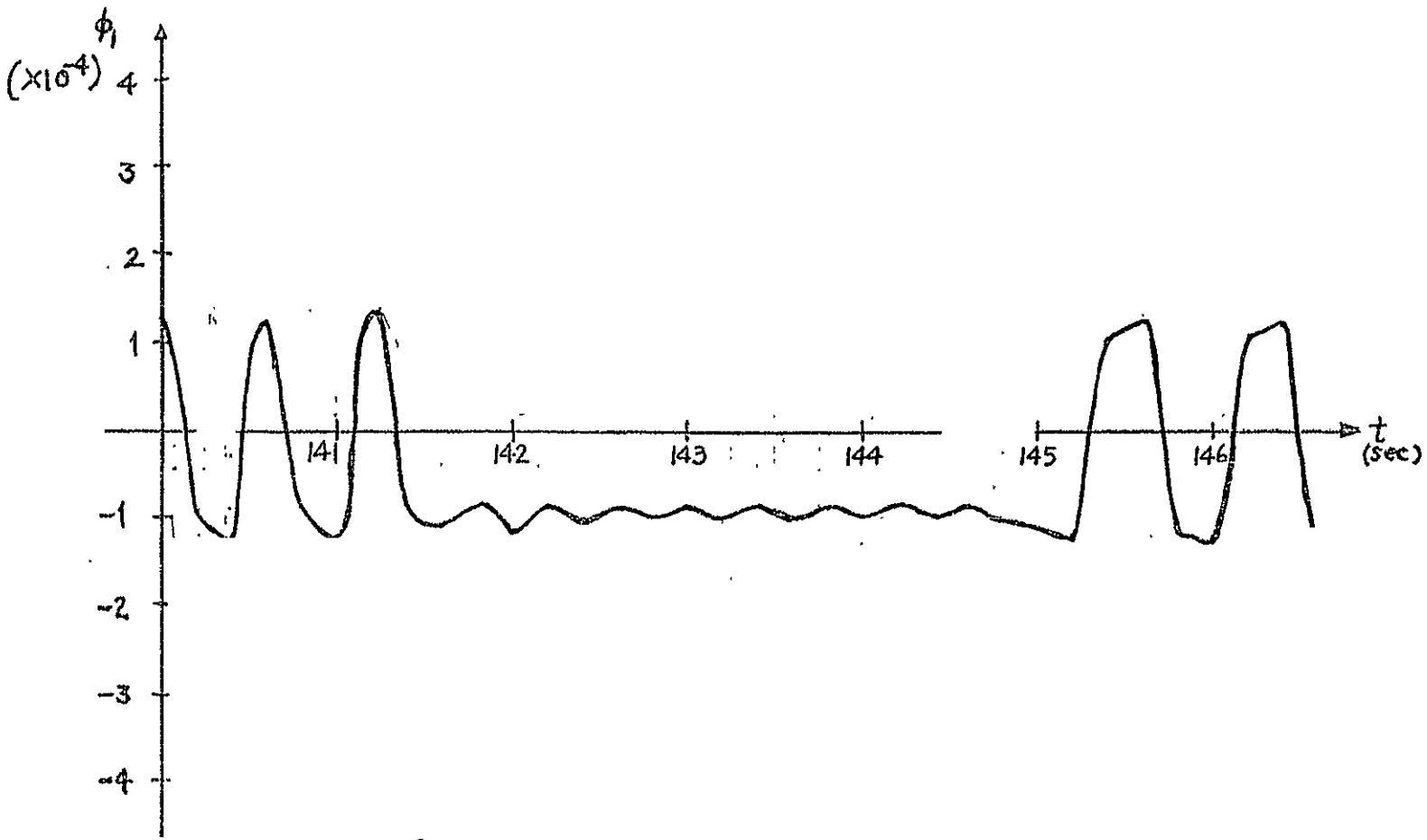

Figure 8-9. Time response near steady state of ϕ_1 dynamics with 12-bit A/D and D/A converters.

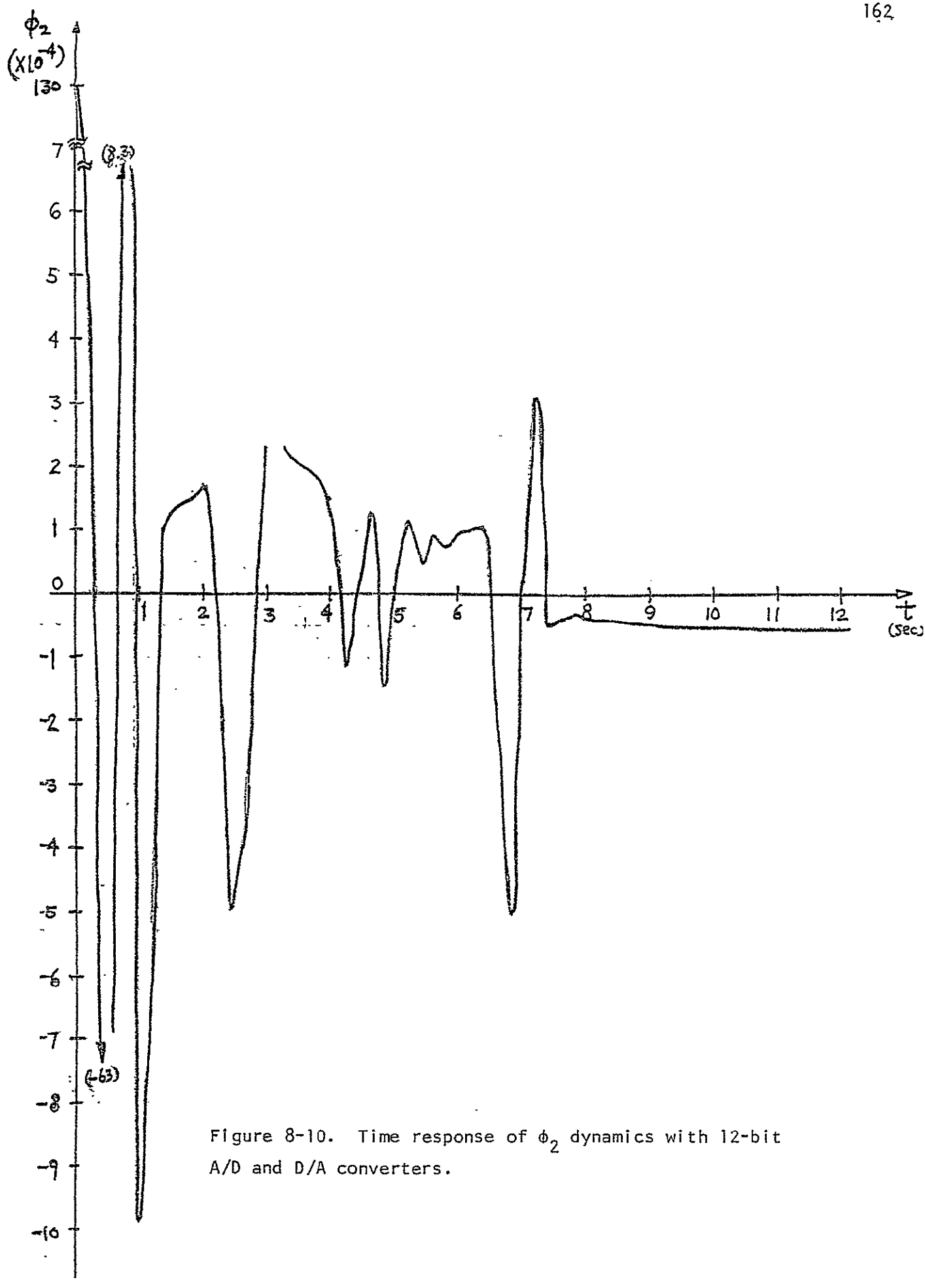

Figure 8-10. Time response of ϕ_2 dynamics with 12-bit A/D and D/A converters.

In a similar fashion the time response of the ϕ_2 dynamics with the 12-bit A/D and D/A converters in the ASPS system was obtained and plotted as shown in Fig. 8-10. Again, the steady-state error of ϕ_2 due to quantization is very close to that of ϕ_1.

Figure 8-11 illustrates the time response near the steady state of x with 8-bit A/D and D/A converters. Figure 8-12 illustrates the time response of ϕ_1 under the same condition. In these cases, the steady-state errors due to quantization are all less than one quantization level, 2^{-8}. As expected, the steady-state error due to quantization is directly related to the quantization level. In general, large quantization levels will result in large steady-state errors.

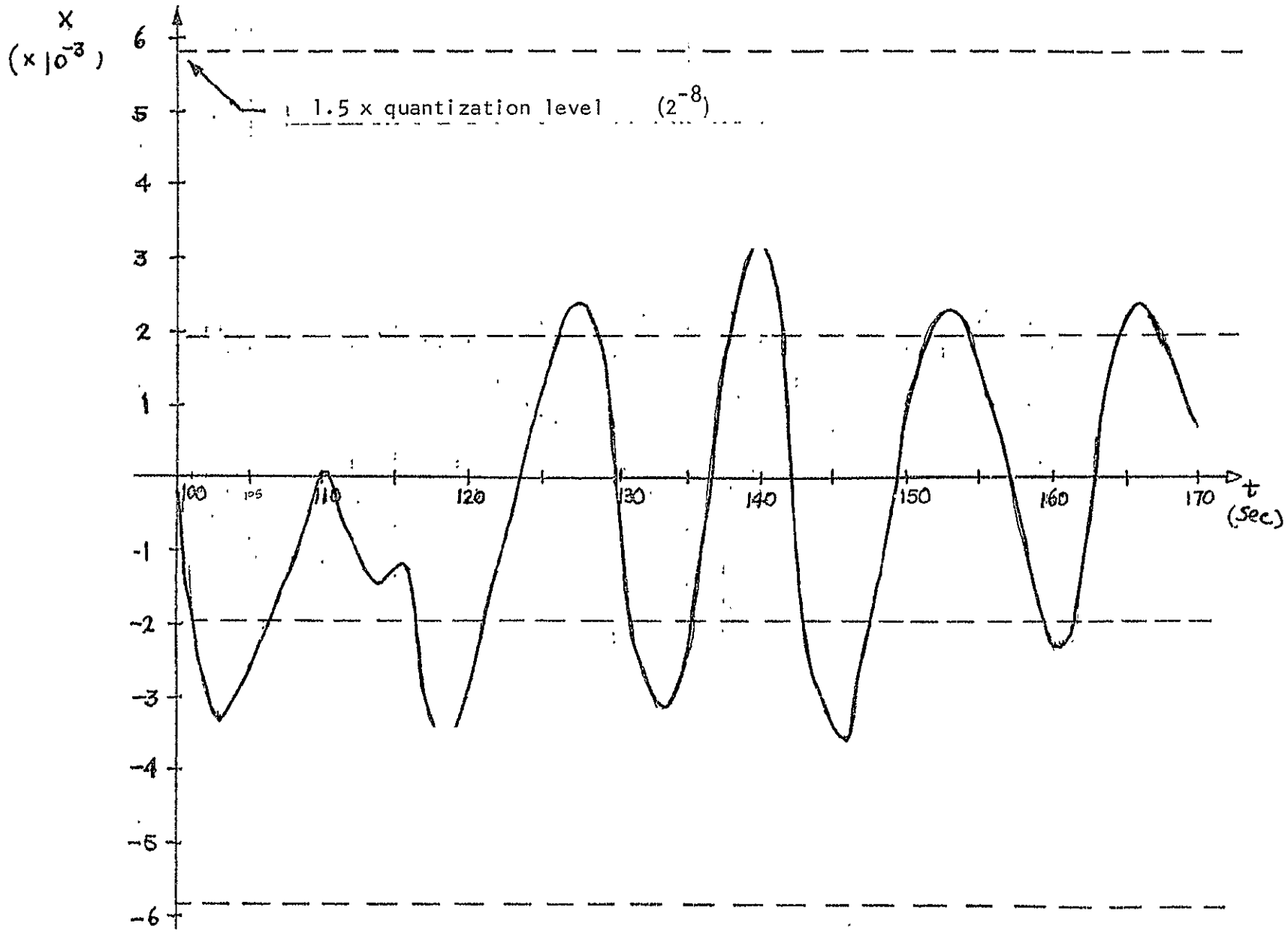

Figure 8-11. Time response of x near steady state with 8-bit A/D and D/A converters.

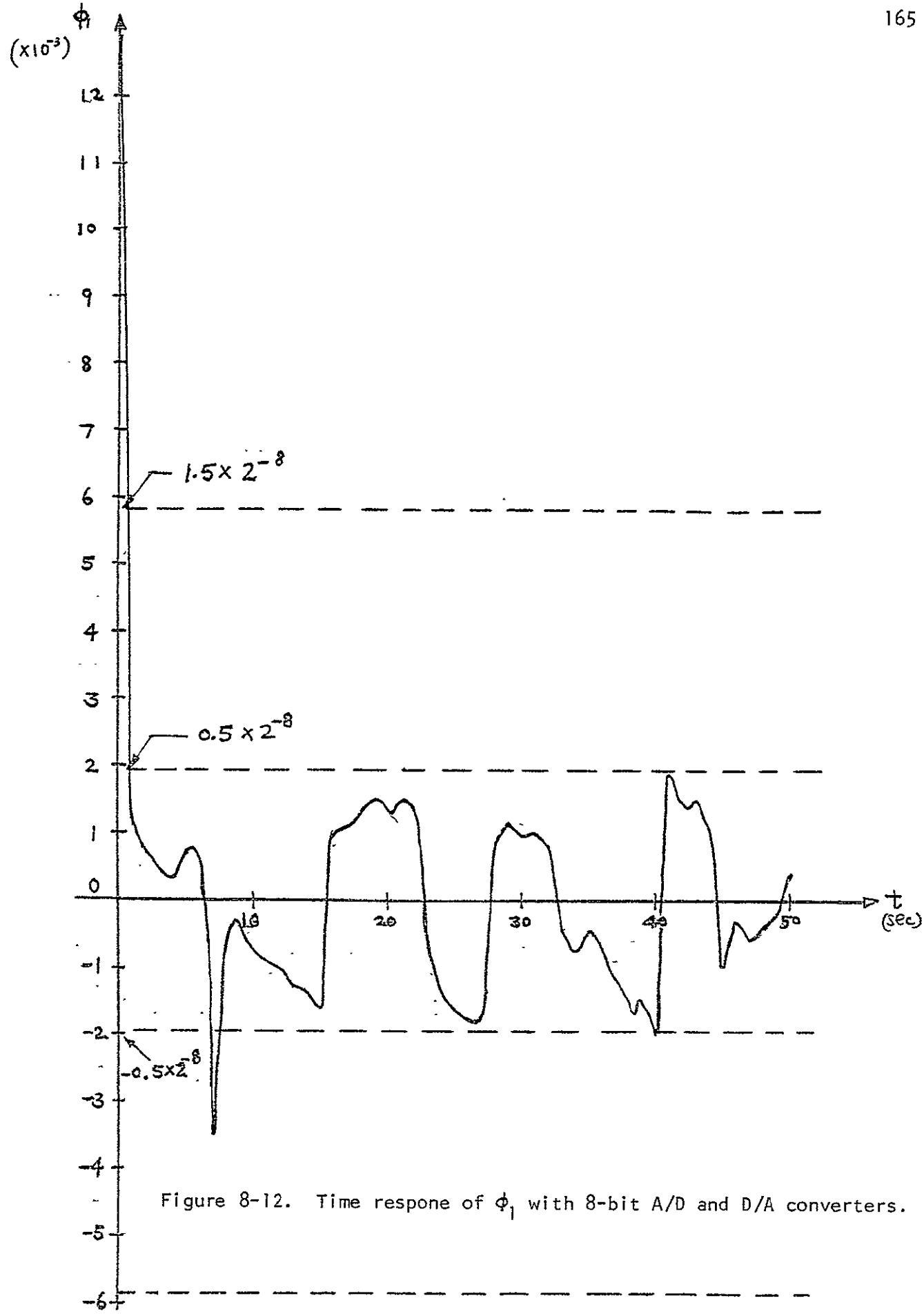

Figure 8-12. Time respone of ϕ_1 with 8-bit A/D and D/A converters.

IX. NONLINEAR SPRING EFFECTS ON THE DIGITAL ASPS

9.1 Introduction

The analysis and design of the digital ASPS conducted in the preceding chapters were based on the system model that the spring characteristics of the wire-cable torque were linear. On the ASPS a wire cable is attached to the center of the payload mounting surface with the other end of the cable attached to the shuttle frame. Similarly, there is another cable attached between the pallet and the shuttle (see Figure 1-2.).

For the linear analysis and design, the spring constant of the payload is designated by the constant K_s (z and x dynamics), and the spring constant of the ϕ_1 and ϕ_2 dynamics are designated by K_{s1} and K_{s2}, respectively.

The nonlinear spring characteristic of the wire-cable torque is shown in Fig. 9-1. The spring parameters are given by H_{WF} and K_s, as shown in the figure. The abscissa is shown as z_1, but the same characteristics are assumed for x, ϕ_1 and ϕ_2.

The objective of this chapter is to investigate the effects of the nonlinear spring characteristics on the performance of the digital ASPS with quantization. Since the overall ASPS with the nonlinear spring and quantizers is a high-order digital control system with multiple nonlinearities, no analytical methods are available to conduct a closed-form study of the system. Thus, computer simulations are conducted for the studies. The listings of the simulation program are given in Table 9-1.

9.2 Effects of the Nonlinear Spring on the X-Dynamics

Since the nonlinear spring characteristic shown in Fig. 9-1 can be interpreted as the superposition of a velocity-dependent force (or torque) to the

Table 9-1. Computer listings of Digital ASPS with Wire-Cable Nonlinearity and Quantization.

```
 TYPE SIMOT.F)
      DIMENSION PRNT(5),Y(8),DERY(8),AUX(8,6)
      EXTERNAL FCT,OUTP
      COMMON X,XDOT,PHI1,PHI1DT,PHI1IN,PHI2,PHI2DT,PHI2IN,P,
     &  V1,V2,V3,AJ,AMI,AKSX,AKSP,AKSS,A33,TPRT,RB,DELTA,
     &  A0,B0,C0,D0,E,F,TEND,H,
     &  NPRT,IV1,IV2,IV3,LINE
      OPEN(UNIT=6,DEVICE='DSK',FILE='FOR20.DAT',ACCESS='SEQOUT')

      LINE=0
      TSP=0.1
      H=2.**-12
      TEND=200.
      TPRT=0.2
      TINT=1.0E-2
C-----SET INITIAL CONDITIO
      X=-1.688E-5
      XDOT=-5.302E-6
      PHI1=6.756E-7
      PHI1DT=5.090E-7
      PHI1IN=3.549E-7
      PHI2=1.774E-6
      PHI2DT=6.753E-6
      PHI2IN=-1.211E-
      AMI=500.
      AKSX=1.051
      AKSP=0.005
      AKSS=0.005
      AJ=503.
      A33=2805.15
      RB=1.956
      A0=RB
      B0=1./AMI
      C0=AMI*RB/A33
      D0=AJ/A33
      E=1./A33
      F=1./AJ
      DELTA=1.-A0*C0-D0
      T=9.7801E1
      NPRT=0
      PRMT(3)=TINT
      PRMT(4)=0.01*2.E-3
      DO 99 I=1,8
99    DERY(I)=0.125
      NOIM=8
10    IF(T.GE.TEND) CALL EXIT

C------DATA SAMPLING AND A/D CONVERSION

      GX=100.
```

```
      GP1=50.
      GP2=50.

      V1=3.56536865234375E2*Q(X,GX)+6.739349605734375E2*
   &    Q(XDOT,GX)
   &    -2.9714966015625E5*Q(PHI1IN,GP1)-2.1922931640625E5*
   &    Q(PHI1,GP1)
   &    -2.161712646484375E4*Q(PHI1DT,GP1)
      V2=-6.993476318359375E2*Q(X,GX)-1.318359375E3*Q(XDOT,GX)
   &    +7.1025085156 25E5*Q(PHI1IN,GP1)+5.241546640625E5*
   &    Q(PHI1,GP1)
   &    +5.16693115234375E4*Q(PHI1DT,GP1)+1.5837097265625E5*
   &    Q(PHI2IN,GP2)
   &    +8.5496521484375E4*Q(PHI2,GP2)+7.79922485351 5625E3*
   &    Q(PHI2DT,GP2)
      V3=1.27349853515625E5*Q(PHI1IN,GP1)+9.3988037109375E4*
   &    Q(PHI1,GP1)
   &    +9.26498413085937 5E3*Q(PHI1DT,GP1)+1.5837097265625E5*
   &   Q(PHI2IN,GP2)
   &    +8.5496521484375E4*Q(PHI2,GP2)+7.7992248535156 25E3*
   &    Q(PHI2DT,GP2)

      GV1=1./ABS(V1)
      GV2=1./ABS(V2)
      GV3=1./ABS(V3)
      V1=Q(V1,GV1)
      V2=Q(V2,GV2)
      V3=Q(V3,GV3)
      PRMT(1)=T
      PRMT(2)=T+TSP
      Y(1)=X
      Y(2)=XDOT
      Y(3)=PHI1IN
      Y(4)=PHI1
      Y(5)=PHI1DT
      Y(6)=PHI2IN
      Y(7)=PHI2
      Y(8)=PHI2DT

      CALL RKGS(PRMT,Y,DERY,NDIM,IHLF,FCT,OUTP,AUX)
      GO TO 10
      END

      SUBROUTINE FCT(XX,Y,DERY)
      DIMENSION  Y(8),DERY(8)
      COMMON X,XDOT,PHI1,PHI1DT,PHI1IN,PHI2,PHI2DT,PHI2IN,
   &  V1,V2,V3,AJ,AMT,AKSX,AKSP,AKSS,A33,TPRT,RB,DELTA,
   &  A0,B0,C0,D0,E,F,TEND,H,
   &  NPRT,IV1,IV2,IV3,LINE
      HX=0.00279
      HP1=0.00279
```

ORIGINAL PAGE IS
OF POOR QUALITY

```
      HP2=0.00279
      IF(Y(2).LT.0.) HX=-HX
      IF(Y(5).LT.0.) HP1=-HP1
      IF(Y(8).LT.0.) HP2=-HP2
      DERY(1)=Y(2)
      DERY(2)=((-V1*B0-AKSX*B0*Y(1)-B0*HX)*(1.-D0)+A0*((-V2-AKSP*
     &          Y(4)-HP1)*E+(V3+AKSS*Y(7)+HP2)*F*D0))/DELTA
      DERY(3)=Y(4)
      DERY(4)=Y(5)
      DERY(5)=((-V2-AKSP*Y(4)-HP1)*E-(V1+AKSX*Y(1)+HX)*B0*C0
     &          +(V3+AKSS*Y(7)+HP2)*D0*F)/DELTA
      DERY(6)=Y(7)
      DERY(7)=Y(8)
      DERY(8)=((-V3-AKSS*Y(7)-HP2)*F*(1.-A0*C0)+(V2+AKSP*Y(4)+HP1)*E
     &          +(V1+AKSX*Y(1)+HX)*B0*C0)/DELTA
      RETURN
      END
      SUBROUTINE OUTP(XX,Y,DERY,IHLF,NDIM,PRMT)
      DIMENSION Y(8),DERY(8),PRMT(5)
      COMMON X,XDOT,PHI1,PHI1DT,PHI1IN,PHI2,PHI2DT,PHI2IN,T,
     &  V1,V2,V3,AJ,AMI,AKSX,AKSP,AKSS,A33,TPRT,RB,DELTA,
     &  A0,B0,C0,D0,E,F,TEND,H,
     &  NPRT,IV1,IV2,IV3,LINE
      IF(XX.GT.TEND) PRMT(5)=1.
      T=XX
      IF(XX.LT.TPRT*FLOAT(NPRT)) RETURN
      LINE=LINE+1
      WRITE(6,100) IHLF,XX,(Y(I),I=1,8),V1,V2
100   FORMAT(1X,I2,3X,1PE10.4,1P8E11.3,2X,1P2E11.3)
      X=Y(1)
      XDOT=Y(2)
      PHI1IN=Y(3)
      PHI1=Y(4)
      PHI1DT=Y(5)
      PHI2IN=Y(6)
      PHI2=Y(7)
      PHI2DT=Y(8)
      NPRT=NPRT+1
      IF(LINE.LT.5) GO TO 200
      WRITE(5,100) IHLF,XX,(Y(I),I=1,8),V1,V2
      LINE=0
200   RETURN
      END
      FUNCTION Q(XX,G)
      COMMON X,XDOT,PHI1,PHI1DT,PHI1IN,PHI2,PHI2DT,PHI2IN,T,
     &  V1,V2,V3,AJ,AMI,AKSX,AKSP,AKSS,A33,TPRT,RB,DELTA,
     &  A0,B0,C0,D0,E,F,TEND,H,
     &  NPRT,IV1,IV2,IV3,LINE
      HG=H/G
      IF(XX.LT.0.) GO TO 20
      IV=(XX/HG)+0.5
      GO TO 30
20    IV=(XX/HG)-0.5
30    Q=FLOAT(IV)*HG
      RETURN
      END
```

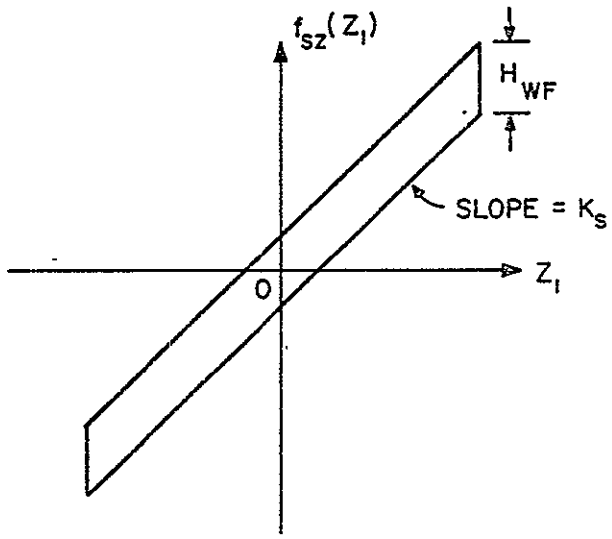

Figure 9-1. Nonlinear spring characteristic for the wire-cable torque of the digital ASPS.

linear characteristic of the ideal linear spring, it is expected that the gross effect is some damping effects on the system dynamics. The computer simulation results show that there are no sustained oscillations as a result of the nonlinear spring characteristics.

Figure 9-2 shows the transient responses of the x-dynamics of the digital ASPS with feedback control as designed in the preceding chapters. A 12-bit quantization is used. The initial value of x is 2×10^{-3}, and H_{WF} is varied from 0 to 0.008. Notice that when H = 0, the springs are ideal, and the response of x is oscillatory. The initial overshoot of the x-dynamics responses is due to the quantization effects. The final steady-state error of x when H_{WF} = 0 is small with a non-zero mean, but the response is relatively slow. As shown in Fig. 9-2, when the value of H_{WF} is increased, the time response becomes faster in reaching its steady state. In fact, when H_{WF} = 0.0028, the response of x resembles that of a deadbeat response, and the steady-state is nearly zero. However, as the value of H_{WF} increases further, the steady-state error increases. When H_{WF} = 0.008, the steady-state error is very large, and the response is also very slow. Thus, the transient responses in

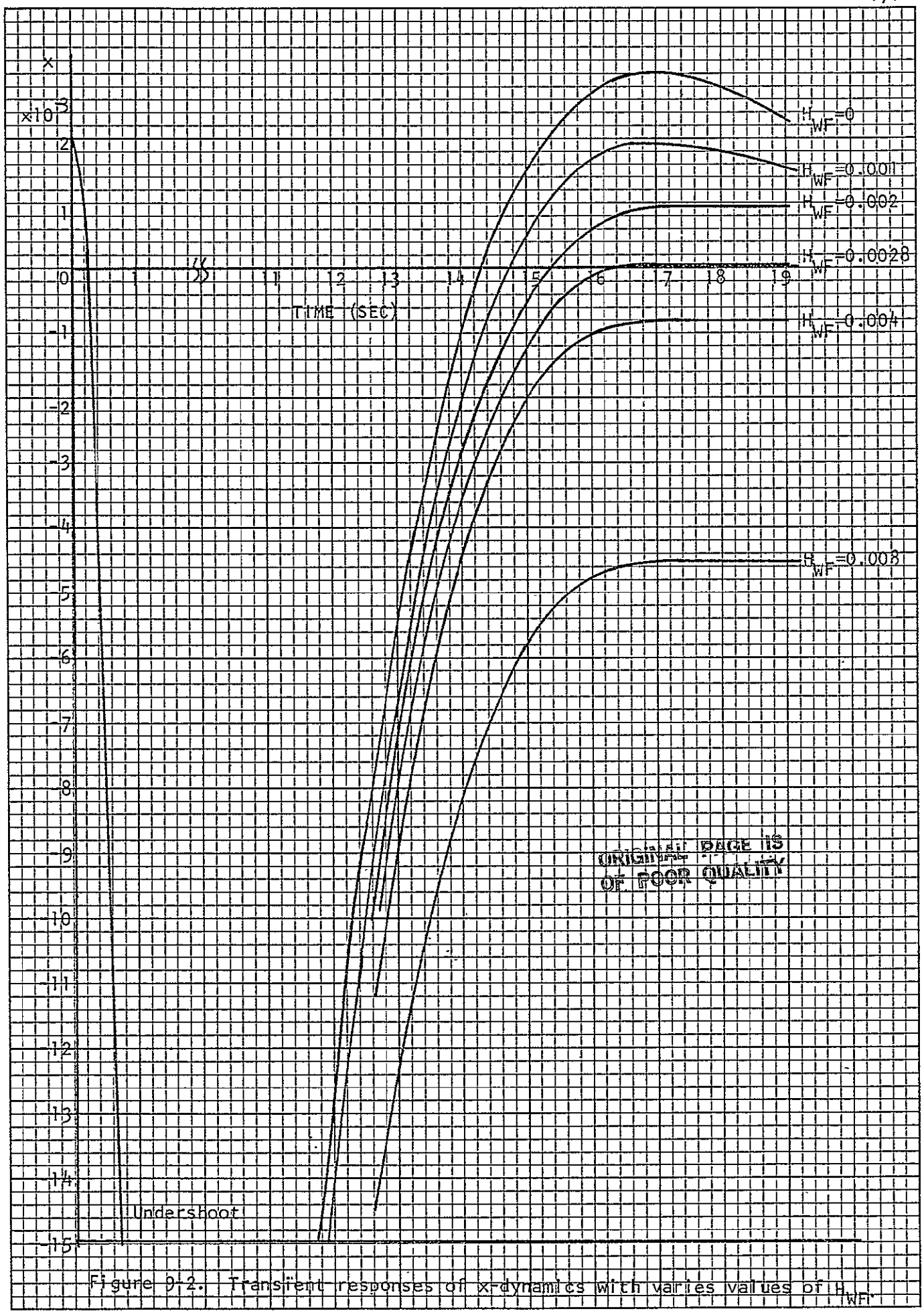

Figure 9-2. Transient responses of x-dynamics with varies values of H_{WF}.

Figure 9-2 clearly show that the nonlinear spring parameter H_{WF} can be used to improve the x-dynamic response if the value of H_{WF} can be controlled to some extent.

9.3 Effects of the Nonlinear Spring on the ϕ_1 and ϕ_2 Dynamics

The computer simulation results show that the nonlinear spring has little effects on the responses of the ϕ_1 and ϕ_2 dynamics. Since these two response components are relatively fast, the above-mentioned results were expected. However, different values of H_{WF} did give slight difference on the steady-state error of the responses. These error trajectories tend to have zero mean as expected due to the effect of the integral feedback in the system. Figures 9-3 and 9-4 show the transient responses of ϕ_1 and ϕ_2, respectively when $H_{WF} = 0$. Figures 9-6 and 9-7 illustrate the steady-state responses of ϕ_1 and ϕ_2, respectively, as compared with the steady-state response of x shown in Figure 9-5.

Figures 9-8, 9-9 and 9-10 illustrate the time responses of x, ϕ_1 and ϕ_2 for $H_{WF} = 0.001$. When $H_{WF} = 0.0028$ it was shown in Figure 9-2 that the x-component has a deadbeat response. However, this value of H_{WF} did not improve the ϕ_1 and ϕ_2 responses, as shown in Figures 9-11 and 9-12.

The conclusions on the investigations in this chapter is that the nonlinear spring effect due to the wire-cables on the ASPS does not appreciably harm the responses of the system. Except for the steady-state error when the value of H_{WF} is large, the transient responses are not much affected. There would be no sustained oscillations generated due to the nonlinear spring characteristic.

TIME	PHI1
0.0000E+00	1.300E-02
2.0000E-01	-3.890E-05
4.0000E-01	-5.139E-03
6.0000E-01	-3.455E-04
8.0000E-01	-1.215E-03
1.0000E+00	-3.335E-05
1.2000E+00	-3.091E-04
1.4000E+00	3.952E-05
1.6100E+00	-4.557E-05
1.8100E+00	-1.147E-04
2.0100E+00	-1.692E-04
2.2000E+00	-1.528E-05
2.4000E+00	5.718E-05
2.6000E+00	1.445E-07
2.8000E+00	5.620E-05
3.0100E+00	1.861E-05
3.2100E+00	-1.165E-05
3.4100E+00	-3.524E-05
3.6100E+00	-5.284E-05
3.8100E+00	-6.514E-05
4.0100E+00	-7.286E-05
4.2000E+00	4.887E-05
4.4000E+00	5.597E-05
4.6000E+00	4.117E-05
4.8000E+00	4.902E-05
5.0000E+00	3.131E-05
5.2000E+00	3.999E-05
5.4000E+00	3.075E-05
5.6000E+00	2.974E-05
5.8000E+00	1.763E-05
6.0000E+00	2.303E-05
6.2000E+00	1.243E-05
6.4000E+00	1.889E-05
6.6000E+00	1.608E-05
6.8000E+00	2.489E-05
7.0000E+00	1.436E-05

Figure 9-3. Transient response of ϕ_1 dynamics with $H_{WF} = 0$.

TIME	PHI2
0.0000E+00	1.300E-02
2.0000E-01	2.849E-03
4.0000E-01	-3.675E-03
6.0000E-01	9.337E-04
8.0000E-01	1.293E-04
1.0000E+00	-1.567E-03
1.2000E+00	-9.869E-04
1.4000E+00	-5.086E-04
1.6100E+00	-5.127E-04
1.8100E+00	-5.189E-04
2.0100E+00	-5.265E-04
2.2000E+00	-6.592E-04
2.4000E+00	-5.508E-04
2.6000E+00	-3.659E-04
2.8000E+00	-3.268E-04
3.0100E+00	-3.167E-04
3.2100E+00	-3.078E-04
3.4100E+00	-3.003E-04
3.6100E+00	-2.939E-04
3.8100E+00	-2.886E-04
4.0100E+00	-2.840E-04
4.2000E+00	-2.700E-04
4.4000E+00	-2.072E-04
4.6000E+00	-1.671E-04
4.8000E+00	-1.401E-04
5.0000E+00	-1.071E-04
5.2000E+00	-8.897E-05
5.4000E+00	-7.093E-05
5.6000E+00	-6.463E-05
5.8000E+00	-4.870E-05
6.0000E+00	-4.096E-05
6.2000E+00	-3.477E-05
6.4000E+00	-2.993E-05
6.6000E+00	-2.493E-05
6.8000E+00	-2.116E-05
7.0000E+00	-1.857E-05
7.2000E+00	-1.664E-05
7.4000E+00	-1.442E-05
7.6000E+00	-2.034E-05
7.8000E+00	-9.968E-06
8.0000E+00	-7.090E-06
8.2000E+00	-1.335E-05
8.4000E+00	-1.127E-05
8.6000E+00	-1.303E-06
8.8000E+00	8.740E-07

Figure 9-4. Transient response of ϕ_2 dynamics with $H_{WF} = 0$.

Figure 9-5. Steady-state response of the x-dynamics with $H_{WF}=0$ (sensor gain $G_x = 100$).

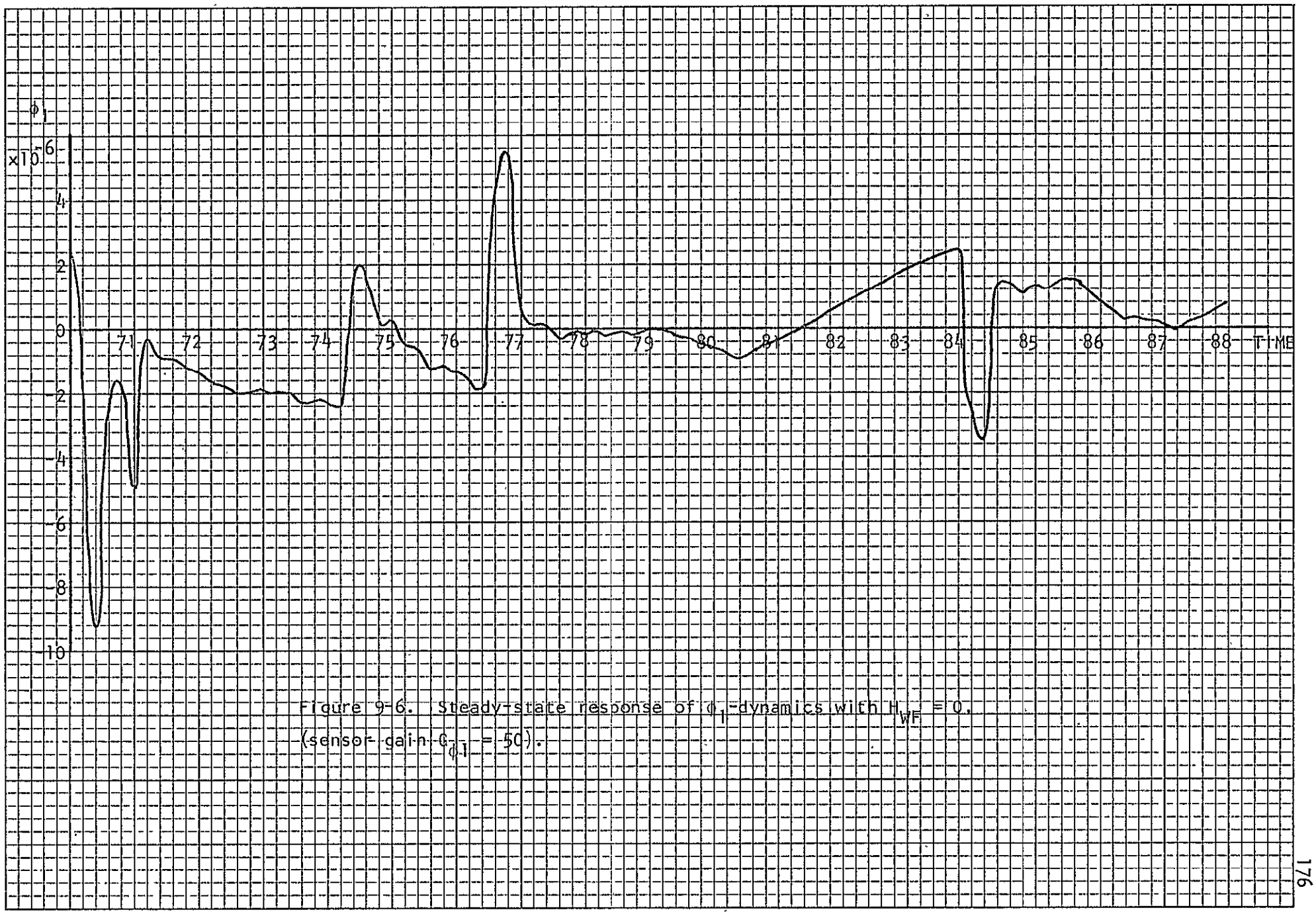

Figure 9-6. Steady-state response of ϕ_1-dynamics with $H_{WF} = 0$, (sensor gain $G_{\phi_1} = 50$).

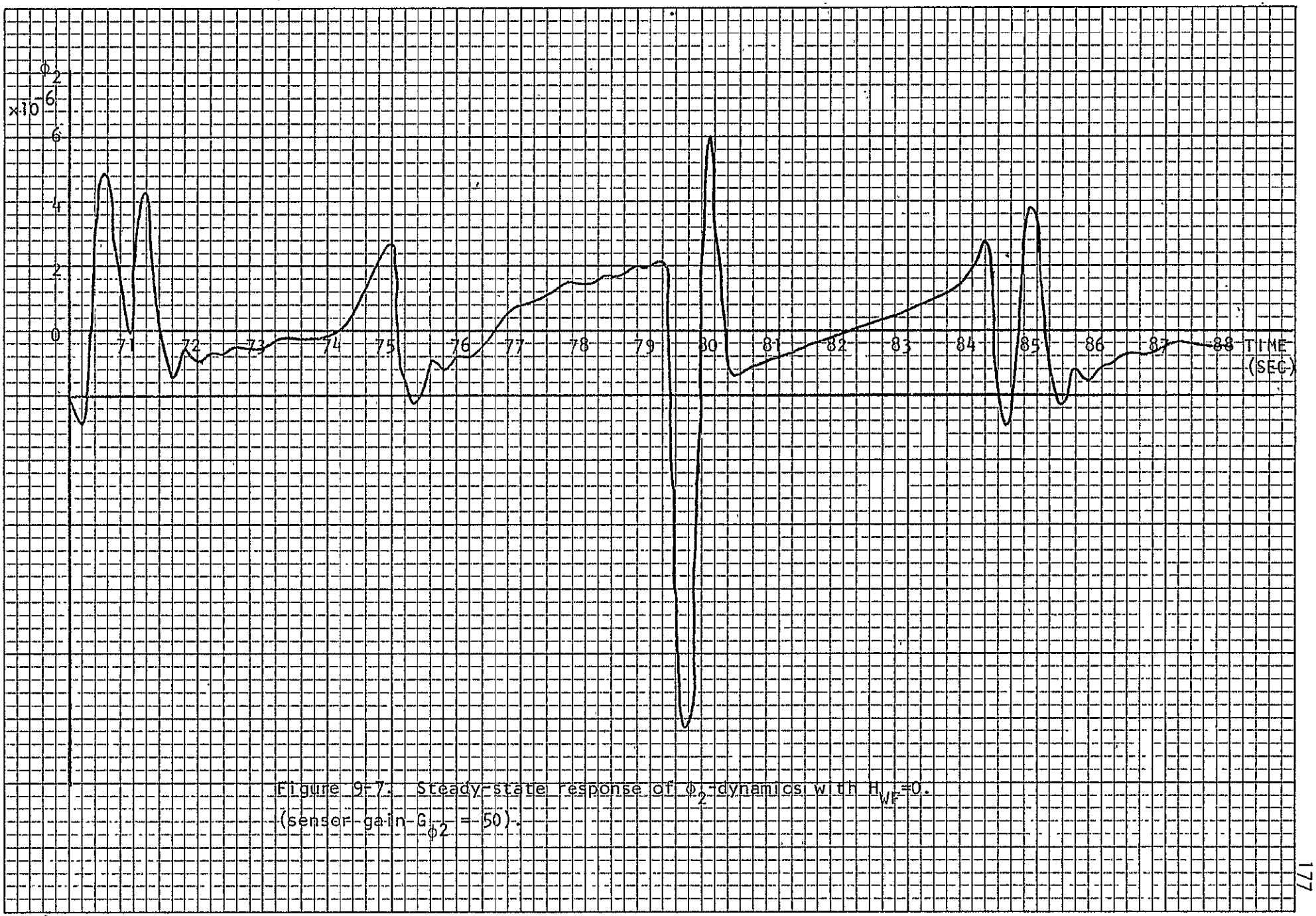

Figure 9-7. Steady-state response of ϕ_2-dynamics with $H_{WF}=0$. (sensor-gain-$G_{\phi 2} = -50$).

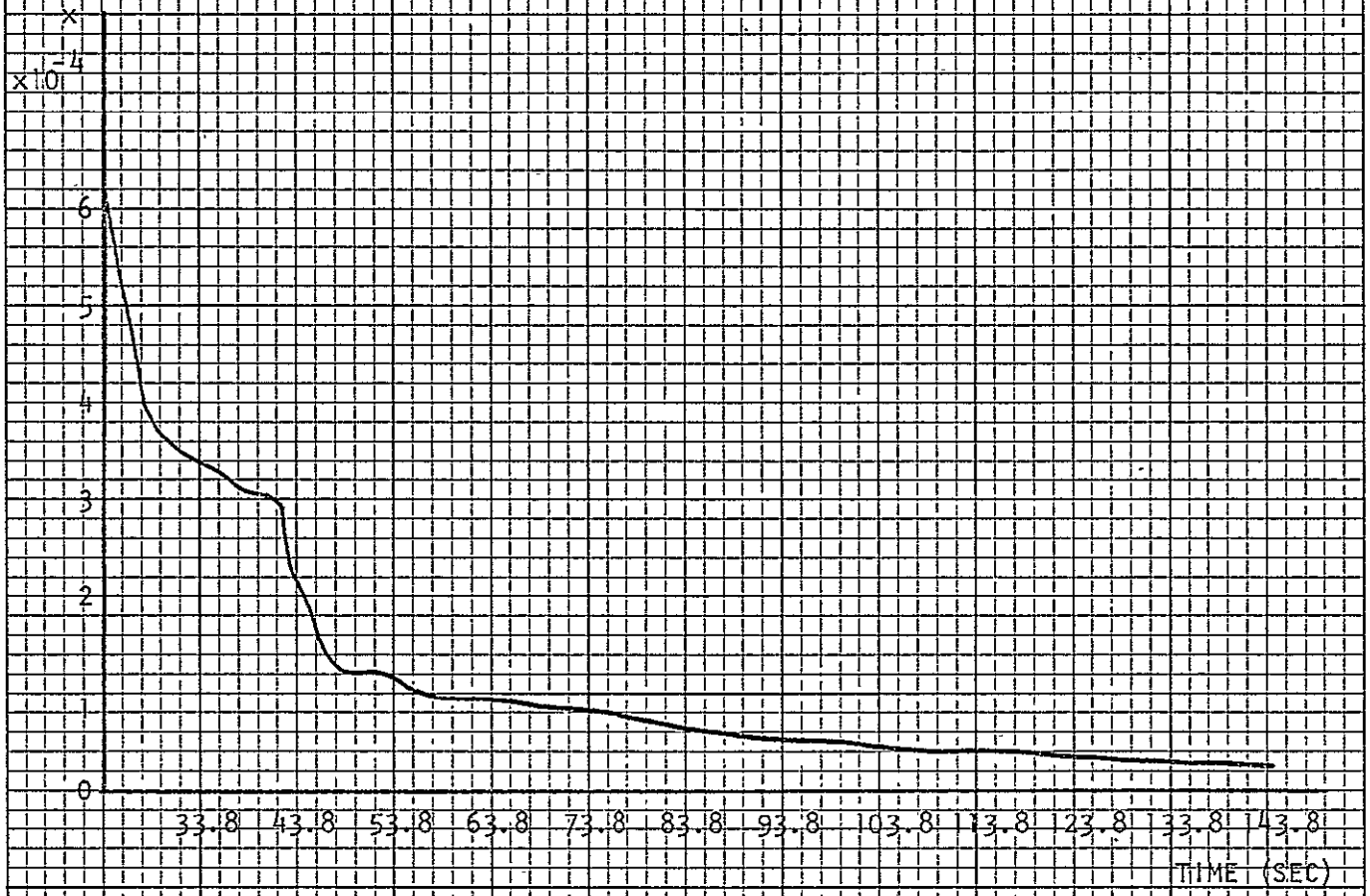

Figure 9-8. Time response of x-dynamics with $H_{WF} = 0.001$. (sensor gain $G_x = 100$).

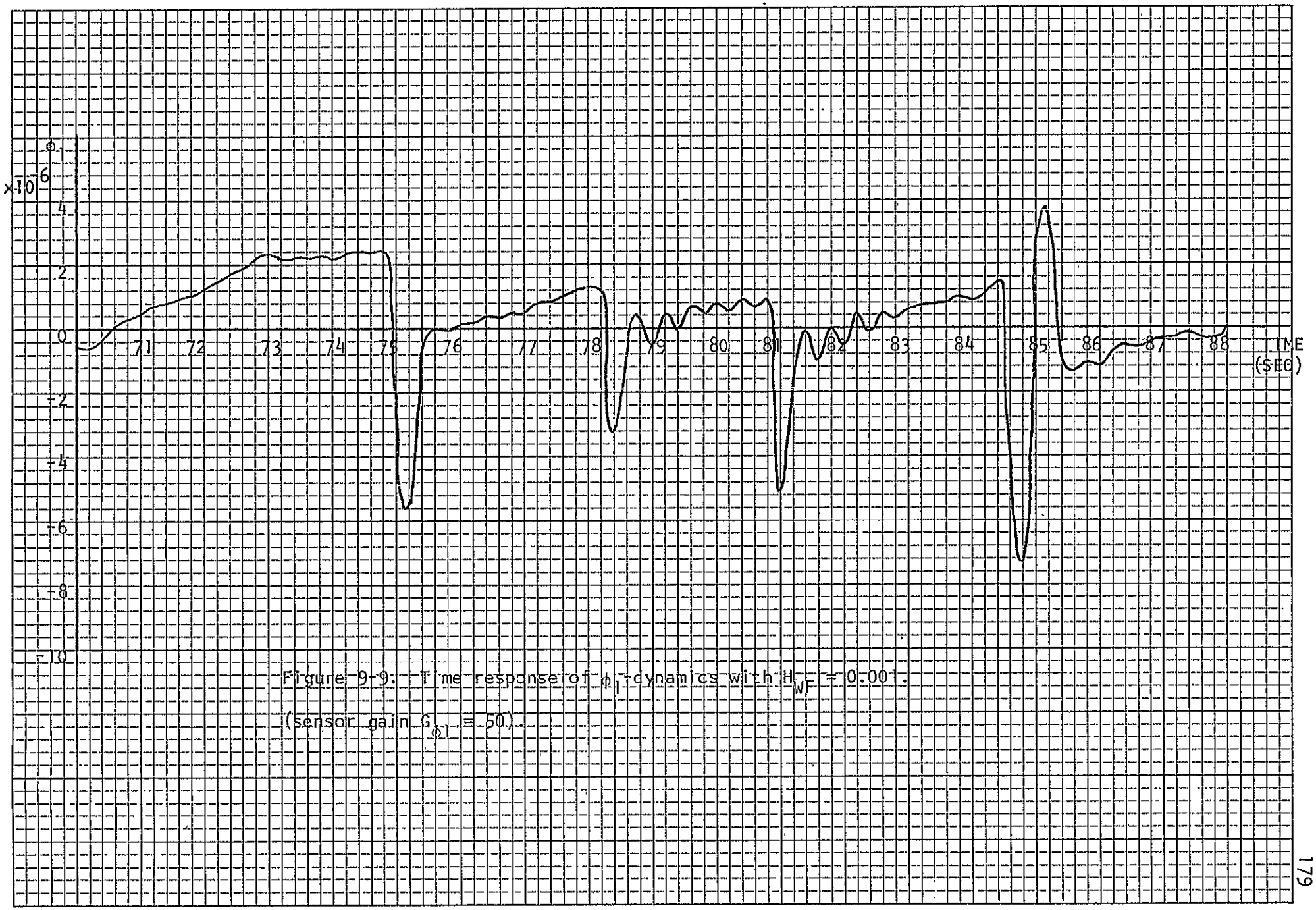

Figure 9-9: Time response of ϕ_1-dynamics with $H_{WF} = 0.00$; (sensor gain $G_{\phi_1} = 50$).

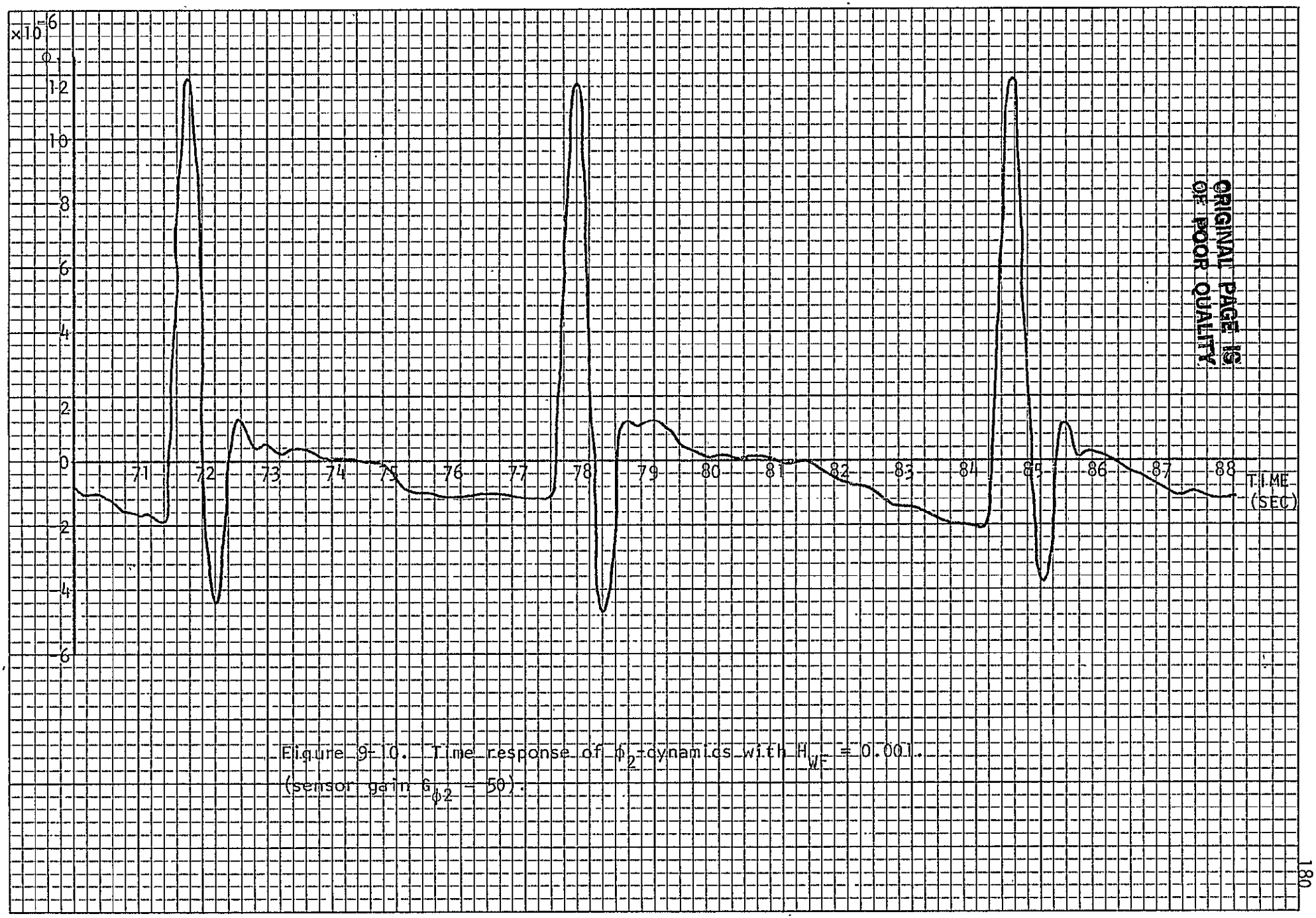

Figure 9-10. Time response of ϕ_2-dynamics with $H_{WF} = 0.001$. (sensor gain $G_{\phi 2} = 50$).

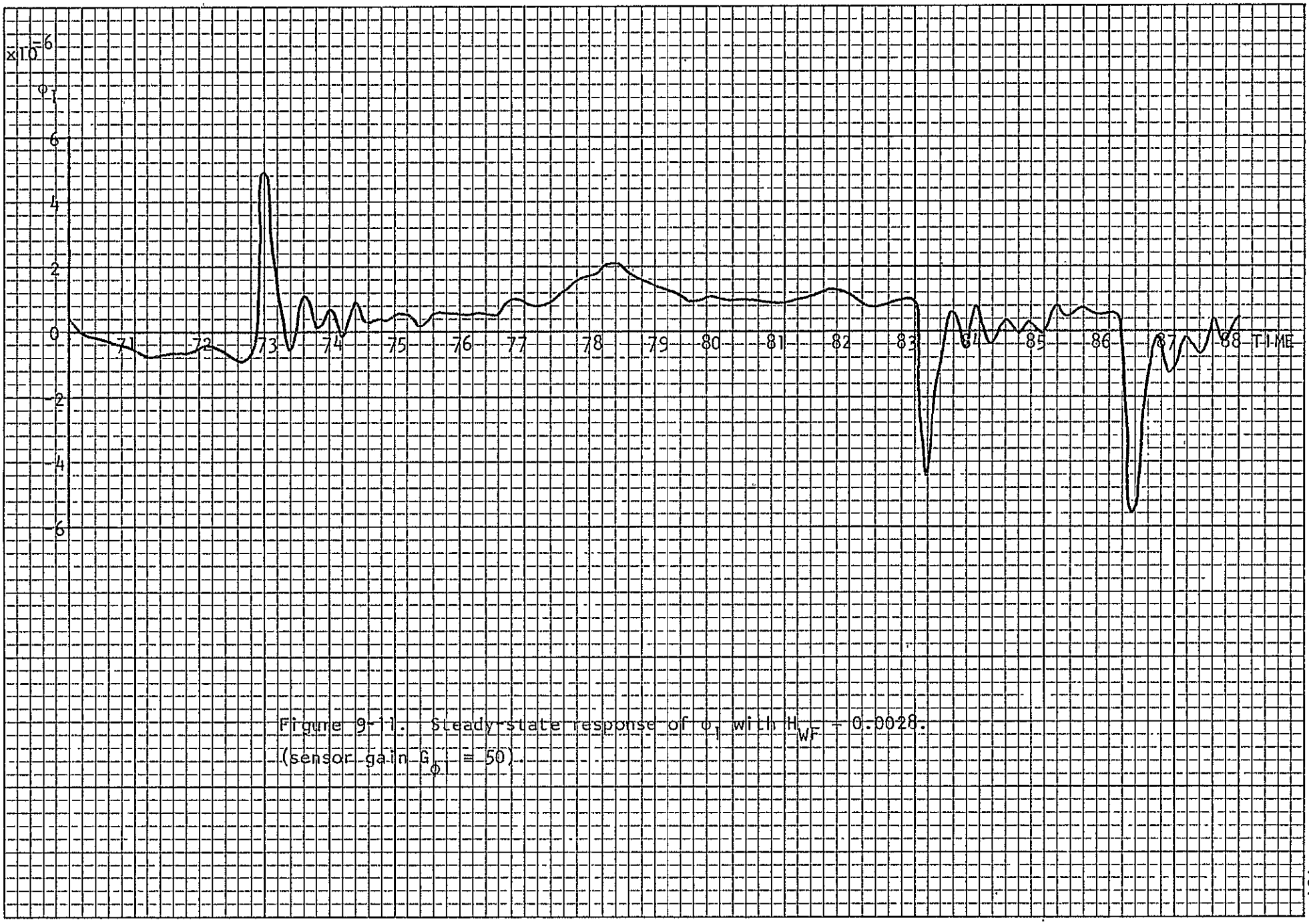

Figure 9-11. Steady-state response of ϕ_1 with $H_{WF} = 0.0028$. (sensor gain $G_\phi = 50$).

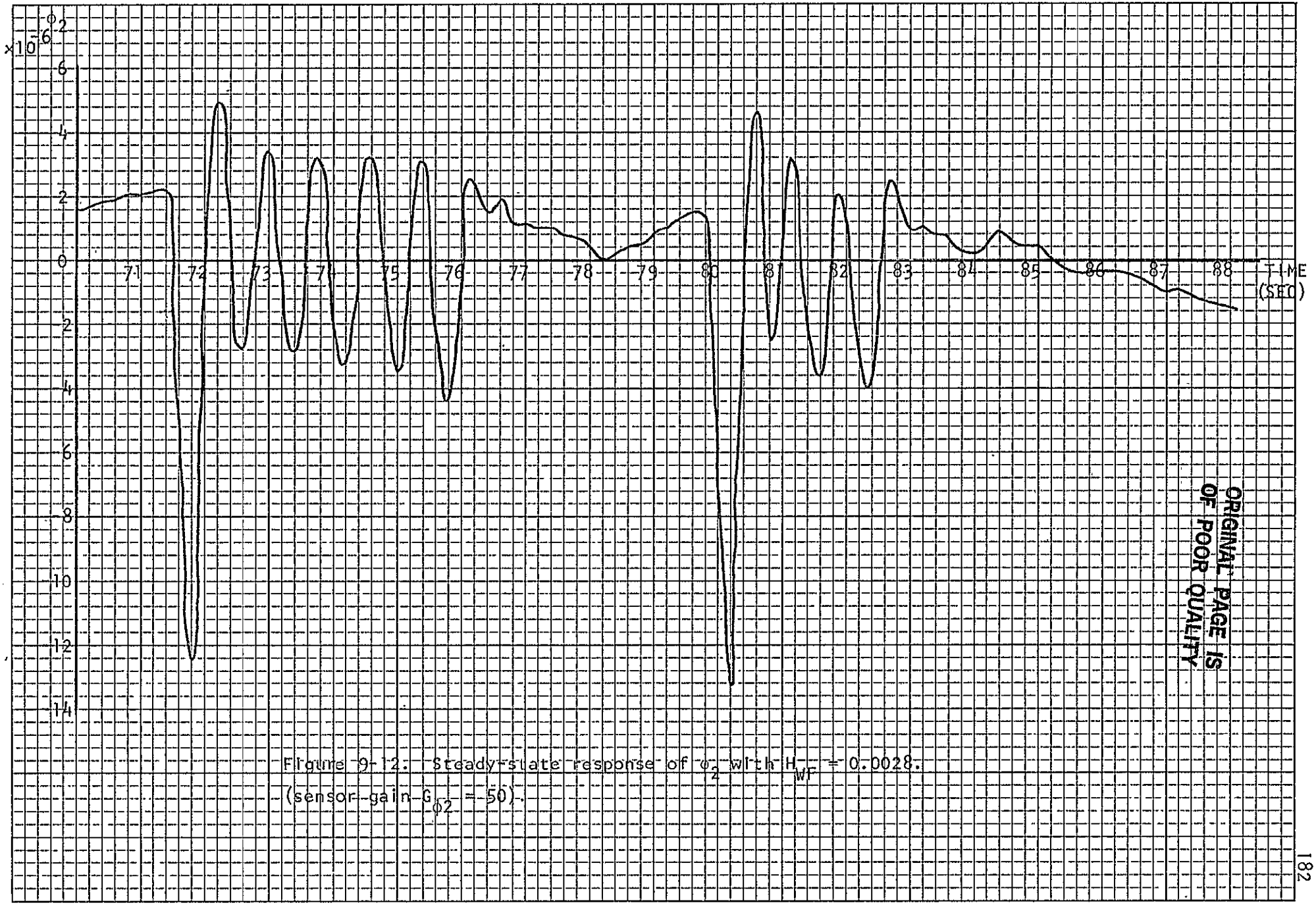

Figure 9-12. Steady-state response of ϕ_2 with $H_{WF} = 0.0028$. (sensor-gain-$G_{\phi 2} = -50$).

References

1. Technical Report, Space Shuttle Experiment Pointing Mount (EPM) Systems, An Evaluation of Concepts and Technologies, Jet Propulsion Laboratory 701-1, April 1, 1977.

2. H. B. Waites, Equations of Motion Derivation for a Simplified ASPS Model, Memorandum, NASA, October 1977.

3. B. C. Kuo, DIGITAL CONTROL SYSTEMS, SRL Publishing Company, 1977.

4. Final Report, Stability Analysis of the Low-Cost Large Space Telescope System, Systems Research Laboratory, June 30, 1975.